

UNIVERSITY OF LJUBLJANA
FACULTY OF MATHEMATICS AND PHYSICS

Mag. Andrija Volkanovski

**Impact of offsite power system reliability on nuclear
power plant safety**

Doctoral thesis

ADVISER: prof. dr. Borut Mayko
CO-ADVISER: doc. dr. Marko Čepin

Ljubljana, 2008

UNIVERZA V LJUBLJANI
FAKULTETA ZA MATEMATIKO IN FIZIKO

Mag. Andrija Volkanovski

**Vpliv zanesljivosti zunanjega električnega napajanja
na varnost jedrske elektrarne**

Doktorska disertacija

MENTOR: prof. dr. Borut Mavko
SOMENTOR: doc. dr. Marko Čepin

Ljubljana, 2008

*Unlike the fairy tale Rumpelstiltskin, do not think that by having named the devil that you have destroyed him.
Positive verification of his demise is required.*

**System Safety Handbook for the
Acquisition Manager, U.S. Air Force**

Acknowledgements/Zahvale

To Ministry of Higher Education, Science and Technology, Republic of Slovenia (contract number 1000-05-310016), and the Reactor Engineering Division of the Jožef Stefan Institute for provided financial support.

To mentor prof. dr. Borut Mavko for accepting the responsibility of mentorship and guiding me as a young researcher, honoring me to work with internationally recognized expert and researcher of his rank.

To co-mentor and research advisor doc. dr. Marko Čepin, for his support, guidelines, always open door of his office, thousands of e-mails, reviews, comments, discussions, teaching me to do things right and, even more important, to do the right things. I'm especially thankful for his supportive words in the times when I needed them most. Marko, thank you.

To all colleagues from Reactor Engineering Division.

To Republic of Slovenia and all citizens for accepting and supporting me and my family.

To my Parents.

To son Aleksandar for reminding me what matters most in life.

To wife Sanja, for always being there as my partner.

Impact of offsite power system reliability on nuclear power plant safety

Keywords:

- Loss of offsite power
- Core damage frequency
- Fault tree
- Power flow method
- Power system reliability
- Nuclear safety

Abstract: The nuclear power plant (NPP) safety and the power system reliability are mutually interdependent parameters. The safe operation of the nuclear power plant results in delivering a large amount of electrical energy to the power system and contributes to its stable operation. On the other side, the power system delivers the electrical energy to the house load of the nuclear power plant, which is especially important during the shutdown and the startup of the plant.

The loss of offsite power (LOOP) initiating event occurs when all electrical power to the plant from external sources is lost. In spite of the fact that NPP is equipped with the emergency diesel generators in such case, the safety of the plant is decreased at the loss of offsite power. This is confirmed with the results of the probabilistic safety assessment, that show that the contribution of the scenarios connected with the loss of offsite power to the overall risk is several tenths of percents.

The current methodologies used for the estimation of the LOOP initiating event frequency are performed generally, not accounting the actual state and the specifics of the power system.

A new method for the estimation of the LOOP initiating event frequency is developed. The method combines the linear network flow method with the fault tree analysis features. A computer program consisting of 4622 lines of code supporting this method has been written. The developed method accounts power flows through interconnections, voltages of the substations and the local weather conditions. The viable pathways of power delivery to the house load of the NPP are identified and the consequent fault tree is built. The consequent fault trees are built for other loads in the system.

The following results are obtained from the quantitative and qualitative analysis of the constructed fault tree: the minimal cut sets, which are combinations of components failures, resulting in a failure of the power delivery to the house load of the NPP, the weighted power system reliability and the importance measures of the components and groups of the components of the power system. The importance measures identify the most important elements of the power system from the aspect of nuclear safety. The frequency of the LOOP initiating event is assessed based on the unreliability of the power delivery to the house load of the NPP. The impact of changes in the power system to the safety of the NPP is evaluated.

The verification of the developed method was performed on small examples. The applicability of the method on the real power systems is validated on a large standard reliability test system. The method is applied on the simplified Slovenian power system.

The reliability of the Slovenian power system and the impact of selected changes in the power system to the safety of the NPP are evaluated. The importance of the NPP Krško for the reliable operation of the Slovenian power system is verified. Installation of new diesel generator for providing emergency electrical power would improve safety. Installation of new line Krško-Beričevó is identified as a mean for improved safety and as a prerequisite for additional nuclear power plant at Krško site.

PACS: 28.50.Hw, 28.41.Ak, 28.41.Te, 84.32.Dd, 84.37.+q, 84.70.+p, 84.32.-y

Vpliv zanesljivosti zunanjega električnega napajanja na varnost jedrske elektrarne

- Ključne besede:**
- Izguba zunanjega napajanja
 - Frekvenca poškodbe sredice
 - Drevo odpovedi
 - Metoda pretokov moči
 - Zanesljivost elektroenergetskega sistema
 - Jedrska varnost

Povzetek: Varnost jedrskih elektrarn in zanesljivost elektroenergetskega sistema sta medsebojno povezana. Varno delovanje jedrske elektrarne daje velike količine električne energije v elektroenergetski sistem in hkrati kot močan vir prispeva k njeni kakovosti. Po drugi strani elektroenergetski sistem daje električno energijo za lastno rabo jedrske elektrarne, kar je še posebej pomembno v času njene zaustavitve in zagona.

Začetni dogodek izguba zunanjega napajanja je neželen dogodek, ki se zgodi, če jedrska elektrarna izgubi vse vire zunanjega električnega napajanja. Čeprav je elektrarna opremljena z dizelskimi generatorji, ki se v takem primeru zaženejo, je varnost elektrarne ob tem dogodku poslabšana. To kažejo tudi rezultati verjetnostnih varnostnih analiz, kjer izguba zunanjega napajanja prispeva k kazalcem tveganja nekaj deset odstotkov celote.

Trenutne metode za ocenjevanje frekvence izgube zunanjega napajanja so splošne in ne upoštevajo dejanskega stanja elektroenergetskega omrežja in njegovih specifičnih značilnosti. Zato je bila razvita nova metoda za ocenjevanje frekvence začetnega dogodka izguba zunanjega napajanja. Metoda združuje linearni model pretokov moči in analizo dreves odpovedi. Lastni računalniški program v dolžini 4622 vrstic je bil napisan za izvedbo metode. V okviru metode so upoštevani pretoki moči med vozlišči, ki predstavljajo transformatorske postaje, in napetosti v njih. Upoštevane so normalne razmere in tudi delovanje pri odpovedi enega daljnovoda. Lokalne vremenske razmere so upoštevane. Identificirane so možne poti dobave električne energije porabnikom, med katerimi je tudi lastna raba jedrske elektrarne. Za vsak porabnik posebej je razvito odgovarjajoče drevo odpovedi.

Rezultati kvalitativne in kvantitativne analize drevesa odpovedi so naslednji: najkrajše poti odpovedi, ki predstavljajo kombinacije odpovedi komponent in ki lahko pomenijo odpovedi sistema, in v konkretnem primeru pomenijo izpad dobave zunanje električne energije za lastno rabo jedrske elektrarne, zanesljivost elektroenergetskega sistema in merila pomembnosti komponent ter skupin komponent sistema. Merila pomembnosti identificirajo najpomembnejše komponente sistema s stališča jedrske varnosti. Frekvenca začetnega dogodka izguba zunanjega napajanja je ocenjena na osnovi nezanesljivosti elektroenergetskega sistema za dobavo lastne rabe jedrske elektrarne. Proučen je vpliv sprememb v elektroenergetskem sistemu na varnost jedrske elektrarne.

Metoda je bila preverjena na majhnih primerih. Preizkušena je bila na velikem standardnem primeru elektroenergetskega sistema. Uporabljena je za slovenski elektroenergetski sistem.

Rezultati kažejo zanesljivost slovenskega elektroenergetskega sistema. Ocenjen je vpliv določenih sprememb na zanesljivost elektroenergetskega sistema in na varnost jedrske elektrarne. Dodaten dizelski generator v jedrski elektrarni znatno prispeva k njeni večji varnosti. Potrjen je njen pomen v elektroenergetskem sistemu. Izgradnja daljnovoda Krško-Beričovo pomeni izboljšano varnost jedrske elektrarne v Krškem in je hkrati predpogoj za postavitev nove jedrske elektrarne v Krškem.

PACS: 28.50.Hw, 28.41.Ak, 28.41.Te, 84.32.Dd, 84.37.+q, 84.70.+p, 84.32.-y

Table of contents

1	INTRODUCTION	1
1.1	OBJECTIVES AND GOALS	2
1.2	THE OUTLINE	4
2	REVIEW OF ACTIVITIES OF POWER SYSTEM ANALYSIS	5
3	PROBABILISTIC SAFETY ASSESSMENT	7
3.1	PROBABILISTIC SAFETY ASSESSMENT FUNDAMENTALS	7
3.2	PSA MODELING.....	12
3.2.1	<i>Event Tree Analysis</i>	12
3.2.2	<i>Fault tree analysis</i>	16
3.3	PSA APPLICATIONS AND RISK-INFORMED DECISION MAKING	25
3.4	POWER SYSTEM ANALYSIS METHODS	25
3.4.1	<i>Percent Reserve Evaluation</i>	26
3.4.2	<i>Loss-of-the-Largest-Generating-Unit Method</i>	26
3.4.3	<i>Loss-of-Load-Probability Method</i>	27
3.4.4	<i>Applications of probability theory to power systems</i>	27
3.4.5	<i>Additional Reliability Measures</i>	27
4	NEW METHOD DESCRIPTION	31
4.1	DEFINITION OF RELIABILITY AND IMPORTANCE INDICES	31
4.2	FAULT TREE CONSTRUCTION PROCEDURE	32
4.2.1	<i>Fault tree construction of loads</i>	33
4.2.2	<i>Fault tree construction of substations</i>	37
4.3	APPROXIMATE DC LOAD FLOW MODEL AND LINE OVERLOAD TEST	39
4.3.1	<i>Direct current (DC) model</i>	42
4.3.2	<i>Relation between line power flows and injected power of generators</i>	44
4.3.3	<i>Calculation of the elements of the matrix [H]</i>	45
4.3.4	<i>Modifications of the matrix [H]</i>	46
4.3.5	<i>Modifications of the matrix [H] in case of the load failure</i>	47
4.3.6	<i>Network separation resulting from the line failure</i>	48
4.3.7	<i>Separated model of the power system</i>	49
4.3.8	<i>Improvement of the reactive power flow calculations</i>	52
4.3.9	<i>Line overload and substation voltage test</i>	53
4.4	DESCRIPTION OF THE COMPUTER CODE.....	54
5	MODELS AND RESULTS OF THE POWER SYSTEM RELIABILITY ANALYSIS	57
5.1	IEEE TEST SYSTEM	57
5.2	THE RESULTS FOR THE IEEE TEST SYSTEM	57
5.2.1	<i>The results for IEEE-RTS without consideration of the substations voltages</i>	58
5.2.2	<i>Change of the cut off used in the analysis</i>	62
5.2.3	<i>The results for IEEE-RTS with the consideration of the substations voltages</i>	62
5.2.4	<i>Summary of the results obtained for the IEEE RTS</i>	66
5.3	SLOVENIAN POWER SYSTEM.....	66
5.4	RESULTS FOR THE SLOVENIAN POWER SYSTEM	70
5.4.1	<i>Basic Slovenian power system without consideration of voltages</i>	70
5.4.2	<i>Basic Slovenian power system with the consideration of voltages</i>	73
5.5	ANALYSIS OF THE CONFIGURATIONS OF THE SLOVENIAN POWER SYSTEM	74
5.5.1	<i>Slovenian power system with the single NPP Krško - Beričevo line</i>	74
5.5.2	<i>Slovenian power system with the double Krško - Beričevo line</i>	78
5.5.3	<i>Slovenian power system with the new NPP in Krško and proportional increase of the load</i>	81
5.5.4	<i>Slovenian power system with the new NPP in Krško and increase of the load in the substation Divača</i> 84	
5.5.5	<i>Summary of the results obtained for the Slovenian Power System</i>	86
6	IMPACT OF OFFSITE POWER SYSTEM RELIABILITY ON NUCLEAR POWER PLANT SAFETY	88

6.1	LOOP DATA ANALYSIS.....	88
6.2	METHOD FOR CALCULATION OF LOSS OF OFFSITE POWER IE FREQUENCY	92
6.3	IMPACT OF LOOP FREQUENCY ON CDF OF NPP	93
6.3.1	<i>NPP power system.....</i>	<i>94</i>
6.3.2	<i>NPP PSA model.....</i>	<i>96</i>
6.3.3	<i>Sensitivity analysis of CDF</i>	<i>101</i>
6.4	IMPLICATION OF GRID RELATED LOOP ON PLANT CDF	104
6.4.1	<i>Implication of Grid related LOOP on plant CDF in IEEE RTS.....</i>	<i>105</i>
6.4.2	<i>Implication of Grid related LOOP on CDF in Slovenian power system</i>	<i>107</i>
7	CONCLUSIONS.....	109
8	REFERENCES	111
	APPENDIX A: PRINCIPLES OF ENGINEERING SAFETY.....	115
	APPENDIX B: SUBSTATIONS CONFIGURATIONS.....	117
	APPENDIX C: VERIFICATION OF THE METHOD AND COMPUTER CODE.....	135
	APPENDIX D: RELIABILITY PARAMETERS.....	148

List of Figures

FIGURE 2-1 HIERARCHICAL LEVELS IN ELECTRICAL POWER SYSTEMS	5
FIGURE 3-1 ACTIVITIES IN PSA	11
FIGURE 3-2 EVENT TREE DEVELOPMENT PROCESS	12
FIGURE 3-3 EXAMPLE EVENT TREE	13
FIGURE 3-4 SYSTEMS A AND B FAULT TREES AND PART OF THE EVENT TREE SEQUENCE	15
FIGURE 3-5 FAULT TREE DEVELOPMENT PROCESS	17
FIGURE 3-6 EXAMPLE HPIS	22
FIGURE 3-7 HPIS FAULT TREE	24
FIGURE 3-8 RELATION COST-RELIABILITY FOR POWER SYSTEMS	25
FIGURE 4-1 AN EXAMPLE POWER SYSTEM	33
FIGURE 4-2 ADJACENCY MATRIX A OF AN EXAMPLE SYSTEM	33
FIGURE 4-3 ROOTED TREE FOR SUBSTATION 1	34
FIGURE 4-4 DISCARDED AND ACCEPTED FLOW PATHS FOR TEST SYSTEM	35
FIGURE 4-5 MODULAR FAULT TREE USED FOR FAULT TREE CONSTRUCTION	35
FIGURE 4-6 OPTIONAL CONSTRUCTION OF THE GENERATOR FAILURE GATE	36
FIGURE 4-7 PART OF THE FAULT TREE BUILT FOR LOAD 1 IN THE SUBSTATION 1	37
FIGURE 4-8 EXAMPLE SUBSTATION AND SIMPLIFIED MODEL OF THE SUBSTATION	38
FIGURE 4-9 FAULT TREE FOR SIMPLIFIED SUBSTATION REPRESENTATION	39
FIGURE 4-10 NOTATION FOR ACTIVE AND REACTIVE POWER AT A TYPICAL BUS I IN POWER FLOW STUDIES	41
FIGURE 4-11 TWO REGIONS SYSTEM	48
FIGURE 4-12 π CIRCUIT OF A MEDIUM-LENGTH TRANSMISSION LINE	49
FIGURE 4-13 EQUIVALENT CIRCUIT OF A MEDIUM-LENGTH LINE	52
FIGURE 4-14 BLOCK DIAGRAM OF THE PROGRAM	55
FIGURE 5-1 IEEE-96 RELIABILITY TEST SYSTEM	58
FIGURE 5-2 BASIC CONFIGURATION OF SLOVENIAN POWER SYSTEM	67
FIGURE 5-3 SLOVENIAN POWER SYSTEM USED IN THE CONSTRUCTION OF THE MODEL	69
FIGURE 5-4 SLOVENIAN POWER SYSTEM WITH THE ADDED LINE NPP KRŠKO – BERIČEVO	76
FIGURE 5-5 SLOVENIAN POWER SYSTEM WITH THE DOUBLE LINE BETWEEN NPP KRŠKO – BERIČEVO	80
FIGURE 5-6 SLOVENIAN POWER SYSTEM WITH THE TWO NPP KRŠKO AND SINGLE LINE NPP KRŠKO – BERIČEVO	82
FIGURE 6-1 LOOP EVENT COUNTS BY CAUSE	91
FIGURE 6-2 EXAMPLE OF AN OFFSITE POWER SYSTEM	94
FIGURE 6-3 CONTRIBUTION OF ACCIDENT GROUPS FOR SURRY UNIT 1 CDF FROM MODEL	98
FIGURE 6-4 CONTRIBUTION OF LOOP AND SBO TO ALL LOOP ACCIDENT GROUP FOR SURRY UNIT 1 CDF	98
FIGURE 6-5 CDF CONTRIBUTION BY INITIATING EVENTS FOR NPP KRŠKO	99
FIGURE 6-6 UNAVAILABILITY OF THE EMERGENCY AC POWER SYSTEM FROM EDG RELIABILITY	101
FIGURE 6-7 UNAVAILABILITY OF THE EMERGENCY AC POWER SYSTEM FROM EDG RELIABILITY, CCF NOT ACCOUNTED	102
FIGURE 6-8 DEPENDENCY OF CDF FROM EDG RELIABILITY	103
FIGURE 6-9 DEPENDENCY OF CDF FROM LOOP FREQUENCY	103
FIGURE 6-10 DEPENDENCY OF CDF FROM LOOP IE FREQUENCY, IEEE SYSTEM	106
FIGURE 6-11 DEPENDENCY OF CDF FROM LOOP IE FREQUENCY, SLOVENIAN POWER SYSTEM	108

List of Tables

TABLE 3-1 LAWS OF THE BOOLEAN ALGEBRA	19
TABLE 3-2 IDENTIFIED MINIMAL CUT SETS FOR HPIS	23
TABLE 5-1 IDENTIFIED MCS FOR POWER DELIVERY TO THE LOAD IN THE SUBSTATION 18	59
TABLE 5-2 IDENTIFIED MCS FOR POWER DELIVERY TO THE LOAD IN THE SUBSTATION 21	59
TABLE 5-3 CALCULATED UNRELIABILITIES FOR THE IEEE RTS	60
TABLE 5-4 BASIC EVENTS WITH THE LARGEST NRRW	60
TABLE 5-5 BASIC EVENTS WITH THE LARGEST NRAW	60
TABLE 5-6 BASIC EVENTS WITH THE LARGEST RRW FOR LOAD IN THE SUBSTATION 18	61
TABLE 5-7 BASIC EVENTS WITH THE LARGEST RAW FOR LOAD IN THE SUBSTATION 18	61
TABLE 5-8 BASIC EVENTS WITH THE LARGEST RRW FOR LOAD IN THE SUBSTATION 21	61
TABLE 5-9 BASIC EVENTS WITH THE LARGEST RAW FOR LOAD IN THE SUBSTATION 21	62
TABLE 5-10 USED TRUNCATION LIMITS IN ANALYSIS.....	62
TABLE 5-11 IDENTIFIED MCS FOR POWER DELIVERY TO THE LOAD IN THE SUBSTATION 18	63
TABLE 5-12 IDENTIFIED MCS FOR POWER DELIVERY TO THE LOAD IN THE SUBSTATION 21	63
TABLE 5-13 CALCULATED UNRELIABILITIES FOR THE IEEE RTS	63
TABLE 5-14 CALCULATED VOLTAGES IN THE SUBSTATIONS OF THE IEEE RTS FOR NORMAL REGIME	64
TABLE 5-15 BASIC EVENTS WITH THE LARGEST NRRW	64
TABLE 5-16 BASIC EVENTS WITH THE LARGEST NRAW	65
TABLE 5-17 THE RRW AND RAW IMPORTANCE MEASURES FOR THE LOAD IN THE SUBSTATION 18.....	65
TABLE 5-18 BASIC EVENTS WITH THE LARGEST RRW FOR THE LOAD IN THE SUBSTATION 21	65
TABLE 5-19 BASIC EVENTS WITH THE LARGEST RAW FOR THE LOAD IN THE SUBSTATION 21	66
TABLE 5-20 THE SUBSTATIONS NUMBERS USED IN CONSTRUCTION OF THE BASIC EVENTS	68
TABLE 5-21 IDENTIFIED MCS FOR POWER DELIVERY TO NPP KRŠKO	70
TABLE 5-22 OBTAINED UNRELIABILITIES FOR THE BASIC CONFIGURATION OF THE SLOVENIAN POWER SYSTEM ...	70
TABLE 5-23 OBTAINED RELIABILITY FOR THE BASIC CONFIGURATION OF THE SLOVENIAN POWER SYSTEM	70
TABLE 5-24 BASIC EVENTS WITH THE LARGEST NRRW	71
TABLE 5-25 BASIC EVENTS WITH THE LARGEST NRAW	71
TABLE 5-26 BASIC EVENTS WITH THE LARGEST RRW FOR NPP KRŠKO	72
TABLE 5-27 BASIC EVENTS WITH THE LARGEST RAW FOR NPP KRŠKO.....	72
TABLE 5-28 CALCULATED VOLTAGES IN SUBSTATIONS FOR THE BASIC SLOVENIAN POWER SYSTEM	73
TABLE 5-29 CALCULATED POWER FLOWS THROUGH LINES FOR THE BASIC SLOVENIAN POWER SYSTEM.....	74
TABLE 5-30 IDENTIFIED MCS FOR POWER DELIVERY TO THE NPP KRŠKO	75
TABLE 5-31 OBTAINED UNRELIABILITIES FOR CONFIGURATION WITH THE SINGLE NPP KRŠKO-BERIČEVO LINE... 75	75
TABLE 5-32 BASIC EVENTS WITH THE LARGEST NRRW, SINGLE NPP KRŠKO – BERIČEVO LINE ADDED	76
TABLE 5-33 BASIC EVENTS WITH THE LARGEST NRAW, SINGLE NPP KRŠKO – BERIČEVO LINE ADDED.....	77
TABLE 5-34 BASIC EVENTS WITH THE LARGEST RRW FOR THE NPP KRŠKO	77
TABLE 5-35 BASIC EVENTS WITH THE LARGEST RAW FOR THE NPP KRŠKO.....	77
TABLE 5-36 CALCULATED POWER FLOWS THROUGH LINES FOR SLOVENIAN POWER SYSTEM, SINGLE NPP KRŠKO – BERIČEVO LINE	78
TABLE 5-37 IDENTIFIED MCS FOR POWER DELIVERY TO THE NPP KRŠKO	79
TABLE 5-38 OBTAINED UNRELIABILITIES FOR CONFIGURATION WITH THE DOUBLE NPP KRŠKO-BERIČEVO LINE ..	79
TABLE 5-39 BASIC EVENTS WITH THE LARGEST RRW FOR THE NPP KRŠKO	80
TABLE 5-40 BASIC EVENTS WITH THE LARGEST RAW FOR THE NPP KRŠKO.....	80
TABLE 5-41 CALCULATED POWER FLOWS THROUGH LINES OF THE SLOVENIAN POWER SYSTEM, DOUBLE NPP KRŠKO – BERIČEVO LINE.....	81
TABLE 5-42 IDENTIFIED MCS FOR POWER DELIVERY TO THE NPP KRŠKO	82
TABLE 5-43 OBTAINED UNRELIABILITIES FOR CONFIGURATION WITH THE PROPORTIONALLY INCREASED LOAD ...	82
TABLE 5-44 BASIC EVENTS WITH THE LARGEST NRRW, NEW NPP AND SINGLE NPP KRŠKO – BERIČEVO LINE ADDED.....	83
TABLE 5-45 BASIC EVENTS WITH THE LARGEST NRAW, NEW NPP AND SINGLE NPP KRŠKO – BERIČEVO LINE ADDED.....	83
TABLE 5-46 OBTAINED UNRELIABILITIES FOR CONFIGURATION WITH THE PROPORTIONALLY INCREASED LOAD, DOUBLE NPP KRŠKO – BERIČEVO LINE.....	84
TABLE 5-47 IDENTIFIED MCS FOR THE POWER DELIVERY TO THE NPP KRŠKO	84
TABLE 5-48 OBTAINED UNRELIABILITY FOR INCREASED LOAD IN DIVAČA AND SINGLE NPP KRŠKO–BERIČEVO LINE ADDED.....	84
TABLE 5-49 OBTAINED RELIABILITY FOR INCREASED LOAD IN DIVAČA AND SINGLE NPP KRŠKO – BERIČEVO LINE ADDED.....	84

TABLE 5-50 OBTAINED UNRELIABILITIES FOR INCREASED LOAD IN DIVAČA AND DOUBLE NPP KRŠKO – BERIČEVO LINE ADDED.....	85
TABLE 5-51 SUMMARIZED RESULTS FOR THE SLOVENIAN POWER SYSTEM.....	86
TABLE 6-1 PLANT-LEVEL LOOP FREQUENCIES	89
TABLE 6-2 LOOP FREQUENCY COMPARISON WITH THE PREVIOUS REPORTS	89
TABLE 6-3 LOOP DURATION DATA ANALYSIS OF PROBABILITIES OF EXCEEDANCE	90
TABLE 6-4 LOOP DURATION COMPARISON	90
TABLE 6-5 EDG PARAMETERS.....	95
TABLE 6-6 EDG CCF UNAVAILABILITY	95
TABLE 6-7 EVENT TREES AND INITIATING EVENTS FOR SURRY UNIT 1 PSA	96
TABLE 6-8 SBO IE FREQUENCY.....	97
TABLE 6-9 COMPARISON OF THE RESULTS FOR DOMINANT ACCIDENT SEQUENCES BY IE TYPE.....	97
TABLE 6-10 DESCRIPTION OF THE INITIATING EVENTS	99
TABLE 6-11 THE IDENTIFIED IMPORTANT BE IN THE MODEL	100
TABLE 6-12 IDENTIFIED MCS FOR EMERGENCY AC POWER SYSTEM FAILURE.....	102
TABLE 6-13 BASIC EVENT DESCRIPTION	102
TABLE 6-14 SHARE OF EACH LOOP DATA CATEGORY INTO OVERALL LOOP.....	104
TABLE 6-15 DESCRIPTION OF THE POWER SYSTEM MODELS AND OBTAINED UNRELIABILITIES FOR IEEE RTS	105
TABLE 6-16 CDF AND LOOP FREQUENCY FOR IEEE RTS	105
TABLE 6-17 DESCRIPTION OF THE POWER SYSTEM MODELS AND OBTAINED UNRELIABILITIES FOR NPP KRŠKO .	107
TABLE 6-18 THE OBTAINED LOOP IE FOR THE NPP KRŠKO	107

List of Abbreviations

AC - Alternating Current
ASAI - Average Service Availability Index
ASIDI - Average System Interruption Duration Index
ASIFI - Average System Interruption Frequency Index
ATWS – Anticipated Transient Without Scram
BE – Basic Event
CAIDI - Customer Average Interruption Duration Index
CAIFI - Customer Average Interruption Frequency Index
CCF – Common Cause Failure
CDF - Core Damage Frequency
CEMIn - Customers Experiencing Multiple Interruptions
CEMSMIn - Customers Multiple Sustained Interruption and Momentary Interruption Events
CTAIDI - Customer Total Average Interruption Duration Index
DC - Direct Current
ECCS - Emergency Core Cooling System
EDG - Emergency Diesel Generators
EPS - Emergency Power Supply
ESWRL - Extremely Severe Weather Related Losses
ET – Event Tree
FT - Fault tree
FV - Fussell - Vesely Importance
GD - Grid Disturbances
HPIS - High Pressure Injection System
IE – Initiating Event
IEEE - Institute of Electrical and Electronics Engineers
LOCA – Loss of Coolant Accident
LOLP – Loss of Load Probability
LOOP - Loss of Offsite Power
MAIFI - Momentary Average Interruption Frequency Index
MAIFI_E - Momentary Average Interruption Event Frequency Index
MCS - Minimal Cut Set
NPP - Nuclear power plant
NRAW – Network Risk Achievement Worth
NRC - Nuclear regulatory commission
NRRW – Network Risk Reduction Worth
PCL - Plant Centered Losses
PSA - Probabilistic Safety Assessment
RAW - Risk Achievement Worth
RCS - Reactor Coolant System
RDF - Risk Decrease Factor
RIF - Risk Increase Factor
RRW - Risk Reduction Worth
RTS - Reliability Test System
RWST - Refueling Water Storage Tank
SAIDI - System Average Interruption Duration Index
SAIFI - System Average Interruption Frequency Index
SBO - Station Blackout
SGTR – Steam Generator Tube Rupture
SWRL - Severe Weather Related Losses

1 Introduction

Nuclear power plants are complex facilities, which produce electrical energy based on the principles of the nuclear fission. Nuclear fuel in the nuclear reactor is used to produce thermal energy in a form of hot steam, using steam turbines and generators being transformed into electrical energy. Structures, systems and components in nuclear power plants comply with the strict technical standards in order that the operation of the plant is safe and effective.

The prime purpose of the nuclear safety is prevention of the release of radioactive materials formed in the fuel, ensuring that the operation of nuclear power plants does not contribute significantly to individual and societal health risk. The main specific issue of the nuclear safety is the need for removing the decay heat, which is necessary even for a reactor in shutdown.

Nuclear safety is achieved by implementation of a set of measures and actions including multiple barriers integrity approach, defense-in-depth and safety principles^{1,2}.

The multiple barriers integrity is sustained with the provision of effective cooling of the fuel in all modes of operation of the nuclear power plant, inside and outside of the core. The barriers include material of fuel pellets themselves, the cladding of the fuel rods, the integrity of reactor coolant system and the containment, which capture the radioactive substances even if the other barriers fail.

The measures constituting the three-level defense-in-depth approach have to be taken in order to ensure that the facilities are operated and the activities are conducted so as to achieve the highest standards of safety that can reasonably be achieved:

- The prevention level is related to control the radiation exposure of people and the release of radioactive material to the environment with the appropriate design, construction, installation and supervision of the nuclear power plant.
- The protection level is related to restriction of the likelihood of undesired events with the installation of protection and safety systems, which put the plant into a safer state if predefined safety limits are exceeded.
- The mitigation level supplements the first two in sense that it relates to the activities, which mitigate the consequences of undesired events, if they occur.

The safety principles such as redundancy (the use of more components or systems than minimally necessary for realization of the function), independence, diversity, fail-safe principle (means that the component is put to a safer state, if it has failed) and single failure criterion (means that failure of the single component can not endanger the fulfillment of any safety function) are listed and explained in more details in Appendix A.

The nuclear power plant is equipped with the continuous and reliable source of electrical energy in order to sustain the effective cooling of the fuel. In normal operation, the preferred source of electrical energy for self consumption is alternating current [AC] electrical energy from the generator bus through unit transformers. During the startup, shutdown or maintenance of the nuclear power plant (NPP), the offsite power system is the preferred source of electrical energy. The self consumption of the NPP depends on several factors including the design of the plant, selection of cooling system for residual heat and is normally in the range of 5-10% of the net installed power of the plant (electrical). In case of power system failure, the generator is disconnected from power system and the output power of turbine-generator is throttled down in order nuclear power plant to continue to provide energy for its own consumption. If throttle down of the power is unsuccessful, there are backup diesel generators, which provide energy until normal conditions in the power system are restored.

In case of the NPP Krško, the normal power supply to the plant auxiliaries is from the generator bus through two unit transformers. The offsite power supplies are from two Electric Power Distribution Systems: a 400 kV and a 110 kV transmission network. The 400 kV

switchyard have standard two bus configuration with the three transmission terminals. Two of the 400 kV lines are coming from Zagreb and one from Maribor, each capable of transmitting the full plant electric power. The 110 kV transmission line is connected to combined gas-steam power plant Brestanica, which serves as the alternate preferred source. The onsite emergency power sources are two diesel electric generators. In the event of a breakdown of the 110kV system, Brestanica automatically cut-off all users except NPP Krško (island operation mode).

The onsite power system of NPP Krško consists of two distinct subsystems:

- Non-Class 1E Power System.
- Class 1E Power System (Engineered Safety Features Power System).

The onsite emergency power sources are two diesel electric generators connected to Class 1E Power System.

The NPP safety and reliability depends partly on the network reliability and vice versa. The failure of the power system results in a loss of offsite power initiating event, which is important contributor to the overall core damage frequency (CDF), is a measure of risk and thus safety of the corresponding NPP. The disconnection of the NPP from the power system results in the deficit of generation directly affecting the reliability and stability of the power system. This interaction between NPP from one side and power system from the other is in the main focus of this thesis.

1.1 Objectives and goals

The offsite power system of a nuclear power plant provides the preferred source of electrical power to station equipment³ during the normal operation:

- Emergency cooling for the reactor following planned or unplanned shutdowns.
- Auxiliary systems for plant startup and safe shutdown.

The loss of offsite power (LOOP) initiating event (IE) occurs when all electrical power to the plant from external sources is lost. That event results in simultaneous loss of electrical power to all unit safety buses, requiring the emergency diesel generators to start and supply power to the safety buses for the equipment, which is essential for safe operation of the plant⁴. A total loss of all AC power as a result of complete failure of both offsite and onsite AC power sources is referred to as a “station blackout” (SBO).

Risk analyses performed for NPP indicate that the LOOP can be a significant contributor to the plant risk, contributing more than 70 percent of the overall risk at some plants. Normally, the plant risk due to LOOP is in the range of 20 to 30 percents^{5,6}. Therefore, the loss of offsite power (LOOP) and its subsequent restoration are important inputs to the plant risk models. These inputs must reflect current industry performance in order that the plant risk models accurately estimate the risk associated with the LOOP.

One particularly important subset of LOOP initiated scenarios involves SBO situations, in which the affected plant must achieve safe shutdown, relying on components that do not require AC power, such as turbine or diesel-driven pumps. Thus, the reliability of such components, the direct current (DC) battery depletion times, and the characteristics of offsite power restoration are important contributors to SBO risk.

The NPP must have the capability to withstand a SBO and to maintain the core cooling for a specified duration taking into account the regulatory requirements and guides^{7,8,9}, e.g. SBO rule¹⁰.

On August 14, 2003, a widespread loss of the USA electrical power grid (blackout) resulted in LOOP at nine commercial NPP (in period of time less of two minutes) in the U.S., as well as eleven in Canada¹¹. Major contributors to the domino effect that resulted in plant after plant tripping off-line resulting with the collapse of the electrical grid were: poor maintenance of transmission lines, lack of sensor and relay repair, poor communications between load

dispatchers and power plant operators and a lack of understanding of transmission system interdependencies resulting with the overload of lines.

As a result of the 2003 blackout, the Nuclear Regulatory Commission (NRC) initiated a comprehensive program to review grid stability and offsite power issues as they relate to NPP^{8, 12}.

The Forsmark-1 NPP on 25th of July 2006 experienced a SBO event¹³. The cause was shown to be a failure in the 400 kV switchyard of the NPP. Two of the four auxiliary diesel generators failed to start resulting with the lost of power on two of four Class 1E redundant trains. This caused a coastdown of recirculation pumps, shutdown of the turbines and eventually reactor scram. After 23 minutes the operators managed to start the failed generators manually, but this event clearly indicate the impact of LOOP on NPP safety.

The NRC study on effects of deregulation and changes in grid operation to nuclear power plant performance clearly re-enforces the need to understand the conditions of the grid throughout the year to assure that the risk due to potential grid conditions remains acceptable¹⁴. Evermore the NRC risk-informed regulatory strategy¹⁵ depends on plants having access to reliable offsite power. For each light-water-cooled nuclear power plant operating license application⁸ submitted after September 27, 2007, in its final safety analysis report the applicant shall submit information for:

- The redundancy of the onsite emergency ac power sources.
- The reliability of the onsite emergency ac power sources.
- The expected frequency of loss of offsite power.
- The probable time needed to restore offsite power.

Two of the issues that are of particular concern for new reactors include:

- Should new units be designed to withstand a load rejection without shutting down.
- What is the impact of bringing large generators onto the grid.

Taking into account the new environment after 11th of September and threats on major infrastructures including the power systems, the need for more detailed analysis of power system reliability come forward¹⁶.

Data analysis⁶ from year 1986 through year 2004 reveals that SBO risk was low when evaluated on an average annual basis due to the plant modifications in response to the SBO rule. However, when focus is on grid-related LOOP events, the SBO risk has increased. Current results⁶ show that the grid initiated LOOP events contribute 52 percent to the SBO core damage frequency (CDF). Severe and extreme weather events, which are generally related to grid events, contribute another 13 percent. The increasing number of grid-related LOOP events in years 2003 and 2004 is a cause of concern. Additionally, if only data⁶ from the “summer” period is considered, the LOOP increases by approximately a factor of two.

By NRC methodology, there are three major LOOP event categories: plant centered, grid related, and weather related. Grid related LOOP events are defined as LOOP that are strictly associated with the loss of the transmission and distribution system due to insufficient generating capacity, excessive loads or dynamic instability. Although the grid failure may also be caused by other factors, such as severe weather conditions, these events are not considered grid related by the NRC since they are caused by external events.

In the methodology and guidance documents issued by NRC, grid disturbances are estimated from the site susceptibility to grid related LOOP^{17,18}. Based on the expected frequency, plant is classified in specific group for which predetermined frequency is given. Severe weather related losses are estimated using simple relation, which includes site vulnerability to effects of salt spray, snowfall, tornadoes, storms and a number of transmission lines connected to the plant.

The proposed NRC methodology has two major deficiencies:

1. Estimation of the grid-related LOOP is based only on a historical data for the site susceptibility to grid related LOOP, not accounting the overall grid structure and the analytical methodology to estimate the corresponding frequency. The proposed NRC approach does not provide qualitative and quantitative identification of major contributors to grid related LOOP and consequent actions to decrease the frequency, thus improving the plant reliability and safety.

2. Grid related and severe weather initiated LOOP are closely related¹⁹, but that correlation is not included in the NRC methodology. In the estimation of the severe weather related losses, the ambient temperature, which has direct impact on the overall power system reliability⁸, is excluded from calculations.

Enlisted deficiencies in current methodologies indicate necessity for development of the new method for estimation of the LOOP initiating events and detail analysis of the impact that power system state has on the performance and risk of the nuclear power plants.

The main objective of the thesis is development of a method, which can be used to assess and improve the safety of the nuclear power plants, which operate in power system using the methods, tools and models known from probabilistic safety assessment^{20,21,22,23,24,25,26}. The method is developed combining linear network flow method with the fault tree analysis features, and computer program based on this method is compiled.

Proposed method is applied to a test system used in bulk power system reliability evaluation studies²⁷ and model of the Slovenian power system. Analysis of LOOP IE frequency and resulting core damage frequency of NPP in test systems is done.

1.2 The outline

Section 2 reviews main activities in area of power system analysis together with the current state of art in the field. Description of the methods used in the Probabilistic Safety Analysis together with the applications of probability theory to the power systems reliability estimation is given in section 3. In section 4, detail description of the developed method is given. In sections 5 the obtained results for the IEEE (Institute of Electrical and Electronics Engineers) test system and Slovenian power system are given. In section 6 the obtained results from the sensitivity analysis of the LOOP IE and CDF of the reference plant are presented. Final conclusions and remarks are given in section 7.

2 Review of activities of power system analysis

The review of main activities in the area of power system analysis is presented together with the state of the art in the field.

The power systems are usually large, complex and, in many ways, nonlinear systems. The power systems include multiple components such as generators, switching substations, power lines and loads. The post-fault phenomena in a power system are dynamic in nature and dependent on the grid connection and load flows in different parts of the grid. Therefore, the evaluation of the overall system reliability is extremely complex as it is necessary to include detailed modelling of both generation and transmission facilities and their auxiliary elements.

The power system is usually divided into segments, which can be analyzed separately²⁸. These segments are referred to as generation, transmission and distribution functional zones. These functional zones can be combined to form a series of hierarchical levels for the purpose of conducting system reliability analysis. Hierarchical Level I reliability assessment concerns only the generation facilities. Evaluation of the composite or bulk generation and transmission facilities is designated as Hierarchical Level II study. The entire system evaluation is designated as Hierarchical Level III assessment, as shown on Figure 2-1. System reliability is usually predicted using one or more indices, which quantify expected system reliability performance, implemented using the criteria based on acceptable values of these indices.

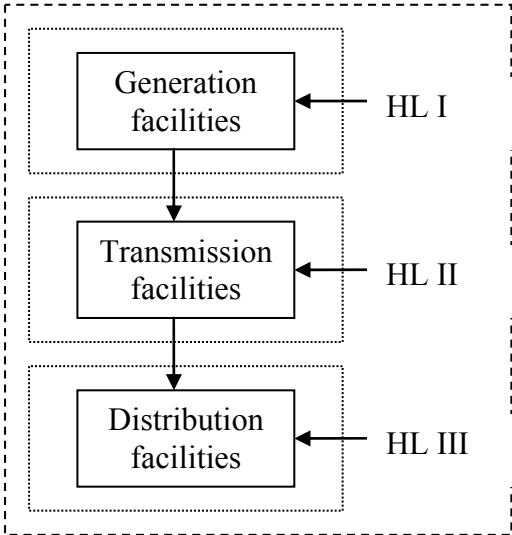


Figure 2-1 Hierarchical levels in electrical power systems

The overall problem of Hierarchical Level III reliability evaluation can be quite complex in most systems as it involves starting at the generating points and terminating at the individual load points.

The application of probability methods in power systems came into prominence only in the last three decades considering that the industry itself is more than a century old and that discussions on probability concepts appeared in Italian manuscripts seven centuries ago²⁹.

Most of the approaches for determination of power system reliability use certain approximation or simplification of the problem in order to degrade the problem to a solvable level. Quasi-transient approach³⁰ and examination of cascading failure using linear programming³¹ were proposed assuming only single component failure and identification of only one critical point in system, not accounting for the probability of failure of components. Evaluation of system reliability concerning only the generation facilities and their adequacy to

satisfy load using heuristic methodologies was proposed. This methodology, as other HL I reliability assessments, exclude transmission from analysis^{32,33}.

The minimal cut set and frequency duration method are used for the planning and design of industrial and commercial electric power distribution systems and their reliability evaluation, but this method is applicable only to small distribution systems³⁴. Screening method for the identification and ranking of infrastructure vulnerabilities, including small power system, due to terrorism based on minimal cut set approach was proposed, but the whole analysis is conditional on the assumed presence of a minor threat³⁵. Event tree method was proposed for the analysis of infrastructures risk from terrorism with the example application on a small power system, but the method lacks of conditional success rate for a network failure, which is estimated by authors and not by a strict method³⁶. An application of Monte Carlo network analysis for reliability assessment of multiple infrastructures, including power system, for terrorist actions³⁷ is proposed, but this method is inadequate when infrastructures are analyzed individually.

Application of the sum-of-disjoint products technique for evaluating stochastic network reliability is proposed³⁸, considering only one path between source and sink nodes and assuming that each node is perfectly reliable.

Hybrid model that includes both power system dynamic simulations and event trees for the protection was anticipated for power system reliability estimation, accounting only failure of lines protection³⁹.

Several variations of Monte Carlo simulation methods including cellular automata and system state transition sampling approach were developed to probabilistically evaluate composite power system long-term reliability^{40,41,42,43,44,45,46}. Deficiency of these methods is that they can only be used for Hierarchical Level II study and convergence problem that they encompass.

Recent probabilistic method for transmission grid security evaluation uses event trees and fault trees and combines them with the power system dynamic simulations. Only substation protection and trip operations after line faults are modeled with the event trees. Power system security is studied with a substation model that would include possible malfunctions of the protection and circuit breakers. Only single faults of lines, as result of the protection failure, were accounted in the analysis^{47,48}.

Review of the activities in the area of PSA and power system analysis indicate that these two methodologies haven't been integrated in formal matter as it was done in this thesis, thus providing solution to problems foreseen in the both areas.

3 Probabilistic Safety Assessment

The report⁴⁹ entitled "Reactor Safety Study: An Assessment of Accident Risk in U.S. Commercial Nuclear Power Plants"- WASH 1400 was the first detailed analysis to provide a realistic assessment of the risks associated with the utilization of commercial NPP. A systematic probabilistic method for assessment of reliability and safety of complex systems was developed and applied. In most countries, the method is referred to as Probabilistic Safety Assessment (PSA). In the United States, the method is referred to as Probabilistic Risk Analysis (PRA). The event tree and the fault tree are two basic methods used in Probabilistic Safety Assessment, which is a standardized method for assessment of nuclear power plant safety^{50,51}.

There are number of techniques used to perform system modelling. These techniques are grouped into two major categories, inductive and deductive techniques.

Inductive analysis begins with the consideration of specific event and goes on to consider the general effect of that specific event in terms of system operability. Event tree analysis is an inductive technique, which organizes and characterizes potential accidents in a methodological manner⁵². It is suitable for modelling the complex sequences of events and for their efficient evaluation.

In system modelling, a deductive analysis is one that begins with a general system operability state and proceeds to deduce the specific events that could give rise to that operability state. Fault tree analysis is the deductive modelling approach used in the PSA to identify and assess the combinations of the undesired events in the context of the system operation and its environment that can lead to the undesired state of the system^{53, 54}. The undesired state of the system is represented by a top event. The logical gates integrate the primary events to the top event. The primary events are the events, which are not further developed, e.g. the basic events and the house events. The fault tree is based on Boolean algebra and probabilistic basis that relates probability calculations to Boolean logic functions.

3.1 Probabilistic Safety Assessment Fundamentals

The basic definitions and relations of the probability theory are presented in this section.

The PSA purports to assess risk. In the context of PSA, the concept of risk can be defined^{55, 58, 84} as "the likelihood of experiencing a defined set of undesired consequences".

The assessment of risk with the respect to nuclear power plants is intended to achieve four general objectives:

- To identify initiating events and event sequences, which are significant contributor to risk.
- To provide a realistic quantitative measure of the likelihood of these risk contributors.
- To provide a realistic evaluation of the potential consequences associated with the hypothetical accident sequences.
- To provide a reasonable risk-based framework for making decisions regarding nuclear plant design, operation and sitting.

The probability defines quantitatively the likelihood of an event or events. In the context of PSA the concept of probability is thought of in three ways, each with its own applications.

In the classical concept, the probability of occurrence of event A is defined as:

$$P(A) = \frac{N_A}{N} \quad (3.1)$$

Where:

N_A – Number of occurrences of the event A.

N - Mutually exclusive and equally likely random experiments.

The empirical (frequentist) concept is the second approach with the relative frequency interpretation of the probability:

$$P(A) = \lim_{n \rightarrow \infty} \frac{N_A}{N} \quad (3.2)$$

Where:

N_A – Number of occurrences of the event A.

N – Mutually exclusive and equally likely random experiments.

n – Number of experiments.

The third definition of probability is the subjective concept and really represents the degree of belief that a given event may occur.

Availability is the measure used for continuously operated systems that can tolerate failures, and is defined⁵⁵ as the probability of the component/device/system to be available when required.

Component unavailability is defined⁵⁵ in general as the probability of being in a failed state when required. The point unavailability is the probability that the component is down at the time. Interval unavailability is associated with the some interval and is the fraction of time that the component is down (ratio of downtime to some cycle time).

The unavailability is denoted with the symbol Q and standard forms are:

$$Q = \lambda t \quad (3.3)$$

Where:

λ – Component failure rate.

t – Average fault duration time (detection plus repair time).

Or:

$$Q = \frac{t_D}{t_T} \quad (3.4)$$

Where:

t_D – Average downtime.

t_T – Total cycle time.

The Eq. (3.3) is of the point type and Eq. (3.4) is of the interval type.

The failure probability is defined in general as the probability of failure in specified time interval (required operation time, mission time or standby time). The failure probability is also called the unreliability (one minus the reliability). The failure probability is denoted with U and for non-repairable component (component failure rate λ is constant) have form:

$$U = 1 - e^{-\lambda t} \cong \lambda t \quad (3.5)$$

It's notified that in the PSA terminology⁵⁵ the standard denotation for the unreliability is with the letter "P". The unreliability is denoted with U in order not to mismatch with the probability.

The approximation in the Eq. (3.5) is accurate to within 5% for unreliability U less than 0.1; it is on the conservative side and is small compared to uncertainties in λ .

Comparison of the Eqs. (3.3) and (3.5) show that they are identical but only in case of constant λ and small probabilities. For this specific case the component/system unreliability is equal to its unavailability.

The simplified description of reliability defines it as a probability⁵⁶ that an item can perform its intended function for a specified interval under stated conditions. Reliability as a measure is suitable for quantifying the adequacy of mission oriented systems (systems functioning without failure).

There are probability rules, which permit to combine of the probabilities associated with the individual events, to give the probability of overall system behavior. These rules with their description are given.

Rule 1 – Independent events.

Two events are said to be independent if the occurrence of one event does not affect the probability of the occurrence of the other event.

Rule 2 – Mutually exclusive events

Two events are said to be mutually exclusive (or disjoint) if they cannot happen at the same time.

Rule 3 – Complementary events.

Two outcomes of an event are said to be complementary if, when one outcome doesn't occur, the other must. If the two outcomes A and B have probabilities P(A) and P(B), then:

$$P(A) + P(B) = 1 \quad (3.6)$$

Rule 4 – Conditional events.

Conditional events are events that occur conditionally on the occurrence of another event or events. The conditional probability of event A occurring given that event B has occurred is described mathematically as P(A|B) and can be deduced from Eq. (3.4):

$$P(A|B) = \frac{\text{number of ways A and B can occur}}{\text{number of ways B can occur}} \quad (3.7)$$

Rule 5 – Simultaneous occurrence of events.

The simultaneous occurrence of two events A and B is the occurrence of both A and B event. Mathematically is known as the intersection of the two events and is represented as: (A∩B), (A AND B) or (AB). In this rule there are two cases to consider: when events are independent or when they are dependent.

If two events are independent the probability that they both occur is:

$$P(A \cap B) = P(A) \cdot P(B) \quad (3.8)$$

If there are n independent events, the principle can be extending to give:

$$P(A_1 \cap A_2 \cap A_3 \cap \dots \cap A_n) = P(A_1) \cdot P(A_2) \cdot \dots \cdot P(A_n) \quad (3.9)$$

In case of dependent events, the probability of occurrence of both events will be:

$$\begin{aligned} P(A \cap B) &= P(B|A) \cdot P(A) \\ &= P(A|B) \cdot P(B) \end{aligned} \quad (3.10)$$

Rule 6 – Occurrence of at least one of two events.

The occurrence of at least one of two events A and B is the occurrence of A or B or both events and is expressed as: (A ∪ B), (A OR B) or (A+B). In this rule there are three cases to consider: the events are independent but not mutually exclusive, the events are independent and mutually exclusive and third case when events are not independent.

The probability of occurrence of at least one of the events that are independent but not mutually exclusive is given by expression:

$$P(A \cup B) = P(A) + P(B) - P(A) \cdot P(B) \quad (3.11)$$

In case of mutually exclusive events by definition the probability of their simultaneous occurrence P(A)P(B) must be zero, therefore probability of the union of the two events will be:

$$P(A \cup B) = P(A) + P(B) \quad (3.12)$$

If there are n independent and mutually exclusive events, the union probability will be:

$$P(A_1 \cup A_2 \cup A_3 \dots \cup A_n) = \sum_{i=1}^n P(A_i) \quad (3.13)$$

If the two events A and B are not independent the probability of the union of the events will be:

$$\begin{aligned}
P(A \cup B) &= P(A) + P(B) - P(A \cap B) \\
&= P(A) + P(B) - P(B | A) \cdot P(A) \\
&= P(A) + P(B) - P(A | B) \cdot P(B)
\end{aligned} \tag{3.14}$$

Rule 7 – Application of conditional probability.

The probability of occurrence of an event A dependent upon a number of mutually exclusive events B_i is calculated as:

$$P(A) = \sum_{i=1}^n P(A | B_i) \cdot P(B_i) \tag{3.15}$$

The parameters that are associated with the reliability evaluation are described by probability distributions. Two main types of distributions are discrete and continuous. Discrete distributions represent random variables that can assume only certain discrete values whereas continuous distributions represent random variables that can assume an infinite number of values within a finite range. The two most important discrete distributions are the binomial and Poisson distribution and continuous distributions include the normal (or Gaussian), exponential, Weibull, gamma and Rayleigh distribution.

All random variables (discrete and continuous) have a cumulative distribution function. It is a function giving the probability that the random variable X is less than or equal to x, for every value x. The cumulative distribution function F(x) formally is defined as:

$$F(x) = P(X \leq x) \tag{3.16}$$

$$-\infty < x < \infty$$

The cumulative distribution function for a discrete random variable is found by summing up the probabilities and for a continuous random variable as integral of its probability density function.

The probability density function of a continuous random variable is a function, which can be integrated to obtain the probability, that the random variable takes a value in a given interval. More formally, the probability density function, f(x), of a continuous random variable X is the derivative of the cumulative distribution function F(x):

$$f(x) = \frac{dF(x)}{dx} \tag{3.17}$$

The probability density function f(x) can be formulated, accounting the definition of the cumulative distribution function F(x) given by Eq. (3.16), as:

$$\int_a^b f(x)dx = F(b) - F(a) = P(a \leq x \leq b) \tag{3.18}$$

The cumulative distribution function, as shown by Eq. (3.16), increases from zero to unity as the random variable increases. The random variable in reliability evaluation is frequently time. The cumulative distribution function in reliability terminology is known as the cumulative failure distribution function or unreliability. The complementary the cumulative failure distribution is the survivor function also referred as reliability, designated as R(t):

$$R(t) = 1 - U(t) \tag{3.19}$$

The failure density function f(t) is defined as derivate of the cumulative failure distribution function U(t):

$$f(t) = \frac{dU(t)}{dt} = -\frac{dR(t)}{dt} \tag{3.20}$$

The failure rate is one of the most extensively used functions in reliability evaluation, designated as $\lambda(t)$ and referred as hazard rate or force of mortality. The mathematical description of the failure rate is:

$$\lambda(t) = \frac{\text{number_of_failures_per_unit_time}}{\text{number_of_components_exposed_to_failure}} \quad (3.21)$$

The general expression for the failure rate $\lambda(t)$ at time t is:

$$\lambda(t) = -\frac{1}{R(t)} \cdot \frac{dR(t)}{dt} = \frac{f(t)}{R(t)} \quad (3.22)$$

The relation between survivor function (reliability) $R(t)$ and failure rate $\lambda(t)$, from Eq. (3.22), can be expressed as:

$$R(t) = \exp\left[-\int_0^t \lambda(t)dt\right] \quad (3.23)$$

In case of constant and time independent failure rate λ Eq. (3.23) transforms into exponential distribution:

$$R(t) = e^{-\lambda t} \quad (3.24)$$

Using the Eq. (3.24) equation (3.5) is obtained.

Input data for the initiating events and component failures is necessary in order to realize quantitative PSA. The development of a data base for accident sequence quantification involves the collection and analysis of data and the evaluation of the appropriate reliability models. Uncertainty analysis is performed in order to measure the accuracy of the quantitative results in PSA⁵⁷. There are two sources of uncertainty in the data base for component and system failure: natural variability of failure rates and imperfect knowledge of the actual behavior. The uncertainty in the PSA additionally includes the incomplete analysis, incorrectness of the models and sequence quantification. The primary methods for treating uncertainty in PSA are bounding analysis and sensitivity analysis.

The PSA is generally divided into three broad areas: system modeling, accident process analysis and accident consequence analysis. The activities that comprise a risk assessment are given on Figure 3-1.

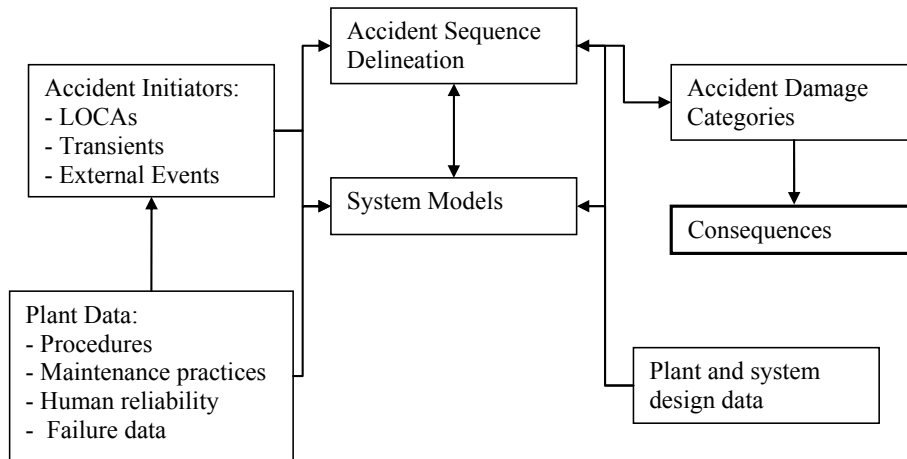


Figure 3-1 Activities in PSA

The system modeling is the basic element of Level 1 PSA. There are different system modeling techniques and two of them are used exclusively and comprehensively in PSA: event tree analysis and fault tree analysis. Detail description of both techniques is given in the following sections.

Formal definition⁵³ of a system defines it as: "A deterministic entity comprising an interacting collection of discrete elements". The plant damage states identified in the system modeling task are used as the starting point for accident process analysis (Level 2 PSA). The accident process analysis assesses the reactor core behavior and containment response under

accident conditions. The outcome of the accident process analysis is the identification of potential releases to the environment in terms of their energies, magnitudes and timing. The accident consequence analysis (Level 3 PSA), using local weather data, the probable radiological dispersion and depletion mechanisms, develops estimates of population radiological doses and environmental contamination.

3.2 PSA Modeling

The first step in a PSA, as shown on Figure 3-1, is the identification of potential accident initiators. Accident initiators, also known as initiating events (IE) are undesired events, which present a challenge to the plant, in that if they are not successfully responded to, core damage may result. Initiating events are typically divided into two broad groups: transients and loss-of-coolant accidents (LOCA). These groups are then subdivided in terms of the systems required to respond to the initiator. The subdivision of the LOCAs depends upon the size and location of the break. The accident initiators are grouped on basis of systems required to respond to the initiating event in order to decrease their number on feasible level. Data on the frequency of initiating events is generally obtained from several sources and the largest body of that data is generic.

3.2.1 Event Tree Analysis

Event tree analysis is the technique⁵⁸ used to define potential accident sequences associated with a particular initiating event or set of initiating events. The event tree model describes the logical interrelationships between potential system successes and failures as they respond to the initiating event.

The general tasks included in the process of development of event trees are given on Figure 3-2.

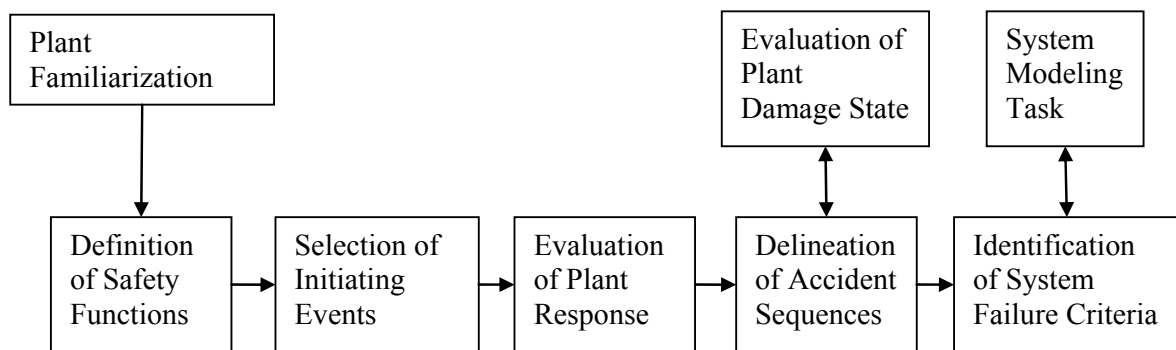


Figure 3-2 Event tree development process

The purpose of first task, plant familiarization, is to provide information necessary for the identification of initiating events, the identification of the success criteria for systems that must directly perform the required safety functions and the identification of the dependences between the frontline system and the support systems, which they require for proper functioning.

The functions that must be performed to control the sources of energy in the plant and the radiation hazards are called safety functions. Safety functions are defined by a group of actions that prevent core melting, prevent containment failure or minimize radionuclide releases and they are identified in second step of the event tree development process. Definition of the necessary safety functions forms the preliminary basis for grouping accident initiating events.

A comprehensive list of initiating events is necessary to select and compile during third step of the development of ET in order to make certain that the event trees include all potentially significant accident sequences. The selection of initiating events consists of two steps:

- Definition of possible events.
- Grouping of identified IE's by the safety function to be performed or combinations of systems responses.

Once IE's have been identified and grouped, it's necessary to determine the response of the plant to each IE group. Two distinct methods exist for evaluation of plant response: functional and systemic event trees. The functional event tree is an intermediate analytical step for sorting out the complex relationship between accident initiators and system responses. The systemic event tree explicitly defines the response of key plant systems using detailed event sequence analysis.

The description of accident sequences is accomplished by developing detailed system event trees developed from either functional event trees or event sequence diagrams. The event trees developed from functional event trees are quantified using the method of fault tree linking, whereas event trees developed from sequence diagrams are quantified using event trees with the boundary conditions. The accident sequence delineation is the most important step in event tree development process.

Each heading in the system event trees is quantified using detailed system models in order to determine the likelihood of system failure. The system models for event tree headings require predefined failure criteria based on the success criteria defined for each event tree heading and correlation with the previous failures in the accident sequence (previous failures in the accident sequence may result with the system unavailability or necessity of different system components operation in order to accomplish successful operation).

A sample event tree from corresponding reference⁵⁸ is presented on Figure 3-3 to illustrate event tree construction process. The example used is a LOCA IE associated with a simple imaginary reactor system.

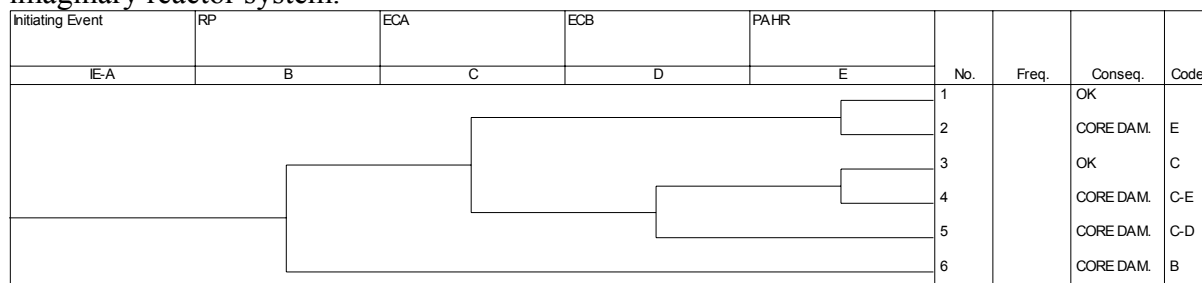


Figure 3-3 Example event tree

The various event possibilities or the systems that need to function to mitigate the consequences of the accident are listed on the top of the event tree and they include:

- The initiating event IE-A, assumed to be pipe break in the primary coolant system of reactor.
- RP, operation of the reactor protection system to shut down the reactor.
- ECA, injection of emergency coolant by pump A.
- ECB, injection of emergency coolant by pump B.
- PAHR, post-accident decay heat removal.

The placement of the events across the tree is based upon the time sequence in which they occur or some logical order, reflecting operational interdependence. Consequently the initiating event IE-A is first and PAHR is shown as the last event on the tree.

The various sequences are represented by the paths developed with the success (upward path) or failure (downward path) of the events. The far right column of the tree identifies the sequences, for example second sequence is the sequence that starts with the initiating event IE-A and ending with the failure of PAHR function E. For this example event tree it is

assumed that either emergency coolant pump A or B is sufficient the emergency coolant requirement. In the column consequences is the final consequence for each accident sequence identified in the event tree. On Figure 3-3 two consequences are identified: core damage and no core damage (OK consequence). Accident sequence can result with the new initiating event (e.g. seal LOCA or anticipated transient without scram), and they are analyzed in separate event tree. The core damage criterion is developed using design basis approach and typical value⁵⁹ for Westinghouse-type PWR is that hottest core fuel/clad node temperature does not exceed 650°C. Exception is allowed when core is reflooded before significant cladding oxidation has occurred, but time above 650°C is limited to 30 minutes and highest temperature may never exceed 1075°C.

The total number of possible sequences in the sample problem is 16, which are reduced to four core damage sequences (eliminating⁶⁰ branches that have zero conditional probability for at least one event). For example, all sequences on Figure 3-3 with the failed reactor protection system RP will result with the core damage. The sequences resulting with the core damage are evaluated further using containment event tree whereby the failure modes of the various barriers, which prevent the release of the radioactivity to the environment are probabilistically evaluated.

The elements to be considered for the accident sequence quantification process are the initiating event, the event tree resulting from the initiating event, the system fault trees and their resulting Boolean failure equations, and the containment failure modes possible for each combination of IE and safety system failures and successes. The event tree sequence is a particular combination of safety system failures and successes for a given initiating event and it doesn't include a containment failure mode.

The event tree sequence quantification process consists of the following steps:

- For each sequence, reduce by Boolean algebra the system failure and success equations to obtain the sequence reduced Boolean equation (the sequence cut sets).
- Quantify the component faults and outages in each cut set, accomplished on system level.
- Assess recovery at the sequence level.
- Assess human errors.
- Quantify the cut sets of the sequence failure equations.

A major portion of the quantification process is involved with the obtaining the Boolean equations for each event tree sequence. They are obtained by Boolean reduction of the Boolean failure and success equations for the systems that fail and succeed on each event tree path in order to account common components that must be Boolean reduced.

An example is used to illustrate the requirement of consideration of system successes as well as failures during event tree sequences quantification. On Figure 3-4 are given fault trees for two hypothetical systems A and B. Two faults result in system failure for each of these systems with the fault C1 appearing in both systems. A portion of the event tree involving these two systems is given on bottom of the Figure 3-4, with the sequence 1 when both systems fail and sequence 2 when system B fails while system A succeeds.

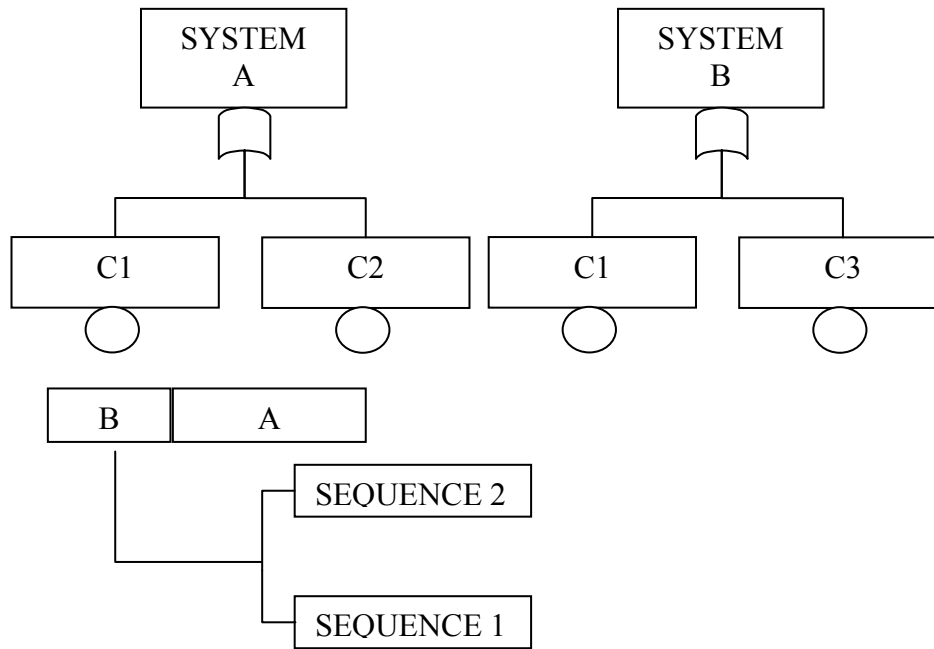


Figure 3-4 Systems A and B fault trees and part of the event tree sequence

The Boolean equation for sequence 1 is:

$$Q_1 = A \cdot B = (C1 + C2) \cdot (C1 + C3) = C1 + C2 \cdot C3 \quad (3.25)$$

The Eq. (3.25) clearly indicate that it's not correct to simply multiply the failure probabilities of systems A and B, because the common term, C1, would appear twice. The sequence equation correctly states that both systems fail if C1 occurs or if C2 and C3 occur.

The Boolean equation for sequence 2 is:

$$Q_2 = \bar{A} \cdot B = \overline{(C1 + C2)} \cdot (C1 + C3) = \bar{C1} \cdot \bar{C2} \cdot C3 \cong C3 \quad (3.26)$$

The last term in Eq. (3.26) is approximation obtained if the success terms are ignored. The Eq. (3.26) correctly states that the only way for system B failure and system A to succeed is for C3 to occur. If C1 were to occur, both A and B would fail, which is contrary to the system success/failure combination implied by sequence 2.

Thus, the Boolean-reduced equations for event tree sequences must be quantified in order to correctly account for common components among systems.

The quantification of the accident sequences requires incorporation of the frequency of the initiating event. For small event/large fault tree method, the initiating event is a simple multiplier to each sequence on the event tree. Using the fault tree event tree linking approach the accident sequences in the event trees are expressed as:

$$F_{ASj} = F_{IE} \sum_{i=1}^n Q_{MCSi} \quad (3.27)$$

Where:

F_{ASj} - Accident sequence frequency for ASj.

F_{IE} - Initiating event frequency.

n - Number of minimal cut sets.

Q_{MCSi} - Probability of i-th minimal cut set.

The sequence quantification proceeds in two stages. In first stage accident sequence frequencies are calculated without accounting post-accident corrections and using screening

values for human error probabilities. The results of this calculation are used to generate the list of important human errors analyzed further during human performance subtask. In second stage recovery of misposition or actual faults on a cutset-specific basis is accounted.

In order to make sequences quantification practical, it may be necessary to truncate considering only those cutsets whose probability is above some cutoff or number of events in cutset is smaller than truncation limit called truncation value. Truncation is approximation with the generally uncontrolled consequences on the results⁷¹.

After plant-specific human error probabilities have been derived, the sequences can be requantified using these values. The final results are obtained by applying appropriate multiplicative factors to each cutset probability, in order to include the possibility that operator action will eliminate one of the faults in the cutset, and thereby prevent core damage. The uncertainty evaluation is performed using the plant-specific gamma posteriors for the initiating event frequencies and the component failure rates together with the error ranges identified for human error rates and recovery probabilities, and following results are obtained:

- Overall core damage frequency.
- The frequency of each bin.
- The frequency of accident sequences contributing the top 99% of total core damage frequency.

The purpose of the importance evaluations is to identify the important accident sequences, system failures, component failures and human errors with the regard to core damage frequency. The purpose of the sensitivity analysis is to determine how sensitive the core damage frequency is to possible dependencies among component failures and human errors and to address those assumptions suspected of having a potential significant impact on the results.

The final summarized products resulting from accident sequence quantification and event tree analysis are:

- Minimal cut sets for systems involved in the sequence.
- Binning of all accident sequences on the basis of accident sequence characteristics.
- Point estimates for the dominant accident sequences.
- Estimate of the core damage frequency, which is an expression of the likelihood that, given the way a reactor is designed and operated, an accident could cause the fuel in the reactor to be damaged.
- Plant-specific error bounds on frequencies of dominant accident sequences and on the core-damage frequency.
- Importance measures for accident sequences, systems, cut sets and components.
- Sensitivity studies showing effects of dependences and human errors.
- Engineering insights into systems, components and procedures that most affect risk.

3.2.2 Fault tree analysis

Fault tree analysis is the tool used to evaluate the ways in which nuclear plant systems might fail to perform their intended functions.

The standard definition^{53, 54} of the fault tree technique defines it as: “An analytical technique, whereby an undesired state of a system is specified (usually a state that is critical from a safety standpoint), and the system is then analyzed in the context of its environment and operation to find all credible ways in which the undesired event can occur”. If fault tree analysis is the technique by which system fault trees are developed, a workable definition of a fault tree might be: “a graphical depiction of the logical interrelationship between postulated fault events as they contribute to the occurrence of the top event”.

Fault tree analysis is a deductive technique in that it goes from effect to cause. Fault tree analysis begins with a hypothetical undesired state of the system, the top event, and

deductively identifies the credible events and combinations of the events that might produce that system state. Undesired event definition provides a means of defining the undesired system operability state (top event) in terms of its constituent fault events. Event relationships depict the logical interrelationships between system fault events as they relate to the top event. Logic diagram serves as a roadmap of the system fault paths. Unavailability tool qualitatively identifies how a system may become unavailable. The fault tree analysis when combined with the quantitative techniques provides a means of calculating system failure probabilities. The PSA Procedures Guides identifies⁵⁸ five essential tasks in the fault tree development, depicted on Figure 3-5.

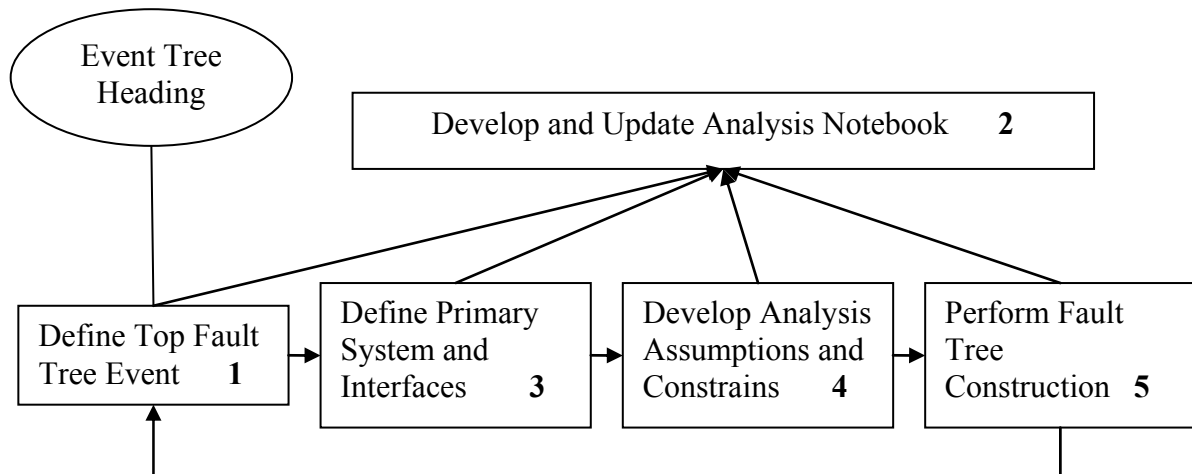


Figure 3-5 Fault Tree development process

The entire fault tree analysis activity is based on the particular associated top event, therefore the statement of the top event should be clear, accurate and appropriately specific. Top event definition is the process of developing such a top event.

A system, as previously defined in the section 3.1, is a collection of discrete elements that interact to perform, in total or in part, a function or set of functions. To perform a fault tree analysis, clear definition of system boundaries is necessary.

Standard symbols and notations have been developed to facilitate fault tree analysis approach⁵³. The logical gates integrate the primary events to the top event. The primary events are the events, which are not further developed, e.g. the basic events and the house events. The basic events are the ultimate parts of the fault tree, representing the undesired events, e.g. the component failures, the missed actuation signals⁶¹, the human errors^{62, 63, 64}, the unavailability's due to the test and maintenance activities^{65, 66, 67, 68, 69, 73} or common cause contributions⁷⁰.

The house events represent the conditions set either to true or false, which support the modeling of connections between the gates and the basic events, and enable that the fault tree better represents the system operation and its environment.

Generic to the problem-solving process is the need to establish assumptions and conditions, and for the fault tree analysis process issues that must be addressed are:

- Passive failures.
- Inadvertent operation.
- Secondary failure postulation.
- Errors of commission.
- System operating states.

During the fault tree development process it's necessary to account Common Cause Failures (CCF). The CCF are defined as failures of dependent components from shared root causes⁷⁰. The CCF can result from:

- Common cause initiating event resulting with the plant transient and increased unavailability of several systems (e.g. earthquake).
- Intersystem dependency on joint event probability (e.g. fire resulting with the loss of two systems).
- Intercomponent dependency (e.g. battery overrun).

Dependent events must be considered not only in the quantification, but also in the definition of the accident sequences in the PSA. The common cause failures are modeled using common cause basic events, which are basic events that represent multiple failures of components from shared root causes. The quantification of the common cause basic events is through selection of the appropriate⁷⁰ common cause model (e.g. Beta factor, Multiple Greek letters, and Alpha factor).

Two types of results are obtained in a fault tree evaluation: qualitative and quantitative results. Qualitative results include:

- Minimal cut sets (combinations of components failures causing system failure).
- Qualitative importance (qualitative rankings of contributions to system failure).
- Common cause potentials (Minimal cut sets potentially susceptible to a single failure cause).

The quantitative results include:

- Numerical probabilities (probabilities of system and cut set failures).
- Quantitative importance (quantitative ranking of contributions to system failure).
- Sensitivity evaluations (effects of changes in models and data, error determinations).

For the qualitative evaluations, the minimal cut sets are obtained by Boolean reduction, using laws of Boolean algebra given in Table 3-1. The basic steps of Boolean reduction are:

- Express fault tree logic as Boolean equation.
- Apply rules of Boolean algebra to reduce terms.
- Treat results as a reduced form of Boolean equation.
- Redraw fault tree diagram to identify fault relationship.

The classic fault tree is mathematically represented^{20, 53} by a set of Boolean equations:

$$G_i = f(G_p, B_j, H_s); i, p \in \{1..P\}, j \in \{1..J\}, s \in \{1..S\} \quad (3.28)$$

Where:

G_p - Gate p.

B_j - Basic event j.

H_s - House event s.

P - Number of gates in the fault tree.

J - Number of basic events in the fault tree.

S - Number of house events.

The qualitative importance of the cut sets is identified by ordering the minimal cut sets according to their size (number of basic events in the set). Because the failure probabilities associated with the minimal cut sets often decrease by orders of the magnitude as the size of the cut set increases, the ranking according to size gives a gross indication of the importance of the minimal cut set. The identified minimal cut sets are screened in order to identify the minimal cut sets that are potentially susceptible to common cause failures.

Table 3-1 Laws of the Boolean algebra

Boolean Law	Expression
Commutative Law	$X+Y=Y+X$ $XY=YX$
Associate Law	$(X+Y)+Z=X+(Y+Z)$ $(XY)Z=X(YZ)$
Distributive Law	$X(Y+Z)=XY+XZ$ $(X+Y)Z=XZ+YZ$
Identity Law	$XX=X$ $X+X=X$
Redundancy Law	$X(X+Y)=X$ $X+XY=X$
Complementary Law	$X+X'=1$ $XX'=0$ $(X')'=X$
De Morgan's Theorem	$(XY)'=X'+Y'$ $(X+Y)'=X'Y'$

The quantitative fault tree evaluation includes the following steps:

- Determination of the component failure probabilities.
- Calculation of the minimal cut set probabilities.
- Calculation of the system failure (top event) probability (unavailability).

The quantitative measures of the importance of each cut set and of each component (basic event) can also be obtained. The term component represents any basic primary event shown in the event tree. For components two failure probability models are considered: constant failure rate per time and constant failure rate per cycle. Using these constant failure rate models the time-dependent effects such as component burn-in and wear-out are ignored.

The calculation of the component unreliability in case of the constant failure rate per time model is described in the 3.1 and given by Eq. (3.5). The failure rate λ can be either a standby failure rate or an operating failure rate. In case of the standby failure rate λ the time period t used in the Eq. (3.5) should be standby time, in the case of the operating failure rate, the t is the actual operating time period. In case of components that have both operational modes, the proper failure rate should be used with the proper time period. In case of the nonrepairable components the component unreliability is equal to component unavailability, therefore:

$$Q(t) \cong \lambda \cdot t \quad (3.29)$$

Where:

$Q(t)$ - Component unavailability at time t .

λ – Component failure rate.

For repairable failures, the component unavailability $Q(t)$ is not equal to the unreliability. If the repair process restores the component to a state where it is essentially as good as new, the unavailability of the component is calculated using two approaches.

The first approach is when component is monitored and in this case the unavailability $Q(t)$ quickly reaches a constant asymptotic value Q_M given by:

$$Q_M = \frac{\lambda \cdot T_D}{1 + \lambda \cdot T_D} \cong \lambda \cdot T_D \quad (3.30)$$

Where:

Q_M – Unavailability of the monitored component.

T_D – The average online downtime obtained by statistically averaging the downtime distribution.

λ – Component failure rate.

For components not monitored but periodically tested, any failures occurring are not detectable until the test is performed. The total average unavailability Q_T for periodically tested components is given as:

$$Q_T = \frac{\lambda \cdot T}{2} + \lambda \cdot T_R \quad (3.31)$$

Where:

Q_M – Unavailability of the periodically tested component.

T_R – The average repair time obtained from downtime considerations.

T – The interval of the periodic tests.

λ – Component failure rate.

In general, the T_R is small compared to the T , therefore the Eq. (3.31) can be approximated as:

$$Q_T \cong \frac{\lambda \cdot T}{2}, T_R \ll T \quad (3.32)$$

The constant failure rate per cycle model, also called p-model, is applied when failures are inherent to the component and are not caused by external mechanisms associated with the exposure time. The reliability characteristics of the p-model are based on the one characterizing value p , the probability of failure per cycle or per demand. For n demands in time t and assuming independent failures, the reliability (R_c) and the unavailability (Q_c) are given by:

$$R_c = 1 - Q_c = (1 - p)^n \quad (3.33)$$

$$Q_c \cong np, np < 0.1 \quad (3.34)$$

Where:

R_c - The reliability of the component.

Q_c – The component unavailability.

n - Number of cycles.

p - The probability of failure per cycle.

As noted in the above equations, the reliability and unavailability do not depend explicitly on time but on the number of cycles (demands) occurring in that time.

Once the components (basic events) reliability characteristics are obtained, the reliability characteristics of the minimal cut sets can be evaluated. For a fault tree of a standby system, such as nuclear safety system, the characteristic of principal concern is minimal cut set unavailability denoted as Q_{MCS} .

$$Q_{MCSi} = Q_{B1} \cdot Q_{B2} | Q_{B1} \cdot Q_{B3} | Q_{B1} \cap Q_{B2} \cdot \dots \cdot Q_{Bm} | Q_{B1} \cap Q_{B2} \cap \dots \cap Q_{Bm-1} \quad (3.35)$$

Where:

Q_{MCSi} – The minimal cut set i probability.

Q_{Bj} – The probability of occurrence of basic event B_j (component unavailability).

Assuming the component failures are mutually independent²⁰, recall from the section 3.1 that the probability of an intersection is simply the product of the component probabilities result with the following expression for calculation of the minimal cut set probability:

$$Q_{MCSi} = \prod_{j=1}^m Q_{Bj} \quad (3.36)$$

Where:

Q_{MCSi} – The minimal cut set i probability.

Q_{Bj} – The probability of occurrence of basic event B_j (component unavailability).

m - Number of basic events in minimal cut set i .

The probability of occurrence of basic event Bj is expressed as:

$$Q_{Bj} = Q_{Bj}(T_j, \lambda_j, q_j) \quad (3.37)$$

Where:

Tj - Considered time interval.

λ_j - Failure rate of the equipment modelled in the basic event j.

q_j - Probability of failure of equipment modelled in basic event j.

Once the minimal cut sets are quantified, the next step is determination of the system unavailability (top event probability) denoted Q_{GD} defined as a probability that the system is down at specific time point and unable to operate if called on. The top event probability is given as:

$$Q_{GD} = \sum_{i=1}^n Q_{MCSi} - \sum_{i<j} Q_{MCSi \cap MCSj} + \sum_{i<j<k} Q_{MCSi \cap MCSj \cap MCSk} - \dots + (-1)^{n-1} Q_{\bigcap_{i=1}^n MCSi} \quad (3.38)$$

Where:

Q_{GD} - Top event probability.

Q_{MCSi} - Probability of occurrence of MCSi.

$Q_{MCSi \cap MCSj}$ - probability of occurrence of MCSi and MCSj simultaneously.

If the minimal cut sets are not assumed as mutually independent, the second and the next elements in Equation (3.38) are written as follows:

$$Q_{MCSi \cap MCSj} = Q_{MCSi} \cdot Q_{MCSj | MCSi} \quad (3.39)$$

$$Q_{MCSi \cap MCSj \cap \dots \cap MCSn} = Q_{MCSi} \cdot Q_{MCSj | MCSi} \cdot \dots \cdot Q_{MCSn | MCSi \cap MCSj \cap \dots \cap MCS_{n-1}} \quad (3.40)$$

If the minimal cut sets are assumed as mutually independent, the second and the next terms in Eq. (3.38) are written as:

$$Q_{MCSi \cap MCSj} = Q_{MCSi} \cdot Q_{MCSj} \quad (3.41)$$

$$Q_{MCSi \cap MCSj \cap \dots \cap MCSn} = Q_{MCSi} \cdot Q_{MCSj} \cdot \dots \cdot Q_{MCSn} \quad (3.42)$$

In either case, the Eq. (3.38) can be simplified and approximated accounting only the first term as:

$$Q_{GD} = \sum_{i=1}^n Q_{MCSi} \quad (3.43)$$

For Q_{MCSi} less than 0.1, the approximate results stay in 10% of accuracy in the conservative side. The approximate results show²⁰ slightly higher failure probabilities than the exact value.

If Q_{MCSi} have larger values, exact formulation as given by Eq. (3.38) is necessary.

In addition, the quantitative results obtainable from fault tree analysis include importance measures for each minimal cut set and each component failure. The importance measures are divided in two groups. The first group consists of the measure that is called Fussell-Vesely Importance (FV)^{71,72} and gives fractional contribution to the system unavailability:

$$FV_k = 1 - \frac{Q_{GD}(Q_k = 0)}{Q_{GD}} = 1 - \frac{1}{RRW_k} \quad (3.44)$$

Where:

FV_k – Fussell-Vesely importance for component k.

Q_{GD} – Top event probability.

$Q_{GD}(Q_k=0)$ – Top event probability when failure probability of component k is set to 0.

RRW_k – Risk Reduction Worth for component k.

The second group of the importance measures depicts the change of the system unavailability when the contributor's failure probability is set to 0 or 1. These importance measures are

named Risk Achievement Worth (RAW), also named as Risk Increase Factor (RIF) and Risk Reduction worth (RRW), also named as Risk Decrease Factor (RDF), and they are defined as:

$$RAW_k = \frac{Q_{GD}(Q_k = 1)}{Q_{GD}} \quad (3.45)$$

$$RRW_k = \frac{Q_{GD}}{Q_{GD}(Q_k = 0)} \quad (3.46)$$

Where:

RAW_k – Risk Achievement Worth for component k.

RRW_k – Risk Reduction Worth for component k.

$Q_{GD}(Q_k=1)$ – Top event probability when failure probability of component k is set to 1.

$Q_{GD}(Q_k=0)$ – Top event probability when failure probability of component k is set to 0.

Q_{GD} – Top event probability.

The presented importance measures are also used in the event tree analysis, with the substitution of the Q_{GD} (top event probability) with the calculated core damage frequency of the corresponding plant.

An example of construction of the fault tree, for the High Pressure Injection System (HPIS) of a NPP is presented. A simplified HPIS of a NPP with the Pressurized Water Reactor is shown on Figure 3-6, taken from corresponding reference⁷³. This system is normally in stand-by and consists of three pumps and seven valves organized as shown on Figure 3-6. Under accidental conditions the HPIS can be used to remove heat from the reactor in those events in which steam generators are unavailable. For example, in case of a Small-Break Loss-Of-Coolant Accident the HPIS safety function draws water from the Refueling Water Storage Tank (RWST) and must discharge it into the cold legs of the Reactor Cooling System through any of the two injection paths. Normally, pumps discharge into the injection paths A and B through valves 26 and 27, although crossover valves 409, 410 and 411 provide alternative flow paths in case of failure of the normal feed.

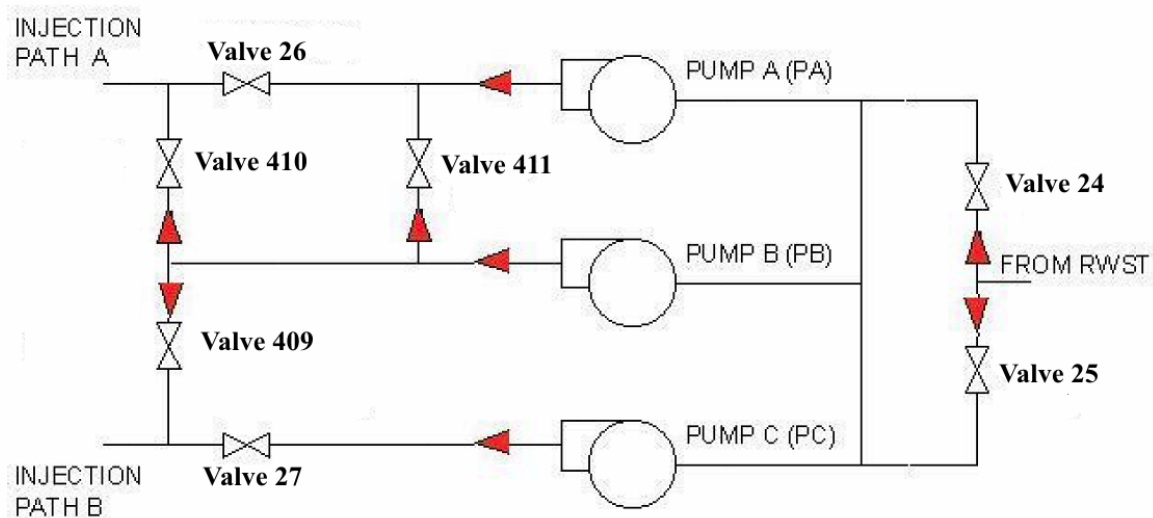


Figure 3-6 Example HPIS

Several analysis assumptions and constrains are applied during construction of the fault tree for the HPIS given on Figure 3-6:

- No passive failures are considered in the fault tree (e.g. pipe breaks).
- No secondary failures are considered (e.g. loss of the power).
- Flow through lines is limited to direction marked with the red squares on Figure 3-6.
- An inexhaustible fluid supply is available to the pumps from RWST.
- Common cause failures are not accounted during fault tree construction.

The common cause failures were excluded from the fault tree construction as a result of the space limitation.

The constructed fault tree for the HPIS is given on Figure 3-7. The top event of the fault tree given on Figure 3-7 is failure of the HPIS to deliver coolant flow through one of the two injection paths A and B. The identified MCS together with the calculated probability are given in Table 3-2.

Table 3-2 Identified minimal cut sets for HPIS

No. MCS	Probability	Event 1	Event 2	Event 3	Event 4	Event 5
1	5.89E-08	FAILURE PA	FAILURE PB	FAILURE PC		
2	8.82E-11	FAILURE PB	FAILURE PC	FAILURE V26		
3	8.82E-11	FAILURE PA	FAILURE PB	FAILURE V27		
4	3.40E-11	FAILURE V24	FAILURE V25			
5	1.32E-13	FAILURE PB	FAILURE V26	FAILURE V27		
6	7.71E-19	FAILURE PC	FAILURE V26	FAILURE V409	FAILURE V410	
7	3.00E-21	FAILURE PA	FAILURE PC	FAILURE V409	FAILURE V410	FAILURE V411
8	1.16E-21	FAILURE V26	FAILURE V27	FAILURE V409	FAILURE V410	
9	4.49E-24	FAILURE PA	FAILURE V27	FAILURE V409	FAILURE V410	FAILURE V411

Nine minimal cut sets are identified for the HPIS given on Figure 3-6. The main contributor to the top event probability corresponding to system failure is from the minimal cut set resulting from failure of all three pumps.

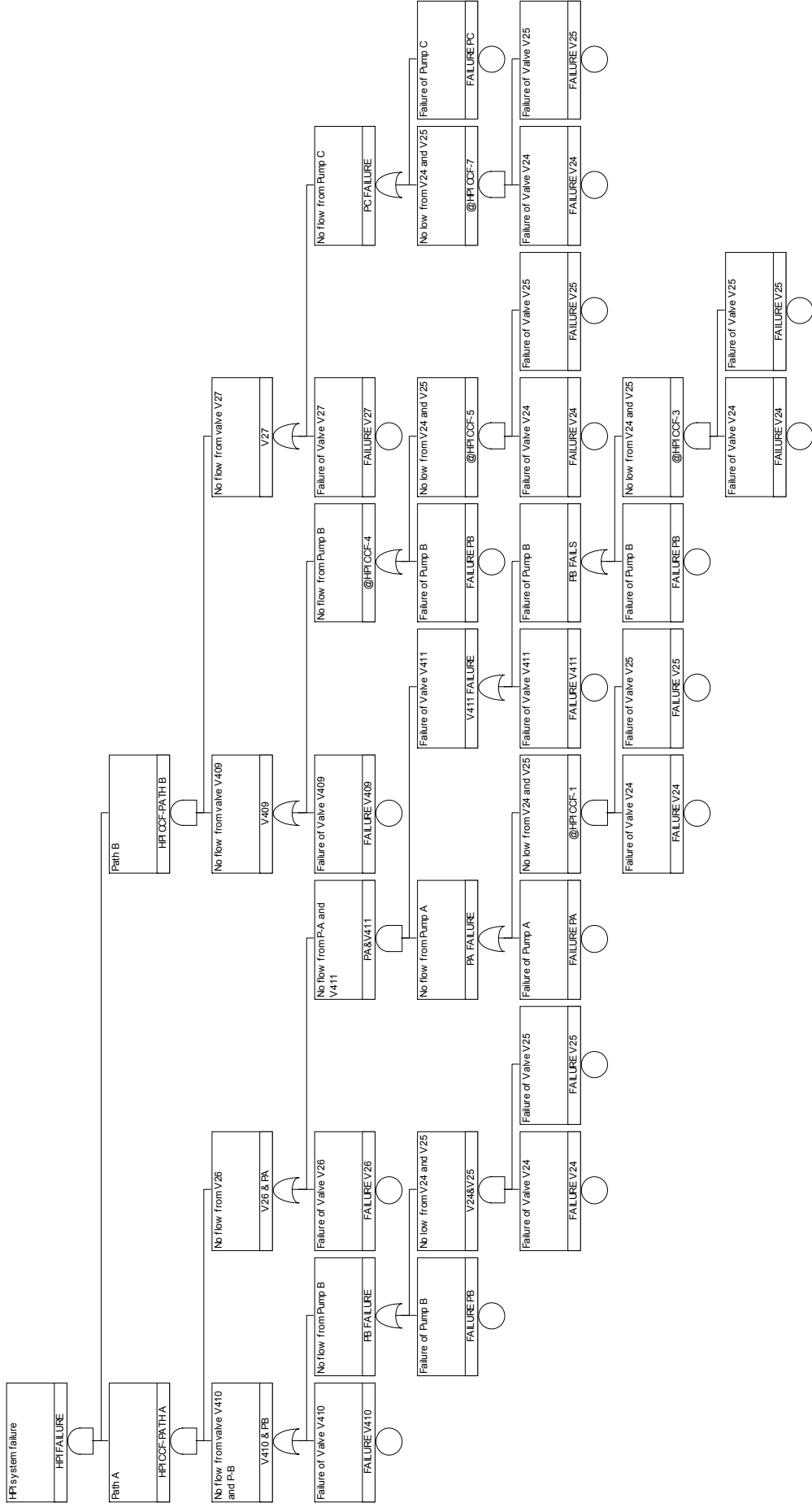


Figure 3-7 HPIs fault tree

3.3 PSA applications and Risk-Informed decision making

The Nuclear Regulatory Commission policy statement⁷⁴ on the PSA encourages greater use of this analysis technique to improve safety decision making and regulatory efficiency.

Licensee-initiated changes that are consistent with the currently approved regulatory NRC positions (e.g., regulatory guides, standard review plans, branch technical positions, or the Standard Technical Specifications) are normally evaluated using the traditional engineering analyses. In the case of the licensee-initiated change requests that go beyond current NRC positions, evaluation can be made using traditional engineering analyses as well as the risk-informed approach⁷⁵. In the areas in which the results of risk analyses are used to justify regulatory action the corresponding regulatory guides are applied^{15, 76, 77, 78}.

The Nuclear Regulatory Commission reviews new reactor license applications⁷⁹ in accordance with the Standard Review Plan⁸⁰ (SRP). The SRP is a guide for conducting safety reviews of applications to construct and operate nuclear power plants and the review of applications to approve standard designs and sites for nuclear power plants. The risk insights are developed from probabilistic evaluations (PSA) and traditional evaluations (e.g., defense-in-depth, expert panel). Risk insights are developed to facilitate identification of potential design and performance issues that could be adverse to the plant risk⁸¹.

3.4 Power system analysis methods

The primary technical function of a power system is to provide electrical energy to its customers as economically as possible with an acceptable degree of continuity and quality, known as reliability⁸². The two constraints of economics and reliability are competitive since increased reliability of supply generally requires increased capital investment, as shown on Figure 3-8. These two constraints are balanced in many different ways in different countries and by different utilities, although generally they are all based on various sets of deterministic criteria.

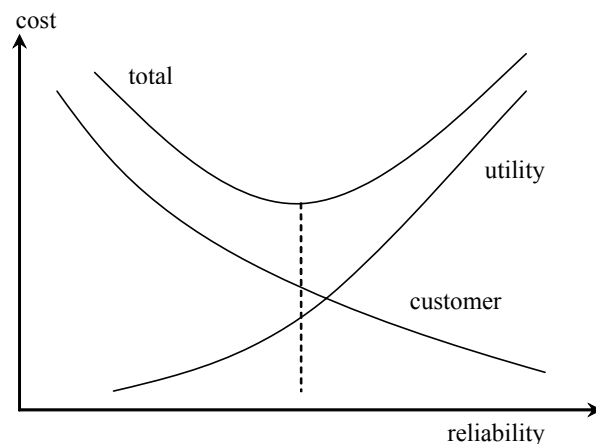


Figure 3-8 Relation Cost-Reliability for power systems

A wide range of appropriate indices can be determined using probability theory. A single all-purpose formula or technique does not exist. The approach used and the resulting formulas depend on the problem and the assumptions utilized. Many assumptions must be made in all practical applications of probability and statistical theory. The validity of the analysis is directly related to the validity of the model used to represent the system. Actual failure distributions rarely completely fit the analytical descriptions used in the analysis, and care must be taken to ensure that significant errors are not introduced through oversimplification of a problem.

The most important aspect is that it is necessary to have a complete understanding of the engineering implications of the system. No amount of probability theory can circumvent this important engineering function. Probability theory is only a tool that enables an engineer to transform knowledge of the system into a prediction of its likely future behavior. Only after this understanding has been achieved, a model can be derived and the most appropriate evaluation technique chosen. Both of these must reflect and respond to the way the system operates and fails.

There are two main categories of evaluation techniques: analytical and simulation. Analytical techniques represent the system by a mathematical model and evaluate the indices from this model using mathematical solutions. Monte Carlo simulation methods, however, estimate the indices by simulating the actual process and random behavior of the system. The method therefore treats the problem as a series of real experiments. There are merits and demerits in both methods. Generally Monte Carlo simulation requires a large amount of computing time and is not used extensively if alternative analytical methods are available. In theory, however, it can include any system effect or system process that may have to be approximated in analytical methods. The predicted indices are only as good as the model derived for the system, the appropriateness of the evaluation technique and the quality of the input data used in the models and techniques.

Three historical methods used to determine power system reliability and generation adequacy are presented in this section.

3.4.1 Percent Reserve Evaluation

The earliest method and most easily computed criterion for evaluation of generation system adequacy is the percent generation reserve margin approach. This method is sensitive to only two factors at one point in time.

Percent reserve evaluation computes the generation capacity exceeding annual peak load. It is calculated by comparing the total installed generating capacity at peak with the peak load. The criterion is based on past experience requiring reserve margins in the range of 15-25% to meet demand. The load demand support meant that the frequency and magnitude of emergency power purchases from neighboring power systems was reasonable and/or the number of curtailments was small.

There are, however, disadvantages to the percent reserves approach. It is insensitive to forced outage rates and unit size considerations, power transfer capacity and failures in transmission network as well as to differing load characteristics of power systems. Although this approach is a useful step in the analysis of generation reserve problems, it does not provide a complete answer to how much generation capacity is required to adequately serve load demands.

3.4.2 Loss-of-the-Largest-Generating-Unit Method

Loss-of-the-largest-generating-unit method provides a degree of sophistication over the percent reserve margin method by reflecting the effect of unit size on reserve requirements. With the loss-of-the-largest-unit method, required reserve margin is calculated by adding the size of the largest unit divided by the peak load plus a constant reserve value.

For example, if reserve requirements are 15% plus the largest unit, and the largest unit is 500 MW in a power system with a 5000-MW peak load, then the reserve requirement is $15\% + 500/5000 - (100\%)$, or 25%. This approach begins to explicitly recognize the impact of a single outage, that is, loss of the largest generating unit. Probabilistic measures are necessary to extend this method to include multiple simultaneous outages.

Loss-of-the-largest-unit method, although simple, has a distinct advantage over the generation reserve margin method. As larger units are added to a system, the percent reserves for a system are implicitly increased by this method as needed. But similarly as percent reserve

evaluation method, it is insensitive to forced outage rates of the units and power transfer capacity and failures in transmission network.

3.4.3 Loss-of-Load-Probability Method

Loss of load probability consists of two segments in which the generating unit unavailability is characterized by random outage rate (forced) and scheduled outage rate. The effect of random outages is evaluated probabilistically, while that of scheduled outages is evaluated deterministically.

The measure, termed "loss-of-load-probability" (LOLP) index, provides a consistent and sensitive measure of generation system reliability. The term "loss of load probability" is misleading in two respects. First, this index is not a probability, but is an expected number of days per year of capacity deficiency. Second, it is not a loss of load, but rather a deficiency of installed available capacity. Despite the misnomers, LOLP is the most widely accepted approach for determining reserves in the utility industry today.

In power system analysis the application of LOLP is only limited to estimation of generation adequacy and its application for overall system analysis is constrained.

3.4.4 Applications of probability theory to power systems

The following topics illustrate some areas, in which probability theory has and still is applied to power system applications. Some areas are highly developed and used in practice whilst others are in the development stage.

Structural reliability is of concern in many disciplines including that of line design. Factors that affect short-circuit currents include fault location, fault type and system conditions. Since they are random events, the fault current can also be described by a probability density function. Taking into account the likelihood as well as the magnitude can have a major impact on short-circuit rating. Previous conservative ratings could be increased if probabilistic analyses are subsequently included. The stability of a system, in a similar manner to that of short-circuit current analysis, is dependent on many random factors including the location of a disturbance, injected powers, fault type, fault clearing times, system impedances, and system configuration. Techniques have been developed⁸² that enable the probability of stability to be evaluated as a function of these variables. Power injections, loads, generation as well as the network configurations all vary randomly with the time. Probabilistic load flow techniques take these factors into account and evaluate relevant probability density functions for parameters such as line flows, bus voltages and reactive power injections. Reliability assessment is the most extensively studied application area.

3.4.5 Additional Reliability Measures

The standard⁸³ distribution reliability indices and factors that affect their calculation are given. The indices are intended to be applied to distribution systems, substations, circuits, and defined regions.

The first set represents the sustained interruption indices:

- System average interruption frequency index (SAIFI)

The system average interruption frequency index indicates how often the average customer experiences a sustained interruption over a predefined period of time. Mathematically, this is given in Equation (3.47):

$$SAIFI = \frac{\sum Total_Number_of_Customers_Interrupted}{Total_Number_of_Customers_Served} \quad (3.47)$$

- System average interruption duration index (SAIDI)

This index indicates the total duration of interruption for the average customer during a predefined period of time. It is commonly measured in customer minutes or customer hours of interruption. Mathematically, this is given in Eq. (3.48):

$$SAIDI = \frac{\sum Customers_Interruption_Durations}{Total_Number_of_Customers_Served} \quad (3.48)$$

- Customer average interruption duration index (CAIDI)

CAIDI represents the average time required to restore service. Mathematically, this is given in Eq. (3.49):

$$CAIDI = \frac{\sum Customers_Interruption_Durations}{Total_Number_of_Customers_Interrupted} \quad (3.49)$$

- Customer total average interruption duration index (CTAIDI)

This index represents the total average time in the reporting period that customers who actually experienced an interruption were without power. This index is a hybrid of CAIDI and is similarly calculated except that those customers with the multiple interruptions are counted only once. Mathematically, this is given in Eq. (3.50):

$$CTAIDI = \frac{\sum Customers_Interruption_Durations}{Total_Number_of_Customers_Interrupted} \quad (3.50)$$

- Customer average interruption frequency index (CAIFI)

This index gives the average frequency of sustained interruptions for those customers experiencing sustained interruptions. The customer is counted once regardless of the number of times interrupted for this calculation. Mathematically, this is given in Eq. (3.51):

$$CAIFI = \frac{\sum Total_Number_of_Customers_Interrupted}{Total_Number_of_Customers_Interrupted} \quad (3.51)$$

- Average service availability index (ASAI)

The average service availability index represents the fraction of time (often in percentage) that a customer has received power during the defined reporting period. Mathematically, this is given in Eq. (3.52):

$$ASAI = \frac{\sum Customers_Hours_Service_Availability}{Customers_Hours_Service_Demand} \quad (3.52)$$

- Customers experiencing multiple interruptions (CEMI_n)

This index indicates the ratio of individual customers experiencing more than n sustained interruptions to the total number of customers served. Mathematically is given in Eq. (3.53):

$$CEMI_n = \frac{Total_Num_of_Cust_experience_morethan_n_sustained_interr}{Total_numer_of_customers_Served} \quad (3.53)$$

The next set of the reliability indices are the load based indices:
 - Average system interruption frequency index (ASIFI)

The calculation of this index is based on load rather than customers affected. ASIFI is sometimes used to measure distribution performance in areas that serve relatively few customers having relatively large concentrations of load, predominantly industrial/commercial customers. Theoretically, in a system with the homogeneous load distribution, ASIFI would be the same as SAIFI. Mathematically, this is given in Eq. (3.54):

$$ASIFI = \frac{\sum Total_Connected_kVA_of_Load_Interrupted}{Total_Connected_kVA_Served} \quad (3.54)$$

- Average system interruption duration index (ASIDI)

The calculation of this index is based on load rather than customers affected. Its use, limitations, and philosophy are stated in the ASIFI definition. Mathematically, this is given in Eq. (3.55):

$$ASIDI = \frac{\sum Connected_kVA_Duration_of_Load_Interrupted}{Total_Connected_kVA_Served} \quad (3.55)$$

The additional, named momentary, indices used in the practice are the following three:

- Momentary average interruption frequency index (MAIFI)

This index indicates the average frequency of momentary interruptions. Mathematically, this is given in Eq.(3.56):

$$MAIFI = \frac{\sum Total_Number_of_Customers_Momentary_Interruptions}{Total_Number_of_Customers_Served} \quad (3.56)$$

- Momentary average interruption event frequency index (MAIFI_E)

This index indicates the average frequency of momentary interruption events. This index does not include the events immediately preceding a lockout as given in (3.57):

$$MAIFI_E = \frac{\sum Total_Number_of_Cust_Momentary_Interruption_Events}{Total_Number_of_Customers_Served} \quad (3.57)$$

- Customers experiencing multiple sustained interruption and momentary interruption events (CEMSMI_n)

This index is the ratio of individual customers experiencing more than n of both sustained interruptions and momentary interruption events to the total customers served. Its purpose is to help identify customer issues that cannot be observed by using averages. Mathematically, this is given in Eq. (3.58):

$$CEMSMI_n = \frac{Total_Number_Cust_Exper_More_Than_n_Interruption}{Total_Number_of_Customers_Served} \quad (3.58)$$

Both duration and frequency of customer interruptions must be examined at various system levels in order to adequately measure performance. The most commonly used indices are

SAIFI, SAIDI, CAIDI and ASAI. All of these indices provide information about average system performance. Many utilities also calculate indices on a feeder basis to provide more detailed information for decision making. Averages give general performance trends for the utility; however, using averages will lead to loss of detail that could be critical to decision making. For example, using system averages alone will not provide information about the interruption duration experienced by any specific customer. It is difficult for most utilities to provide information on a customer basis. The tracking of specific details surrounding specific interruptions rather than averages will be, in the future, accomplished by improving tracking capabilities.

4 New method description

A description of the developed method and its procedures is given in the following sections. Relations used for load point reliability indices calculations are presented, followed by the explanation of the developed method.

4.1 Definition of reliability and importance indices

In order to estimate the frequency of Loss of Offsite Power initiating event, it is necessary to develop method for estimation of the load supplying capability of the power system to each load point of the system. Fault tree analysis approach was selected for estimation of reliability indices of the power delivery to the house loads of the NPP in the system.

The corresponding fault tree is built for each load in the system. The unreliability of the power delivery to the i -th load (U_{GD_i}) is calculated through the top event probability of the respective fault tree, and the weighted unreliabilities of power delivery to all loads are considered to get the overall measure of the power system reliability:

$$R_{PS} = 1 - \sum_{i=1}^{NL} U_{GD_i} \frac{K_i}{K} = 1 - U_{PS} \quad (4.1)$$

Where:

R_{PS} - Power system reliability.

U_{PS} – Weighted system unreliability.

U_{GD_i} - Unreliability of the power delivery to the i -th load (top event probability of the respective fault tree).

NL - Number of loads in system.

K_i - Size of i -th load [MW].

$\frac{K_i}{K}$ - Weighting factor for i -th load.

$$K = \sum_{i=1}^{NL} K_i \quad (4.2)$$

The fault tree analysis is performed for each load in the power system and the weighted system unreliability, given by Eq. (4.1), is calculated.

New risk importance measures are developed for the power system: Network Risk Achievement Worth (NRAW) and Network Risk Reduction Worth (NRRW). They are defined using the definition of the importance measures for fault tree given in Eqs. (3.45) and (3.46) and the weighted system unreliability expression given in Eq. (4.1). As the term network is a descriptive term for the power system, NRAW and NRRW can be expressed as power system risk achievement worth and power system risk reduction worth.

The $NRAW^k$ is defined as:

$$NRAW^k = \frac{U_{PS}(U_k = 1)}{U_{PS}} = \frac{\sum_{i=1}^{NL} U_{GD_i}(U_k = 1)K_i}{\sum_{i=1}^{NL} U_{GD_i}K_i} = \frac{\sum_{i=1}^{NL} U_{GD_i}K_i RAW_{GD_i}^k}{\sum_{i=1}^{NL} U_{GD_i}K_i} \quad (4.3)$$

$$RAW_{GD_i}^k = \frac{U_{GD_i}(U_k = 1)}{U_{GD_i}} \quad (4.4)$$

Where:

$NRAW^k$ – Network risk achievement worth of the element k.

U_{PS} – Weighted unreliability of the power system.

$U_{PS}(U_k=1)$ – Weighted unreliability of the power system when unreliability of the element k is set to 1.

$U_{GD_i}(U_k=1)$ – Unreliability of the power delivery to the i-th load when unreliability of the element k is set to 1.

NL- Number of loads in the system.

U_{GD_i} – Unreliability of the power delivery to the i-th load.

$RAW^k_{GD_i}$ – Value of RAW for element k corresponding to the load i.

K_i – Capacity of i-th load.

The $NRRW^k$ is defined as:

$$NRRW^k = \frac{U_{PS}}{U_{PS}(U_k = 0)} = \frac{\sum_{i=1}^{NL} U_{GD_i} K_i}{\sum_{i=1}^{NL} U_{GD_i}(U_k = 0) K_i} = \frac{\sum_{i=1}^{NL} U_{GD_i} K_i}{\sum_{i=1}^{NL} \frac{U_{GD_i} K_i}{RRW^k_{GD_i}}} \quad (4.5)$$

$$RRW^k_{GD_i} = \frac{U_{GD_i}}{U_{GD_i}(U_k = 0)} \quad (4.6)$$

Where:

$NRRW^k$ – Network risk reduction worth of the element k.

$U_{PS}(U_k=0)$ – Weighted unreliability of the power system when unreliability of element k is set to 0.

$U_{GD_i}(U_k=0)$ – Unreliability of the power delivery to the i-th load when unreliability of element k is set to 0.

$RRW^k_{GD_i}$ – Value of the RRW for element k corresponding to the load i.

The system importance measures $NRAW$ and $NRRW$ for elements groups are defined similarly as importance measures for single elements, substituting Q_{PS} and Q_{GD_i} in Eqs.(4.5) and (4.6) with the:

$U_{PS}(U_g=1)$ – Weighted system unreliability when unreliability of elements in group g is set to 1.

$U_{GD_i}(U_g=1)$ – Unreliability of the power delivery to i-th load when unreliability of the elements in group g is set to 1.

$U_{PS}(U_g=0)$ – Weighted system unreliability when unreliability of elements in group g is set to 0.

$U_{GD_i}(U_g=0)$ – Unreliability of the power delivery to i-th load when unreliability of elements in group g is set to 0.

Elements groups may contain elements (components) of same type, elements corresponding to specific substation or/any other combination.

4.2 Fault tree construction procedure

Switching substations are important elements of the power systems. A generator and/or a load can be connected to each switching substation. The switching substations are interconnected with the power lines, through which the power is transferred from generators and other switching substations to the loads. The main task of the analysis is to identify the possible interruptions of the power delivery to the load, to evaluate the probability of those interruptions and to recognize the main contributing elements.

In order to start with the fault tree analysis, the corresponding fault tree should be built first for each switching substation connected to a load. The principle of continuum of energy

delivery is taken in account during the analysis. The fault tree structure corresponds to the power system configuration and includes all possible flow paths of the power supply from the generators to the loads. The power transfer limitations and common cause failures (CCF) of power lines are included in the model together with the power flows and size of the generators and loads in the power system. Common cause failures are failures of multiple equipment items occurring from the single cause that is common to all of them.

The procedure of building fault trees for loads can be divided in three steps:

- Building of fault trees for the loads including load flow calculation and energy flowpaths examination.
 - Construction of fault trees for each substation.
 - Qualitative and quantitative evaluation of the fault trees.
- These steps are described in details in the following sections.

4.2.1 Fault tree construction of loads

The first step in developing the corresponding fault trees for loads is the identification of all the possible energy delivery flow paths from adjacency matrix of the corresponding power system. The six nodes system shown on Figure 4-1, is presented as an example for the description of the method.

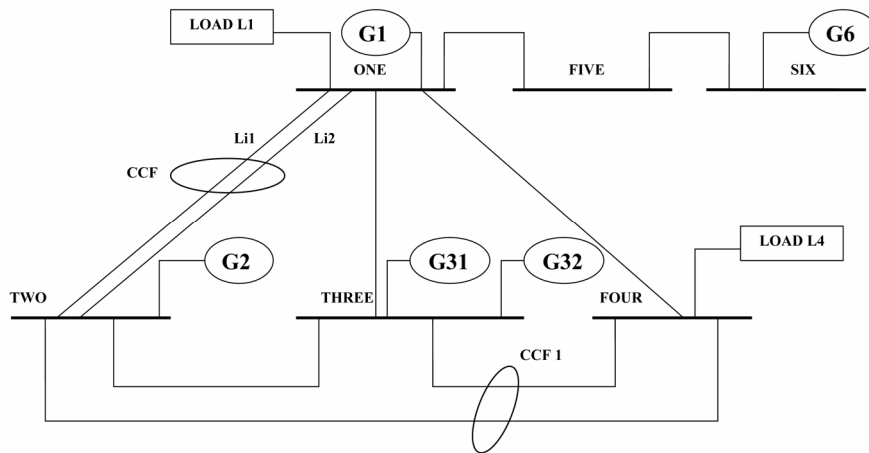


Figure 4-1 An example power system

The system consist of six substations, five generators in substations 1, 2, 3 and 6 and two loads in substations 1 and 4. There are multiple generators (two in substation three) and multiple lines (marked Li1 and Li2 on Figure 4-1) between substations 1 and 2 in the example system. The lines for which common cause failures (CCF) are accounted are marked on Figure 4-1, CCF of lines due to the common tower and CCF1 of lines that are assumed to be on a common right-of way for part of their length.

The adjacency matrix A of a simple graph is a matrix with the rows and columns labeled by graph vertices, with a 1 or 0 in position (v_i, v_j) according to whether graph vertices v_i and v_j are adjacent or not. The adjacency matrix A of an example system is given on Figure 4-2.

$$A = \begin{bmatrix} 0 & 1 & 1 & 1 & 1 & 0 \\ 1 & 0 & 1 & 1 & 0 & 0 \\ 1 & 1 & 0 & 1 & 0 & 0 \\ 1 & 1 & 1 & 0 & 0 & 0 \\ 1 & 0 & 0 & 0 & 0 & 1 \\ 0 & 0 & 0 & 0 & 1 & 0 \end{bmatrix}$$

Figure 4-2 Adjacency matrix A of an example system

Using the adjacency matrix A , all possible flow paths between generation (source) and consumer (load) substations are identified, using developed recursive procedure for formation of rooted trees of the graph of the system. Used recursive procedure is standard recursion with the marking of passed nodes in order to avoid closed cycles.

The energy flow paths between the load and other substations in system are identified using the rooted tree. A rooted tree is a tree in which a labeled node is singled out. The rooted tree for substation 1 on Figure 4-1 is given on Figure 4-3. Dashed lines identify the energy flow paths between substations 3 and 6 and the substation 1.

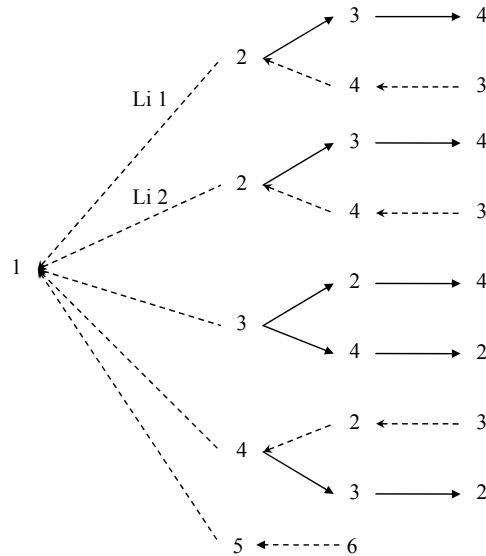


Figure 4-3 Rooted tree for substation 1

The identified flow paths of energy delivery between substations are tested for consistency, namely:

1. Only a part of the flow path ending with the substation, directly connected to generators with the total installed capacity equal or larger than load, is taken further for the overload test.
2. If there is overloaded line in the flow path obtained from previous test, then that flow path is discarded.
3. If there is substation with the disrupted voltages in the flow path obtained from previous test, then that flow path is discarded.

Test of overloaded lines in a flow path and voltages in the substations is performed using direct current (DC) model given in details in the section 4.3.1.

In the consistency tests it is assumed that the energy is delivered to the load only from the substations, where total installed capacity of generators is equal or larger compared to load. This assumption does not correspond to real power systems, where each generator have share of energy delivered to each load in a power system. Taking into account that all possible combinations of flow paths of all substations with the generators and loads are included in the model, it is postulated, that the model corresponds to the state of the real power system. This postulation is based on a fact that distributed generation (generation from multiple small generators) in most of the power systems have small share of total energy produced and the majority of the loads in separate substations are smaller than net installed power of the generators in the nodes.

Example of consistency test, for the system given on Figure 4-1 is given on Figure 4-4. Let the total installed capacity of generator in substation 2 is smaller than load in substation 1, line 2-4 is overloaded for specific flow path corresponding to energy delivery from substation 3 to substation 1 and voltage in substation 5 is higher than nominal in case of the failure of the line 1-3. In that case, only flow paths marked with the dark solid lines on Figure 4-4 are

accepted for fault tree construction. All other flow paths are discarded due to the lack of generator (black dashed lines, substation 4), smaller generation than load (green lines, substation 2), violated voltage (blue line from substation 6) or overload of the line (red dashed line between substation 2 and 4 shows overloaded line; red line between substations 2 and 3 is discarded too).

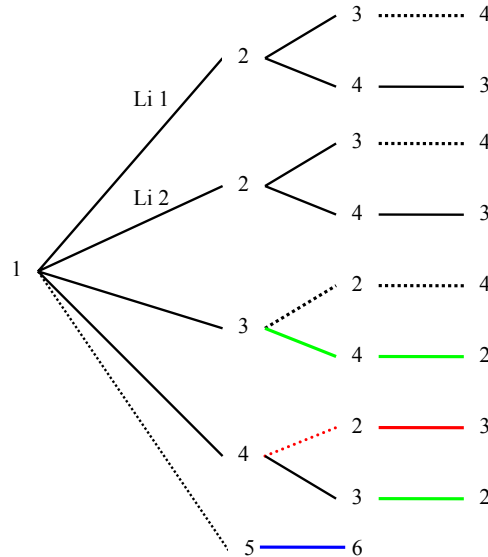


Figure 4-4 Discarded and accepted flow paths for test system

Flow paths accepted in previous test of consistency, are used in next step for the fault tree construction. The fault tree for each substation connected to a load, is created using the modular fault tree, shown on Figure 4-5 with the structure and the failure probabilities inserted depending on the elements modelled. Basic events (BE) marked in red squares are optional, depending on if there are CCF between lines or there are multiple generators in the substation.

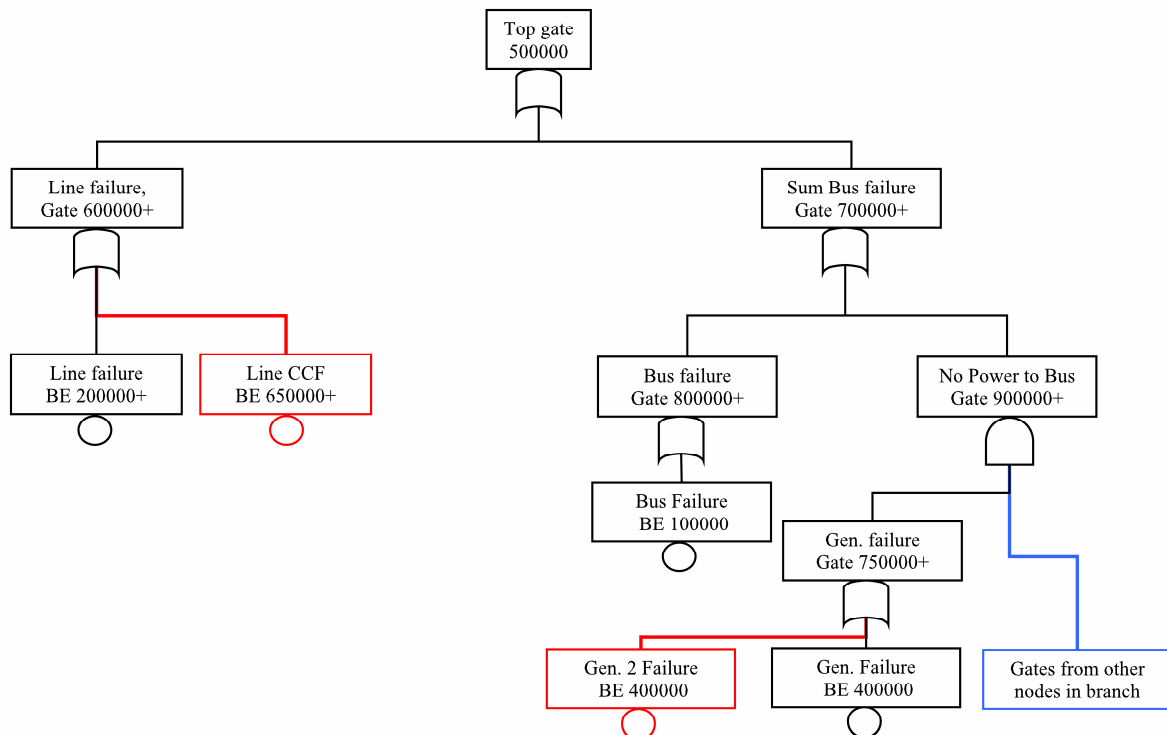


Figure 4-5 Modular fault tree used for fault tree construction

Procedure of building the fault tree includes following steps:

1. Add OR gate (top gate named 500000) corresponding to the failure of the power delivery to the substation.
2. If previously added gate is top gate exclude line failures gate, else add OR gate for those failures (named 600000 or above) and corresponding basic events for line failures and CCF of lines (named with the numbers starting from 200000 and 650000).
3. Add OR gate corresponding to substation failure (named with the numbers starting from 700000).
4. Add OR gates corresponding to substation failure (named with the numbers starting from 800000) and corresponding basic events (named with the numbers starting from 100000).
5. Add AND gate corresponding to failure to deliver energy to specific substation (named 900000 or above).
6. Add OR gates corresponding to generators failure in that substation (750000 and above) or no energy from other substations connected to that substation (500001 and above).
7. Go to step 2 until all energy flow paths are accounted.

If there are multiple generators in the substation, as described in the step 6 of the procedure, the failure of any of them will result with the failure of all generators in that substation. The variation of step 6 was tested, with the change of added gates (750000 and above) from OR type to AND type, and then adding OR gates (780000 and above) of all combinations of generators (comparable to Loss of Load Probability method³²) larger or equal to the load as shown on Figure 4-6. With this procedure more exact fault tree is constructed and deficiency identified in the consistency testing of the energy flow paths concerning generators is reduced. This approach wasn't selected in developed method as a result of the truncation limitations of the MCS identification module.

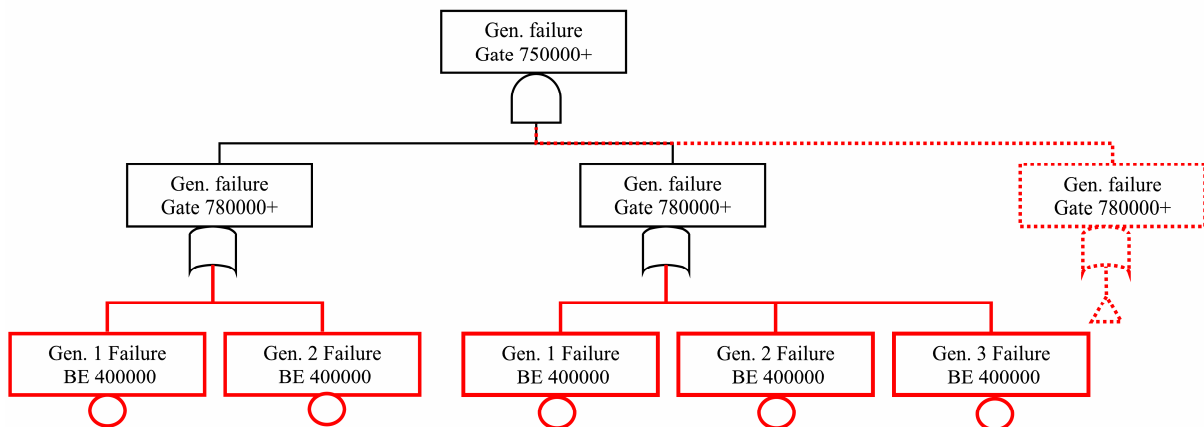


Figure 4-6 Optional construction of the generator failure gate

Common cause failures (CCF) of lines are modelled using the Beta factor⁸⁴. Part of fault tree built for substation 1 based on flow paths identified on Figure 4-4 is given on Figure 4-7. Branches of the fault tree marked with the blue dashed lines are developed further and are not given on Figure 4-7. Fault trees for all loads in the system are analyzed by computer code for fault tree analysis with a bottom up algorithm. Minimal cut sets (MCS) satisfying predefined cut-off, are identified. The default cut-off limit used for identification of MCS is either a limiting number of BE in a MCS, which should be eight or less, either limiting probability of calculated MCS, e.g. $Q_{MCS} < 10^{-14}$. During the analysis in certain cases the default cut-off has shown to be unsuitable and was changed in order to improve the number of identified MCS and obtained results. Quantitative analysis is performed according to the equations given in section 4.1.

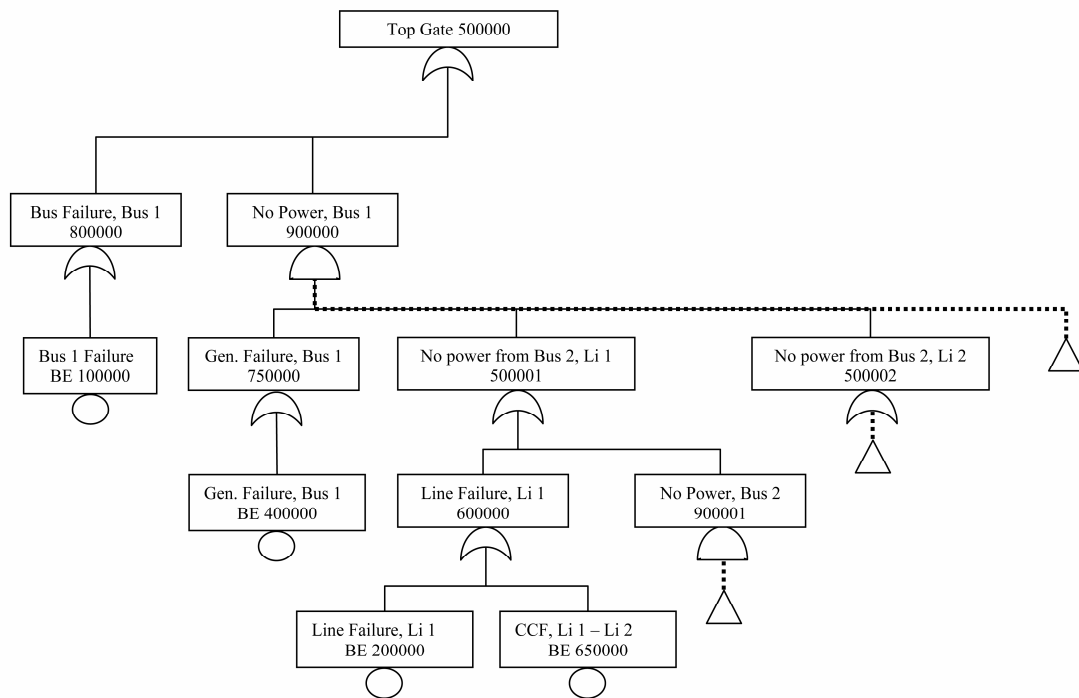


Figure 4-7 Part of the fault tree built for load 1 in the substation 1

The evaluation of the network reliability is a NP-hard problem³⁸ requiring processor power and memory allocation. Two major elements identify the size of the problem and the necessary processing time. The first is the size of the fault trees built for each of the loads in the system. Fault trees size depend on the number of substations (correlated to size of adjacency matrix), loads (number of generated fault trees), lines in the power system (related to number of possible energy flow paths) and size of the loads and generators and their disposition in the system (number of accepted flow paths accounting power transfer capabilities of the lines). Second element is efficiency of used fault tree analysis module and used truncation limits in the calculations and this element is most time-demanding and limiting in the method.

During the construction of the fault tree model for each of the substations in the system, the following important issues are considered:

- Logical looping was avoided by careful consideration of the flow paths.
- All ends of flow paths are considered in order not to double count contributions, modelled previously in the tree.

The verification of a proper fault tree modelling was done through examination of minimal cut sets of small test systems in sense:

- If all minimal cut sets are really minimal.
- If all expected minimal cut sets appear in their respective listing.

The results of the verification of the procedure, fault tree modelling and powerflow calculations are given in Appendix C.

4.2.2 Fault tree construction of substations

Example of a switching substation, consisting of load, two buses, four generators and three lines (top of the figure) together with the corresponding simplified model representation of the substation (down) is given on Figure 4-8.

Switching substations used in the model correspond to the substations in real power systems, which normally include several components as circuit breakers, protective relays, cut-out switches, disconnect switches, lightning arresters, fuses, transformers and other communication and protection equipment.

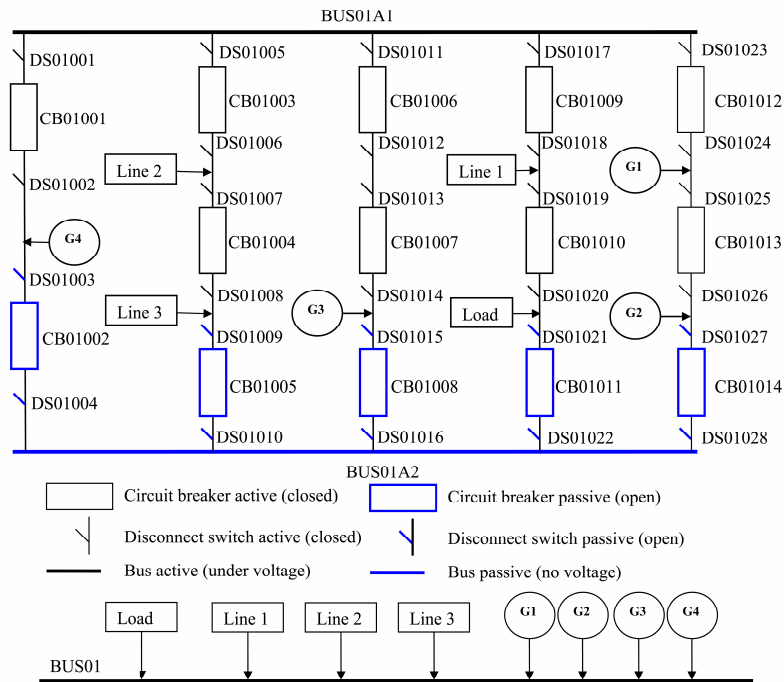


Figure 4-8 Example substation and simplified model of the substation

Complexity of the substation depends on its configuration (single bus, sectionalized single bus, breaker-and-a-half, double bus double breaker, and ring bus) and number of generators, lines and loads connected into it.

Before starting the building of the fault tree for the substation it's necessary to define the function it has in the power system and to identify events, which represent failure of the bus. One or more of the four major functions are realized through substations:

- Transfer of energy from generators to the system.
- Interconnection of lines and generators.
- Delivery of energy to loads.
- Protection of lines and substation elements from faults (short currents, lightning).

Additional functions (measurement of energy, integration of data and communications equipment and similar) are realized in substations but those function are irrelevant for the model. Protection equipment and its functions are also excluded from the analysis in order to decrease complexity of the model. The final model used for the representation of the substation, as given on Figure 4-8, accounts energy flow paths between lines, loads and generators. In the simplified substation representation, given on bottom of Figure 4-8, bus BUS01 failure will result with the interruption of energy delivery from generators and lines to load, disruption of power delivery from generators to lines and disruption of energy exchange between power lines. Disruption of energy delivery paths through elements of the substation is accounted during the construction of the fault tree.

Fault tree of simplified substation model on Figure 4-9 shows that the following events are considered in the model as substation failure:

- Failure of any generator and all lines to deliver energy to load resulting from the substation components failures.
- Failure of any generator to deliver energy to line due to the substation components failures.

- Failure of any line to deliver energy to another line as a result of the substation components failures.

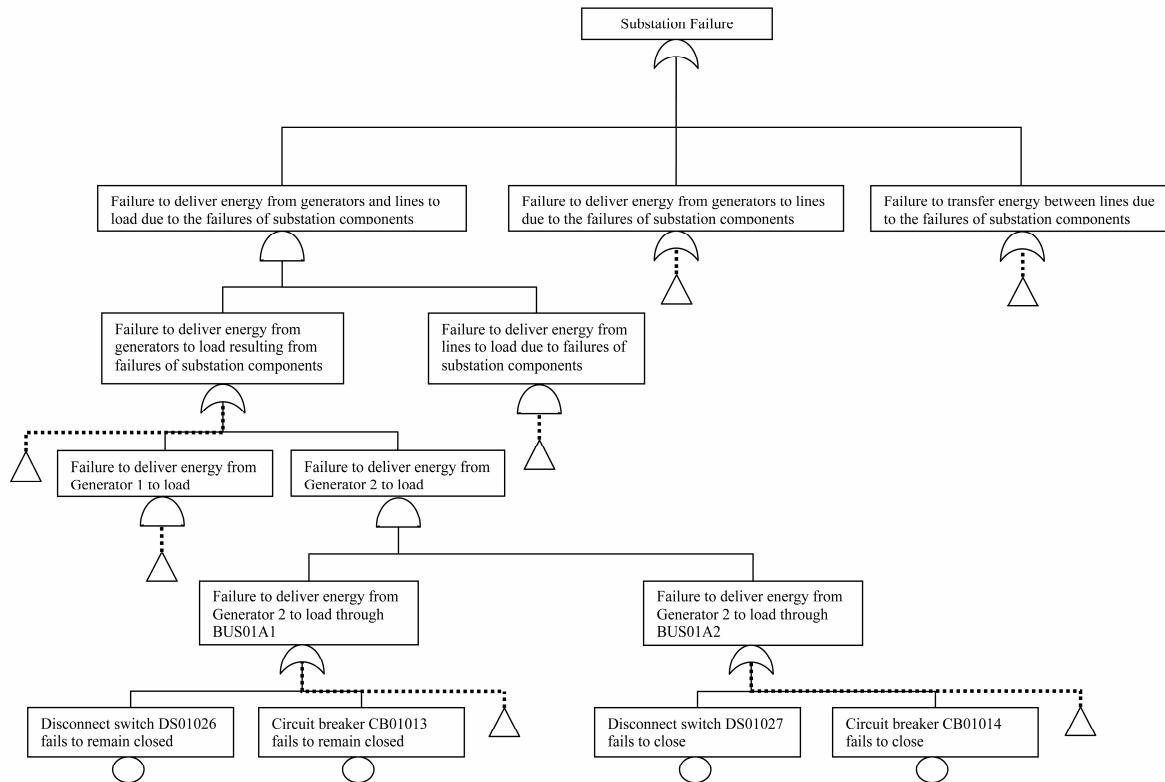


Figure 4-9 Fault tree for simplified substation representation

On Figure 4-9, gates are represented with the boxes with the logical operators, boxes with the circles represent basic events and triangles symbolize continuation of the model or transfer to other FT.

Type and number of events taken as substation failure in the model are conservative but they correspond to the simplified representation of the substation shown on Figure 4-8. Normal states of the circuit breakers and disconnect switches (normally open or normally closed) are assumed and modelled in the fault tree using two failure probabilities (active and passive) for each of the substation elements (fails to close, fails to remain closed), including the buses. Building of the fault trees and calculation of top event probability and corresponding importance measures is done using commercial software⁸⁵.

Configurations of the substations used in the analysis are given in Appendix B.

4.3 Approximate DC load flow model and line overload test

The approximate direct current (DC) power flow model is obtained from the alternating current (AC) power system model, approximating that voltages in all buses are equal to nominal, considering the differences of angles of voltages are very small and neglecting the losses in power system. DC power flow model gives a linear relationship between the power flows through the lines and the power injection at the nodes.

The principal information obtained from a power-flow study is the magnitude and the phase angle of the voltage at each bus and the real and reactive power flowing in each line. Obtained information can be used in further analyses complementary with the other methods for safety and reliability assessment.

The power-flow problem solving can be done using the bus admittance matrix Y_{bus} or the driving-point and transfer impedances that compose Z_{bus} . The starting point of the analysis is the single-line diagram of the system. Transmission lines are represented by their per-phase nominal π equivalent circuit for the medium length line⁸⁶. A medium length lines are roughly between 80 km and 240 km long. A medium length line can be represented sufficiently well by series resistance R and series inductance X as lumped parameters, as shown on Figure 4-13, with the half the capacitance to neutral of the line lumped at each end of the equivalent circuit. Shunt conductance G is usually neglected in overhead transmission lines when calculating voltage and current. The same circuit represents the short line if capacitors are omitted. The lumped parameter representation can be used for lines up to 320 km long.

If the total shunt admittance, usually pure capacitance, of the line is divided into two equal parts placed at the sending and receiving ends of the line, the circuit is called a nominal π as shown on Figure 4-12 and on Figure 4-13.

For each line numerical values for the series impedance Z and the total line-charging admittance Y (usually in terms of line-charging megavars at nominal voltage of the system) are necessary to determine all the elements of the $N \times N$ bus admittance matrix with the typical element Y_{ij} :

$$Y_{ij} = |Y_{ij}| \angle \delta_{ij} = |Y_{ij}| \cos \delta_{ij} + j |Y_{ij}| \sin \delta_{ij} = G_{ij} + jB_{ij} \quad (4.7)$$

Where:

Y_{ij} – Element i-j of the bus admittance matrix, measured in Siemens.

$|Y_{ij}|$ - The magnitude of the admittance matrix i-j element.

δ_{ij} – The phase of the admittance matrix i-j element.

G_{ij} – The conductance of the admittance matrix i-j element, measured in Siemens.

B_{ij} – The susceptance of the admittance matrix i-j element, measured in Siemens.

Other essential information includes transformer ratings and impedances, shunt capacitor ratings and transformer tap settings. In advance of each power-flow study to certain bus voltages and power injections must be given known values.

The voltage at a typical bus i of the system in polar coordinates is given by:

$$U_i = |U_i| \angle \theta_i = |U_i| (\cos \theta_i + j \sin \theta_i) \quad (4.8)$$

Where:

U_i – The voltage in bus i .

$|U_i|$ - The magnitude of the voltage in the bus i .

θ_i - The phase of the voltage in the bus i .

The voltage at another bus j is similarly written by changing the subscript from i to j . The net current injected into the network at bus i in terms of the elements Y_{in} of Y_{bus} is given by the summation:

$$I_i = Y_{i1}U_1 + Y_{i2}U_2 + \dots + Y_{iN}U_N = \sum_{n=1}^N Y_{in}U_n \quad (4.9)$$

Where:

I_i - The net current injected at bus i .

U_n - The voltage in bus n .

Y_{in} – The element i-n of the admittance matrix.

N - Number of buses in the system.

Let P_i and Q_i denote the net real and reactive power entering the network at the bus i . Then, the complex conjugate of the power injected at bus i is:

$$P_i - jQ_i = U_i^* \sum_{n=1}^N Y_{in}U_n \quad (4.10)$$

Where:

- P_i – The net active power injected at the bus i.
- Q_i - The net reactive power injected at the bus i.
- U_i^* – The conjugate of the voltage of the bus i.
- U_n - The voltage in bus n.
- Y_{in} – The element i-n of the admittance matrix.
- N- Number of buses in the system.

Entering substitution from Eq. (4.7) and (4.8) in Eq. (4.10) following relation is obtained:

$$P_i - jQ_i = \sum_{n=1}^N |Y_{in} U_i U_n| \angle \delta_{in} + \theta_n - \theta_i \quad (4.11)$$

Where:

- δ_{ij} – The phase of the admittance matrix i-n element.
- θ_i - The phase of the voltage in the bus i.

Expanding Eq. (4.11) and equating real and reactive parts following equation is obtained:

$$P_i = \sum_{n=1}^N |Y_{in} U_i U_n| \cos(\delta_{in} + \theta_n - \theta_i) \quad (4.12)$$

$$Q_i = - \sum_{n=1}^N |Y_{in} U_i U_n| \sin(\delta_{in} + \theta_n - \theta_i) \quad (4.13)$$

Equations (4.12) and (4.13), using Eq. (4.7) can be written as:

$$P_i = |U_i| \left[\sum_{n=1}^N |U_n| \cdot [G_{in} \cos(\theta_i - \theta_n) + B_{in} \sin(\theta_i - \theta_n)] \right] \quad (4.14)$$

$$Q_i = |U_i| \left[\sum_{n=1}^N |U_n| \cdot [G_{in} \sin(\theta_i - \theta_n) - B_{in} \cos(\theta_i - \theta_n)] \right] \quad (4.15)$$

$i = 1, N$

Equations (4.14) and (4.15) define Alternated Current (AC) model⁸⁷ for the net real P_i and reactive power Q_i entering the network at the bus i.

Let P_{gi} denote the scheduled power being generated at bus i and P_{di} denote the scheduled power demand of the load at that bus. Same notation goes for reactive power at bus i as shown on Figure 4-10.

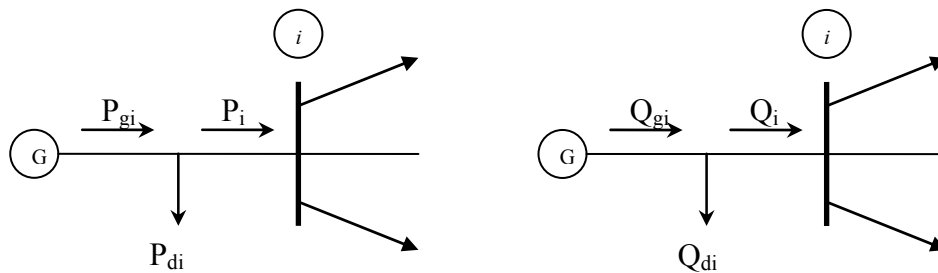


Figure 4-10 Notation for active and reactive power at a typical bus i in power flow studies

Net real and reactive power entering the network at the bus i is given by equations:

$$P_i = P_{gi} - P_{di} \quad (4.16)$$

$$Q_i = Q_{gi} - Q_{di} \quad (4.17)$$

$i = 1, N$

Where:

- P_i – The net active power injected at the bus i.
- P_{gi} – The active power generated at bus i.
- P_{di} - The scheduled power demand of the load at bus i.
- N- Number of buses in the system.

For all buses in the system, except for the slack bus, the values for scheduled power being generated at buses P_{gi} and Q_{gi} are given, together with the scheduled power demand of the loads P_{di} and Q_{di} . These values, using Eq. (4.16) and (4.17) define the net real and reactive power injected into the network.

Using input data, Eqs. (4.14) and (4.15) can be solved, obtaining the module and phase angle of voltages in all buses except the slack bus.

Calculated voltages of the buses can be used for calculation of power flows through lines in the power system, given by equations:

$$P_k = |U_t|^2 Y_{tl} \sin \rho_{tl} + |U_t| \cdot |U_l| \cdot |Y_{tl}| \sin(\theta_t - \theta_l - \rho_{tl}) \quad (4.18)$$

$$Q_k = |U_t|^2 Y_{tl} \cos \rho_{tl} - |U_t| \cdot |U_l| \cdot |Y_{tl}| \cos(\theta_t - \theta_l - \rho_{tl}) - \frac{|U_t|^2 P_k}{2} \quad (4.19)$$

$$\rho_{tl} = \arctg\left(\frac{R_k}{X_k}\right) \quad (4.20)$$

$$k = 1, M$$

Where:

k - The line between buses t-l.

P_k - The net active power flow through line k.

Q_k - The reactive power flow through line k.

$|U_t|$ - The magnitude of the voltage in the bus t.

$|Y_{t-l}|$ - The magnitude of the admittance matrix t-l element.

θ_t - The phase of the voltage in the bus t.

ρ_{tl} - The phase of the impedance.

R_k - The resistance of the line k.

X_k - The reactance of the line k.

M - number of lines in the system

System of equations given by Eqs. (4.14) and (4.15) is linear and it is solved with the iterative approaches (the Gauss-Seidel method and the Newton - Raphson method) but their major characteristic of them is slow calculation time and problems with the convergence⁸⁶.

Major characteristic of approximate methods for power flow calculations is linear approximation of the Eqs. (4.14) and (4.15), modifying the problem on level to be solvable fast without iterations, and with the small demand for computer memory and processor power.

4.3.1 Direct current (DC) model

The DC power flow model greatly simplifies the calculations by making a number of approximations including:

1. Exclusion of the reactive power balance equations from analysis.
2. Assumption that all substations voltages are equal to one per unit.
3. The losses of the interconnections are neglected.

The named approximations presented as equations will be:

$$|U_i| \approx 1 pu; \quad i = 1, N \quad (4.21)$$

$$\sin(\theta_i - \theta_k) \approx \theta_i - \theta_k; \quad i = 1, N; k = 1, N \quad (4.22)$$

$$\cos(\theta_i - \theta_k) \approx 1; \quad i = 1, N; k = 1, N \quad (4.23)$$

Where:

$|U_i|$ - The magnitude of the voltage in the bus i.

θ_i - The phase of the voltage in the bus i.

Approximation given by Eq. (4.21) states that the magnitude voltage in all buses in the analyzed system is equal to nominal voltage, well corresponding for normal regime balanced networks. Equations (4.22) and (4.23) state that difference in angles (phase) of voltages in high voltage networks is very small and this approximation correspond to the state in the real systems^{88,89}.

Substituting approximations given by Eqs. (4.21), (4.22) and (4.23) in Eq. (4.14), following simplified equation is obtained for net real injected power at buses:

$$P_i = \sum_{n=1}^N [G_{in} + B_{in}(\theta_i - \theta_n)] = \sum_{n=1}^N G_{in} + \theta_i \sum_{n=1}^N B_{in} - \sum_{n=1}^N B_{in} \theta_n \quad (4.24)$$

$i = 1, N$

Where:

P_i – The net active power injected at the bus i .

N - Number of buses in the system.

G_{in} – The conductance of the admittance matrix i - n element.

B_{in} – The susceptance of the admittance matrix i - n element.

θ_i - The phase of the voltage in the bus i .

If there are no shunt active resistance in the network, accounting the definition of matrixes $[G]$ and $[B]$ of the conductances and susceptances of lines in network the following result is obtained:

$$\sum_{n=1}^N B_{in} = 0 \quad \sum_{n=1}^N G_{in} = 0 \quad i = 1, N \quad (4.25)$$

Following relation is obtained from the substitution of Eq.(4.25) in Eq. (4.24):

$$P_i = \sum_{n=1}^N [-B_{in}] \theta_n \quad i = 1, N \quad (4.26)$$

Improved results are obtained if the series active resistance of the network elements is neglected^{88,89} during the formation of matrix $[B]$ of lines susceptances.

The relation between net injected reactive power and voltages is obtained following the same procedure:

$$[Q_i] = [-B][U] \quad (4.27)$$

$i = 1, N$

Where:

$[Q_i]$ – The matrix of the injected reactive powers in the buses.

$[B]$ – The matrix of susceptances of lines.

$[U]$ – The matrix of the voltages in the buses.

Unknown angles of voltages in linear system of Eq. (4.26) are calculated as:

$$[\theta] = [Z][P_i] \quad (4.28)$$

Where:

$$[Z] = [-B]^{-1} \quad (4.29)$$

Where:

$[\theta]$ – The matrix of the voltage phases.

$[Z]$ – The matrix of the network impedances.

If approximations given by Eqs. (4.21), (4.22) and (4.23) are introduced in Eq. (4.18) then active power flow in line k between buses (t - l) will be:

$$P_{bk} = Y_{tl}(\theta_t - \theta_l) = \frac{\theta_t - \theta_l}{X_k} \quad (4.30)$$

$k = 1, M$

Where:

P_{bk} – The real (active) power flow through line k.

X_k – The reactance of the line k between buses t-l.

θ_t - The phase (angle) of the voltage in the bus t.

Equation (4.30) states that active power flow in line depends only on line impedance and difference of the voltage angles on both ends of line.

4.3.2 Relation between line power flows and injected power of generators

Correlation of the matrix of difference of the voltage angles of lines and voltage angles in buses is given in form:

$$[\theta_b] = [A]^T [\theta] \quad (4.31)$$

Where:

$[\theta_b]$ - The matrix of difference of voltage angles of lines.

$[A]$ – The adjacency matrix of the network.

$[\theta]$ - The matrix of voltage angles in buses of network.

Accounting Eq. (4.30), the active power flows through lines can be written in matrix form as:

$$[P_b] = [Y_b][\theta_b] \quad (4.32)$$

Where:

$[P_b]$ – The matrix of net real (active) power flows through interconnections.

$[Y_b]$ – The admittance matrix of the network.

$[\theta_b]$ - The matrix of difference of voltage angles in lines.

With the substitution of $[\theta_b]$ from Eq. (4.31) and $[\theta]$ from Eq. (4.28) into (4.32):

$$[P_b] = [Y_b][A]^T [Z][P_i] \quad (4.33)$$

Where:

$[A]^T$ – The transpose adjacency matrix of the network.

$[Z]$ – The impedance matrix of the network.

$[P_i]$ – The matrix of injected active power in the buses of the network.

Substituting $[P_i]$ from Eq. (4.16), Eq. (4.33) transforms into:

$$[P_b] = [Y_b][A]^T [Z][[P_g] - [P_d]] \quad (4.34)$$

Where:

$[P_g]$ – The matrix of the active power generated at the buses.

$[P_d]$ - The matrix of the power demand of the load at the buses.

With the introduction of the approximation^{88, 89} that power of loads in all buses of system is proportional to the sum power of the system P_s (equal to the sum of all loads in system), independently of the size of P_s matrix $[P_d]$ can be written in form:

$$[P_d] = [\alpha]P_s \quad (4.35)$$

Where:

P_s – The sum of the power system load active power.

$[\alpha]$ – The matrix of the loads share in the summary system load.

Elements of matrix $[\alpha]$ are defined as:

$$\alpha_i = \frac{P_{di}}{P_s} \quad (4.36)$$

$i = 1, N$

Data for load distribution is included in the input data, therefore the elements of matrix $[\alpha]$ are defined.

As stated previously, line losses are neglected in DC model, therefore:

$$P_{gs} = P_s \quad (4.37)$$

Where:

P_{gs} – The sum of generated active power in the system.

The P_{gs} , total power generated by the generators in the system, is given as:

$$P_{gs} = [L]^T [P_g] \quad (4.38)$$

Where:

[L] – The matrix column with the dimensions (Nx1) and elements equal to 1.

Introducing the Eqs. (4.36), (4.37) and (4.38) in Eq. (4.35), matrix $[P_d]$ of the power demand of the load at the buses is obtained as:

$$[P_d] = [\alpha][L]^T [P_g] \quad (4.39)$$

Substituting Eq. (4.39) in (4.34), following relation is obtained for power flows through lines:

$$[P_b] = [Y_b] \cdot [A]^T \cdot [Z] \cdot [E] - [\alpha][L]^T \cdot [P_g] \quad (4.40)$$

Equation (4.40) defines relation between power flows through lines and power of generators and can be written in form:

$$[P_b] = [H] \cdot [P_g] \quad (4.41)$$

Where:

$$[H] = [Y_b] \cdot [A]^T \cdot [Z] \cdot [E] - [\alpha][L]^T \quad (4.42)$$

Matrix $[H]$ given by Eq. (4.42) have dimensions (MxN). Taking account that not all buses have generators, matrix $[P_g]$ is sparsely filled. With the reduction of matrixes $[H]$ and $[P_g]$, multiplication with the zero elements is avoided in Eq. (4.41).

Dimensions of the matrix $[H]$ after reduction are (MxNG), including only columns corresponding to buses with the generators.

4.3.3 Calculation of the elements of the matrix [H]

Calculation of the elements of the matrix $[H]$ can be done using relation given by Eq. (4.42).

This approach, accounting that matrixes $[A]$ and $[Y_b]$ are sparsely filled, is unproductive.

The relation for the matrix $[H]$ given by Eq. (4.42) can be written in form:

$$[H] = [W] \cdot [F] \quad (4.43)$$

Where:

$$[W] = [Y_b][A]^T [Z] \quad (4.44)$$

$$[F] = [E] - [\alpha][L]^T \quad (4.45)$$

Matrix $[Y_b]$ is diagonal matrix with the elements equal to lines admittances given as:

$$Y_{ii} = \frac{1}{X_i} \quad (4.46)$$

$$Y_{ij} = 0; j \neq i$$

$$i = 1, M; j = 1, M$$

Where:

X_i – The reactance of the line i .

Transpose adjacency matrix $[A]^T$ is sparsely filled matrix, giving information about interconnection of the buses with the lines.

Taking notation that the lines are directed from bus with the smaller to bus with the larger index, elements of row l of matrix $[A]$ corresponding to line $l(m-n)$ are:

$$A_{lj} = 0; j = 1, N; j \neq m; j \neq n$$

$$A_{im} = 1; A_{in} = -1; (m < n) \quad (4.47)$$

Elements of the matrix [F] are:

$$F_{ij} = -\alpha_i; j = 1, N; j \neq i$$

$$F_{ii} = 1 - \alpha_i; i = 1, N \quad (4.48)$$

With the substitution and multiplication in the Eq. (4.44) following relation is obtained for the elements of the matrix [W]:

$$W_{lj} = \frac{(Z_{mj} - Z_{nj})}{X_l}; j = 1, N \quad (4.49)$$

The relation for calculation of the elements of matrix [H] is obtained with the substitution of Eqs. (4.48) and (4.49) in (4.43), as:

$$H_{lj} = \frac{Z_{mj} - Z_{nj}}{X_l} - \sum_{i=1}^N \frac{\alpha_i (Z_{im} - Z_{in})}{X_l}; l = 1, M \quad (4.50)$$

Sum on the right side of the Eq. (4.50) is constant for all elements of row l, therefore Eq. (4.50) can be written as:

$$H_{lj} = \frac{Z_{mj} - Z_{nj}}{X_l} - S_l; j = 1, NG, l = 1, M$$

$$S_l = \sum_{i=1}^N \frac{\alpha_i (Z_{im} - Z_{in})}{X_l} \quad (4.51)$$

Where:

H_{lj} – The element l-j of the matrix [H].

Z_{mj} – The element m-j of the impedance matrix [Z].

S_l – The element l of the assisting matrix [S].

4.3.4 Modifications of the matrix [H]

Line failures and change of the load distribution result in change of the elements of matrix [H]. Elements of matrix [H] can be calculated using Eq. (4.51) but this approach is inefficient from the aspect of the calculation time. Therefore, several procedures for correction of the elements of the matrix [H] are developed in case of line failure or addition of new line, improving the calculations.

The matrix [Z] in case of line failure or addition of new line is changed resulting with the change of matrix [H].

New matrix [Z] resulting from new state of the system can be obtained from matrix [Z] of the previous state using relation:

$$[Z'] = [Z] + [DZ] \quad (4.52)$$

In the case of failure or switch off of the line k(l-t) elements of correction matrix [DZ] can be obtained using relation:

$$DZ_{ij} = -\frac{(Z_{ti} - Z_{li})(Z_{tj} - Z_{lj})}{ZVPQ} \quad (4.53)$$

$$i = 1, N; j = 1, N$$

Where:

$$ZVPQ = Z_{tt} + Z_{ll} - 2Z_{tl} - X_k \quad (4.54)$$

The Eq. (4.53) in case of the addition of new line k(l-t) to the system, will change in the term ZVPQ calculated as:

$$ZVPQ = Z_{tt} + Z_{ll} - 2Z_{tl} + X_k \quad (4.55)$$

Correction of the matrix [H] is done using matrix [DH] and following relation:

$$[H'] = [H] + [DH] \quad (4.56)$$

Making the substitution from Eq. (4.43) and (4.44):

$$[DH] = [Y_b][A]^T[Z][F] \quad (4.57)$$

Elements of matrix [DH] are calculated with the expression:

$$DH_{lj} = -\frac{DZ_{mj} - DZ_{nj}}{X_l} - \sum_{i=1}^N \frac{\alpha_i(DZ_{im} - DZ_{in})}{X_l}; l = 1, M \quad (4.58)$$

Sum on the right side of the Eq. (4.58) is constant for all elements of row l , therefore equation can be written as:

$$DH_{lj} = -\frac{DZ_{mj} - DZ_{nj}}{X_l} - DS_l; j = 1, NG$$

$$DS_l = \sum_{i=1}^N \frac{\alpha_i(DZ_{im} - DZ_{in})}{X_l} \quad (4.59)$$

Elements of k^{th} row of the matrix $[H']$ have zero values resulting from setting $X_l = \infty$ corresponding to the switching off of the line l in the system.

$$[H'_{lj}] = 0; j = 1, NG \quad (4.60)$$

4.3.5 Modifications of the matrix [H] in case of the load failure

Load failure of one or more loads result with the change of overall distribution of the load in the system resulting with the change of the matrix $[\alpha]$:

$$[\alpha'] = [\alpha] + [D\alpha] \quad (4.61)$$

Where:

$[\alpha']$ – The final matrix of the share of the loads in total system load.

$[\alpha]$ – The matrix of the share of the loads in total system load.

$[D\alpha]$ – The matrix of the change of the share of the loads in summary system load.

Changes of the matrix $[\alpha]$ results in the changes of the matrix $[F]$:

$$[F'] = [E] - ([\alpha] + [D\alpha])[L]^T \quad (4.62)$$

Equation (4.62) can be written as:

$$[F'] = [F] + [DF] \quad (4.63)$$

Where:

$$[DF] = [D\alpha][L]^T \quad (4.64)$$

Where:

$[L]$ – The matrix column with the dimensions (Nx1) and elements equal to 1.

Equation (4.64) defines elements of the matrix $[DF]$ with the relation:

$$DF_{ij} = \alpha'_i - \alpha_i \quad (4.65)$$

$i = 1, N; j = 1, N$

Elements of the matrix $[H']$ are obtained from Eq. (4.56) and values of $[DH]$ calculated as:

$$[DH] = [Y_b] \cdot [A] \cdot [Z] \cdot [DF] \quad (4.66)$$

Replacing values of $[DF]$ defined by Eq. (4.65) in the Eq. (4.66), values of $[DH]$ are obtained as:

$$DH_{lj} = -\frac{1}{X_l} \sum_{i=1}^N (\alpha'_i - \alpha_i)(Z_{im} - Z_{in}) \quad (4.67)$$

$l = 1, M$

Where:

DH_{lj} – The element l-j of the correction matrix [DH].

X_l – The reactance of the line l.

Z_{im} – The element i-m of the impedance matrix [Z].

α_i – Share of the load i in total system load.

α'_i – Correction of the load i share.

Equation (4.67) shows that values of DH for same row l are equal resulting with the fast and efficient correction of matrix [H].

4.3.6 Network separation resulting from the line failure

For the system shown on Figure 4-11, failure of line k(l-t) result with the system separation on two independent parts. For indication of network separation the ZVPQ is used, calculated with the Eq. (4.54).

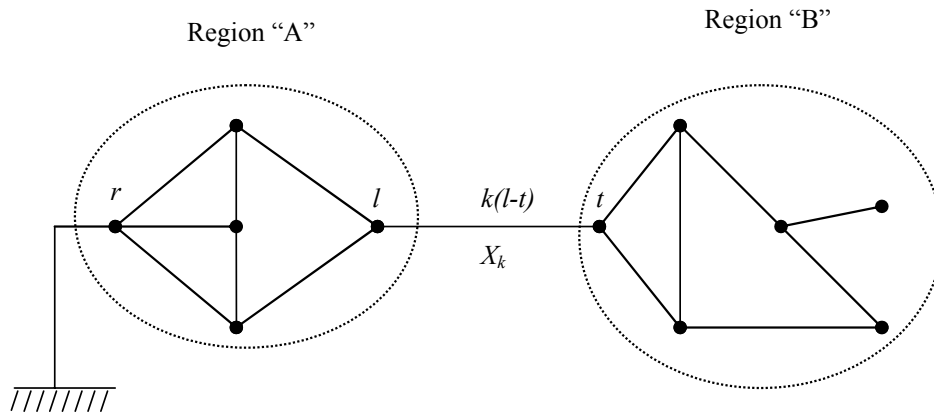


Figure 4-11 Two regions system

In case of network separation due to line k failure following relation is satisfied:

$$Z_{tt} + Z_{ll} - 2Z_{tl} = X_k \quad (4.68)$$

Where:

Z_{tt} – The element t-t of the impedance matrix [Z].

X_k – The reactance of the line k.

Therefore:

$$ZVPQ = Z_{tt} + Z_{ll} - 2Z_{tl} - X_k = 0 \quad (4.69)$$

As a result of finite arithmetic's and rounding errors, the ZVPQ may be different from zero but still near that value, indicating separation of the network.

If ZVPQ indicate separation of the network, then it's necessary to identify buses, constituting separated part of the network, shown as Region "B" on Figure 4-11.

If network is separated, due to the line failure, then, accounting Eq. (4.53), it is necessary to divide with the ZVPQ, resulting in division by zero.

For those buses, for which dividend is different from zero:

$$Z_{ii} - Z_{li} \neq 0 \quad (4.70)$$

the infinite input impedance is obtained, indicating that buses are located in the separated Region "B" of the network.

For those buses, for which dividend is equal to zero:

$$Z_{ii} - Z_{li} = 0 \quad (4.71)$$

the term 0/0 is obtained for element of $[DZ]$ matrix, and the input impedance remains the same as before line k(l-t) failure.

Comparison of the subtraction terms given by Eqs. (4.70) and (4.71) is normally done using value near but not exactly equal to zero.

4.3.7 Separated model of the power system

Power flows of active and reactive power in the power system can be calculated from voltages of buses in the system.

Nominal π circuit of a medium-length transmission line is given on Figure 4-12.

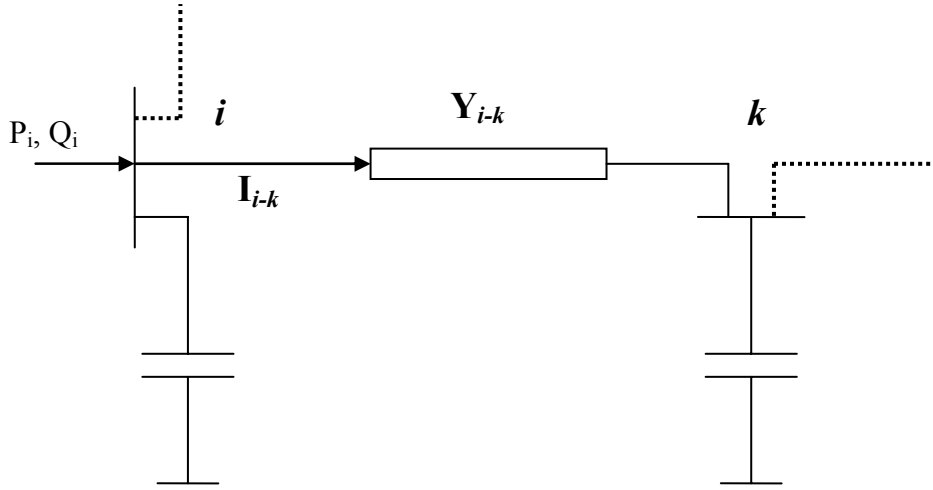


Figure 4-12 π circuit of a medium-length transmission line

Current flowing from bus i to bus k is given as:

$$\underline{I}_{i-k} = \underline{Y}_{i-k} (\underline{U}_i - \underline{U}_k) \quad (4.72)$$

Where:

\underline{I}_{i-k} - Current (complex) from bus i to bus k.

\underline{Y}_{i-k} - Admittance (complex) of the line i-k.

\underline{U}_i - Voltage (complex) in the bus i.

Using Eq. (4.72), the power flowing from bus i to bus k is given as:

$$\underline{S}_{i-k} = \underline{U}_i \underline{I}_{i-k}^* = \underline{U}_i^2 \underline{Y}_{i-k}^* - \underline{Y}_{i-k}^* \underline{U}_i \underline{U}_k^* \quad (4.73)$$

Where:

\underline{S}_{i-k} - Power (complex) flowing from bus i to bus k.

\underline{I}_{i-k}^* - Conjugate (complex) of the current flowing from bus i to bus k.

\underline{U}_i - Voltage (complex) in bus i.

With the introduction of the substitutions:

$$\underline{U}_i = |U_i| \angle \theta_i = |U_i| (\cos \theta_i + j \sin \theta_i) = U_i \exp(j\theta_i) \quad (4.74)$$

$$\underline{Y}_{i-k} = Y_{i-k} \exp \left[-j \left(\frac{\pi}{2} - \delta_{i-k} \right) \right] \quad (4.75)$$

in Eq. (4.73), the following result is obtained:

$$P_{i-k} = Y_{i-k} U_i^2 \sin \alpha_{i-k} + Y_{i-k} U_i U_k \sin(\theta_i - \theta_k - \delta_{i-k}) \quad (4.76)$$

$$Q_{i-k} = Y_{i-k} U_i^2 \cos \alpha_{i-k} - Y_{i-k} U_i U_k \cos(\theta_i - \theta_k - \delta_{i-k}) \quad (4.77)$$

Where:

P_{i-k} - The net real (active) power flow through line i-k.

Q_{i-k} - The reactive power flow through line i-k.

Y_{i-k} - The magnitude of the admittance of the line i-k.

U_i - The magnitude of the voltage in the bus i.

θ_i - The phase of the voltage in the bus i.

δ_{i-k} - The phase of the admittance of the line i-k.

Kirchhoff's First Law states that the sum of currents entering a junction equals the sum of currents leaving, resulting in the following relations for powers:

$$P_i = \sum_{\substack{k=1 \\ k \neq i}}^N P_{i-k} \quad (4.78)$$

$$Q_i = \sum_{\substack{k=1 \\ k \neq i}}^N Q_{i-k} - Q_i^c \quad (4.79)$$

Where:

P_i - The net real (active) power injected at bus i.

P_{i-k} - The net real (active) power flow through line i-k.

Q_i - The reactive power injected at bus i.

Q_{i-k} - The reactive power flow through line i-k.

Q_i^c - Sum capacitive reactive power of all lines connected to node i.

N - The number of the buses in the network.

For a high voltage network, the following approximations^{88,89} can be introduced:

$$\delta_{i-k} \approx 0 \quad (4.80)$$

$$\sin(\theta_i - \theta_k) \approx \theta_i - \theta_k \quad (4.81)$$

$$|U_i| \approx U_n, i = 1, N \quad (4.82)$$

If approximations given by Eqs. (4.80) and (4.81) are introduced in Eq. (4.76), the following relation for active power flows is obtained:

$$P_{i-k} = B_{i-k} U_i U_k (\theta_i - \theta_k) \quad (4.83)$$

B_{i-k} - The susceptance of the line i-k.

On the basis of Eqs. (4.78) and (4.83), the following result is obtained for injected active power in node i:

$$P_i = U_n^2 \left[\sum_{\substack{k=1 \\ k \neq i}}^N B_{i-k} \theta_i - \sum_{\substack{k=1 \\ k \neq i}}^N B_{i-k} \theta_k \right] \quad (4.84)$$

Equation (4.84) is satisfied for each node, therefore it can be written in matrix form:

$$[P'] = U_n^2 [B'] \cdot [d\theta'] \quad (4.85)$$

Where:

$[P']$ - The matrix of the active power injected into buses.

U_n - The nominal voltage of the network.

$[B']$ - The matrix of the network susceptance.

$[d\theta']$ - The matrix of the differences of voltage angles (phases).

The equation (4.84) shows that diagonal elements of matrix $[B']$ are equal to the negative sum of non-diagonal elements resulting with the singularity of matrix $[B']$. The sum of all injected

power in node is equal to zero corresponding the fact that losses are neglected resulting with the equality between power of generators and power of loads in the system.

As a result of the singularity of the matrix $[B']$, for given injected power, $[P']$, only difference of the voltage angles (but not their actual value) from slack bus can be calculated.

Using Eq. (4.85), the angle differences are calculated and those values are substituted in the Eq. (4.83) in order to calculate active power flows.

With the introduction of the approximation:

$$\cos(\theta_i - \theta_k) \approx 1 \quad (4.86)$$

and substitution of Eqs. (4.80) and (4.86), Eq. (4.77) transforms into:

$$Q_{i-k} = B_{i-k} U_i^2 - B_{i-k} U_i U_k \quad (4.87)$$

Where:

Q_{i-k} - The reactive power flow through line i-k.

B_{i-k} - The susceptance of the line i-k.

U_i - The magnitude of the voltage in the bus i.

Replacing Eq. (4.87) in Eq. (4.79), the following relation is obtained for injected reactive power:

$$Q_i + Q_k^c = U_i^2 \sum_{\substack{k=1 \\ k \neq i}}^N B_{i-k} - U_i \sum_{\substack{k=1 \\ k \neq i}}^N B_{i-k} U_k \quad (4.88)$$

If products of squares with the voltage differences, given by Eq. (4.88), are neglected and introduction of the following relation for the bus voltages:

$$U_j = U_n + \Delta U_j; j = 1, n \quad (4.89)$$

Where:

U_j - The magnitude of the voltage in the bus j.

U_n - The nominal voltage of the network.

ΔU_j - The difference of the magnitude of the voltage in the bus j from the nominal voltage.

The following relation is obtained:

$$Q_i + Q_i^c = U_n \sum_{\substack{k=1 \\ k \neq i}}^n B_{i-k} \Delta U_i - U_n \sum_{\substack{k=1 \\ k \neq i}}^n B_{i-k} \Delta U_k \quad (4.90)$$

On the basis of Eq. (4.90), the following matrix relation can be written:

$$[Q'] + [Q^c] = U_n [B'] \cdot [\Delta U'] \quad (4.91)$$

Where:

$[Q']$ - The matrix of the reactive power injected into buses.

$[Q^c]$ - The matrix of the sum reactive powers of lines connected to corresponding node.

U_n - The magnitude of the nominal voltage of the network.

$[B']$ - The matrix of the network susceptance.

$[\Delta U']$ - The matrix of the differences of voltage angles (phases).

Matrix $[B']$ is the same as used for active power calculations in Eq. (4.85).

Using Eq. (4.91) the voltage difference of the voltages in the nodes compared to slack node can be calculated. Using calculated voltages, using Eq. (4.87), flows of reactive power through lines can be calculated. Equations (4.91) and (4.85) define separated model of the network, with the split calculations of the active and reactive power flows.

4.3.8 Improvement of the reactive power flow calculations

As a result of the singularity of the matrix $[B']$, the losses of the reactive power in Eq. (4.91) are not included. The losses of reactive power can't be neglected, especially in regimes of maximum load, which are most critical from the aspect of reliability. Therefore, the improvement of calculations of reactive power flows and inclusion of losses in those calculations, is needed.

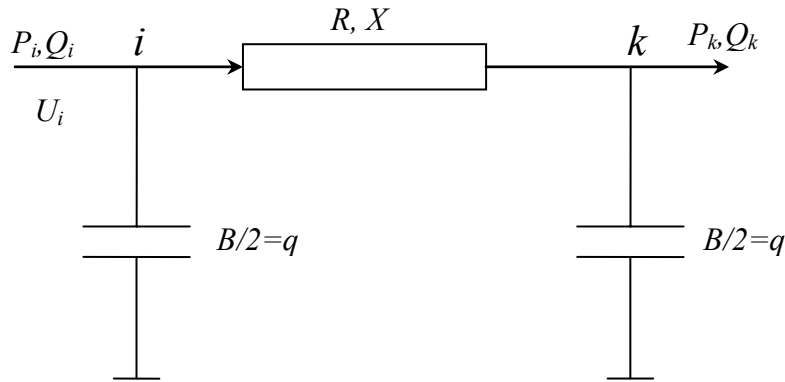


Figure 4-13 Equivalent circuit of a medium-length line

The q is equivalent reactive power generated from line between nodes i and k , calculated using relation:

$$q = \frac{\Delta Q_c - \Delta Q_x}{2} \quad (4.92)$$

Where:

$$\Delta Q_x = X \left(\frac{P_{i-k}}{U_n} \right)^2 \quad (4.93)$$

$$\Delta Q_c = BU_n^2 \quad (4.94)$$

Where:

X – The line i - k reactance.

U_n – The magnitude of the nominal voltage.

P_{i-k} – The active power flow through line i - k .

B – The line i - k susceptance.

From equivalent circuit of a line given on Figure 4-13, the following relation is obtained:

$$Q_i + q + \frac{R}{X} P_{i-k} - \frac{U_n \Delta U_{i-k}}{X} = 0 \quad (4.95)$$

Where:

Q_i – The injected reactive power at node i .

q – The reactive power generated from line between nodes i and k .

R – The resistance of the line between nodes i and k .

X – The reactance of the line between nodes i and k .

P_{i-k} – The active power flow between nodes i and k .

U_n – The magnitude of the nominal voltage.

ΔU_{i-k} – The difference of the magnitude of the voltage between nodes i and k .

Equation (4.95) is satisfied for all branches of the network including transformers with the capacity equal to zero.

Equation (4.95) can be represented in a matrix form as:

$$[Q_{gi}] - [Q_{di}] + [q] + [A] \cdot [B_b] \cdot [R_b] \cdot [P_b] - U_n [B] \cdot [\Delta U] = 0 \quad (4.96)$$

Where:

$[Q_{gi}]$ - The matrix of the generated reactive power in corresponding buses.

$[Q_{di}]$ - The matrix of the reactive power demand in corresponding buses.

$[q]$ - The matrix of the generated reactive power from the lines.

$[A]$ - The adjacency matrix.

$[B_b]$ - The lines reactance matrix.

$[R_b]$ - The lines resistance matrix.

$[P_b]$ - The matrix of the active power flow through lines.

U_n - The magnitude of the nominal voltage.

$[B]$ - The lines susceptance matrix.

$[\Delta U]$ - The matrix of the difference of the magnitude of the voltage compared to nominal.

The Eq. (4.96) can be rewritten in the form:

$$[Q] - U_n [B] \cdot [\Delta U] = 0 \quad (4.97)$$

Where:

$$[Q] = [Q_{gi}] - [Q_{di}] + [q] + [A] \cdot [B_b] \cdot [R_b] \cdot [P_b] \quad (4.98)$$

Equation (4.97) represents more exact model for flows of reactive power and voltages compared to Eq. (4.91).

Solving the Eq. (4.97), the voltage differences $[\Delta U]$ used for calculation of the reactive power flows are obtained.

4.3.9 Line overload and substation voltage test

Using the approximate DC flow method presented in the previous chapters, the flows of power (active and reactive) through lines and the voltages in the substations are calculated for normal and for the single line failure regimes.

In the calculations of the continuous load ratings of the line, the reactive power flows through line are accounted as:

$$P_{line} = \sqrt{P_{th}^2 - Q_{flow}^2} \quad (4.99)$$

Where:

P_{line} - Continuous load rating of the line.

P_{th} - Thermal load rating of the line.

Q_{flow} - Maximum reactive power flow through line.

Thermal load rating of the line P_{th} is updated with the ambient temperature, multiplying it with the correction factor defined as:

$$k_{corr} = \sqrt{\frac{80 - T_{amb}}{40}} \quad (4.100)$$

Where:

k_{corr} - Correction factor for continuous load rating.

T_{amb} - The ambient temperature in C° .

Using updated continuous load rating, the lines are tested with the power flows calculated in simulations, identifying the lines that have flows larger than rating given with the Eq. (4.99).

Identified overloaded lines are stored in matrixes: pprgr(overloaded line), nppgr(counter) and prgr(percentage of overload). The substation voltages are compared to predefined nominal values and those, who are outside predefined nominal range, are identified and stored in

matrixes n_{ap} (substation with the voltage problem), n_{map} (counter), p_{nap} (voltage in substation). These matrixes are used for checking overload lines and voltages in flow paths.

The procedure for consistency testing contains the following steps:

1. Compare flows through the lines that constitute tested flow path, with the continuous load rating of those lines, when lines, which are not included in the flow path fail (single line failure).
2. If overloaded line is found in step 1, then discard that flow path and check next flow path.
3. Check, if there are violated voltages (outside predetermined nominal range) in the substations constituting flow path, when lines, that are not included in the flow path, fail.
4. If flow path passes overload and voltage tests, accept it for the fault tree construction.
5. Go to step 1, until all flow paths are checked.

The voltage consistency test described in the step 3 of the procedure can be omitted from the test procedure. Namely, the application of the voltages consistency tests for specific power systems configurations results in a large increase of the unreliability of the power delivery resulting from the discarded energy flow paths. This is case for the power system configurations with the non-uniform distribution of the generated and consumed reactive power, resulting with substations voltages outside the nominal range. The voltage consistency test for these power system configurations can be omitted from the test procedure.

Many power systems are built or have been designed with the relatively strong transmission network. When analysis is done to those systems⁴³, several modifications are made in order to weaken the system for conducting the transmission reliability studies. Those modifications are mostly connected with the disconnection of multiple lines in the power system. With the disconnection of lines, the overall structure and power flows within the system are changed, not corresponding to flows in a real system. In the proposed method, the power flows in normal and single line failure regime are accounted together with the voltages in the substations. Only selected energy paths are accounted in the fault tree construction discarding those, which are overloaded, as a result of limitations of transfer capacity or violated voltages. Discarded flow paths depending on power flows have direct implication on reliability of power delivery and on overall power system reliability (a smaller number of flow paths results in a smaller number of alternative power delivery paths and increased unreliability). Reduction of the number of flow paths reduces the number of gates in a fault tree and the fault tree size.

4.4 Description of the computer code

A computer code was developed on the basis of the method described in the previous chapters. The code was created in the Compaq Visual Fortran Professional Edition v 6.0.0 environment, and it includes 4622 lines. The Figure 4-14 shows the block diagram of the code. The first step of the code includes the subroutines for reading input parameters of the network used for power flow and reliability calculations. The adjacency matrix is created simultaneously during this step. Next section of the code creates matrix H that, as shown in section 4.3.3, is used for power flow calculations. The power flows through lines and voltages in the substations are calculated for normal and for the single line failure regime in the following section of the code. The obtained results are stored and used during consistency tests. The next section of the code is the procedure for the construction of the fault trees for loads in the system and contain the following steps:

- Using the adjacency matrix identify all energy flow paths with the procedure described in the section 4.2.1.
- Identified energy flow paths test for consistency as shown in the section 4.3.9.
- Accepted energy flow paths use for fault tree construction as described in the section 4.2.1.
- Convert the identification of the basic events from numbers to names.

- Save constructed fault trees in external file.

The following naming practice was used for the names of the basic events:

- The names of the generators basic events are in the form “G2 101-1” where “G” is for generator, following number “2” identifies the failure mode, “101” identifies the substation where it is connected, and final number “-1” identifies the specific generator in the power plant.

- The lines basic events are in form “L1-101 103” where “L” stands for line failure, following number “1” or “2” identifying the failure mode of the line (1 for line failure, 2 for CCF), “101” identifies the starting substation of the line and “103” the end substation of the line.

- The substations basic events are in the form “B1-101” where “B” is for the substation, “1” is failure mode and “101” is the identification of the substation.

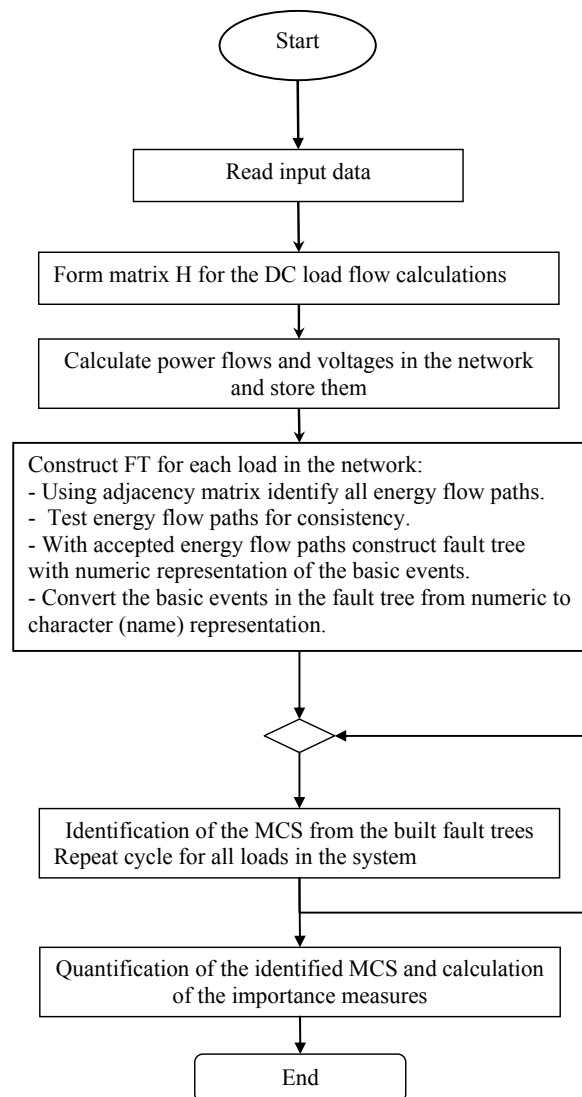


Figure 4-14 Block diagram of the program

After the construction of the fault trees, the next step is their qualitative analysis and identification of the minimal cut sets from each of the created fault trees. This step is the most time consuming part of the evaluations.

The identified MCS are stored in array and used in the last procedure of the code where, quantification of the MCS is done using the reliability parameters. Rare event approximation, given in the section 3.2.1, is used for the MCS quantification. Quantitative results include

calculation of the top event probabilities and calculation of the importance measures for elements and elements groups.

The computer code is optimized for speed with the application of the efficient algorithms and optimal usage of the memory. The structure of the code is built to allow future parallelization of the program in order to increase its efficiency. The use of the separate subroutines and variables organized into modules was applied during the writing of the code, improving the readability and description of the program.

5 Models and Results of the Power System Reliability Analysis

In the following chapters, the selected results obtained from the developed method are presented. The analysis was done for two systems: the IEEE Reliability Test System²⁷ and simplified Slovenian Power System. The IEEE Reliability Test System was selected because it is a standardized test system used in power system reliability analysis, because the input data for the parameters of the system exist and because the complexity of the test network is similar to the complexity of the real system. The IEEE Reliability Test System includes two nuclear power plants situated in separate substations, allowing testing of the applicability of the developed method for estimation of the Loss of Offsite Power initiating event frequency for the corresponding NPP. After verification of the developed method on the IEEE test system, the practical application of the method was realized on the simplified Slovenian Power System including nuclear power plant Krško. The implications of the addition of new lines and change of generation and load are investigated for Slovenian Power System and the obtained results are presented.

5.1 IEEE test system

The IEEE reliability test system²⁷ is given on Figure 5-1, consisting of: 24 substations, 18 substations directly connected to loads, 7 substations connected to 32 generators and interconnected with the 38 power lines. For 14 lines, the common cause failures (CCF) were considered. The IEEE reliability test system is selected, because it's specially designed to be used for different static and dynamic analyses and because of the availability of the reliability parameters of the system elements, including two nuclear power plants among generating capacities. The parameters used in the analysis are given in the Appendix D.

The nuclear power plants in the IEEE RTS are situated in the substations 18 and 21. The load of size 20 MW was added in the substation 21 in order to account house load of the NPP in the analysis.

5.2 The results for the IEEE test system

The obtained results for the IEEE test system are presented in the following sections. Analysis was done with and without consideration of the substations voltages in the flow paths test procedure. The application of the substations voltages consistency test in the method for specific power system configurations results in the large unreliabilities of power delivery, therefore analysis with both approaches is done.

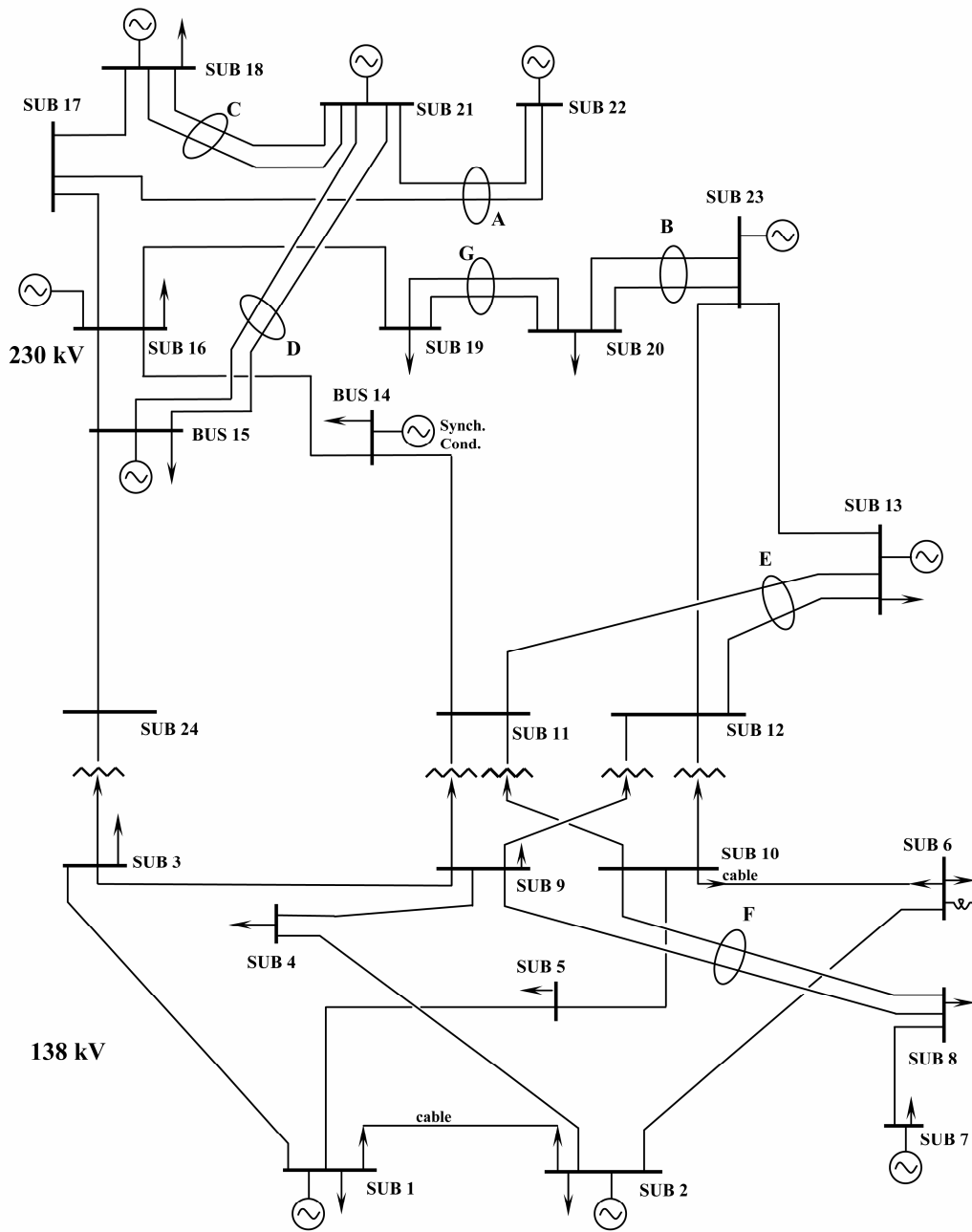


Figure 5-1 IEEE-96 Reliability test system

5.2.1 The results for IEEE-RTS without consideration of the substations voltages

The analysis of the IEEE RTS was done without consideration of the substations voltages in the energy flow path consistency tests. From the fault trees built for the loads in the system, the MCS were identified and ordered by their contribution to the top event probability. Ten the most important MCS identified from the fault tree built for the load in the substations 18 are given in Table 5-1. The basic event BE “G2 118- 1” corresponds to the failure of the generator in the substation 118, BE “G2 121- 1” to the generator failure in substation 121, the BE “G2 123- 3” to the failure of the generator 3 in the substation 123. Line failures are identified with the BE “L1-117 118” corresponding to the failure of the line between substation 117 and substation 118 and BE “L2-118 121” for the CCF of lines between

substation 118 and 121. The basic event BE “B1-118” identifies the failure of the substation 118.

Table 5-1 Identified MCS for power delivery to the load in the substation 18

No.	Event 1	Event 2	Event 3	Event 4
1	G2 118- 1	G2 121- 1	G2 123- 3	
2	G2 118- 1	G2 121- 1	G2 123- 2	
3	G2 118- 1	G2 121- 1	G2 123- 1	
4	G2 118- 1	L2-118 121	L1-117 118	
5	G2 118- 1	L1-118 121	L1-117 118	
6	B1-118			
7	G2 118- 1	G2 121- 1	L1-116 117	L2-115 121
8	G2 118- 1	G2 121- 1	L1-116 117	L1-115 121
9	G2 118- 1	G2 121- 1	B1-123	
10	G2 118- 1	B1-121	G2 123- 3	

The identified MCS for the house load of the nuclear power plant in the substation 21 are given in Table 5-2.

Table 5-2 Identified MCS for power delivery to the load in the substation 21

No.	Event 1	Event 2	Event 3	Event 4	Event 5
1	B1-121				
2	G2 121- 1	G2 122- 3	G2 118- 1	L1-116 117	L2-115 121
3	G2 121- 1	G2 122- 5	G2 118- 1	L1-116 117	L1-115 121
4	G2 121- 1	G2 122- 5	G2 118- 1	L1-116 117	L2-115 121
5	G2 121- 1	G2 122- 1	G2 118- 1	L1-116 117	L1-115 121
6	G2 121- 1	G2 122- 3	G2 118- 1	L1-116 117	L1-115 121
7	G2 121- 1	G2 122- 4	G2 118- 1	L1-116 117	L1-115 121
8	G2 121- 1	G2 122- 4	G2 118- 1	L1-116 117	L2-115 121
9	G2 121- 1	G2 122- 6	G2 118- 1	L1-116 117	L1-115 121
10	G2 121- 1	G2 122- 6	G2 118- 1	L1-116 117	L2-115 121

The unreliability of the power delivery to the corresponding loads was calculated using the identified MCS. The obtained results are given in Table 5-3.

The first column in Table 5-3 identifies substation where load is connected. The second column gives the unreliability of the power delivery to the respective load. The third column gives the weighting factor equal to the share of the load (the last column in the table) in the total system load. The fourth column gives the product of the unreliability and the weighting factor. The fifth column shows the load size in the substation. The results in Table 5-3 show that the largest unreliability is obtained for the loads situated in the substations 15, 18 and 13. This result is obtained due to the size of the corresponding loads and unreliabilities of the related substations where they are connected. The unreliability of the power delivery to the house load of the nuclear power plant connected in the substation 21 is substantially smaller than the value obtained for the load in the substation 18. This result is obtained as a result of the larger load in the substation 18 (sum of house load of the nuclear power plant and the load of other consumers) and more reliable interconnection of substation 21 with the rest of the power system through substations 22 and 15.

Table 5-3 Calculated unreliabilities for the IEEE RTS

Load substation	The unreliability of the power delivery to the load	Weighting factor	Weighted unreliability of the power delivery	Capacity [MW]
15	2.31E-03	1.10E-01	2.54E-04	317
18	2.30E-03	1.16E-01	2.66E-04	333
13	1.39E-04	9.20E-02	1.28E-05	265
20	4.47E-05	4.44E-02	1.99E-06	128
7	4.11E-05	4.34E-02	1.79E-06	125
9	9.96E-06	6.08E-02	6.05E-07	175
10	9.96E-06	6.77E-02	6.74E-07	195
14	3.71E-06	6.74E-02	2.50E-07	194
19	3.55E-06	6.28E-02	2.23E-07	181
3	2.56E-06	6.25E-02	1.60E-07	180
6	7.29E-07	4.72E-02	3.44E-08	136
8	6.56E-07	5.94E-02	3.90E-08	171
4	1.88E-07	2.57E-02	4.83E-09	74
5	1.51E-07	2.47E-02	3.71E-09	71
2	3.59E-08	3.37E-02	1.21E-09	97
1	3.57E-08	3.75E-02	1.34E-09	108
21	2.26E-08	1.04E-02	2.36E-10	30
16	1.99E-08	3.47E-02	6.91E-10	100
Weighted system unreliability			5.39E-04	
System reliability			0.99946	

The obtained NRRW importance measure, for selected elements of the power system, are given in Table 5-4.

Table 5-4 Basic events with the largest NRRW

BE	BE description	NRRW
G2 118- 1	Generator 118- 1 failure	1.04E+02
G2 121- 1	Generator 121- 1 failure	1.04E+02
G2 123- 3	Generator 123- 3 failure	1.98E+00
G2 123- 1	Generator 123- 1 failure	1.33E+00
G2 123- 2	Generator 123- 2 failure	1.33E+00

The results in Table 5-4 show that elements with the largest NRRW importance measure are: generator situated in substation 18 (BE “G2 118- 1”), substation 21 (BE “G2 121- 1”) and generators in substation 23 (BE “G2 123- 1”, BE “G2 123- 2” and BE “G2 123- 3”). The obtained high NRRW importance measures for these generators are resulting from their size. The obtained NRAW importance measures, for selected elements of the power system are given in Table 5-5.

Table 5-5 Basic events with the largest NRAW

BE	BE description	NRAW
B1-118	Substation 118 failure	2.20E+02
B1-115	Substation 115 failure	2.05E+02
B1-113	Substation 113 failure	1.72E+02
L1-107 108	Line 107 – 108 failure	1.07E+01
G2 118- 1	Generator 118-1 failure	8.26E+00

The results in Table 5-5 show that elements with the largest NRAW in IEEE RTS are: substations 18, 15 and 13 (BE “B1-118”, BE “B1-115” and BE “B1-113”), line between substation 7 and substation 8 (BE “L1-107 108”) and generator connected in substation 18 (BE “G2 118- 1”). The large NRAW for substations 18, 15 and 13 is resulting from the size of the loads connected in those substations. The failure of the line between substation 7 and substation 8 will disconnect substation 7 from the power system. The large NRAW for the generator of nuclear power plant situated in substation 18 is anticipated accounting that this unit is the largest in the power system.

The results obtained for the RRW importance measures from the fault tree built for the power delivery to the load in the substation 18, are given in Table 5-6.

Table 5-6 Basic events with the largest RRW for load in the substation 18

BE	BE description	RRW
G2 118- 1	Generator 118-1 failure	1.17E+05
G2 121- 1	Generator 121-1 failure	5.56E+04
G2 123- 3	Generator 123-3 failure	2.00E+00
G2 123- 1	Generator 123-1 failure	1.33E+00
G2 123- 2	Generator 123-2 failure	1.33E+00

Elements that have the largest RRW values are generators situated in substations 18, 21 and 23, and these elements are important from the aspect of nuclear safety and unreliability of the power delivery to the load in the substation 18, which partly includes the house load of the nuclear power plant.

The results obtained for the RAW importance measures from the fault tree built for the power delivery to the load in the substation 18, are given in Table 5-7.

Table 5-7 Basic events with the largest RAW for load in the substation 18

BE	BE description	RAW
B1-118	Substation 118 failure	4.33E+02
G2 118- 1	Generator 118-1 failure	8.33E+00
G2 121- 1	Generator 121-1 failure	8.33E+00
G2 123- 1	Generator 123-1 failure	7.00E+00
G2 123- 2	Generator 123-2 failure	7.00E+00

The large RAW obtained for the substation 18 (BE “B1-118”) identified in Table 5-7 is expected, accounting that failure of substation will directly interrupt offsite power delivery to the house load of the nuclear power plant connected into it. The failure of the generator of the nuclear power plant situated in the substation 18 (BE “G2 118- 1”) together with the nuclear power plant situated in the substation 21 (BE “G2 121- 1”) are identified in Table 5-7.

The obtained results for the RRW importance measures for the power delivery to the house load of the nuclear power plant in the substation 21 are given in Table 5-8.

Table 5-8 Basic events with the largest RRW for load in the substation 21

BE	BE description	RRW
B1-121	Substation 121 failure	1.05E+02
G2 121- 1	Generator 121-1 failure	1.31E+00
L2-115 121	CCF 115 – 121 lines	1.25E+00
G2 118- 1	Generator 118-1 failure	1.12E+00
L1-116 117	Line 116 – 117 failure	1.01E+00

Table 5-8 show that the elements with the largest RRW for the nuclear power plant in substation 21, are: substation 21 (BE “B1-121”) and generator of the nuclear power plant connected into it (BE “G2 121- 1”), generator of the nuclear power plant in substation 18 (BE

“G2 118- 1”), line between substation 16 and substation 17 (BE “L1-116 117”) and CCF of lines between substation 115 and 121 (BE “L2-115 121”). The appearance of line between substation 16 and substation 17 in Table 5-8 is resulting from the fact that the failure of this line will disrupt energy flow in top region of the power system, where substation 21 and corresponding nuclear power plant are situated. The CCF of lines between substations 15 and 21 degrades interconnection between the substation 21 and the power system.

The results obtained for the RAW for the power delivery to the house load of the nuclear power plant in the substation 21, are given in Table 5-9.

Table 5-9 Basic events with the largest RAW for load in the substation 21

BE	BE description	RAW
B1-121	Substation 121 failure	4.42E+07
L1-116 117	Line 116 – 117 failure	2.07E+01
L2-115 121	CCF 115 – 121 lines	1.95E+01
B1-115	Substation 115 failure	1.93E+01
L2-118 121	CCF 118 – 121 lines	2.84E+00

The same elements are identified to have high RAW values as those identified for the RRW. The substation 15 failure (BE “B1-115”) and CCF of lines between substation 18 and substation 21 (BE “L2-118 121”) are additionally identified.

To summarize, the obtained results show that the major contributors to the weighted system unreliability are substations 18 and 21 and adjacent nuclear power plants. From the aspect of the nuclear safety, the major contributors to the unreliability of the power delivery to the house loads of the nuclear power plants are identified using the obtained importance measures. The CCF of the lines between substations 118 and 121 and CCF of the lines between substations 116 and 117 are identified as important from the aspect of the nuclear safety.

5.2.2 Change of the cut off used in the analysis

The analysis of the fault trees built for the loads situated in the substations 16 and substation 20 of the IEEE RTS, with the default truncation limits given in Table 5-10 resulted with the code failure to identify the MCS. This result is obtained because of the large number of the MCS that passed default cutoffs. The multiple (four) lines are connected in both substations, and default cutoff will result with the inclusion of all branches bellow AND gate (related to power delivery from other substations through those lines) in the fault tree, exceeding the capabilities of MCS identification module⁹⁰. The selection of the appropriate truncation limit was done by trials of different cutoffs. The selected truncation limits used in the analysis for loads in the substations 16 and 20 are given in Table 5-10.

Table 5-10 Used truncation limits in analysis

Analysis	Default cutoff	Load 16	Load 20
Probability cutoff	1.00E-12	1.00E-09	1.00E-14
Number of BE in MCS	7	7	5

5.2.3 The results for IEEE-RTS with the consideration of the substations voltages

Analysis of the IEEE RTS, with the inclusion of the substations voltages in the energy flow paths consistency test procedure was done and the obtained results are presented. The identified MCS from the fault trees built for the house load of the nuclear power plants in the substations 18 and 21 are given in Table 5-11 and in Table 5-12.

Table 5-11 Identified MCS for power delivery to the load in the substation 18

No.	Event 1	Event 2	Event 3	Event 4
1	G2 118- 1	G2 121- 1		
2	G2 118- 1	L2-118 121	L1-117 118	
3	B1-118			
4	G2 118- 1	B1-121		
5	G2 118- 1	L2-118 121	L2-121 122	L2-115 121
6	G2 118- 1	L2-118 121	L2-121 122	L1-116 117
7	G2 118- 1	L2-118 121	L2-121 122	L1-115 116
8	G2 118- 1	L2-118 121	L2-117 122	L2-115 121
9	G2 118- 1	L1-118 121	L3-118 121	L1-117 118
10	G2 118- 1	L2-118 121	L2-117 122	L1-116 117

Table 5-12 Identified MCS for power delivery to the load in the substation 21

No.	Event 1	Event 2	Event 3	Event 4	Event 5
1	G2 121- 1	G2 122- 1	G2 118- 1	G2 116- 1	G2 115- 6
2	G2 121- 1	G2 122- 2	G2 118- 1	G2 116- 1	G2 115- 6
3	G2 121- 1	G2 122- 5	G2 118- 1	G2 116- 1	G2 115- 6
4	G2 121- 1	G2 122- 3	G2 118- 1	G2 116- 1	G2 115- 6
5	G2 121- 1	G2 122- 4	G2 118- 1	G2 116- 1	G2 115- 6
6	G2 121- 1	G2 122- 6	G2 118- 1	G2 116- 1	G2 115- 6
7	G2 121- 1	G2 122- 4	G2 118- 1	G2 116- 1	G2 115- 4
8	G2 121- 1	G2 122- 1	G2 118- 1	G2 116- 1	G2 115- 3
9	G2 121- 1	G2 122- 4	G2 118- 1	G2 116- 1	G2 115- 2
10	G2 121- 1	G2 122- 5	G2 118- 1	G2 116- 1	G2 115- 1

Table 5-13 Calculated unreliabilities for the IEEE RTS

Load substation	The unreliability of the power delivery to the load	Weighting factor	Weighted unreliability of the power delivery	Capacity [MW]
1	2.40E-01	3.75E-02	9.00E-03	108
2	2.40E-01	3.37E-02	8.08E-03	97
7	1.20E-01	4.34E-02	5.21E-03	125
15	1.44E-02	1.10E-01	1.59E-03	317
18	1.44E-02	1.16E-01	1.67E-03	333
20	4.43E-05	4.44E-02	1.97E-06	128
16	2.49E-05	3.47E-02	8.65E-07	100
9	7.40E-06	6.08E-02	4.50E-07	175
10	7.40E-06	6.77E-02	5.01E-07	195
21	5.21E-06	1.04E-02	5.42E-08	30
8	6.22E-07	5.94E-02	3.69E-08	171
19	6.22E-07	6.28E-02	3.91E-08	181
13	5.15E-09	9.20E-02	4.74E-10	265
3	2.33E-09	6.25E-02	1.46E-10	180
14	2.33E-09	6.74E-02	1.57E-10	194
4	1.56E-09	2.57E-02	4.01E-11	74
5	1.56E-09	2.47E-02	3.85E-11	71
6	1.56E-09	4.72E-02	7.37E-11	136
Weighted system unreliability			2.55E-02	
System reliability			0.9745	

Using the identified MCS the unreliability of the power delivery to the corresponding loads was calculated with the obtained results given in Table 5-13.

The results in Table 5-13 show that the largest unreliability of the power delivery is obtained for the loads in the substations 1, 2 and 7. The comparison of the results in Table 5-13 and results in Table 5-3 (voltages not accounted in the method) indicate substantial change of the results. The obtained unreliabilities for these substations are result of the low voltages in these and adjacent substations, as shown in Table 5-14.

Table 5-14 Calculated voltages in the substations of the IEEE RTS for normal regime

Load substation	Substation Identification	Load(MW)	Load(Mvar)	Un(%)	Un(kV)
1	101	108	22	79.63	109.9
2	102	97	20	79.38	109.5
3	103	180	37	84.05	116
4	104	74	15	78.07	107.7
5	105	71	14	77.69	107.2
6	106	136	28	75.82	104.6
7	107	125	25	80.23	110.7
8	108	171	35	77.02	106.3
9	109	175	36	80.72	111.4
10	110	195	40	78.69	108.6
11	111	0	0	83.77	192.7
12	112	0	0	83.23	191.4
13	113	265	54	85.97	197.7
14	114	194	39	87.57	201.4
15	115	317	64	101.39	233.2
16	116	100	20	97.39	224
17	117	0	0	100.16	230.4
18	118	333	68	101.97	234.5
19	119	181	37	94.46	217.3
20	120	128	26	93.18	214.3
21	121	20	0	102.63	236
22	122	0	0	101.29	233
23	123	0	0	92.97	213.8
24	124	0	0	92.77	213.4

The weighted system unreliability in Table 5-13 is larger than in Table 5-3 obtained without consideration of the substations voltages. This result is obtained because introduction of the voltages in the energy flow path test procedure results in a larger numbers of discarded flow paths. This results in the decreased number of the alternative flow paths of power delivery to the corresponding loads and the increased unreliability of power delivery.

The NRRW for selected elements of the power system are given in Table 5-15.

Table 5-15 Basic events with the largest NRRW

BE	BE description	NRRW
G2 101- 1	Generator 101-1 failure	1.17E+00
G2 101- 2	Generator 101-2 failure	1.17E+00
G2 102- 1	Generator 102-1 failure	1.16E+00
G2 121- 1	Generator 121-1 failure	1.15E+00
G2 118- 1	Generator 118-1 failure	1.15E+00

The results in Table 5-15 show that elements with the largest NRRW importance measure are: generators in substation 1 (BE “G2 101- 1” and BE “G2 101- 2”), generator in substation 2 (BE “G2 102- 1”), generator in substation 21 (BE “G2 121- 1”) and substation 18 (BE “G2 118- 1”). The ranking in Table 5-15 of the generators in substation 1 and 2 is result of the low voltages in those and adjacent substations.

Table 5-16 show NRAW for selected elements of the power system are given in.

Table 5-16 Basic events with the largest NRAW

BE	BE description	NRAW
B1-118	Substation 118 failure	6.04E+00
B1-115	Substation 115 failure	5.36E+00
B1-113	Substation 113 failure	4.60E+00
G2 107- 1	Generator 107-1 failure	2.63E+00
L1-115 116	Line 115-116 failure	1.06E+00
L2-115 121	CCF 115-121 line	1.01E+00

The results in Table 5-16 identify the following elements: substation 18 failure (BE “B1-118”), substation 15 (BE “B1-115”) and substation 13 failure (BE “B1-113”), substation 7 generator failure (BE “G2 107- 1”), line between substations 15 and 16 failure (BE “L1-115 116”) and CCF of the lines between substations 15 and 21 (BE “L2-115 121”). The cause of the large NRAW for the substations 18, 15 and 13 is described in the section 5.2.1. The large NRAW for generator situated in the substation 7 is result of the weak interconnection (one line only) of the substation 7 to the power system. Failure of line between substations 15 and 16 and CCF of lines between substations 15 and 21 will disrupt power flows to top region of the IEEE RTS.

The results obtained for the importance measures for the load in the substation 18 are given in Table 5-17.

Table 5-17 The RRW and RAW importance measures for the load in the substation 18

BE	BE description	RAW	RRW
G2 118- 1	Generator 118-1 failure	8.33E+00	7.29E+05
G2 121- 1	Generator 121-1 failure	8.33E+00	3.29E+05
B1-118	Substation 118 failure	6.93E+01	1.27E+03
L1-117 118	Line 117-118 failure	1.00E+00	3.04E+02
L2-118 121	CCF 118-121 line	1.00E+00	1.70E+00

The results in Table 5-17 show that the same elements are identified to have the largest RRW and RAW for the load in the substation 18: generator in substations 18 (BE “G2 118- 1”) and 21 (BE “G2 121- 1”), substation 18 failure (BE “B1-118”), line between substation 17 and 18 (BE “L1-117 118”) and CCF of the lines between substation 118 and 121 (BE “L2-118 121”).

The results obtained for the RRW importance measures for the house load of the nuclear power plant in the substation 21 are given in Table 5-18.

Table 5-18 Basic events with the largest RRW for the load in the substation 21

BE	BE description	RRW
G2 121- 1	Generator 121-1 failure	2.32E+02
G2 118- 1	Generator 118-1 failure	2.32E+02
G2 116- 1	Generator 116-1 failure	2.30E+02
G2 115- 6	Generator 115-6 failure	1.50E+00
G2 122- 6	Generator 122-6 failure	1.20E+00

The elements in Table 5-18 include generators in the substation 21, 18, 16 and substation 15. The results obtained for the RAW importance measures from the fault tree built for the power delivery to the house load in the substation 21 are given in Table 5-19.

Table 5-19 Basic events with the largest RAW for the load in the substation 21

BE	BE description	RAW
B1-121	Substation 121 failure	1.92E+05
G2 116- 1	Generator 116-1 failure	2.49E+01
G2 122- 6	Generator 122-6 failure	1.74E+01
G2 122- 1	Generator 122-1 failure	1.74E+01
G2 122- 3	Generator 122-3 failure	1.74E+01

The identified elements in Table 5-19 include substation 121 failure (BE “B1-121”). Other elements in Table 5-19 are equal to those identified in Table 5-18.

Truncation limits shown in Table 5-10 were used in the analysis.

To summarize, the obtained results demonstrate the implication of the introduction of the substations voltages in the test procedure to the results. The increases of the unreliabilities of power delivery for all loads are notified, especially for those situated in substations with the low nominal voltages. The obtained results indicate the need for more strict definition of the intervals of the nominal voltages of the substations from operational experience in order to be applied in the method.

5.2.4 Summary of the results obtained for the IEEE RTS

The most important findings from the obtained results are:

- The applicability of the developed method was tested and confirmed on the IEEE RTS. The obtained results include identified MCS, unreliability of the power delivery to the corresponding loads and importance measures for the specific loads and whole power system. The obtained results for the unreliability of the power delivery to the house loads (self consumption) of the nuclear power plants can be used for the estimation of the Loss of offsite power initiating event and resulting core damage frequency. The obtained results also verify the applicability of the developed method for the quantification of the consequences on the nuclear safety resulting from changes in the power system, and identification of the most important elements of the power system from aspect of nuclear safety.
- The most important contributors to the weighted system unreliability for IEEE RTS are: the substations 18 and 21 together with the nuclear power plants connected in these substations.
- Implication of nominal substations voltage intervals on results indicates the need for precise endorsement of those intervals.
- The unreliability of the power delivery to the house loads of the nuclear power plant situated in the substations 18 and 21 depends on the unreliability of those and adjacent substations, the unreliability of the interconnections to these substations and unreliability of the power plants in adjacent substations. The most important elements from aspect of nuclear safety are identified using the importance measures obtained for the house loads of the nuclear power plants.
- The need for the change of the truncation limits for specific loads in the analysis is notified. The new truncation limits were estimated and applied in the analysis.

5.3 Slovenian power system

The configuration of the Slovenian system used in the analysis is given on Figure 5-2, consisting of: 19 substations, 13 of them directly connected to loads, 5 substations directly connected to actual and 5 to representative generators and 25 interconnections (10 transformers and 15 lines). For 12 interconnections, the common cause failures (CCF) are

considered. The CCF were considered for double lines (Okroglo-Beričevo and RTP Krško-Brestanica), and for double transformers between substations (e.g. Beričevo - Beričevo II). The configuration of the Slovenian power system was constructed on the basis of the system from the corresponding reference⁹¹, given on Figure 5-3. Only 220 kV and 400 kV lines in Slovenian power system were accounted in the basic configuration, including two 110 kV lines connected to power plants in substations Šoštanj and Brestanica. The 110kV line to substation Šoštanj was included in the analysis due to the thermal power plant Šoštanj blocks 1-3 connected into it. The 110kV connection to substation Brestanica was included in the model because power plant Brestanica can be connected directly to nuclear power plant Krško (island mode of operation) as alternative offsite power source to nuclear power plant Krško. Interconnections with the neighboring power systems of Austria, Italy and Croatia weren't included in the analysis. The power flows through interconnections with the neighboring systems were accounted in the loads of corresponding substations, where those lines are connected, in this case substations Divača, Maribor and NPP Krško. The generating units in substations Podlog II and Okroglo were added in the model to represent production from hydro power plants connected to 110 kV network and balance produced power. Parameters of the power system together with the references are given in the Appendix D.

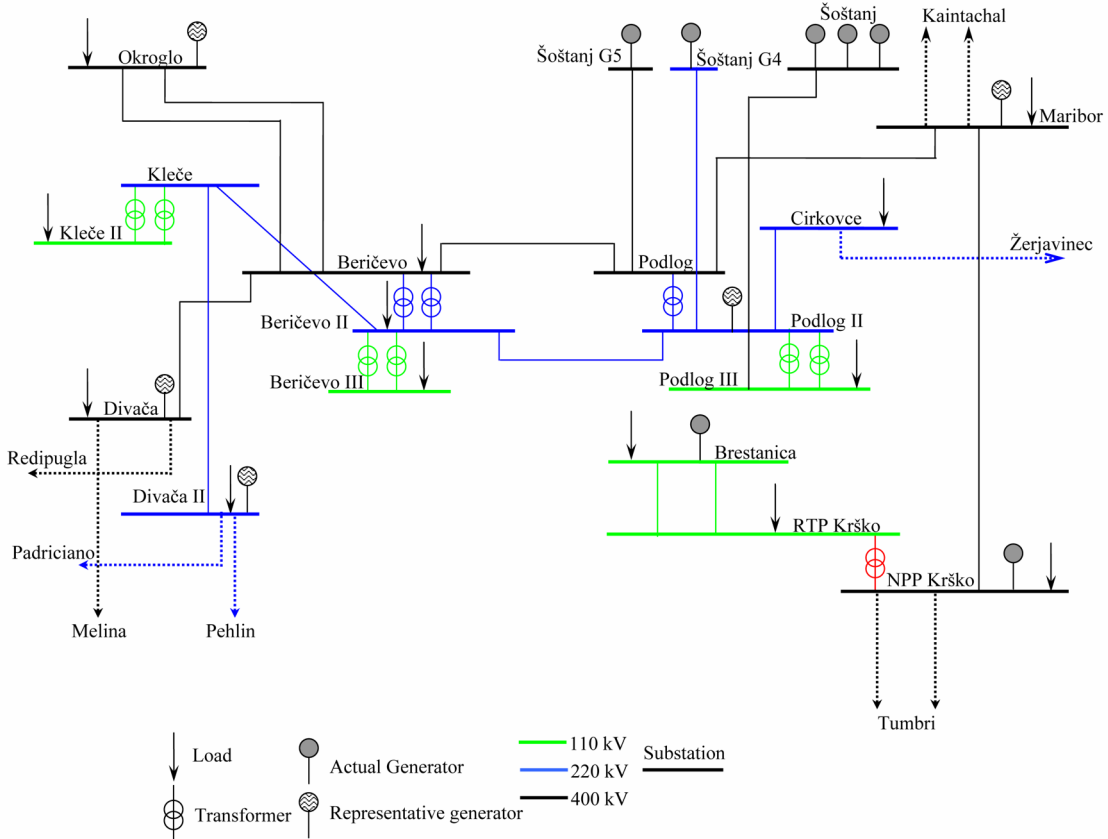


Figure 5-2 Basic configuration of Slovenian power system

The substations of the Slovenian power system on Figure 5-2 are numbered as shown in Table 5-20.

Table 5-20 The substations numbers used in construction of the basic events

Substation number	Substation name	Substation BE identification
1	NPP Krško	101
2	RTP Krško	102
3	Maribor	103
4	Podlog	104
5	Podlog2	105
6	Šoštanj4	106
7	Šoštanj5	107
8	Podlog3	108
9	Šoštanj1	109
10	Cirkovce	110
11	Beričevo	111
12	Beričevo2	112
13	Beričevo3	113
14	Kleče 2	114
15	Kleče	115
16	Divača	116
17	Divača 2	117
18	Okroglo	118
19	Brestanica	119

The NPP Krško is equipped with a two loop Westinghouse Pressurized Light Water Reactor of 2.000 MW thermal power. The power plant's net electrical power is 696 MW. It is connected to the 400kV grid of Slovenia and Croatia.

NEK generates over five billion kWh of electrical energy per year, representing approximately 40% of the total electricity produced in Slovenia and covering the base load throughout the year.

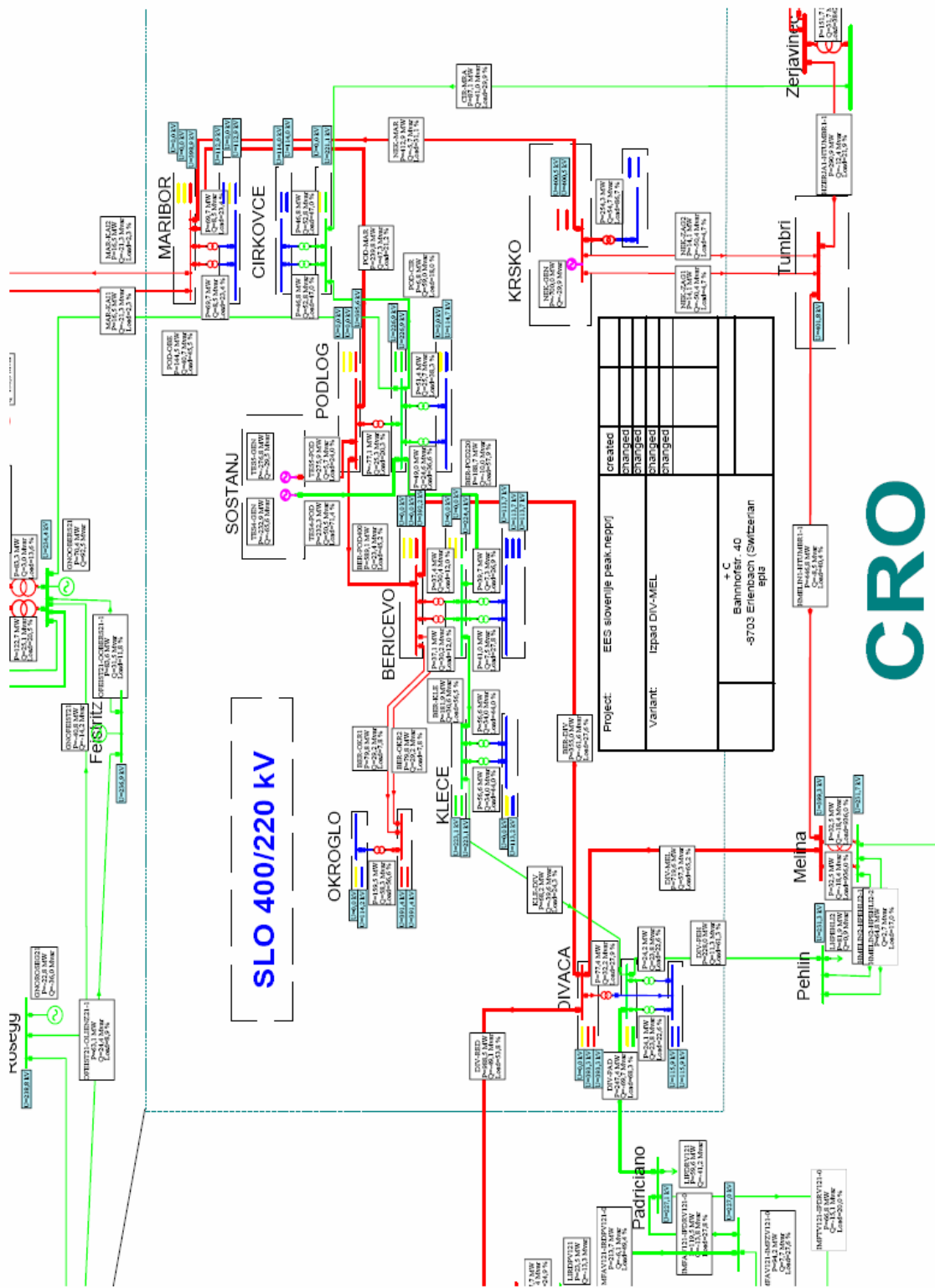


Figure 5-3 Slovenian power system used in the construction of the model

5.4 Results for the Slovenian power system

For the Slovenian Power System, the analysis of the basic configuration was performed without and with the consideration of voltages in procedure described in the section 4.2.1. Implications of the changes on the basic configuration were tested and obtained results are presented in the following sections.

5.4.1 Basic Slovenian power system without consideration of voltages

Analysis of the basic configuration of the Slovenian power system was done and the obtained results are presented. The voltages of the substations were not included in consistency test procedure.

From the fault tree built for the power delivery to substation NPP Krško, the 344 minimal cut sets (MCS) were determined, with the ten most important given in Table 5-21.

Table 5-21 Identified MCS for power delivery to NPP Krško

No.	Event 1	Event 2	Event 3	Event 4	Event 5	Event 6
1	G2 101- 1	L1-101 103	G2 119- 1			
2	G2 101- 1	L1-103 104	G2 119- 1			
3	G2 101- 1	L1-101 103	L1-101 102			
4	G2 101- 1	L1-101 103	L2-102 119			
5	G2 101- 1	L1-103 104	L1-101 102			
6	G2 101- 1	L1-103 104	L2-102 119			
7	G2 101- 1	G2 105- 1	G2 109- 1	G2 106- 1	G2 107- 1	G2 119- 1
8	G2 101- 1	L1-104 111	G2 107- 1	L1-104 105	G2 119- 1	
9	G2 101- 1	G2 105- 1	L1-108 109	G2 106- 1	G2 107- 1	G2 119- 1
10	G2 101- 1	L1-105 112	G2 107- 1	L1-104 105	G2 119-1	

The first MCS in Table 5-21 includes basic events corresponding to the failure of generator in the NPP Krško (BE “G2 101- 1”), line between substations NPP Krško– Maribor failure (BE “L1-101 103”) and failure of the generator in the power plant Brestanica (BE “G2 119- 1”). In the second MCS, the line failure NPP Krško – Maribor is substituted with the basic event corresponding to the failure of the line between substations Podlog – Maribor (BE “L1-103 104”). The transformer failure (BE “L1-101 103”) between substations NPP Krško and RTP Krško is one of the events in the third MCS. In the fourth MCS, the CCF of the lines (BE “L2-102 119”) between substation RTP Krško and substation Brestanica is identified.

The system (top event) unavailability was determined for all loads in the system. As a result of the selection of the constant failure rate per time and unrepairable element model for the constituting elements of the power system, the system unavailability, as shown in section 3.2.2, is equal to system unreliability of the power delivery to the corresponding load. The obtained unreliability of the power delivery to the substation NPP Krško and weighted system unreliability, calculated using Eq. (4.1), is given in Table 5-22. The system reliability is given in Table 5-23.

Table 5-22 Obtained unreliabilities for the basic configuration of the Slovenian power system

Parameter	Weighted system unreliability	Unreliability of power delivery to substation NPP Krško
Value	1.40E-02	1.55E-04

Table 5-23 Obtained reliability for the basic configuration of the Slovenian power system

System reliability	0.986
--------------------	-------

The unreliability of the power delivery to the loads connected in the substations RTP Krško and Beričevo 2 is the major contributor to the weighted system unreliability given in Table 5-22. The simplified Slovenian power system shown on Figure 5-2 doesn't account all lines and generators of the real power system, resulting with the large weighted system unreliability in Table 5-22. The human contribution to the restoration of the power delivery to loads is not considered in the analysis, which means that the results are conservative, i.e. calculated unreliability is larger as it would be, if the human contribution is considered.

The importance measures NRRW and NRAW for selected elements of the power system are given in Table 5-24 and Table 5-25. The results given in Table 5-24 show that elements with the largest NRRW importance measure are: generator in the substation NPP Krško (BE "G2 101- 1"), CCF of lines between substations Beričevo and Okroglo (BE "L2-111 118"), transformer between substation NPP Krško and substation RTP Krško (BE "L1-101 102"), followed by the generators in the substations Šoštanj G4 and Šoštanj G5 (BE "G2 106- 1" and "G2 107- 1"). The large NRRW implies that the reliability of the respective elements is worth to increase in order that the system reliability is significantly increased. This result corresponds to the expected results for the system, because increase of the reliability of the NPP Krško as a largest generator in the Slovenian power system directly implies decrease of the unreliability of the overall system. The same conclusion goes for the generators in the substations Šoštanj G4 and Šoštanj G5.

Table 5-24 Basic events with the largest NRRW

BE	BE description	NRRW
G2 101- 1	Generator 101-1 failure	4.64E+00
L2-111 118	CCF line 111-118	1.08E+00
L1-101 102	Line failure 101-102	1.06E+00
G2 106- 1	Generator 106-1 failure	1.06E+00
G2 107- 1	Generator 107-1 failure	1.06E+00
L1-111 116	Line failure 111-116	1.03E+00
L1-112 115	Line failure 112-115	1.02E+00
L1-105 110	Line failure 105-110	1.01E+00
L2-102 119	CCF line 102-119	1.01E+00
L1-115 117	Line failure 115-117	1.01E+00

The results given in Table 5-25 show that elements with the largest NRAW importance measure are: substations NPP Krško, Beričevo and RTP Krško (BE "B1-101", "B1-111" and "B1-102") and transformer between substations NPP Krško and RTP Krško (BE "L1-101 102").

Table 5-25 Basic events with the largest NRAW

BE	BE description	NRAW
B1-101	Substation 101 failure	2.06E+01
B1-111	Substation 111 failure	1.96E+01
B1-102	Substation 102 failure	1.81E+01
L1-101 102	Line failure 101-102	1.81E+01
B1-112	Substation 112 failure	1.78E+01
G2 101- 1	Generator 101-1 failure	1.46E+01
B1-105	Substation 105 failure	1.18E+01
B1-115	Substation 115 failure	9.54E+00
L1-112 115	Line failure 112-115	9.52E+00
B1-118	Substation 118 failure	9.43E+00

Elements with the largest NRAW should be maintained well, in order that the reliability of the system is not reduced significantly. Obtained results correspond to the expected, because failure of these elements will result with: substation NPP Krško - disconnection of the largest generator in the system, substation Beričevo - disruption of the power flows between East and West part of the Slovenian power system, substation RTP Krško - disruption of the power delivery to the largest load in the system.

The importance measures from the fault tree built for power delivery to the substation NPP Krško, are given in Table 5-26 and Table 5-27.

Table 5-26 Basic events with the largest RRW for NPP Krško

BE	BE description	RRW
G2 101- 1	Generator 101-1 failure	1.13E+05
G2 119- 1	Generator 119-1 failure	3.16E+01
L1-101 103	Line failure 101-103	3.02E+00
L1-103 104	Line failure 103-104	1.49E+00
L1-101 102	Line failure 101-102	1.02E+00
L2-102 119	CCF line 102-119	1.01E+00

The results given in Table 5-26 show that the element with the largest RRW importance measure for power delivery to the substation NPP Krško are: generator in substation NPP Krško and Brestanica (BE “G2 101- 1” and “G2 119- 1”), lines between substations NPP Krško – Maribor (BE “L1-101 103”) and substations Maribor – Podlog (BE “L1-103 104”), transformer between substations NPP Krško - RTP Krško (BE “L1-101 102”), and CCF of lines between substations RTP Krško-Brestanica (BE “L2-102 119”). The large RRW implies that the reliability of the respective elements is worth to increase in order to improve reliability of the power delivery to the substation NPP Krško. Interconnection of the substation NPP Krško to substation Tumbri in Croatia through two 400 kV lines wasn’t accounted. The obtained results in Table 5-26 are expected because: preferred sources of power delivery to substation NPP Krško are: the on-site generator in Krško and generators in power plant Brestanica. The model of the Slovenian power system as shown on Figure 5-3 has radial configuration therefore failure of the lines NPP Krško-Maribor and Maribor-Podlog will directly disrupt power delivery to the substation NPP Krško.

Table 5-27 show that element with the largest RAW importance measure for power delivery to the substation NPP Krško are: substation NPP Krško (BE “B1-101”), substation Podlog (BE “B1-104”) and substation Maribor (BE “B1-103”).

Table 5-27 Basic events with the largest RAW for NPP Krško

BE	BE description	RAW
B1-101	Substation 101 failure	6.44E+03
B1-104	Substation 104 failure	6.95E+01
B1-103	Substation 103 failure	6.64E+01
L1-103 104	Line failure 103-104	6.31E+01
L1-101 103	Line failure 101-103	6.28E+01
G2 101- 1	Generator 101-1 failure	1.83E+01

The elements identified in Table 5-27 should be maintained well, in order that the reliability of power delivery to the substation NPP Krško is not reduced significantly. The obtained results are expected because failure of these elements will result in: substation NPP Krško - disconnection of NPP from power system disrupting power delivery from power system to the house load, substations Podlog and Maribor failure – disruption of power delivery from other generators (excluding Brestanica) in the power system to the substation NPP Krško.

In the analysis of the fault tree constructed for the failure of substation NPP Krško, two elements, namely circuit breaker CB01002 and disconnect switch DS01013 contribute 48.26% of total substation unreliability equal to $Q_{NPP-Krško}=1.381E-09$, and these two elements should be in the focus of the maintenance and upgrade activities.

To summarize, the obtained results show that the most important elements for the Slovenian power system reliability are: substation NPP Krško and corresponding generator, CCF of lines between substations Beričevo – Okroglo, transformer between substations NPP Krško and RTP Krško, generators in the substations Šoštanj G4 and Šoštanj G5 and substation Beričevo. The most important elements for reliability of the power delivery to substation NPP Krško are the corresponding generator and generators in the substation Brestanica.

5.4.2 Basic Slovenian power system with the consideration of voltages

The results obtained for the Slovenian power system with the consideration of the voltages in the substations are identical to the results given in section 5.4.1. This result is obtained, because in the procedure of testing energy flow paths described in section 4.2.1, none of the identified energy flow paths was discarded due to the violation of the voltages, resulting with the construction of identical fault trees. The voltages in the substations for the basic Slovenian power system together with the power flows through lines are given in Table 5-28 and Table 5-29. The obtained results in Table 5-28 show that the voltages in the substations are in the interval of allowed operational voltages as a result of balanced production and selective reposition of reactive power sources in the system. The selection of injected reactive power was done after multiple trials on the basic configuration.

Table 5-28 Calculated voltages in substations for the basic Slovenian power system

No.	Substation Identification	Name	Load(MW)	Load(Mvar)	Un (%)	Un(kV)
1	101	NPP Krško	30	0	101.4	405.6
2	102	RTP Krško	254	54	99.14	218.1
3	103	Maribor	139	17	101.55	406.2
4	104	Podlog	0	0	101.32	405.3
5	105	Podlog 2	0	0	99.6	219.1
6	106	Šoštanj G4	0	0	103.18	227
7	107	Šoštanj G5	0	0	101.81	407.2
8	108	Podlog 3	100.4	50.3	99.36	109.3
9	109	Šoštanj	0	0	107.22	117.9
10	110	Cirkovce	93.6	105.6	94.83	208.6
11	111	Beričevo	115	0	100.96	403.8
12	112	Beričevo 2	74.5	60.6	98.7	217.1
13	113	Beričevo 3	80.7	14.8	97.49	107.2
14	114	Kleče 2	113.2	68	90.95	100
15	115	Kleče	0	0	95.66	210.4
16	116	Divača	77.4	32.2	102.21	408.8
17	117	Divača 2	48.4	47.6	97.09	213.6
18	118	Okroglo	159.5	58.3	100.69	110.8
19	119	Brestanica	70	0	99.23	109.1

The active and reactive power flows shown in Table 5-29 for the basic Slovenian power system are smaller than nominal thermal limitations. The overload tests described in section 4.2.1 didn't identify overloaded line in case of single line failure.

Comparison of the results obtained for examined configurations in following chapters, with and without consideration of voltages in the consistency test, described in section 4.3.9, has

shown that the difference between obtained results is small. Therefore, in the following chapters, the results obtained without consideration of the voltages of the substations are presented.

Table 5-29 Calculated power flows through lines for the basic Slovenian power system

Line No.	Starting substation	End substation	Flow(MW) Start	Flow(Mvar) Start	Flow(MW) End	Flow(Mvar) End
1	101	102	260.2	75.9	-260.2	-52.3
2	101	103	409.9	-53.8	-409.9	36.5
3	103	104	270.9	-10.9	-270.9	-7.9
4	104	107	-246.8	-45.4	246.8	29.5
5	104	111	497.6	1.6	-497.6	-1.5
6	111	118	79.8	-11.9	-79.8	-29.4
7	111	118	79.8	-11.9	-79.8	-29.4
8	111	116	77.4	-110.4	-77.4	74.7
9	115	117	48.4	-37.1	-48.4	31.5
10	112	115	161.6	41.7	-161.6	-35.1
11	105	112	171.1	-3.4	-171.1	8.5
12	105	106	-232.9	-49.2	232.9	66.5
13	105	110	93.6	101.9	-93.6	-98.4
14	111	112	74.6	69.5	-74.6	-66.1
15	111	112	74.6	69.5	-74.6	-66.1
16	104	105	20.6	53.2	-20.6	-52.1
17	108	109	-35	-46.6	35	51.3
18	102	119	0	-1.3	0	0
19	102	119	0	-1.3	0	0
20	112	113	44.2	10.4	-44.2	-8.1
21	112	113	44.2	10.4	-44.2	-8.1
22	105	108	35.8	1.9	-35.8	-0.5
23	105	108	35.8	1.9	-35.8	-0.5
24	114	115	-62	-34.3	62	40.1
25	114	115	-62	-34.3	62	40.1

5.5 Analysis of the configurations of the Slovenian power system

The analysis of the several configurations of the Slovenian power system is done with change of the interconnections and load/generation in the basic configuration presented in section 5.3. The new interconnection between substations NPP Krško – Beričevo is added, single and double, and implication on the results is tested. The increase of the load and addition of the new NPP in the substation NPP Krško is tested with two approaches. The first approach is to increase all loads in the system proportionally with summary increase equal to the size of the new NPP Krško generator. The second selected approach is to increase load only in substation Divača for the size of the new NPP Krško generator. The obtained results from these analysis and power system configurations are given in the following sections.

5.5.1 Slovenian power system with the single NPP Krško - Beričevo line

The new 400 kV line between substation NPP Krško and substation Beričevo was added to the basic model of Slovenian power system and configuration, shown on Figure 5-4, was analyzed.

The number of the identified MCS was 519, with the ten most important MCS given in Table 5-30.

Table 5-30 Identified MCS for power delivery to the NPP Krško

No.	Event 1	Event 2	Event 3	Event 4	Event 5	Event 6
1	G2 101- 1	L1-101 111	L1-101 103	G2 119- 1		
2	G2 101- 1	L1-101 111	L1-103 104	G2 119- 1		
3	G2 101- 1	G2 105- 1	G2 109- 1	G2 106- 1	G2 107- 1	G2 119- 1
4	G2 101- 1	L1-101 111	L1-101 103	L1-101 102		
5	G2 101- 1	L1-101 111	L1-101 103	L2-102 119		
6	G2 101- 1	G2 105- 1	L1-108 109	G2 106- 1	G2 107- 1	G2 119- 1
7	G2 101- 1	L1-101 111	L1-103 104	L1-101 102		
8	G2 101- 1	L1-101 111	L1-103 104	L2-102 119		
9	G2 101- 1	L1-105 112	L1-104 105	G2 107- 1	G2 119- 1	
10	G2 101- 1	G2 105- 1	G2 109- 1	G2 106- 1	L1-104 107	G2 119- 1

The results in Table 5-30 compared to MCS given in Table 5-21 indicate the considerable change resulting from introduction of the new line between substation NPP Krško and substation Beričevo (BE “L1-101 111”). The MCS number 3 in Table 5-30 demonstrate the increase of the importance of other generators resulting from introduction of new line.

The unreliability of the power delivery to the substation NPP Krško and weighted system unreliability is given in Table 5-31.

Table 5-31 Obtained unreliabilities for configuration with the single NPP Krško-Beričevo line

Parameter	Weighted system unreliability	Unreliability of power delivery to substation NPP Krško
Value	1.37E-02	1.80E-06

Compared to the results shown in Table 5-22, decrease of the weighted system unreliability (power system is more reliable) is notified. The change of the weighted system unreliability is small because introduction of the line NPP Krško-Beričevo doesn't affect the reliability of the power delivery to the biggest load in the system situated in the substation RTP Krško. The size of the load in the substation RTP Krško is larger compared to the all generators in the Slovenian power system, except the generator in NPP Krško. Therefore, the reliability of the power supply to the load in the substation RTP Krško is not affected by the changes in the power system.

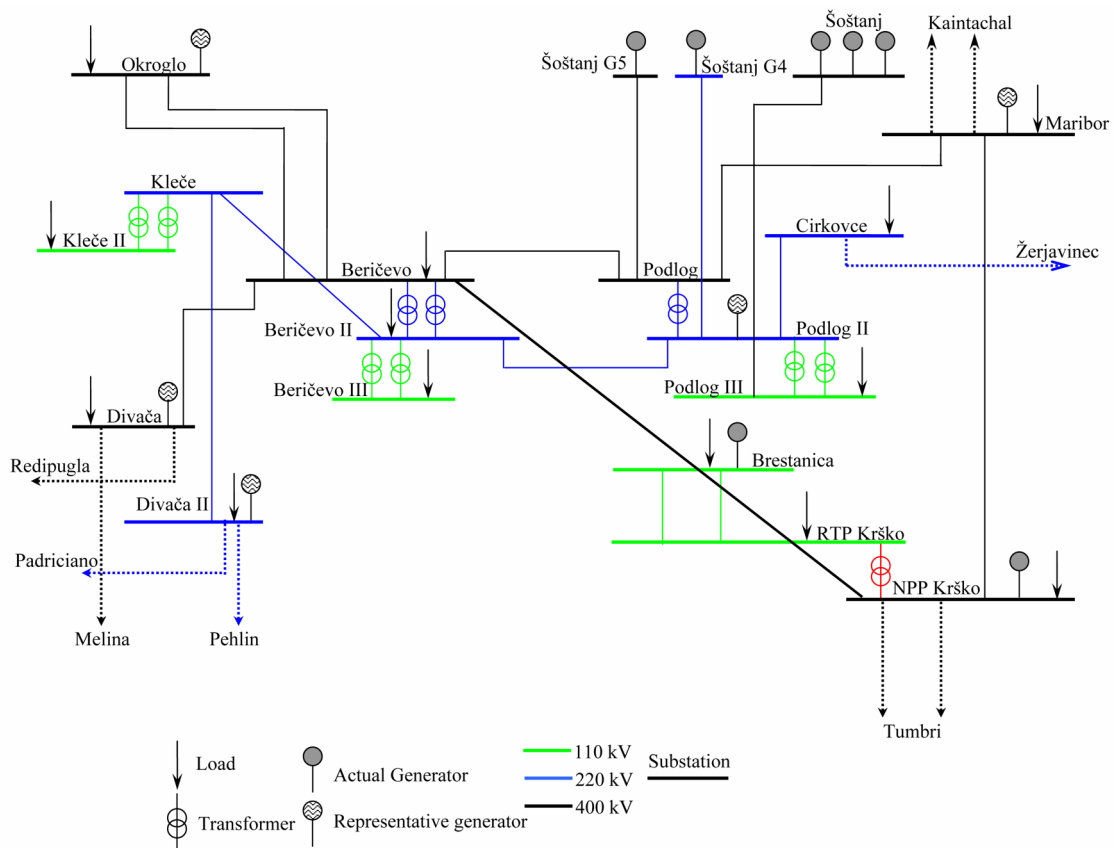


Figure 5-4 Slovenian power system with the added line NPP Krško – Beričevo

Comparison of the results in Table 5-31 and in Table 5-22 shows that unreliability of the power delivery to the house load in the substation NPP Krško decreased significantly. This result is obtained because the new power line introduction increased the number of available energy flow paths to the load in the substation NPP Krško.

The importance measures NRRW and NRAW for selected elements in the power system are given in Table 5-32 and Table 5-33.

Table 5-32 Basic events with the largest NRRW, single NPP Krško – Beričevo line added

BE	BE description	NRRW
G2 101- 1	Generator 101-1 failure	4.83E+00
L2-111 118	CCF line 111-118	1.08E+00
L1-101 102	Line failure 101-102	1.06E+00
G2 106- 1	Generator 106-1 failure	1.05E+00
G2 107- 1	Generator 107-1 failure	1.05E+00
L1-111 116	Line failure 111-116	1.03E+00
L1-112 115	Line failure 112-115	1.02E+00
L2-102 119	CCF line 102-119	1.01E+00
L1-105 110	Line failure 105-110	1.01E+00
L1-115 117	Line failure 115-117	1.01E+00

The results shown in Table 5-32 are comparable to results shown in Table 5-24 with the increase of the NRRW for generator NPP Krško (BE “G2 101- 1”), and appearance of the generators in the substations Šoštanj G4 and Šoštanj G5 (BE “G2 106- 1” and BE “G2 107- 1”). This result is expected, accounting that new line increase the number of flow paths from NPP Krško to other loads in the Slovenian power system.

The results in Table 5-33 show the elements with the largest NRAW importance measure. The same elements as in Table 5-25 are identified: substations NPP Krško, Beričevo and RTP

Krško (BE “B1-101”, “B1-111” and “B1-102”) and transformer between substations NPP Krško and RTP Krško (BE “L1-101 102”).

Table 5-33 Basic events with the largest NRAW, single NPP Krško – Beričevo line added

BE	BE description	NRAW
B1-101	Substation 101 failure	2.09E+01
B1-111	Substation 111 failure	2.00E+01
B1-102	Substation 102 failure	1.84E+01
L1-101 102	Line failure 101-102	1.84E+01
B1-112	Substation 112 failure	1.81E+01
G2 101- 1	Generator 101-1 failure	1.47E+01
B1-105	Substation 105 failure	1.18E+01
B1-115	Substation 115 failure	9.70E+00
L1-112 115	Line failure 112-115	9.68E+00
B1-118	Substation 118 failure	9.58E+00

The results obtained for the importance measures for load in the substation NPP Krško, are given in Table 5-34 and Table 5-35.

Table 5-34 Basic events with the largest RRW for the NPP Krško

BE	BE description	RRW
G2 101- 1	Generator 101-1 failure	1.31E+03
G2 119- 1	Generator 119-1 failure	3.09E+01
L1-101 111	Line failure 101-111	1.27E+01
L1-101 103	Line failure 101-103	2.61E+00
L1-103 104	Line failure 103-104	1.44E+00
G2 107- 1	Generator 107-1 failure	1.08E+00

With the introduction of new line NPP Krško–Beričevo, the same elements identified in Table 5-26 to have the largest RRW are also identified in Table 5-34. The major difference is inclusion of new line NPP Krško–Beričevo with the third largest RRW (BE “L1-101 111”) and generator G5 (BE “G2 107- 1”) in Šoštanj power plant with the sixth largest RRW.

The results in Table 5-35, compared to results given in Table 5-27, show that with the introduction of new line, the RAW and ordering of Slovenian power system elements have changed.

Table 5-35 Basic events with the largest RAW for the NPP Krško

BE	BE description	RAW
B1-101	Substation 101 failure	5.54E+05
B1-105	Substation 105 failure	6.97E+02
L1-101 111	Line failure 101-111	8.62E+01
B1-111	Substation 111 failure	8.11E+01
B1-104	Substation 104 failure	7.79E+01
L1-103 104	Line failure 103-104	5.84E+01

The elements in Table 5-35 identified with the largest RAW are: substation NPP Krško (BE “B1-101”), substation Podlog 2 (BE “B1-105”), line between substation NPP Krško and substation Beričevo (BE “L1-101 111”), substation Beričevo (BE “B1-111”), substation Podlog (BE “B1-104”) and line from it to the substation Maribor (BE “L1-103 104”). The change of the RAW is result of the shift of the power flows from line NPP Krško-Maribor to line NPP Krško–Beričevo and change of the flows through lines connected to substation Podlog.

The active and reactive power flows are shown in Table 5-36. The flow through NPP Krško-Maribor line, compared to the flow given in Table 5-29, has decreased.

Table 5-36 Calculated power flows through lines for Slovenian power system, single NPP Krško – Beričevo line

Line No.	Starting substation	Ending substation	Flow(MW) Start	Flow(Mvar) Start	Flow(MW) End	Flow(Mvar) End
1	101	102	260.2	75.9	-260.2	-52.3
2	101	103	150.1	-81.6	-150.1	32.8
3	103	104	11.1	-7.6	-11.1	-19.6
4	104	107	-246.8	-45.7	246.8	29.5
5	104	111	261.3	11.6	-261.3	-27.2
6	111	118	79.8	-12.2	-79.8	-29.8
7	111	118	79.8	-12.2	-79.8	-29.8
8	111	116	77.4	-111.6	-77.4	75.3
9	115	117	48.4	-37.5	-48.4	31.9
10	112	115	161.6	41.9	-161.6	-35.2
11	105	112	147.6	-2.7	-147.6	5.3
12	105	106	-232.9	-49.1	232.9	66.8
13	105	110	93.6	102.6	-93.6	-99.2
14	111	112	86.6	68.9	-86.6	-64.9
15	111	112	86.6	68.9	-86.6	-64.9
16	104	105	-3.4	54.6	3.4	-53.6
17	108	109	-35	-46.9	35	51.7
18	102	119	0	-1.3	0	0
19	102	119	0	-1.3	0	0
20	112	113	44.2	10.5	-44.2	-8.2
21	112	113	44.2	10.5	-44.2	-8.2
22	105	108	35.8	1.9	-35.8	-0.4
23	105	108	35.8	1.9	-35.8	-0.4
24	114	115	-62	-34.6	62	40.5
25	114	115	-62	-34.6	62	40.5
26	101	111	259.8	-66.7	-259.8	27.7

To summarize, with the introduction of the new line between substation NPP Krško and substation Beričevo, the reliability of the Slovenian power system improved with the considerable improvement of the reliability of the power delivery to the house load in the NPP Krško. The obtained results for network importance measures and power delivery to NPP Krško indicate the importance of the generator and substation NPP Krško for overall reliability of the Slovenian power system. The importance of the lines NPP Krško-Maribor and NPP Krško–Beričevo for reliable power delivery to substation NPP Krško is verified.

5.5.2 Slovenian power system with the double Krško - Beričevo line

The new double 400 kV line was added between substation NPP Krško and substation Beričevo of the Slovenian power system, as shown on Figure 5-5, and this new configuration was analyzed. From the fault tree built for the power delivery to the load in NPP Krško in total 551 MCS were identified, with the ten most important given in Table 5-37.

Table 5-37 Identified MCS for power delivery to the NPP Krško

No.	Event 1	Event 2	Event 3	Event 4	Event 5	Event 6
1	G2 101- 1	G2 105- 1	G2 109- 1	G2 106- 1	G2 107- 1	G2 119- 1
2	G2 101- 1	L2-101 111	L1-101 103	G2 119- 1		
3	G2 101- 1	L2-101 111	L1-103 104	G2 119- 1		
4	G2 101- 1	L1-101 111	L3-101 111	L1-101 103	G2 119- 1	
5	G2 101- 1	G2 105- 1	L1-108 109	G2 106- 1	G2 107- 1	G2 119- 1
6	G2 101- 1	L1-105 112	L1-104 105	G2 107- 1	G2 119- 1	
7	G2 101- 1	L1-101 111	L3-101 111	L1-103 104	G2 119- 1	
8	G2 101- 1	G2 105- 1	G2 109- 1	G2 106- 1	L1-104 107	G2 119- 1
9	G2 101- 1	G2 105- 1	G2 109- 1	G2 106- 1	G2 107- 1	L1-101 102
10	G2 101- 1	L2-101 111	L1-101 103	L1-101 102		

The MCS identified in Table 5-37 show that with the introduction of the double line between substation NPP Krško and substation Beričevo the reliability of the power delivery to the house load in the NPP Krško will depend mainly by the reliability of the generators in the system (BE identified in the first MCS) and CCF of the newly added line (BE “L2-101 111”). The calculated unreliability of the power delivery to the substation NPP Krško and weighted system unreliability is given in Table 5-38.

Table 5-38 Obtained unreliabilities for configuration with the double NPP Krško-Beričevo line

Parameter	Weighted system unreliability	Unreliability of power delivery to substation NPP Krško
Value	1.37E-02	3.23E-07

The results given in Table 5-38 compared to results given in Table 5-31 show that change of the line between substation NPP Krško and substation Beričevo from single to double doesn't affect the weighted system unreliability, resulting from the load in the substation RTP Krško and elaborated in the section 5.5.1. The change of the line from single to double between substation NPP Krško and Beričevo improved the reliability of the power delivery to the house load in the NPP Krško for 5.6 times, resulting from increased redundancy of energy flow path between terminal substations of the newly added line.

The small change of the importance measures NRRW and NRAW is notified in the results in the introduction of the double line, therefore values in Table 5-32 and Table 5-33, obtained for single line can be taken as relevant.

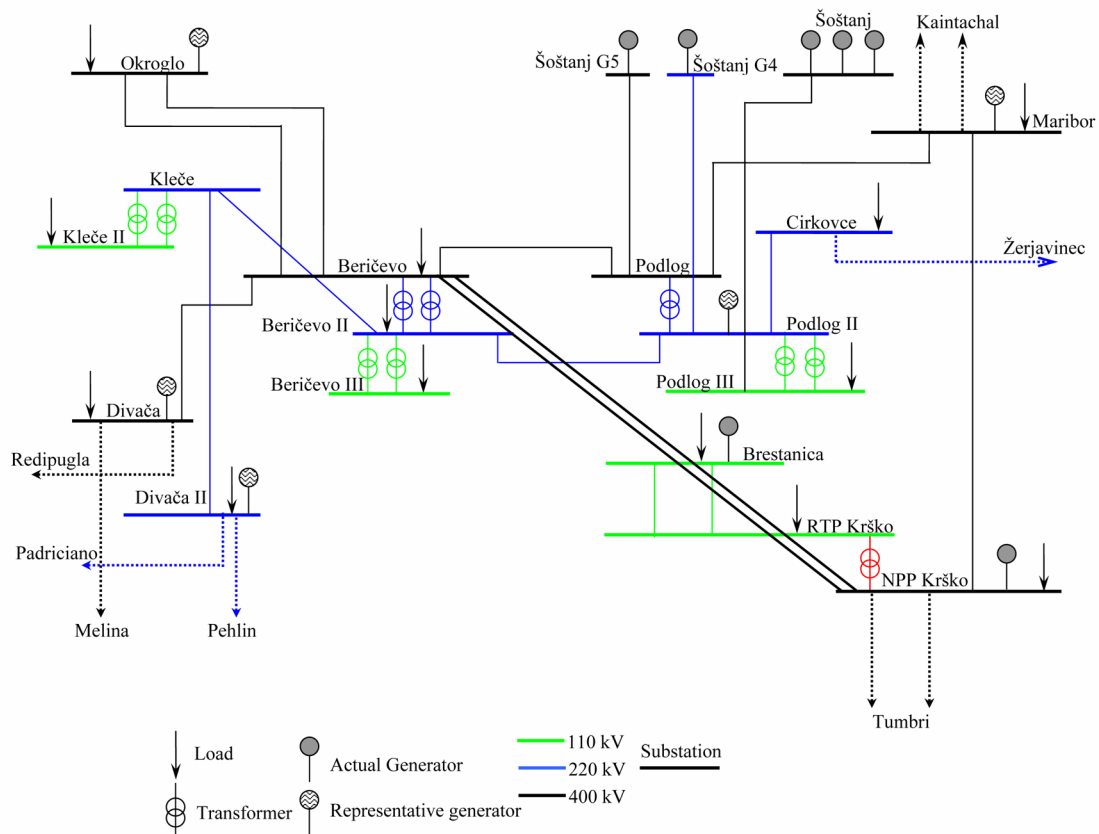


Figure 5-5 Slovenian power system with the double line between NPP Krško – Beričevo

The importance measures from the fault tree built for the power delivery to the house load in the substation NPP Krško, are given in the Table 5-39 and Table 5-40.

Table 5-39 Basic events with the largest RRW for the NPP Krško

BE	BE description	RRW
G2 101- 1	Generator 101-1 failure	2.36E+02
G2 119- 1	Generator 119-1 failure	2.80E+01
L2-101 111	CCF line 101-111	2.04E+00
G2 107- 1	Generator 107-1 failure	1.70E+00
G2 105- 1	Generator 105-1 failure	1.67E+00
G2 106- 1	Generator 106-1 failure	1.65E+00

The results shown in Table 5-39, compared to results in Table 5-34, show decrease of the RRW for generators in the substations NPP Krško and Brestanica and appearance of CCF of lines between substations NPP Krško and Beričevo and generators in substations Šoštanj G4, Šoštanj G5 and Podlog. The results in Table 5-40 compared to results in Table 5-35, show that the obtained RAW have decreased with the substitution of basic event NPP Krško–Beričevo line failure with the CCF of lines between these substations.

Table 5-40 Basic events with the largest RAW for the NPP Krško

BE	BE description	RAW
B1-101	Substation 101 failure	3.07E+06
B1-105	Substation 105 failure	3.95E+03
B1-111	Substation 111 failure	4.91E+02
L2-101 111	CCF line 101-111	4.78E+02
B1-104	Substation 104 failure	1.07E+02
L1-103 104	Line failure 103-104	3.64E+01

The active and reactive power flows in the power system are shown in Table 5-41.

Table 5-41 Calculated power flows through lines of the Slovenian Power system, double NPP Krško – Beričevo line

Line No.	Starting substation	Ending substation	Flow(MW) Start	Flow(Mvar) Start	Flow(MW) End	Flow(Mvar) End
1	101	102	260.2	75.9	-260.2	-52.3
2	101	103	95.2	-80.5	-95.2	28.8
3	103	104	-43.8	-3.6	43.8	-23.4
4	104	107	-246.8	-45.7	246.8	29.5
5	104	111	211.3	15.1	-211.3	-32.8
6	111	118	79.8	-12.2	-79.8	-29.8
7	111	118	79.8	-12.2	-79.8	-29.8
8	111	116	77.4	-111.7	-77.4	75.3
9	115	117	48.4	-37.6	-48.4	31.9
10	112	115	161.6	41.9	-161.6	-35.2
11	105	112	142.7	-2.5	-142.7	4.5
12	105	106	-232.9	-49.1	232.9	66.8
13	105	110	93.6	102.7	-93.6	-99.2
14	111	112	89.2	68.6	-89.2	-64.5
15	111	112	89.2	68.6	-89.2	-64.5
16	104	105	-8.5	54.9	8.5	-54
17	108	109	-35	-47	35	51.7
18	102	119	0	-1.3	0	0
19	102	119	0	-1.3	0	0
20	112	113	44.2	10.5	-44.2	-8.2
21	112	113	44.2	10.5	-44.2	-8.2
22	105	108	35.8	1.9	-35.8	-0.4
23	105	108	35.8	1.9	-35.8	-0.4
24	114	115	-62	-34.7	62	40.5
25	114	115	-62	-34.7	62	40.5
26	101	111	157.3	-64.8	-157.3	16.5
27	101	111	157.3	-64.8	-157.3	16.5

The obtained power flows given in Table 5-41, compared to power flows in Table 5-36, show that flows through line between substation NPP Krško and substation Maribor and line between substation Beričevo and substation Maribor have decreased with the increase of flow in line between substation NPP Krško and substation Beričevo.

To summarize, with the introduction of double lines between substation NPP Krško and substation Beričevo, reliability of the power delivery to the house load in the substation NPP Krško improves and depends on the CCF of the added line.

5.5.3 Slovenian power system with the new NPP in Krško and proportional increase of the load

A new nuclear power plant, with the parameters equal to NPP Krško was added to the substation NPP Krško, as shown on Figure 5-6. The loads in the system were proportionally increased for 700 MW. Values of the other parameters were taken same as the basic system configuration given in the section 5.4.1. The configuration with the single line between substation NPP Krško and substation Beričevo was necessary because operation without this

line is not feasible (the total generated power in the substation NPP Krško, when two nuclear power plants are connected, is larger than transfer capacity of the NPP Krško-Maribor line).

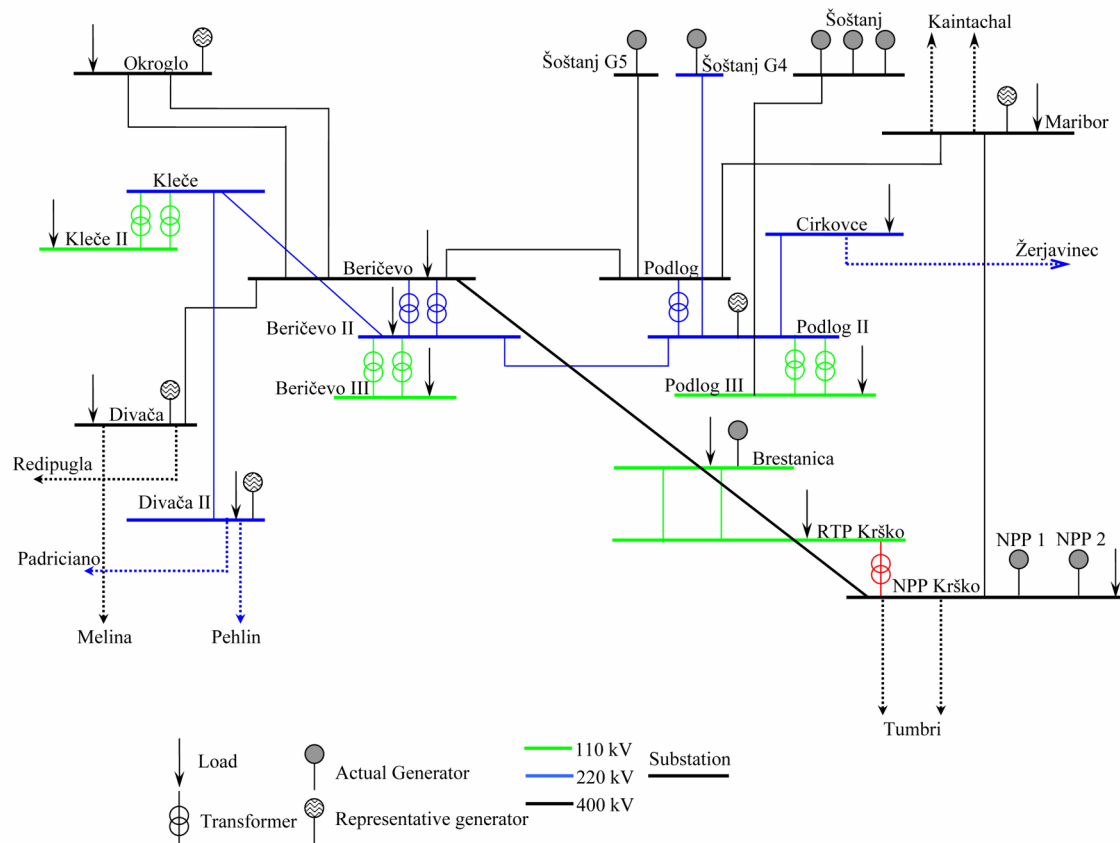


Figure 5-6 Slovenian power system with the two NPP Krško and single line NPP Krško – Beričevo
 From the fault tree built for the power delivery to the load in NPP Krško, 70 MCS were identified, with the ten most important given in Table 5-44.

Table 5-42 Identified MCS for power delivery to the NPP Krško

No.	Event 1	Event 2	Event 3	Event 4
1	G2 101- 2	G2 105- 1	G2 106- 1	G2 107- 1
2	G2 101- 2	L1-101 111	L1-101 103	
3	G2 101- 2	L1-101 111	L1-103 104	
4	G2 101- 2	G2 105- 1	G2 106- 1	L1-104 107
5	G2 101- 2	G2 105- 1	L1-105 106	G2 107- 1
6	G2 101- 2	G2 105- 1	G2 106- 1	B1-107
7	G2 101- 2	G2 105- 1	B1-106	G2 107- 1
8	G2 101- 2	L1-105 112	L1-104 105	G2 107- 1
9	G2 101- 2	G2 105- 1	L1-105 106	L1-104 107
10	G2 101- 2	L2-111 112	L1-104 105	G2 107- 1

The new generator in the substation NPP Krško appears in the identified MCS shown in Table 5-44 because the second generator in NPP Krško is selected as a slack bus, resulting with the smaller output power. Therefore the second generator in NPP Krško is ranked lower in the MCS list. The calculated unreliability of the power delivery to the substation NPP Krško and weighted system unreliability is given in Table 5-43.

Table 5-43 Obtained unreliabilities for configuration with the proportionally increased load

Parameter	Weighted system unreliability	Unreliability of power delivery to NPP Krško
Value	1.40E-02	3.24E-05

The results in Table 5-43 show that Slovenian power system, with the additional nuclear power plant in substation NPP Krško is on the same reliability level as the one given in Table 5-22 for the basic Slovenian power system. The reliability of the power delivery to the substation NPP Krško for self consumption of both plants is improved compared to reliability for the basic configuration.

The importance measures NRRW and NRAW for selected elements in the power system are given in Table 5-44 and Table 5-45.

Table 5-44 Basic events with the largest NRRW, new NPP and single NPP Krško – Beričevo line added

BE	BE description	NRRW
G2 101- 2	Generator 101-2 failure	5.39E+00
G2 107- 1	Generator 107-1 failure	1.10E+00
L2-111 118	CCF line 111-118	1.07E+00
L1-101 102	Line failure 101-102	1.06E+00
G2 106- 1	Generator 106-1 failure	1.04E+00
L1-111 116	Line failure 111-116	1.03E+00
L1-105 110	Line failure 105-110	1.01E+00
L1-115 117	Line failure 115-117	1.01E+00
L1-112 115	Line failure 112-115	1.01E+00
L2-102 119	CCF line 102-119	1.01E+00

The NRRW of the new NPP Krško generator (BE “G2 101- 2”) is larger compared to the current generator in the NPP Krško (BE “G2 101- 1”). The difference of the NRRW for current and new generator in NPP Krško is obtained because existing generator is taken as a slack (balancing bus) in the power system and power of that power plant is smaller than newly added. The NRRW for other power plants and lines are increased due to the increased size of the loads in the system.

The results for the NRAW given in Table 5-45 show increase of the NRAW for substation NPP Krško and substation Beričevo. This is expected accounting the increased power flows through identified substations in the power system.

To summarize, with the introduction of new nuclear power plant in substation Krško, proportional increase of load and single NPP Krško – Beričevo line, the reliability of the power system is increased compared to the current level of reliability together with the increased reliability of power delivery to NPP Krško substation. Increase of the importance of substation Podlog with the corresponding generator and decrease of the importance of generators in substation Brestanica is notified.

Table 5-45 Basic events with the largest NRAW, new NPP and single NPP Krško – Beričevo line added

BE	BE description	NRAW
B1-101	Substation 101 failure	2.21E+01
B1-111	Substation 111 failure	1.92E+01
B1-102	Substation 102 failure	1.77E+01
L1-101 102	Line failure 101-102	1.77E+01
G2 101- 2	Generator 101-2 failure	1.51E+01
B1-112	Substation 112 failure	1.15E+01
B1-105	Substation 105 failure	1.13E+01
B1-118	Substation 118 failure	9.24E+00
L2-111 118	CCF line 111-118	9.17E+00
B1-103	Substation 103 failure	8.21E+00

The line between substation NPP Krško and substation Beričevo was changed from single to double and obtained unreliabilities are given in Table 5-46.

Table 5-46 Obtained unreliabilities for configuration with the proportionally increased load, double NPP Krško – Beričevo line

Parameter	Weighted system unreliability	Unreliability of power delivery to substation NPP Krško
Value	1.40E-02	2.40E-05

The results in Table 5-46 show that with the introduction of double line NPP Krško – Beričevo, the weighted system unreliability will remain on same value and reliability of the power delivery to the substation NPP Krško is improved for a small value. Change of the values calculated for importance measures are small.

To summarize, with the change of the line NPP Krško–Beričevo from single to double, increase of the reliability of the power delivery to the NPP Krško is identified together with the appearance of CCF of the line in the list of elements with the largest RAW.

5.5.4 Slovenian power system with the new NPP in Krško and increase of the load in the substation Divača

The new nuclear power plant, equal to the NPP Krško and single line between substation NPP Krško and substation Beričevo was added to the basic configuration of the Slovenian power system, as shown on Figure 5-6. The load in the substation Divača was increased for the 700MW to simulate export of the produced electricity in the new NPP Krško to the Italian power system. The parameters of other elements were the same as those used for the basic system configuration described in the section 5.4.1.

From the fault tree built for the house load of the both NPP in the substation NPP Krško, 298 MCS were identified with ten most important given in Table 5-47.

The identified MCS given in Table 5-47, compared to the MCS given in Table 5-44, include failure of the generators in the substation Brestanica (BE “G2 119- 1”). The second identified difference is the increase of the number of the basic events in the minimal cut sets.

Table 5-47 Identified MCS for the power delivery to the NPP Krško

No.	Event 1	Event 2	Event 3	Event 4	Event 5
1	G2 101- 2	G2 105- 1	G2 106- 1	G2 107- 1	G2 119- 1
2	G2 101- 2	L1-101 111	L1-101 103	G2 119- 1	
3	G2 101- 2	L1-101 111	L1-103 104	G2 119- 1	
4	G2 101- 2	G2 105- 1	G2 106- 1	L1-104 107	G2 119- 1
5	G2 101- 2	G2 105- 1	G2 106- 1	G2 107- 1	L1-101 102
6	G2 101- 2	G2 105- 1	L1-105 106	G2 107- 1	G2 119- 1
7	G2 101- 2	G2 105- 1	G2 106- 1	G2 107- 1	L2-102 119
8	G2 101- 2	L1-101 111	L1-101 103	L1-101 102	
9	G2 101- 2	G2 105- 1	G2 106- 1	B1-107	G2 119- 1
10	G2 101- 2	L1-101 111	L1-101 103	L2-102 119	

The calculated unreliability of the power delivery to the substation NPP Krško and weighted system unreliability is given in Table 5-48, with the system reliability given in Table 5-50.

Table 5-48 Obtained unreliability for increased load in Divača and single NPP Krško–Beričevo line added

Parameter	Weighted system unreliability	Unreliability of power delivery to substation NPP Krško
Value	3.18E-02	1.80E-06

Table 5-49 Obtained reliability for increased load in Divača and single NPP Krško – Beričevo line added

System reliability	0.968
--------------------	-------

The weighted system unreliability given in Table 5-48 has increased compared to the value given in Table 5-43 obtained for the Slovenian power system with the proportional increase of the load. With the increase of the load in the substation Kleče for the 700 MW only energy flow paths between substation Kleče and substation NPP Krško are accounted in the model.

The unreliability of the power delivery to the house load of the both nuclear power plants in the substation NPP Krško decreases compared to the unreliability obtained from the system with the proportionally increased loads. Unreliability decreased due to the decrease of power flows through adjacent power lines connected to the substation NPP Krško.

To summarize, with the introduction of additional nuclear power plant in the substation NPP Krško and increase of load in the substation Divača, the reliability of the power system decreases compared to the reliability of the system with the basic configuration or system with the proportional increase of the load. The reliability of power delivery to NPP Krško substation is increased and is equal to reliability of the basic configuration with the single NPP Krško – Beričevo line added.

The line between substation NPP Krško and substation Beričevo was changed from single to double and obtained unreliabilities are given in Table 5-50.

Table 5-50 Obtained unreliabilities for increased load in Divača and double NPP Krško – Beričevo line added

Parameter	Weighted system unreliability	Unreliability of power delivery to substation NPP Krško
Value	3.17E-02	3.24E-07

The results given in Table 5-50 show that the change of the line NPP Krško – Beričevo from single to double, decreases the weighted system unreliability and the unreliability of the power delivery to house load in the substation NPP Krško.

In the obtained results for the importance measures, the CCF of the lines between substations NPP Krško and Beričevo is identified with the largest RAW, together with the failure of the generator in the substation Podlog 2 and failure of the substation Beričevo.

5.5.5 Summary of the results obtained for the Slovenian Power System

Several configurations of the simplified Slovenian power system were analyzed. The implication of the introduction of the single and double line between substation NPP Krško and substation Beričevo was foreseen together with the consequences due to the change of the load and introduction of additional nuclear power plant in the power system. The obtained results for the unreliability of the power delivery to the house load of the NPP Krško and weighted system unreliability for all models of the Slovenian power system are given in Table 5-51.

Table 5-51 Summarized results for the Slovenian power system

No.	Power system model	Weighted system unreliability	Unreliability of power delivery to NPP Krško
1.	NPP Krško, basic configuration of the Slovenian power system	1.40E-02	1.55E-04
2.	NPP Krško, single NPP Krško - Beričevo line	1.37E-02	1.80E-06
3.	NPP Krško, double NPP Krško - Beričevo line	1.37E-02	3.23E-07
4.	NPP Krško 1-2, proportional load increase, single NPP Krško - Beričevo line	1.40E-02	3.24E-05
5.	NPP Krško 1-2, proportional load increase, double NPP Krško - Beričevo line	1.40E-02	2.40E-05
6.	NPP Krško 1-2, load increase in Divača, single NPP Krško - Beričevo line	3.18E-02	1.80E-06
7.	NPP Krško 1-2, load increase in Divača, double NPP Krško - Beričevo line	3.17E-02	3.24E-07

The obtained results show the following findings:

- Reliability of the substation NPP Krško and corresponding generator are the most important elements for the overall reliability of the Slovenian power system. This conclusion is supported by the NRRW and NRAW importance measures values obtained for these elements. Obtained result is expected accounting the installed power of the NPP Krško generator as a largest unit in the Slovenian power system and power circulated through substation NPP Krško. With the inclusion of the interconnections to the Croatian power system the increase of the importance of the NPP Krško is expected.
- The introduction of the power line between substation NPP Krško and substation Beričevo improves the overall system reliability and reliability of the power delivery to the house load in the NPP Krško. Obtained result is important from the aspect of the nuclear safety because, improvement of the reliability of the power delivery to the house load (self consumption) of the NPP Krško implies more reliable offsite power and decrease of the loss of offsite power (LOOP) initiating event frequency. The decrease of the LOOP frequency results in the decrease of the core damage frequency and increased safety of the nuclear power plant. The introduction of the line NPP Krško – Beričevo improves, in addition, the reliability of the power delivery to other loads in the system resulting in decrease of the weighted system unreliability.
- The change of the line between substation NPP Krško and substation Beričevo from single to double will additionally improve reliability of power delivery to the house load of the NPP Krško. The obtained results identify the CCF of the interconnection as

an important contributor to the reliability of the power delivery. From the aspect of the nuclear safety, the introduction of the double line will decrease the frequency of the LOOP initiating event, but this decrease will depend on the CCF of the interconnection. Obtained results show that substitution of the interconnection between substation NPP Krško and substation Beričevo from single to double lines doesn't decrease noticeably the weighted system unreliability.

- With the proportional increase of the loads and introduction of the new nuclear power plant in the substation NPP Krško, the unreliability of the power delivery to the house load (sum of the self consumption of the both nuclear power plants) in NPP Krško decreased compared to the unreliability obtained for the single nuclear power plant basic configuration of the Slovenian power system. The necessity of the interconnection between substation NPP Krško and substation Beričevo (single or double) is confirmed.
- With the increase of the load only in the substation Divača, the largest weighted system unreliability is obtained, indicating the lowest level of the power system reliability compared to the values from other scenarios. Contrary to this, the smallest unreliability of the power delivery to the house load, accounting self consumption of both nuclear power plants in NPP Krško, was obtained. The obtained result indicates that from the aspect of the nuclear safety, configuration with the increased load in the substation Divača corresponding to the export to the Italy, is the safest one.
- The obtained results from test configurations indicate that the most important elements of the power system, that contribute to the reliability of the power delivery to the house load of the substation NPP Krško, are generators in the substation Brestanica, lines between substation NPP Krško and substations Maribor and Beričevo and transformer between substation NPP Krško and substation RTP Krško. Accounting the implication of the reliability of the identified elements on the nuclear safety of the NPP Krško, proper actions should be taken to maintain and improve their reliability (for example improvement of the maintenance activities from aspect of quality and optimal time schedule).

6 Impact of Offsite Power System Reliability on Nuclear Power Plant Safety

Alternating current (AC) power is essential for safe operations and accident recovery at commercial nuclear power plants. The AC power is normally supplied by the offsite sources via the electrical grid. Thus, Loss of Offsite Power (LOOP, also referred to as LOSP) and subsequent restoration of offsite power are important inputs to plant probabilistic safety assessments (PSA). The results from statistical and engineering analysis of data for LOOP frequencies and durations at commercial nuclear reactors in the U.S. are presented in continuation. The impact of change of LOOP frequency to the core damage frequency of a specific PSA model of NPP in addition is presented.

6.1 LOOP data analysis

Data on LOOP and offsite power restoration have been analyzed in several reports^{14, 18, 92, 93}. The results from the NRC study⁶, which include data from 1986 through 2004, are presented.

Three categorization schemes are used to classify LOOP events:

- According to whether the plant was shut down or operating when the LOOP occurred and the consequences of the LOOP.
- According to the cause or location: plant centered, switchyard centered, grid related, and weather related.
- According to the length of the LOOP: momentary (offsite power is restored, or is potentially recoverable to at least one safety bus within less than 2 minutes) and sustained categories (require 2 min or more to restore offsite power).

The results in Table 6-1 summarize the LOOP statistical data. The first column in Table 6-1 identifies the operational mode of the plant. The second column specifies LOOP data category. The third identifies the data period. The fourth column includes number of the LOOP events. The fifth column includes the reactor critical or shutdown years used for calculation of the mean frequency given in the sixth column. The units of frequency are given in the last column of the table. The units of frequency are: per reactor critical year (/rcry) or per reactor shutdown year (/rsy). For power mode of operation of the nuclear power plants, grid-related LOOP contribute 52% to the total frequency of $3.6E-2$ per reactor critical year (/rcry), while switchyard-centered LOOP contribute 29%. The remaining two categories of LOOP have frequency contributions of 13% (weather related) and 6% (plant centered). For shutdown operation, switchyard-centered LOOP contribute 51% to the total frequency of $2.0E-1$ per reactor shutdown year (/rsy), while plant-centered and grid related LOOP contribute 26% and 5%, respectively. The summarized LOOP frequency is $2.3E-1$ per reactor year (/ry), with the 12% contribution of the grid related LOOP. The blackout event¹¹ on August 14, 2003, is included in the data of the study⁶. If that event is excluded from the analysis, the overall LOOP frequency for power operation would have been $2.5E-2$ /rcry rather than $3.6E-2$ /rcry.

Comparison of data obtained from previous studies is given in Table 6-2. For power mode of operation, the overall LOOP frequency has decreased from¹⁸ $1.2E-1$ /rcry to $5.8E-2$ /rcry⁹² ending with the current estimate⁶ of $3.6E-2$ /rcry. The relative contributions of the four categories of LOOP have changed significantly, with the increase of the share of the grid related LOOP. The overall shutdown operation LOOP frequency has remained essentially constant in all studies at approximately $2.0E-1$ /rsy.

Table 6-1 Plant-level LOOP frequencies⁶

Mode	LOOP Category Data	Data Period	Number of LOOP Events	Reactor Critical or Shutdown Years	Mean Frequency	Frequency Units*
Power operation	Plant centered	1997–2004	1	724.3	2.07E–03	/rcry
	Switchyard centered	1997–2004	7	724.3	1.04E–02	/rcry
	Grid related	1997–2004	13	724.3	1.86E–02	/rcry
	Weather related	1997–2004	3	724.3	4.83E–03	/rcry
	All	1997–2004	—	—	3.59E–02	/rcry
Shutdown operation	Plant centered	1986–2004	19	383.2	5.09E–02	/rsy
	Switchyard centered	1986–2004	38	383.2	1.00E–01	/rsy
	Grid related	1986–2004	3	383.2	9.13E–03	/rsy
	Weather related	1986–2004	13	383.2	3.52E–02	/rsy
	All	1986–2004	—	—	1.96E–01	/rsy

Table 6-2 LOOP frequency comparison with the previous reports⁶

		NUREG/CR-6890 (1986–2004)		NUREG/CR-5750 (1987–1995)	NUREG/CR-5496 (1980–1996)	NUREG-1032 (1968–1985)
Mode	LOOP Category Data	Mean Frequency	Frequency Units*	Mean Frequency	Mean Frequency	Mean Frequency
Power operation	Plant centered	2.07E–03	/rcry	Categories not distinguished	4.4E–02	8.7E–02
	Switchyard centered	1.04E–02	/rcry		Included in plant centered	Included in plant centered
	Grid related	1.86E–02	/rcry		2.9E–03	1.8E–02
	Weather related	4.83E–03	/rcry		1.2E–02	1.1E–02
	All	3.59E–02	/rcry		4.6E–02	5.8E–02
Shutdown operation	Plant centered	5.09E–02	/rsy	Shutdown not covered	1.8E–01	Shutdown not covered
	Switchyard centered	1.00E–01	/rsy		Included in plant centered	
	Grid related	9.13E–03	/rsy		3.3E–03	
	Weather related	3.52E–02	/rsy		1.2E–02	
	All	1.96E–01	/rsy		1.9E–01	

The results from LOOP duration data analysis⁶ including probabilities of exceedance versus duration are shown in Table 6-3. In Station Blackout regulatory guide¹⁰, it is stated that for NPP with the two emergency diesel generators (EDG), acceptable station blackout duration

capability is 4 and 8 hours respectively (depending on unit average EDG reliability as shown in Table 2 of the corresponding reference¹⁰). The presented results in Table 6-3 show that probabilities of exceedance versus duration of 4 and 8 hours are 1.57E-01 and 6.72E-02 respectively, and this data can be used in the station blackout event trees.

Table 6-3 LOOP duration data analysis⁶ of probabilities of exceedance

Duration (h)	Plant Centered	Switchyard Centered	Grid Related	Weather Related	Composite
0.00	1.00E+00	1.00E+00	1.00E+00	1.00E+00	1.00E+00
0.25	6.87E-01	7.86E-01	9.43E-01	8.64E-01	8.72E-01
0.50	4.79E-01	5.95E-01	8.25E-01	7.73E-01	7.31E-01
1.00	2.77E-01	3.78E-01	6.11E-01	6.56E-01	5.30E-01
1.50	1.83E-01	2.63E-01	4.61E-01	5.78E-01	4.03E-01
2.00	1.29E-01	1.94E-01	3.56E-01	5.20E-01	3.18E-01
2.50	9.64E-02	1.49E-01	2.81E-01	4.75E-01	2.58E-01
3.00	7.44E-02	1.18E-01	2.27E-01	4.39E-01	2.15E-01
4.00	4.77E-02	7.86E-02	1.54E-01	3.82E-01	1.57E-01
5.00	3.28E-02	5.57E-02	1.09E-01	3.40E-01	1.20E-01
6.00	2.37E-02	4.11E-02	8.05E-02	3.07E-01	9.63E-02
7.00	1.78E-02	3.14E-02	6.10E-02	2.80E-01	7.95E-02
8.00	1.37E-02	2.46E-02	4.73E-02	2.58E-01	6.72E-02
9.00	1.08E-02	1.97E-02	3.73E-02	2.39E-01	5.79E-02
10.00	8.67E-03	1.60E-02	3.00E-02	2.23E-01	5.07E-02
11.00	7.07E-03	1.32E-02	2.44E-02	2.09E-01	4.50E-02
12.00	5.85E-03	1.10E-02	2.00E-02	1.97E-01	4.04E-02

Table 6-4 LOOP duration comparison⁶

LOOP Category	Summary Statistic	NUREG/CR-6890 1986-2004	NUREG/CR-5496 1980-1996	NUREG-1032 1968-1985
Plant Centered (including switchyard centered)	Median Duration (h) (Actual Data)	0.50	0.33	0.26
	Mean Duration (h) (Actual Data)	1.52	1.22	0.45
	Type of Fit	Lognormal	Lognormal	Weibull
Grid Related	Median Duration (h) (Actual Data)	1.56	2.38	0.55
	Mean Duration (h) (Actual Data)	2.43	2.64	1.24
	Type of Fit	Lognormal	Lognormal	Weibull
Weather Related (Severe and Extreme)	Median Duration (h)	1.28	1.18	4.50
	(Actual Data) Mean Duration (h) (Actual Data)	14.2	11.8	4.64

A comparison of the results obtained for the LOOP duration is given in Table 6-4. The presented results indicate an increase of the LOOP duration, with the largest increase notified for weather related LOOP. The August 14, 2003, event also influences the duration analyses, because without consideration of that event the average grid-related LOOP duration over 1986–2004 would have been 0.7 h rather than 2.4 h as shown in Table 6-4.

Consequential LOOP are events in which a reactor trip (unrelated to a LOOP) occurred and subsequently a LOOP occurred in response to the reactor trip. In such events, the LOOP would not have occurred if the reactor trip had not occurred. The conditional probability of a consequential LOOP given a reactor trip is $3.0E-3$ over the period⁶ 1986–1996 and $5.3E-3$ over the period 1997–2004. Comparison of the previous data¹⁴ indicates a recent increase in the conditional probability of a consequential LOOP given a reactor trip. The conditional probability of a consequential LOOP given a reactor trip over the five summer months⁶ (when the grid is most likely to be degraded) is $9.1E-3$, indicating seasonal variation of a consequential LOOP.

Of the 148 LOOP events⁶ during the period 1986–2004, there were 10 LOOP that occurred while a plant was in power operation, but the plant did not experience a reactor trip. These events are termed the “no trip” LOOP, or LOOP-NTs. Some plants have unique designs that have enabled them to experience some LOOP without incurring a reactor trip. The ten LOOP-NT events occurred at eight plants. (Nine Mile Point 2 experienced three LOOP-NTs.) However, four of these eight plants also experienced LOOP during power operation that did result in reactor trips. The current data indicate that the probability for LOOP-NTs for current plants is small.

The LOOP data⁶ on Figure 6-1, illustrates the causes and cause breakdowns. Severe weather is both a LOOP category and a LOOP cause on Figure 6-1. The definition of severe weather related LOOP indicates that localized severe weather events such as lightning strikes at a single plant or switchyard are coded as plant-centered or switchyard-centered LOOP, although the cause is severe weather. Approximately 38% of the events are caused by equipment failures, and approximately 30% of the events are caused by human errors. Transformers dominate in the equipment failures and maintenance activities contribute by the largest fraction to the human error events.

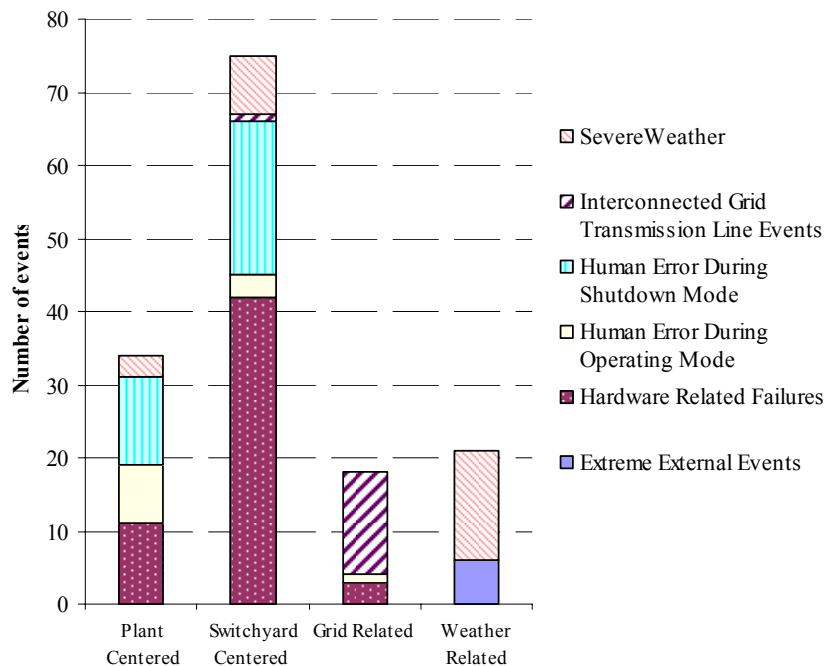


Figure 6-1 LOOP event counts by cause⁶

To summarize, the presented statistical data show that:

- Grid related LOOP are major contributor to LOOP during the power operation mode.
- Overall LOOP frequency decreased and length (duration) increased.
- Conditional probability of a consequential LOOP given a reactor trip increased.
- The probability for LOOP-NTs for current plants is small.
- The interconnected grid and transmission line events are dominant causes for the grid related LOOP.

6.2 Method for calculation of Loss of Offsite Power IE Frequency

A method for calculating the LOOP initiating event frequency consistent with the current NRC guidelines¹⁰ is described in the following chapter. In the proposed method, LOOP IE is a sum of four elements: plant centered losses (PCL), grid disturbances (GD), severe weather related losses (SWRL), and extremely severe weather related losses (ESWRL). Plant centered events are those in which the design and operational characteristics of the plant itself effect likelihood of the loss of the offsite power. The grid related loss of off-site power events are defined as LOOP that are strictly associated with the loss of the transmission and distribution system due to insufficient generating capacity, excessive loads or dynamic instability. Although grid failure may also be caused by the factors such as severe weather conditions these events in current procedures are not considered grid related, since they are caused by external events and accordingly they are covered separately.

There is no formal procedure for estimation of plant and grid related LOOP frequencies. The procedure used in current PSA is to use available statistical data for those IE frequencies and apply it as given, without considering the design of the on-site power system (plant centered) or grid unreliability (grid related).

Severe weather related losses are divided into two groups:

1. Weather caused the event, but did not effect the time to restore power (for example lightning induced event). These events are classified within plant centered losses.
2. Weather initiated the event and created conditions, so that power was not or could not have been restored for a long time. This group includes major storms, hurricanes, high winds, accumulations of snow and ice and tornadoes. This group of LOOP is divided into severe weather related and extreme severe weather related LOOP. The following equation for calculation of severe weather related LOOP is given in the corresponding references^{10,17}:

$$SWRL = 1.310^{-4} * h_1 + b * h_2 + 1.210^{-2} * h_3 + c * h_4 \text{ event/year} \quad (6.101)$$

Where:

h_1 – Annual expectation of snowfall for the site, in inches.

h_2 – Annual expectation of tornadoes (wind speed equal or greater than 113 miles per hour).

b – Value of 12.5 for sites with the transmission lines on two or more rights-of-way spreading out in different directions from the switch-yard, or 72.3 for sites with the transmission lines on one right-of-way.

h_3 – Annual expectation of storms with the wind speed between 75 and 124 mph.

h_4 – Annual expectation of hurricanes at the site.

c – Value of 0 for site not vulnerable to the effects of salt spray and 0.78 for vulnerable site.

The Eq. (6.101) shows that the frequency of severe weather related LOOP for the NPP situated in the regions where probability of hurricanes and tornadoes is small or negligible, depends only from the annual expectation of snowfall at the site. The h_1 is conservatively taken to be equal to the largest measured value in the available meteorological data. Equation (6.101) also indicates that the frequency of SWRL LOOP is smaller than 1E-2 event/year for those power plants.

The frequency of the extreme severe weather related LOOP (ESWRL) is taken to be equal to the annual expectation of storms at a site with the wind velocities equal to or greater than 125 mph. In locations, where registered wind speeds are smaller than 125 mph, the frequency of ESWRL=3.3E-4 event/year is taken conservatively.

The frequency of plant LOOP is obtained as sum of the frequencies of LOOP from all causes, and in certain cases rounded to a larger value to conservatively account uncertainties in the analysis.

Several major deficiencies were identified in the current procedures. The LOOP frequency resulting from plant centered losses and grid disturbances (the dominant contributor to the overall LOOP) is taken from statistical data⁹⁴, without consideration of the unreliability of the specific power system or configuration of the on-site power system of the nuclear power plant. The procedure for estimation of SWRL and ESWRL LOOP frequency is developed from the definitions and classification of the severe and extreme weather groups¹⁰, but the corresponding regulatory guides doesn't specify the adequacy of these procedures for LOOP frequency estimation. Specific extreme weather condition (high temperatures during summer months), that has direct implication⁶ on LOOP frequency, is not accounted in the current procedure.

6.3 Impact of LOOP frequency on CDF of NPP

The Surry⁹⁵ Unit 1 plant is taken as a reference NPP for the analysis of the impact of LOOP initiating event frequency on the CDF. The Surry NPP has two identical units Surry Unit 1 and 2 adjacent to the James River in Surry County, Virginia. Each unit includes a three-coolant-loop, pressurized light water reactor nuclear steam supply system and a turbine generator provided by the Westinghouse Electric Corporation. Both Surry units were updated in 1995 to the core power output of 2546 MW thermal with a gross electrical output of 855 MW electrical.

The selection of the Surry Unit 1 NPP as a reference NPP in the analysis is based on the following comparison:

- Design of the Surry Unit 1 NPP is similar to the NPP Krško. Both NPP have Westinghouse PWR reactors with the two-coolant-loop reactor nuclear steam supply system in NPP Krško and three-coolant-loop in Surry Unit 1 NPP. Both NPP were updated from the initial design output, Surry units (855 MWe) in year 1995 and NPP Krško (696 MWe) in year 2000.
- Both units have similar onsite power system configuration, with the two emergency diesel generators (EDG) per unit.
- The PSA models of NPP are owned by NPP themselves and all their details are mostly not publicly available. The detailed plant model and Level 1 PSA model of the Surry Unit 1 NPP is available^{95, 96}, allowing the use of the model in the study. The PSA model of the Surry Unit 1 NPP is publicly available, because it was one of the five nuclear power plants, which was analyzed in the demonstration study⁹⁵.
- The major difference between Surry Unit 1 NPP and NPP Krško is sharing an interconnection of specific safety systems (auxiliary feedwater system) and elements (one of the EDG) of the Surry Unit 1 NPP with the adjacent Surry Unit 2 NPP. Notifying the differences between Surry Unit 1 NPP and NPP Krško, the results obtained from the Surry Unit 1 PSA is expected to be applicable to the NPP Krško.

The general description of the Surry Unit 1 NPP power system used in the Level 1 PSA model is given in the section 6.3.1. The obtained results from the Level 1 PSA model are given in the section 6.3.2. The results obtained from the sensitivity analysis of the CDF from the EDG unreliability and LOOP frequency are presented in section 6.3.3. The obtained results from the estimation of the LOOP frequency using the new method are presented in section 6.4.

6.3.1 NPP power system

The power system of the nuclear power plants consists of the offsite power system and onsite emergency power system.

The offsite power system at nuclear power plants consist of the following major components:

- Two or more incoming power supplies from the grid.
- One or more switchyards to allow routing and distribution of power within the plant.
- One or more transformers to allow the reduction of voltage to levels needed for safety and non-safety systems within the plant.
- Distribution systems from the transformers to the switchgear buses.

Figure 6-2 shows an example⁹⁷ of an offsite power system design used for nuclear power plants. The offsite power system design shown on Figure 6-2 is similar to the design of the NPP Krško⁹⁸. The solid lines on Figure 6-2 are SBO scoping boundary for license renewal⁹⁴.

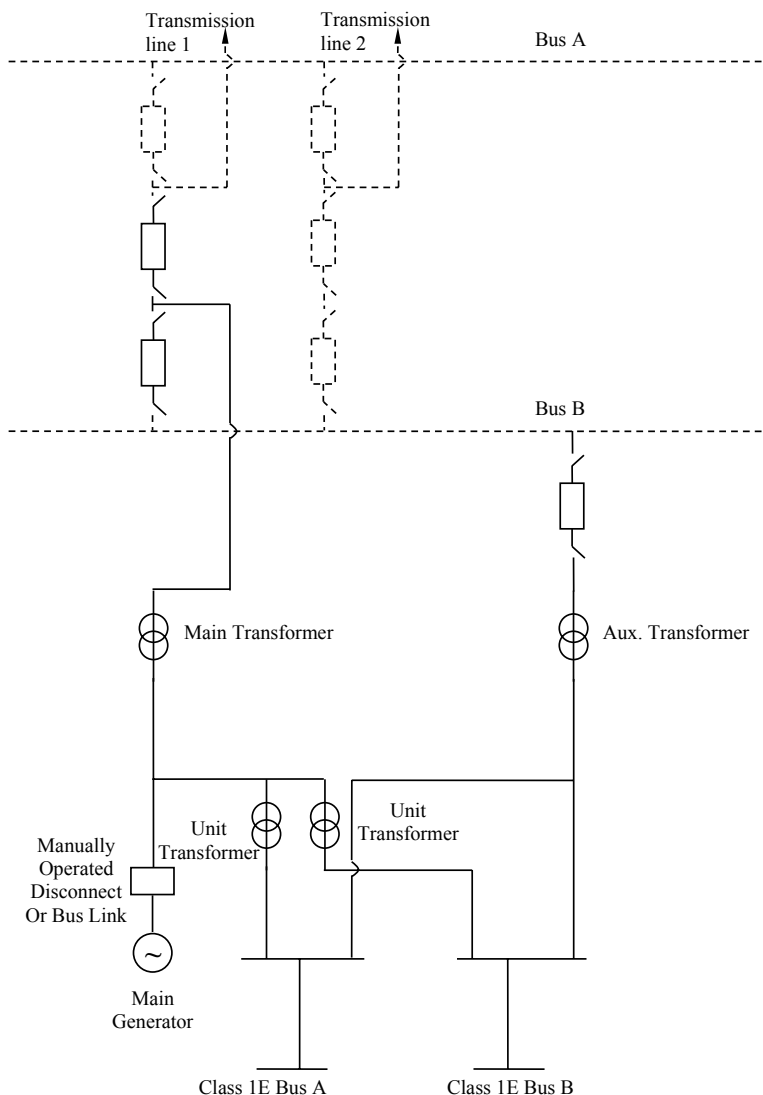


Figure 6-2 Example of an offsite power system⁹⁴

The on-site power system of the nuclear power plants includes safety Class 1E distribution system, emergency diesel generators and batteries.

During normal operation, AC power is typically provided to the safety and non-safety buses from the main generator through the unit transformers; it may also be supplied directly

through the auxiliary transformer. A minimum of two preferred power supply circuits must be provided. Sources of offsite power other than the grid may also be provided as alternate or backup sources of power. These may include nearby (or onsite) gas turbine generators, fossil power plants and hydroelectric power facilities connected directly through dedicated power lines to the auxiliary transformer.

The on-site power system, referred as emergency power system (EPS) provides AC and DC power to safety related components following reactor scram. The EPS is a support system that interfaces with the nearly all front line systems.

The EPS at Surry Unit 1 NPP consist of two 4160 VAC buses, four 480 VAC buses, four 120 VAC vital instrumentation buses, two 125 VDC buses, one dedicated and one shared diesel generator, and their associated components. The EPS at Surry Unit 2 NPP is symmetric to the system of the Surry Unit 1 NPP. Each 4160 VAC bus is normally powered from offsite power sources. Upon loss of offsite power the supply breakers open, the diesel generators start and their associated output breakers close to load the diesel on the emergency buses. Surry has three diesel generators, one dedicated to each unit and a third swing diesel generator shared by the units. In the event that the swing diesel is demanded by both units, the diesel is aligned to the unit at which a safety injection actuation system or consequence limiting control system signal exists. The Surry EPS design does not require load sequences (installed in NPP Krško) for reloading of the buses due to the use of time delays included in the start circuitry of the required pumps. Technical specifications require all three diesel generators to be operable. However, one diesel may be taken out for service for a limited period of time.

Specific assumptions made in the analysis of the EPS are as follows:

- Failure of EDG 2, dedicated to Surry Unit 2 NPP, would result in the inability of the EDG 3 (shared EDG) to supply to Surry Unit 1 NPP.
- The EDG mission time is taken to be equal to 6 hours.
- Battery depletion time is assessed to be 4 hours.
- Cross connection of the buses is not considered.
- Shorts in the buses and motor control centers fail only their respective bus and don't fail the power sources connected into the bus.
- Actuation failures for diesel generators are not explicitly included.
- Alternative source of AC power at the Surry site are not included in the station blackout models.

The EDG parameters used in the Surry Level 1 PSA model are given in Table 6-5.

Table 6-5 EDG parameters

No.	Parameter	Mean unavailability
1	EDG fails to start	2.20E-02
2	EDG fails to run	2.00E-03
3	EDG test and maintenance	6.00E-03
4	EDG circuit breaker - All failures	3.00E-03

The probability for EDG failure to start is calculated from the plant specific data. The common cause failures of the EDG are accounted using unavailability given in Table 6-6.

Table 6-6 EDG CCF unavailability

No.	Parameter	Mean unavailability
1	2 EDG fail to start and run	3.80E-02
2	3 EDG fail to start and run	1.80E-02

6.3.2 NPP PSA model

The PSA model of the Surry Unit 1 NPP is developed on the basis of the plant model and Level 1 PSA analysis given in the corresponding references^{95, 96}. The top events are modeled using large fault trees. The PSA model includes 14 ET, 168 FT and 576 BE. The list of the event trees constructed for Surry Unit 1 PSA are given in Table 6-7.

Table 6-7 Event trees and initiating events for Surry Unit 1 PSA

No.	Event tree name	Initiating event	Description
1.	LOCA-A	Large LOCA	LOCA size 6''-29''
2.	S1	Medium LOCA	LOCA size 2''-6''
3.	S2	Small LOCA	LOCA size 1/2''-2''
4.	S2-Consequence	Small LOCA as consequence	LOCA size 1/2''-2'' as consequence
5.	S3	Very small LOCA	LOCA less than 1/2''
6.	T1-N	LOOP	Loss of offsite power
7.	T1S-N	SBO at Unit 1	Station blackout at Unit 1
8.	T1SS-N	SBO at Unit 1 and Unit 2	Station blackout at both Surry Units
9.	T2	Loss of main feedwater	Loss of main feedwater
10.	T3	Turbine Trip	Turbine trip with the MFW
11.	T5	Loss of DC Bus	No recoverable loss of DC bus
12.	T7-N	Steam generator tube rupture	Steam generator tube rupture (SGTR)
13.	TK	Anticipated trans. without scram	ATWS as consequence
14.	V	Interfacing LOCA	Interfacing LOCA

The developed PSA model of the Surry Unit 1 NPP is not identical to the model the corresponding references^{95, 96}. It is the best completely approximation of the reference model, with the major differences described as follows. The results from developed PSA model for Surry Unit 1 NPP are comparable to the results in corresponding reference^{95, 96}, confirming the applicability of the model.

The event tree number 4 (S2-Consequence) is added to the model in order to quantify the core damage frequency resulting from the sequences, which have Small LOCA as consequence of other initiating events. Event tree number 14 (V-Interfacing LOCA) is added in the plant PSA model in order to directly quantify share of the Interfacing LOCA into total CDF of the plant. The recovery actions of the operators are included in the model with the introduction of the additional branches in the event trees. There are cross ties between the charging systems and auxiliary feedwater systems at Surry Unit 1 and 2, and these interconnections are accounted during FT construction. The fault and event trees are upgraded to account the failure of systems due to the loss of AC power and incorporate operator recovery actions. The failure of the consequence limiting system, auxiliary feedwater system during blackout, primary pressure relief system, recirculation mode transfer system and safety injection actuation system are modeled with fault trees developed from the description given in the corresponding reference⁹⁶. In the reference⁹⁶ failure of these systems is calculated directly from the Boolean expressions. The seal vulnerability sequences were excluded from the event trees because, in the corresponding references⁹⁵, there is no information about their quantification and current actions in Surry NPP to improve the RCP seal/O-ring package⁹⁹.

The station blackout at Surry Unit 1 NPP (event tree T1S-N) is defined as failure of EDG 1 and EDG 3 to provide power to the Surry Unit 1 NPP following a LOOP. The station blackout of both units (event tree T1SS-N) is defined as failure of all three EDG to provide power to Surry Unit 1 NPP following a LOOP initiating event. The EDG 3 is assumed to be unavailable if EDG 2 has failed. The frequency of the Surry Unit 1 NPP station blackout (SBO U1 initiating event) and station blackout of both units (SBO U2 initiating event) are obtained with the construction of the fault trees on the basis of the Boolean equations given in the reference^{95, 96}. The frequencies of the initiating events SBO U1 and SBO U2 used in the model are given in Table 6-8.

Table 6-8 SBO IE frequency

No.	Initiating Event	Frequency [/yr] PSA model
1	SBO at Unit 1	1.6E-04
2	SBO at Both Units	3.3E-05

The frequency of the LOOP initiating event of Surry Unit 1 NPP is estimated to be 7.7E-2 [/yr]. No detailed description of procedure used for LOOP IE frequency estimation is provided in the reference⁹⁵ except the notation that the calculation is based on experience from other plants with the similar switchyard configurations.

The results obtained from the Surry Unit 1 PSA model are obtained by quantification of the model using the commercial software⁸⁵. They are summarized in the following tables and figures.

The contribution of the Accident Groups to CDF obtained for NPP S model is given in Table 6-9. The second column in Table 6-9 contains name of the accident group with included ET given in third column and mean CDF in fourth column.

Table 6-9 Comparison of the results for dominant accident sequences by IE type

No.	Accident Group	Included Event Trees	Mean CDF [/yr] PSA Model
1.	All LOOP	T1-N, T1S-N, T1SS-N	9.63E-06
2.	All LOCA	LOCA-A, S1, S2, S2-Con., S3	6.31E-06
3.	Int. LOCA	V	1.60E-06
4.	All transient	T2, T3, T5	1.52E-06
5.	ATWS	TK	1.99E-06
6.	SGTR	T7-N	4.03E-07
CDF Total			2.15E-05

The contribution of the Accident Groups identified in Table 6-9 to CDF obtained for Surry Unit 1 NPP model is given on Figure 6-3.

The importance analysis is done and the most important BE are identified in Table 6-11.

The RAW importance measure for the initiating events is excluded from the results and marked with the N/A in Table 6-11.

CDF Contribution by Accident Groups

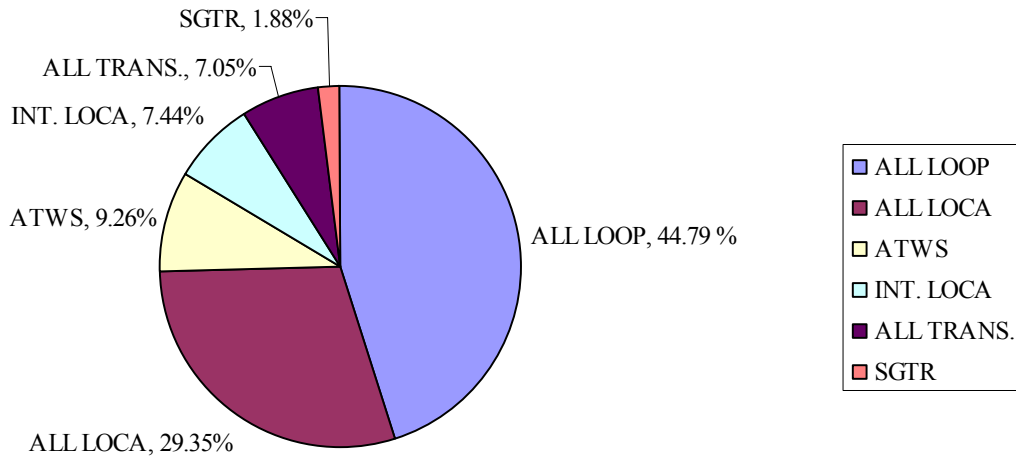


Figure 6-3 Contribution of Accident Groups for Surry Unit 1 CDF from model

The results on Figure 6-3 show that LOOP events are the dominating contributors to the Surry Unit 1 CDF. Division of the LOOP and SBO events to the CDF from the ALL LOOP Accident Group is given on Figure 6-4.

Contribution to ALL LOOP CDF by LOOP and SBO Initiating Events

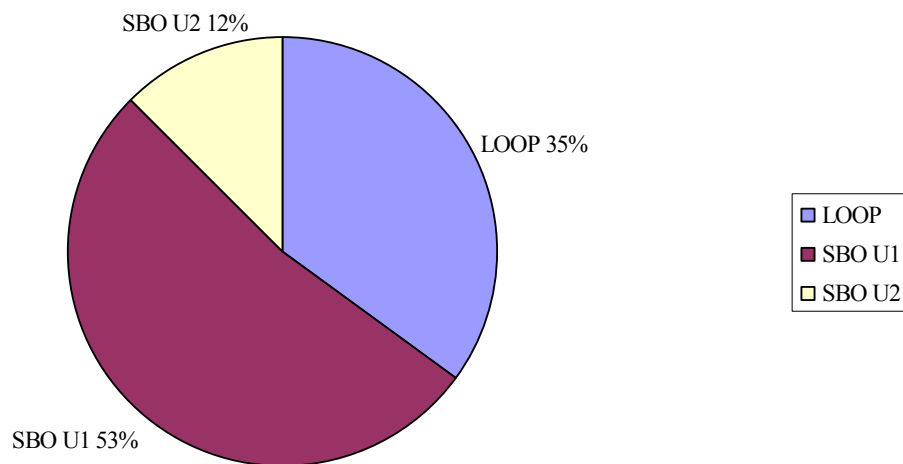


Figure 6-4 Contribution of LOOP and SBO to ALL LOOP Accident Group for Surry Unit 1 CDF
 The Figure 6-4 shows that the main contributor to the CDF from ALL LOOP Accident Group is the SBO U1 initiating event resulting from specific on-site power configuration.

The CDF contribution by Initiating Events¹⁰⁰ for NPP Krško is given on Figure 6-5 with description of the initiating events given in Table 6-10.

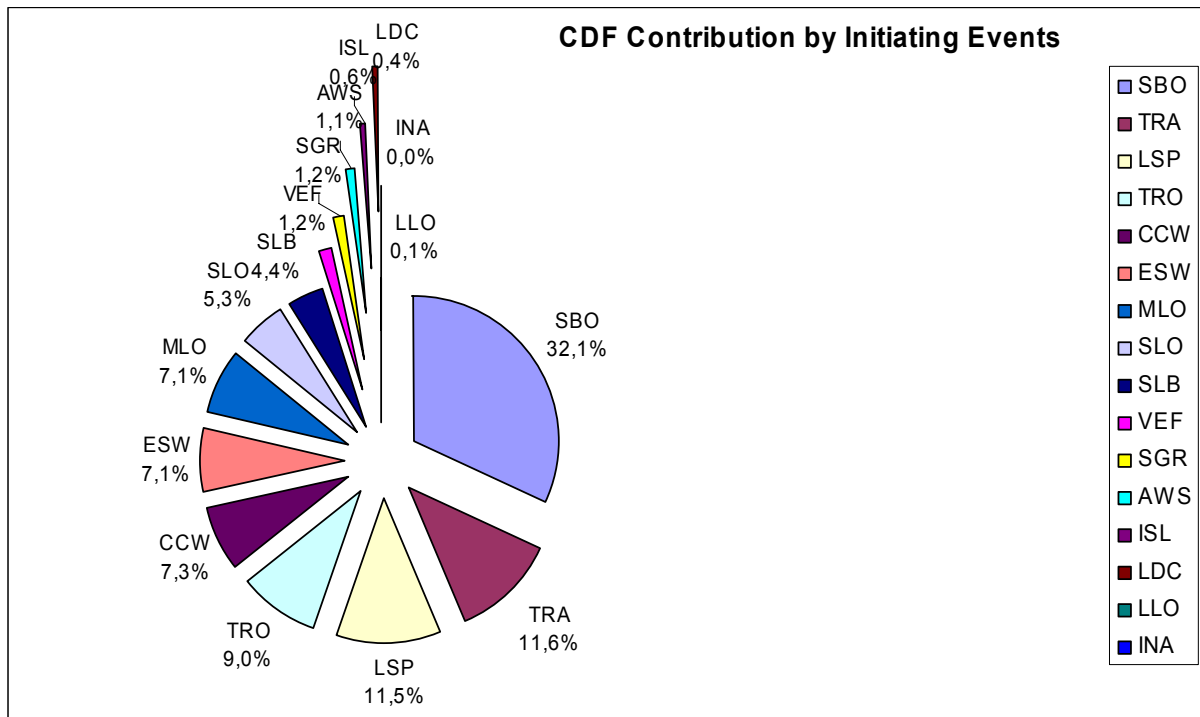


Figure 6-5 CDF contribution by Initiating Events for NPP Krško

Table 6-10 Description of the Initiating events

INITIATING EVENT	IE
ANTICIPATED TRANSIENT WITHOUT SCRAM	AWS
INTERFACING SYSTEMS LOCA	ISL
LARGE LOCA	LLO
LOSS OF 125V DC VITAL BUS	LDC
LOSS OF COMPONENT COOLING WATER SYSTEM	CCW
LOSS OF ESSENTIAL SERVICE WATER SYSTEM	ESW
LOSS OF INSTRUMENT AIR	INA
LOSS OF OFFSITE POWER	LSP
MEDIUM LOCA	MLO
SMALL LOCA	SLO
STATION BLACKOUT	SBO
STEAM GENERATOR TUBE RUPTURE	SGR
STEAM LINE BREAK	SLB
TRANSIENT WITH MFW AVAILABLE	TRA
TRANSIENT WITH MFW UNAVAILABLE	TRO
VESEL FAILURE	VEF

Comparison of the results on Figure 6-3 from Surry Unit 1 NPP and results on Figure 6-5 for NPP Krško justify the selection of the NPP Surry as a reference plant as described in the section 6.3.2.

Table 6-11 The identified important BE in the model

No.	Basic Event	BE description	Type	Value	FV	RRW	RAW
1	LOOP	LOOP initiating event	frequency	7.70E-02 [yr]	4.51E-01	1.82E+00	N/A
2	NRAC-HALFHR	Failure to recover AC power within 30 minutes	probability	6.00E-01	2.90E-01	1.41E+00	1.19E+00
3	NRAC-7HR	Failure to recover AC power within 7 hours	probability	5.00E-02	2.01E-01	1.25E+00	4.81E+00
4	OEP-DGN-FS-DGO1	Failure of EDG 1 to start	probability	2.20E-02	1.61E-01	1.19E+00	8.07E+00
5	S1	Medium LOCA initiating event	frequency	1.00E-03 [yr]	1.49E-01	1.18E+00	N/A
6	RECOV-T1SN-3	Operator recovery action in ET SBO at Unit 1	probability	6.12E-01	1.42E-01	1.17E+00	1.09E+00
7	AFW-TDP-FR-2P6HR	AFW TDP fails to run for 6 hours	probability	3.00E-02	1.03E-01	1.12E+00	4.33E+00
8	AFW-XHE-FO-U1SBO	Operator fails to reconnect AFW	probability	8.20E-02	1.01E-01	1.11E+00	2.13E+00
9	HPI-XHE-FO-FDBLD	Operator fails to establish feed and bleed	probability	7.10E-02	9.40E-02	1.10E+00	2.23E+00
10	R	Failure to manual scram the reactor	frequency	1.70E-01 [yr]	9.30E-02	1.10E+00	1.45E+00
11	ATWS	Anticipated transient without scram IE	frequency	5.00E-04 [yr]	9.30E-02	1.10E+00	N/A
12	OEP-DGN-FS-DGO3	Failure of EDG 3 to start	probability	2.20E-02	8.09E-02	1.09E+00	4.56E+00
13	OEP-DGN-FS-DGO2	Failure of EDG 2 to start	probability	2.20E-02	8.08E-02	1.09E+00	4.55E+00
14	V	Interfacing LOCA initiating event	frequency	1.60E-06 [yr]	7.43E-02	1.08E+00	N/A
15	T2	Loss of main feedwater initiating event	frequency	9.40E-01 [yr]	7.35E-02	1.08E+00	N/A

6.3.3 Sensitivity analysis of CDF

The results of the sensitivity studies are presented in the following sections. It is assumed that they are applicable also to the NPP Krško due to the similarities of the plants and the PSA models.

The correlation of EDG reliability and emergency AC power system unavailability is analyzed, with the obtained results given on Figure 6-6. The probability of failure to start for all three EDG NPP PSA is changed and the emergency AC power system unavailability is calculated. The CCF of the EDG are accounted.

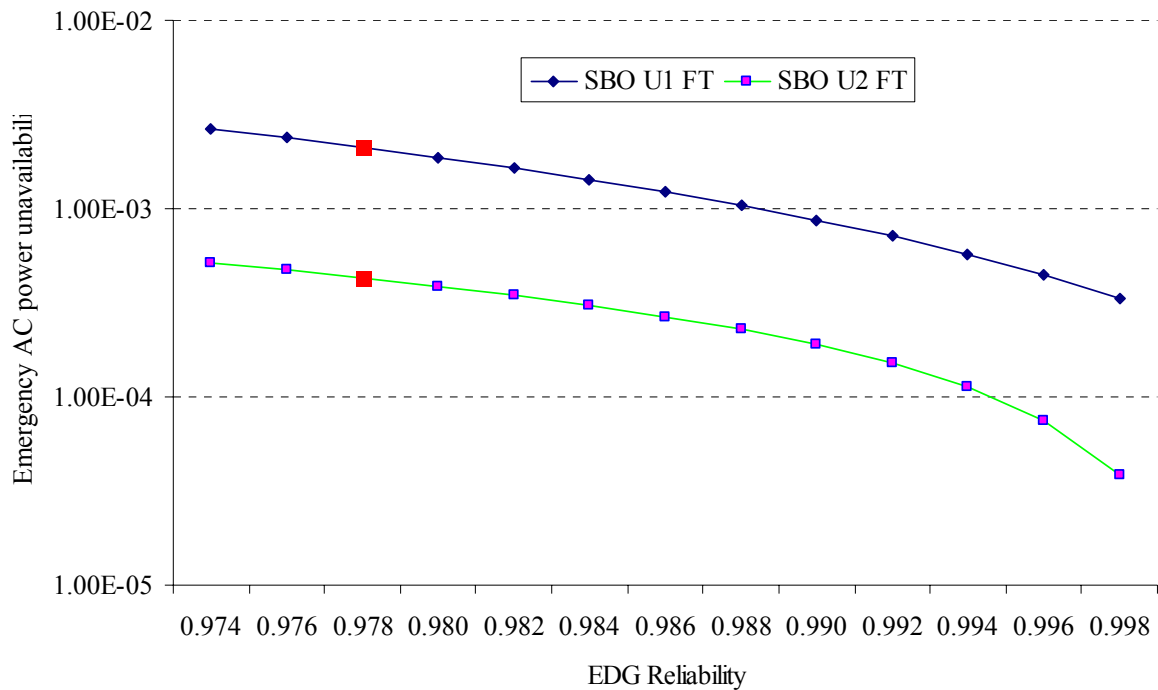


Figure 6-6 Unavailability of the emergency AC power system from EDG reliability

The obtained results on Figure 6-6 show that unavailability of emergency AC power system in the fault tree for station blackout of the Surry Unit 1 (SBO U1 FT) and fault tree for station blackout of both units (SBO U2 FT) depends notably on EDG reliability. With the red squares are marked values of EDG reliabilities used in the model. The ten most important MCS identified for the emergency AC power system failure are given in Table 6-12, where combinations of two EDG failures are identified. The description of the basic events is given in Table 6-13.

Table 6-12 Identified MCS for emergency AC power system failure

MCS No.	Probability	Event 1	Event 2
1	4.84E-04	OEP-DGN-FS-DGO1	OEP-DGN-FS-DGO2
2	4.84E-04	OEP-DGN-FS-DGO1	OEP-DGN-FS-DGO3
3	1.32E-04	OEP-DGN-FS-DGO2	OEP-DGN-MA-DGO1
4	1.32E-04	OEP-DGN-FS-DGO1	OEP-DGN-MA-DGO3
5	1.32E-04	OEP-DGN-FS-DGO3	OEP-DGN-MA-DGO1
6	1.32E-04	OEP-DGN-FS-DGO1	OEP-DGN-MA-DGO2
7	6.60E-05	OEP-CRB-FT-25H3	OEP-DGN-FS-DGO1
8	6.60E-05	OEP-CRB-FT-15H3	OEP-DGN-FS-DGO3
9	6.60E-05	OEP-CRB-FT-15H3	OEP-DGN-FS-DGO2
10	6.60E-05	OEP-CRB-FT-15J3	OEP-DGN-FS-DGO1

Table 6-13 Basic event description

BE name	Description
OEP-DGN-FS-DGO1	Diesel generator 1 fails to start
OEP-DGN-FS-DGO2	Diesel generator 2 fails to start
OEP-DGN-FS-DGO3	Diesel generator 3 fails to start
OEP-DGN-MA-DGO1	Diesel generator 1 in maintenance
OEP-DGN-MA-DGO2	Diesel generator 2 in maintenance
OEP-DGN-MA-DGO3	Diesel generator 3 in maintenance
OEP-CRB-FT-25H3	Failure of circuit breaker 25H3 to remain closed
OEP-CRB-FT-15H3	Failure of circuit breaker 15H3 to remain closed
OEP-CRB-FT-15J3	Failure of circuit breaker 15J3 to remain closed

The obtained results for the unavailability of emergency AC power system from EDG reliability without consideration of EDG CCF are given on Figure 6-7.

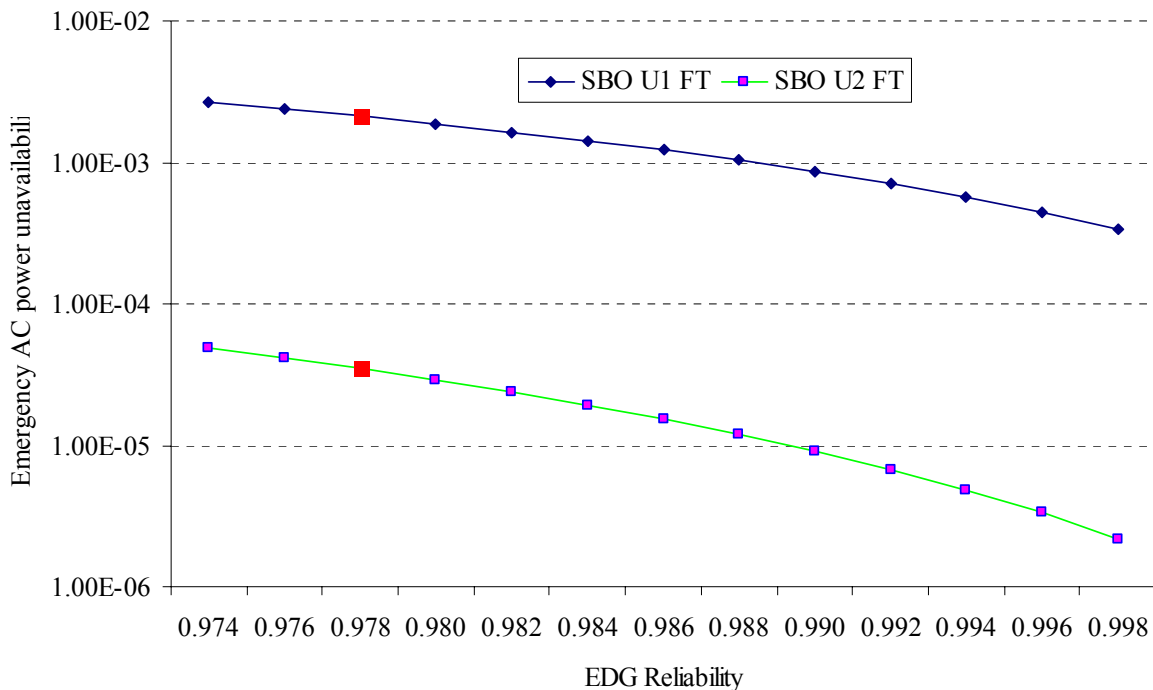


Figure 6-7 Unavailability of the emergency AC power system from EDG reliability, CCF not accounted

The results on Figure 6-7 (without CCF) compared to results on Figure 6-6 (with the CCF) show that unavailability of the emergency AC power system decreased with the exclusion of CCF and this result is more evident for SBO U2 FT. The CCF of all three EDG (BE “BETA-3DG”) is the major contributor to the unavailability of the emergency AC power system in SBO U2 FT. The obtained results on Figure 6-7 and Figure 6-6 are comparable to results provided in the reference¹⁸.

Figure 6-8 shows CDF versus EDG reliability.

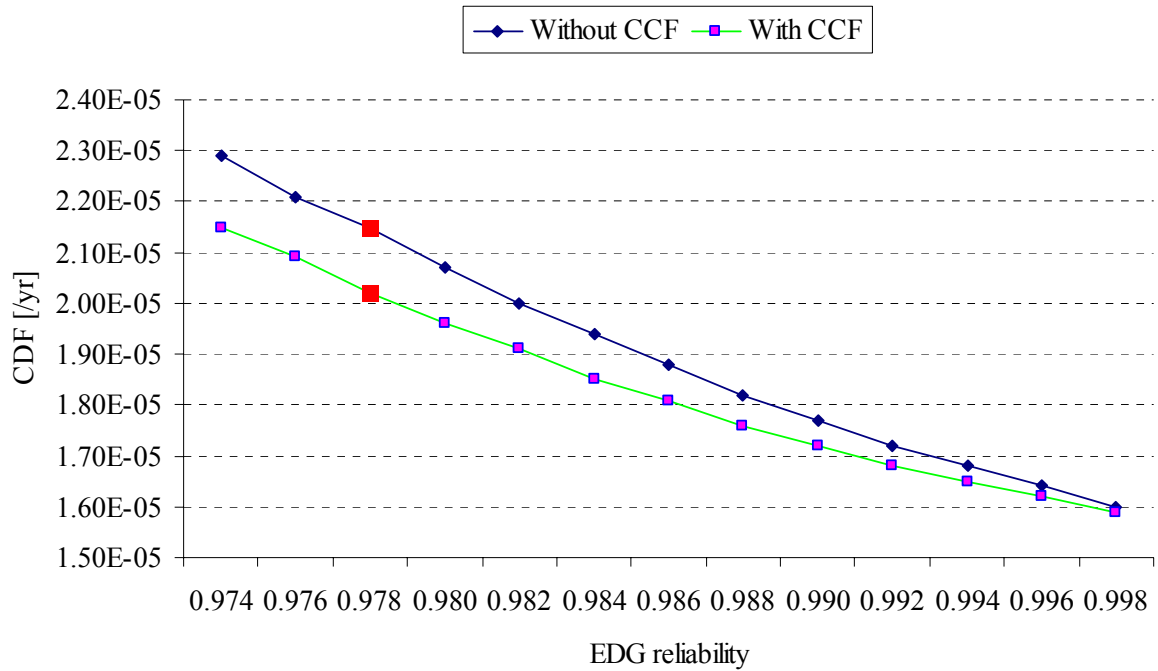


Figure 6-8 Dependency of CDF from EDG reliability

Figure 6-9 shows the sensitivity analysis of the CDF versus LOOP IE frequency.

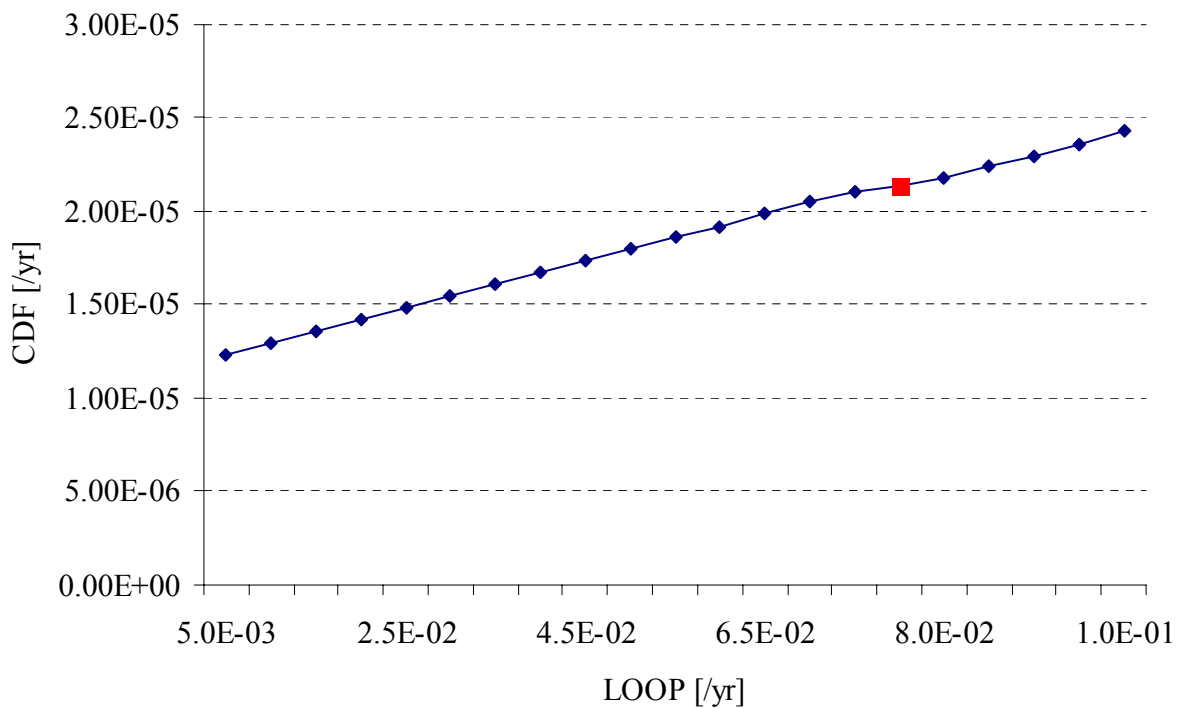


Figure 6-9 Dependency of CDF from LOOP frequency

The red square on Figure 6-9 marks the current LOOP frequency and its respective CDF in the PSA model. The detail cost/benefit analysis¹⁰¹ is necessary to quantify the implication of the CDF change.

6.4 Implication of Grid related LOOP on plant CDF

The results from the sensitivity analysis in the section 6.3.3 show the dependence of the CDF on the LOOP frequency. Two methods for estimation of the LOOP frequency from the unreliability of the power delivery to the house load of the NPP are developed and applied on the IEEE RTS and Slovenian power system.

First approach is used for the assessment of the power system and second approach is used for evaluation of the changes in the power system on the LOOP frequency.

The LOOP category data frequencies are given in Table 6-14. The first column in Table 6-14 identifies the LOOP category with the mean frequency obtained from the statistical data given in the second column. The PSA model LOOP categories are given in the fourth column of the table.

Table 6-14 Share of each LOOP data category into overall LOOP

LOOP Data	Category	Mean Frequency [/yr] NUREG/CR-6890 ⁶	Share %	Mean Frequency [/yr] PSA model ⁹⁵
Plant centered		2.07E-03	5.7	4.44E-03
Switchyard centered		1.04E-02	28.9	2.23E-02
Grid related		1.86E-02	51.8	3.99E-02
Weather related		4.83E-03	13.4	1.04E-02
All		3.59E-02	100.0	7.70E-02

The share of the grid related LOOP is approximately half of the overall LOOP frequency with the switchyard centered failures as the second largest contributor. The frequency of the LOOP IE in the PSA model is approximately twice larger than the mean frequency obtained from the statistical data, as shown in last column in Table 6-14.

The LOOP IE is assessed as a sum of the grid related LOOP and non-grid related LOOP. The non-grid related LOOP include plant, weather and switchyard initiated LOOP that are taken to be constant and equal to the statistical values given in the last column of the Table 6-14.

In the first approach the frequency of the grid related LOOP is assessed from the unreliability of the power delivery to the house load of the NPP. The unreliability of the power delivery to the house load is equal to the unavailability of the power delivery resulting from the usage of the constant failure rate λ and unrepairable component model for the constituting elements of the power system. The Bernoulli's theorem (i.e. the so-called 'law of large numbers') states that in repeated, independent trials with the same probability p of success in each trial, the chance that the percentage of successes differs from the probability p by more than a fixed positive amount, converges to zero as the number of trials goes to infinity, ensuring frequencies converge towards the probability. The LOOP frequency is assessed according to this theorem. The main deficiency of this approach is that it doesn't account the grid related LOOP in the overall LOOP when:

- The obtained unreliability and corresponding grid related LOOP is small compared to the non-grid LOOP.
- When change of the unreliability and corresponding grid-related LOOP, resulting from changes in power system is small.

The second approach is developed and applied in order to account small unreliabilities into the assessment of the LOOP IE frequency. The frequency of the LOOP IE, for the basic configuration of the power system, is taken to be equal to the value available from the

statistical data. For the power system configurations different from the basic configuration, the LOOP IE frequency is obtained as a sum of the non-grid LOOP and product of the grid LOOP with the ratio of the unreliabilities of the power delivery for new and basic configuration, as shown on Eq. (6.102):

$$LOOP_{new} = LOOP_{non-grid} + \frac{U_{new}}{U_{basic}} LOOP_{grid} \text{ [/yr]} \quad (6.102)$$

Where:

$LOOP_{new}$ – The NPP LOOP IE frequency for in the new configuration of the power system.

$LOOP_{non-grid}$ – Sum of the plant, weather and switchyard initiated LOOP.

U_{new} - The unreliability of the power delivery to the house load of the NPP in the new configuration of the power system.

U_{basic} - The unreliability of the power delivery to the house load of the NPP in the basic configuration of the power system.

$LOOP_{grid}$ – The grid related LOOP.

The small changes of the unreliability of the power delivery to the house load of the NPP resulting from the changes in the power system, are accounted in the assessment of LOOP with the second approach.

The obtained results from presented approaches are given in the following sections.

6.4.1 Implication of Grid related LOOP on plant CDF in IEEE RTS

The unreliability of the power delivery to the house load of the nuclear power plants situated in the substation 18 and 21 of the IEEE RTS is summarized in Table 6-15.

Table 6-15 Description of the power system models and obtained unreliabilities for IEEE RTS

No.	Power system model	Unreliability of the power delivery to the house load of NPP
1.	NPP in substation 18 of the IEEE RTS, without consideration of voltages	2.30E-03
2.	NPP in substation 21 of the IEEE RTS, without consideration of voltages	2.26E-08
3.	NPP in substation 18 of the IEEE RTS, with the consideration of voltages	1.44E-02
4.	NPP in substation 21 of the IEEE RTS, with the consideration of voltages	5.21E-06

The obtained LOOP IE frequency for IEEE RTS, using the first approach in section 6.4, are shown in Table 6-16.

Table 6-16 CDF and LOOP frequency for IEEE RTS

No.	Power system model	LOOP frequency [/yr]	CDF [/yr]
1.	NPP in substation 18 of the IEEE RTS, without consideration of voltages	3.94E-02	1.68E-05
2.	NPP in substation 21 of the IEEE RTS, without consideration of voltages	3.71E-02	1.65E-05
3.	NPP in substation 18 of the IEEE RTS, with the consideration of voltages	5.15E-02	1.83E-05
4.	NPP in substation 21 of the IEEE RTS, with the consideration of voltages	3.71E-02	1.65E-05

The CDF of the NPP for IEEE RTS models given in Table 6-16, is given on Figure 6-10.

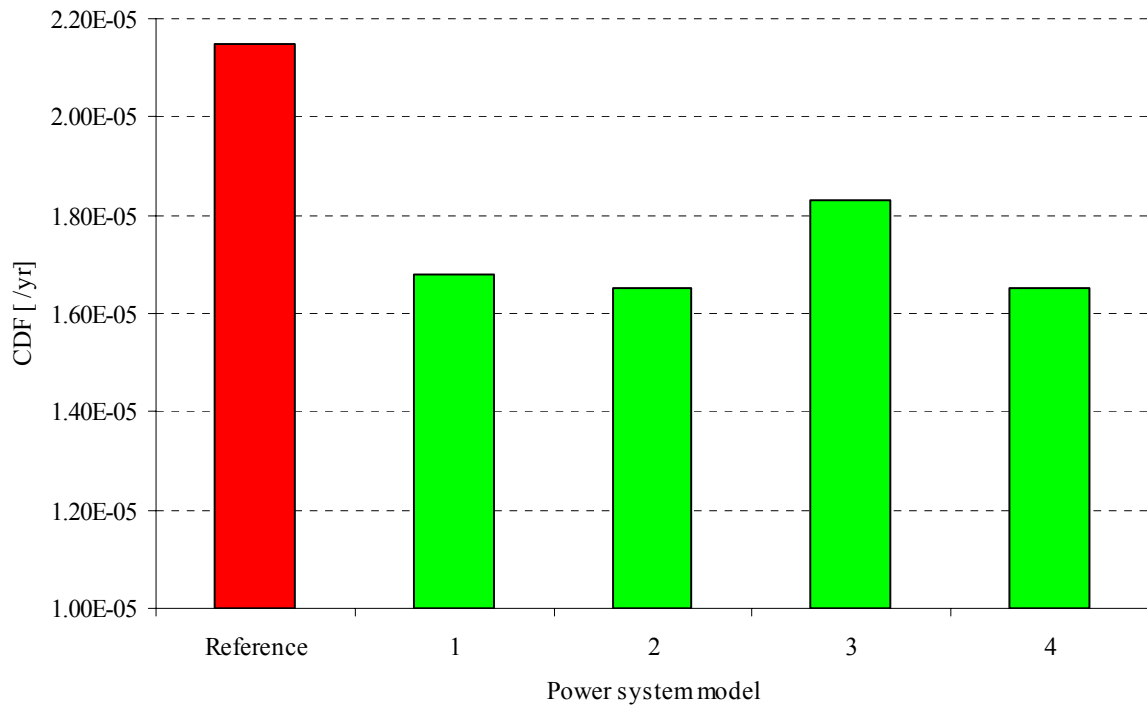


Figure 6-10 Dependency of CDF from LOOP IE frequency, IEEE system

The red column on Figure 6-10 shows the CDF of the NPP obtained in the section 6.3.2 for the initial generic LOOP IE frequency. The blue columns show the CDF of two nuclear power plants in IEEE RTS for both options: with and without consideration of voltages.

The results on Figure 6-10 show that CDF is smaller for all LOOP frequencies compared to the value obtained from the generic LOOP frequency⁹⁵. The results on Figure 6-10 show the increase of the CDF (model 3 compared to model 1) with the introduction of the substation voltages in the method.

6.4.2 Implication of Grid related LOOP on CDF in Slovenian power system

The unreliability of the power delivery to the house load of the NPP Krško for analyzed configurations of the Slovenian power system is given in Table 6-17.

Table 6-17 Description of the power system models and obtained unreliabilities for NPP Krško

No.	Power system model	Unreliability of the power delivery to the house load of NPP Krško
1.	The basic configuration of the Slovenian power system	1.55E-04
2.	Single line NPP Krško – Beričevo is added	1.80E-06
3.	Double line NPP Krško - Beričevo is added	3.23E-07
4.	NPP Krško 2 is added, proportional load increase is assumed, single line NPP Krško – Beričevo is added	3.24E-05
5.	NPP Krško 2 is added, proportional load increase is assumed, double line NPP Krško - Beričevo is added	2.40E-05
6.	NPP Krško 2 is added, load increase in Divača, single line NPP Krško - Beričevo is added	1.80E-06
7.	NPP Krško 2 is added, load increase in Divača, double line NPP Krško - Beričevo is added	3.24E-07

The constant value of the LOOP=3.71E-02 [/yr] is obtained with the application of the first approach from section 6.4 and the unreliabilities given in Table 6-17, as a result of their small value. Therefore, the second approach from section 6.4 is applied.

The obtained LOOP IE frequencies, using the Eq. (6.102), are given in Table 6-18.

Table 6-18 The obtained LOOP IE for the NPP Krško

No.	Power system model	LOOP [/yr]	CDF [/yr]
1.	The basic configuration of the Slovenian power system	7.70E-02	2.15E-05
2.	Single line NPP Krško – Beričevo is added	3.76E-02	1.66E-05
3.	Double line NPP Krško - Beričevo is added	3.72E-02	1.65E-05
4.	NPP Krško 2 is added, proportional load increase is assumed, single line NPP Krško – Beričevo is added	4.54E-02	1.75E-05
5.	NPP Krško 2 is added, proportional load increase is assumed, double line NPP Krško - Beričevo is added	4.33E-02	1.73E-05
6.	NPP Krško 2 is added, load increase in Divača, single line NPP Krško - Beričevo is added	3.76E-02	1.66E-05
7.	NPP Krško 2 is added, load increase in Divača, double line NPP Krško - Beričevo is added	3.72E-02	1.65E-05

The frequency of the LOOP IE, for the basic configuration of the Slovenian power system, is equal to the generic value LOOP_{basic}=7.70E-02 [/yr] from the corresponding reference⁹⁵. The LOOP IE frequency is obtained with Eq. (6.102) for the Slovenian power system configurations different from the basic configuration, with:

LOOP_{non grid} – Sum of the plant, weather and switchyard initiated LOOP in Table 6-14, equal to 3.71E-02 [/yr].

U_{new} - The unreliability of the power delivery to the house load of the NPP for the new configuration of the power system, given in Table 6-17.

U_{basic} - The unreliability of the power delivery to the house load of the NPP for the basic configuration of the power system, given in Table 6-17 with the value $1.55\text{E-}04$ [1/yr] for the NPP Krško.

$\text{LOOP}_{\text{grid}}$ - The grid related LOOP, given in Table 6-14, with the value $3.99\text{E-}02$ [1/yr].

Figure 6-11 shows core damage frequency for the selected configurations of the Slovenian power system.

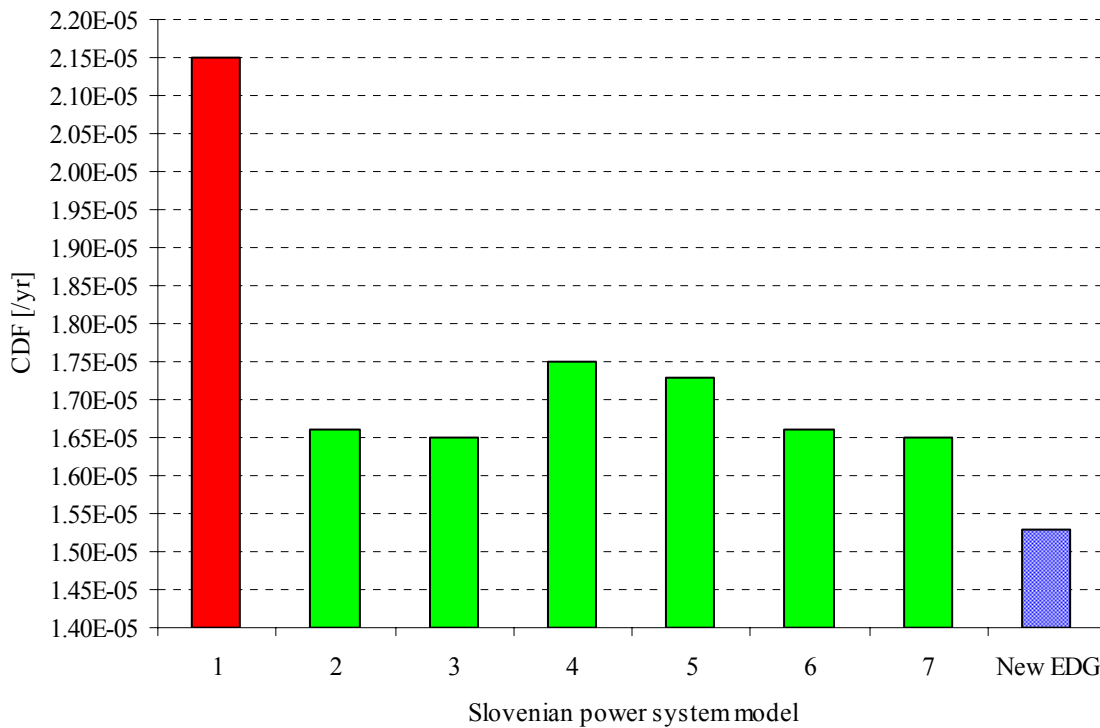


Figure 6-11 Dependency of CDF from LOOP IE frequency, Slovenian power system

The red column shows the basic configuration. Green columns show the variations connected with selected power system configurations. The blue column shows the configuration with additional emergency diesel generator installed at the NPP Krško.

Figure 6-11 shows that obtained CDF is smaller for all configurations (green columns) of the Slovenian power system compared to the CDF obtained for the basic configuration (red column). The addition of the single line between substation NPP Krško and substation Beričevo decreases CDF for $\Delta\text{CDF}=5\text{E-}06$ [1/yr], with the additional decrease of $\Delta\text{CDF}=1\text{E-}07$ [1/yr] with change of the interconnection from single to double. Figure 6-11 shows that, from the aspect of nuclear safety, the safest configuration is the one with the two NPP in the substation NPP Krško, load increase in the substation Divača and double NPP Krško - Beričevo interconnection (power system model 7).

The calculated CDF with the dedicated EDG is $\text{CDF}=1.52\text{E-}05$ [1/yr], with the decrease of the CDF for $\Delta\text{CDF}=6.3\text{E-}06$ [1/yr]. The obtained result show that the decrease of the CDF obtained with the installation of the additional EDG in the NPP is comparable to the decrease obtained with the installation of the line between substations NPP Krško and Beričevo.

The obtained results show that the addition of the new interconnection between substations NPP Krško and Beričevo is comparable, from the aspect of nuclear safety and corresponding CDF as the risk measure, to the installation of the new EDG in NPP Krško.

7 Conclusions

The current methods used for the estimation of the Loss of Offsite Power initiating event frequency do not account the actual state and the specifics of the power system.

The main objectives of the thesis was to develop new and improved method for estimation of the Loss of Offsite Power initiating event frequency, accounting the actual state of the power system and on-site power system configuration of the nuclear power plant, and to evaluate the implications of changes in the power system considering the safety of the nuclear power plants.

The method for assessment of the Loss of Offsite Power initiating event frequency is developed. It is used further for assessment of the nuclear power plant safety. The developed method accounts the power flows through interconnections, configurations of switching substations, their corresponding voltages and the methods and models of probabilistic safety assessment.

The prerequisite for assessment of nuclear power plant safety within the power system is an evaluation of the overall reliability of the power system, which was performed by development of the computer code that integrates the power flows and probabilistic safety assessment. The method for evaluation of the reliability of the power system includes identification of the weak points in the system. The network importance measures identify the most important elements or group of elements for the power system reliability.

The verification of the developed method is performed on small examples. The applicability of the method is confirmed on the standard test system. The implication of the changes of the power system considering the nuclear power plant safety is investigated on the simplified Slovenian power system. The most important elements of the power system from the aspect of nuclear safety are identified using the obtained risk measures.

The obtained results show that:

- Reliability of the substation NPP Krško and the corresponding generator are the most important elements for the overall reliability of the Slovenian power system.
- The change of the line between substation NPP Krško and substation Beričevo from single to double decreases the Loss of Offsite Power initiating event frequency and consequently improves the nuclear power plant safety. This decrease depends on common cause failures of the interconnection.
- Installation of new line Krško-Beričevo is identified as a mean for improved safety and as a prerequisite for additional nuclear power plant at Krško site.
- The introduction of the power line between substation NPP Krško and substation Beričevo decreases the risk similarly as the installation of the additional emergency diesel generator.

The developed method, with the specific modifications, is applicable for the estimation of the reliability of other networks, such as: computer, transport and various goods distribution systems.

The recommendations for the future work and development of the method include improvement of the module used for the identification of the minimal cut sets using faster algorithm (e.g. using binary decision diagrams), improvement of the procedure used for the testing of the energy flow path in order to account generators more realistically and development of the procedure for estimation of the common cause failures of the interconnections. The weather conditions are accounted only with air temperature and its implication on the continuous load rating of the power lines. Estimation of the correlation between grid and weather related events would require more detailed analysis of the weather initiated failures of the power system elements, particularly power lines, and their integration into the model using the common cause failures.

8 References

- ¹ IAEA Fundamental Safety Principles, Safety Standards Series No. SF-1, 15 November, 2006
- ² Moller N., Hansson S. O.; Principles of engineering safety: Risk and uncertainty reduction, Reliability Engineering & System Safety, 2008, 93(6), Pages 798-805
- ³ Sistemi in obrtovanje NE Krško, Knjiga 1, Izobraževalni center za jedrsko tehnologijo "Milan Čopič", 1989
- ⁴ Vaurio J. K., Tammi P.; Modelling the loss and recovery of electric power, Nuclear Engineering and Design, Volume 157, Issues 1-2, 1 July 1995, Pages 281-293
- ⁵ Vrbanić M., Kaštelan B., Krajnc J.; Integrated safety assessment of the NPP Krško modernization, Proceedings of the International Conference Nuclear Energy in Central Europe, Bled, Slovenia, Sept. 11-14, 2000
- ⁶ Reevaluation of Station Blackout Risk at Nuclear Power Plants, NUREG/CR 6890, US NRC, Washington, 2005
- ⁷ General Design Criteria for Nuclear Power Plants, Criterion 17:Electric power systems, NRC Regulations, Title 10, Code of Federal Regulations, Part 50: Domestic Licensing of production and utilization facilities, US NRC, Washington
- ⁸ Loss of all alternating current power, 10 CFR 50.63, NRC Regulations, Title 10, Code of Federal Regulations, Part 50: Domestic Licensing of production and utilization facilities, US NRC, Washington, 2007
- ⁹ Requirements for monitoring the effectiveness of maintenance at nuclear power plants, 10 CFR 50.65, NRC Regulations, Title 10, Code of Federal Regulations, Part 50: Domestic Licensing of production and utilization facilities, US NRC, Washington
- ¹⁰ Station Blackout, Regulatory Guide 1.155, US NRC, Washington, 1988
- ¹¹ Jeffrey S. M.; The NRC and Grid Stability, Commissioner, U. S. Nuclear Regulatory Commission, ANS Executive Conference on Grid Reliability, Stability and Off-Site Power, Denver, Colorado, July 24, 2006
- ¹² Grid Reliability and the Impact on Plant Risk and the Operability of Offsite Power, Generic Letter 2006-02, US NRC, Washington, 2006
- ¹³ RASK- review of the Forsmark unit 1 NPP, SKI, July 26th 2006 Forsmark, Sweden
- ¹⁴ Operating Experience Assessment - Effects of Grid Events on Nuclear Power Plant Performance, NUREG-1784, US NRC, Washington, 2003
- ¹⁵ An approach for using probabilistic risk assessment in risk-informed decision on plant specific changes to the licensing basis, Regulatory Guide 1.174, US NRC, Washington, 2002
- ¹⁶ Holahan M. G.; Expanded Application of PSA to Nuclear Power Plants - A Progress Report, Proceedings of the 8th International Conference on Probabilistic Safety Assessment and Management, May 14-18, New Orleans, 2006
- ¹⁷ Guidelines and Technical Bases for NUMARC Initiatives Addressing Station Blackout at Light Water Reactors, NUMARC 87-00, US NRC, Washington, 1988
- ¹⁸ Evaluation of Station Blackout Accidents at Nuclear Power Plants, NUREG-1032, US NRC, Washington, 1988
- ¹⁹ Carreras A., Newman D. E., Dobson I., Poole A. B.; Evidence for Self-Organized Criticality in Electric Power System Blackouts, Proceedings of the 33rd Annual Hawaii International Conference on System Sciences, January 4-7, 2000
- ²⁰ Čepin M., Mavko B.; A Dynamic Fault Tree, Reliability Engineering & System Safety, 2002, 75(1), Pages 83-91
- ²¹ Čepin M.; Method for Assessing Reliability of a Network Considering Probabilistic Safety Assessment, Proceedings, International Conference Nuclear Energy for New Europe, Bled, Slovenia, 2005
- ²² Čepin M.; Development of new method for assessing reliability of a network, Proceedings of the Eight International Conference on Probabilistic Safety Assessment and Management, May 14-18, 2006, New Orleans, Pages 45/1-45/8
- ²³ Volkanovski A., Čepin M., Mavko B.; Power system reliability analysis using fault trees, Proceedings, International Conference Nuclear Energy for New Europe, Portorož, 2006
- ²⁴ Volkanovski A., Čepin M., Mavko B.; An Application of the Fault Tree Analysis for the Power System Reliability Estimation, Proceedings, International Conference Nuclear Energy for New Europe, Portorož, 2007
- ²⁵ Volkanovski A., Čepin M., Mavko B.; Application of the fault tree analysis for assessment of the power system reliability, Proceedings, ESREL2008 & 17th SRA EUROPE Valencia, Spain, 2008
- ²⁶ Kančev D., Čauševski A., Čepin M., Volkanovski A.; Application of Probabilistic Safety Assessment for Macedonian Electric Power System, Proceedings, International Conference Nuclear Energy for New Europe, Portorož, 2007

- ²⁷ A report prepared by the Reliability Test System Task Force of the Application of Probability Methods Subcommittee, The IEEE Reliability Test System -1996, IEEE Transactions on Power Systems, 1999, 14(3), Pages 1010 – 1020
- ²⁸ Allan R. N., Billinton R.; Reliability Evaluation of Power Systems, Springer, 1996
- ²⁹ Bellhouse D.; Probability And Statistics Ideas In The Classroom - Lessons From History, ISI 55th session, Sydney, Australia 2005
- ³⁰ Koonce A. M., Apostolakis G. E., Cook B. K.; Bulk Power grid risk analysis: Ranking infrastructure elements according to their risk significance, ESD-WP-2006-19, Engineering Systems Division, Working Paper Series, MIT, 2006
- ³¹ Carreras B.A., Lynch V.E., Dobson I., Newman D.E.; Critical points and transitions in an electric power transmission model for cascading failure blackouts, Chaos 2002; 12(4), Pages 985-994
- ³² Volkanovski A., Mavko B., Boševski T., Čauševski A., Čepin M.; Genetic algorithm optimisation of the maintenance scheduling of generating units in a power system, Reliability Engineering & System Safety, 2008, 93(6), Pages 779-789
- ³³ Volkanovski A.; Optimization of the maintenance of the generating units in the power system using genetic algorithm, A Master Thesis, Faculty of electrical engineering – Skopje, Macedonia, 2005, Pages 50+21
- ³⁴ IEEE Gold Book, IEEE Recommended practice for the Design of reliable industrial and commercial power system, ANSI/IEEE Std 493-2007 , 2007
- ³⁵ Apostolakis G. E., Lemon D.M.; Screening Methodology for the Identification and Ranking of Infrastructure Vulnerabilities Due to Terrorism, Risk Analysis, 2005, 25 (2), Pages 361–376
- ³⁶ Garrick B. J., Hall J. E., Kilger M., McDonald J. C., O’Toole T., Probst P. S., Rindskopf P. E., Rosenthal R., Trivelpiece A. W., Van Arsdale L. E., Zebroski E. L.; Confronting the risk of terrorism: making the right decisions, Reliability Engineering & System Safety, 2004, 86, Pages 129-76
- ³⁷ Patterson S. A., Apostolakis G. E.; Identification of critical locations across multiple infrastructures for terrorist actions, Reliability Engineering & System Safety, 2007, 92(9), Pages 1183-1203
- ³⁸ Wei-Chang Y.; An improved sum-of-disjoint-products technique for the symbolic network reliability analysis with known minimal paths Reliability Engineering & System Safety, 2007, 92(2), Pages 260-268
- ³⁹ Miki T., Okitsu D., Kushida M., Ogino T.; Development of a hybrid type assessment method for power system dynamic reliability, IEEE International Conference on Systems, Man and Cybernetics, 1999, IEEE SMC '99 Conference Proceedings, Volume 1, Pages 968–73
- ⁴⁰ Zio E., Podofilini L., Zille V.; A combination of Monte Carlo simulation and cellular automata for computing the availability of complex network systems, Reliability Engineering & System Safety, 2006, 91, Pages 181-190
- ⁴¹ Yishan L.; Short-term and long-term reliability studies in deregulated power system, A doctoral dissertation, Texas A&M University, 2005, Pages 155+4
- ⁴² Ran M.; Deterministic/Probabilistic evaluation in composite system planning, A Master Thesis, University of Saskatchewan, Saskatoon, 2003, Pages 124+35
- ⁴³ Yifeng L.; Bulk System Reliability evaluation in a deregulated power industry, A Master Thesis, University of Saskatchewan, Saskatoon, 2003, Pages 142+45
- ⁴⁴ Rajesh U. N.; Incorporating Substation and Switching Station Related Outages in Composite System Reliability Evaluation, A Master Thesis, University of Saskatchewan, Saskatoon, 2003, Pages 91+25
- ⁴⁵ Hua C.; Generating System Reliability Optimization, A doctoral dissertation, University of Saskatchewan, Saskatoon, 2000, Pages 160
- ⁴⁶ Billinton R., Wangdee W.; Delivery Point Reliability Indices of a Bulk Electric System Using Sequential Monte Carlo Simulation, IEEE Transactions on Power Delivery, 2006, 21(1), Pages 345 – 352
- ⁴⁷ Haarla L., Pulkkinen U., Koskinen M., Jyrinsalo J.; A method for analysing the reliability of a transmission grid, Reliability Engineering & System Safety, 2008, 93(2), Pages 277-287
- ⁴⁸ Pottonen L.; A method for the probabilistic security analysis of transmission grids, A doctoral dissertation, Helsinki University of Technology, 2005, Pages 119+88
- ⁴⁹ Rasmussen N.; Reactor Safety Study, WASH-1400, US NRC, Washington, 1975
- ⁵⁰ Standard for Probabilistic Risk Assessment for Nuclear Power Plant Applications, ASME RA-S-2002, 2002
- ⁵¹ An Approach for Determining the Technical Adequacy of Probabilistic Risk Assessment The results for Risk-Informed Activities, Regulatory Guide 1.200, US NRC, Washington, 2004
- ⁵² Kumamoto H., Henley J. E.; Probabilistic Risk Assessment and Management for Engineers and Scientist, Second Edition, IEEE Press, New York, 1996
- ⁵³ Roberts N. H., Vesely W. E., Haasl D. F., Goldberg F. F.; Fault Tree Handbook, NUREG-0492, US NRC, Washington, 1981
- ⁵⁴ Vesely W. E., Dugan J., Fragola J., Minarick J., Railsback J.; Fault Tree Handbook with Aerospace Applications, National Aeronautics and Space Administration, NASA, 2002

- ⁵⁵ Breeding R. J., Leahy T. J., Young J., Cramond W. R.; Probabilistic Risk Assessment Course Documentation – Volume 1: PRA Fundamentals, NUREG/CR-4350/1, US NRC, Washington, 1985
- ⁵⁶ MIL-HDBK-338B, U.S. Department of Defense (DoD), 1998
- ⁵⁷ Cizelj R. J., Mavko B., Kljenak I.; Component reliability assessment using quantitative and qualitative data, *Reliability Engineering & System Safety*, 71(1), January 2001, Pages 81-95
- ⁵⁸ Haasl D., Young J. Cramond W. R.; Probabilistic Risk Assessment Course Documentation – Volume 4: System reliability and analysis Techniques Session, NUREG/CR-4350/4, US NRC, Washington, 1985
- ⁵⁹ Prior R. P., Chaboteaux J. P., Wolvaardt F. P., Longton M. T., Schene R.; Best estimate success criteria in the Krško IPE, International meeting: PSA/PRA and Severe Accidents, Ljubljana, Slovenia, 1994
- ⁶⁰ Knief R. A.; Nuclear Engineering, Theory and technology of commercial nuclear power, Taylor&Francis, 1992, Washington, 747 Pages
- ⁶¹ Čepin M., Kožuh M., Mavko B., Žunko P.; Raziskava nerazpoložljivosti sistema za sprožitev tehničnih varnostnih ukrepov pri izbranih začetnih dogodkih z uporabo verjetnostnih varnostnih metod, *Elektroteh. vestn.*, 60 (4), 1993, Pages 220-227
- ⁶² Čepin M.; Importance of human contribution within the human reliability analysis (IJS-HRA). *J. loss prev. process ind.*, 2008, 21(3), Pages 268-276
- ⁶³ Prošek A., Čepin M.; Success criteria time windows of operator actions using RELAP5/MOD3.3 within human reliability analysis, *J. loss prev. process ind.*, 2008, 21(3), Pages 260-267
- ⁶⁴ Čepin M.; DEPEND-HRA-A method for consideration of dependency in human reliability analysis, *Reliability Engineering and Systems Safety*, 2008, 93(10), Pages 1452-1460
- ⁶⁵ Čepin M., Mavko B.; Probabilistic safety assessment improves surveillance requirements in technical specifications, *Reliability Engineering and Systems Safety*, 1997, 56 (1), Pages 69-77
- ⁶⁶ Čepin M.; Optimization of safety equipment outages improves safety, *Reliability Engineering & System Safety*, 2002, 77 (1), Pages 71-80
- ⁶⁷ Čepin M., Martorell S.; Evaluation of allowed outage time considering a set of plant configurations, *Reliability Engineering & System Safety*, 2002, 78(3), Pages 259-266
- ⁶⁸ Čepin M.; Optimizacija razporeditve preizkušanja in vzdrževanja varnostne opreme na podlagi najmanjšega tveganja, *Elektroteh. vestn.*, 70(1-2), 2003, Pages 22-26.
- ⁶⁹ Čepin M.; Razvoj kriterijev tveganja za trajne spremembe v jedrski elektrarni, *Elektroteh. vestn.*, 2006, 73(2-3), Pages 149-154
- ⁷⁰ Mosleh A., Fleming K. N.; Procedures for treating Common Cause Failures in safety and reliability studies, NUREG/CR-4780 Vol. 1 and 2, US NRC, Washington, 1988
- ⁷¹ Čepin M.; Analysis of truncation limit in probabilistic safety assessment, *Reliability Engineering and Systems Safety*, 2005, Vol. 87(3), Pages 395-403
- ⁷² W. E. Vesely, Davis T. C., Denning R. S., Saltos N., Measures of Risk Importance and their Applications, NUREG/CR-3385, US NRC, Washington, 1983
- ⁷³ Martorell S., Carlos S., Villanueva J.F., Sanchez A.I., Galvan B., Salazar D., Čepin M.; Use of multiple objective evolutionary algorithms in optimizing surveillance requirements, *Reliability Engineering & System Safety*, 2006, Vol. 91(9), Pages 1027-1038
- ⁷⁴ Use of Probabilistic Risk Assessment Methods in Nuclear Activities: Final Policy Statement, Federal Register, Vol. 60, p. 42622 (60 FR 42622), US NRC, Washington, 1995
- ⁷⁵ Čepin M.; The risk criteria for assessment of temporary changes in a nuclear power plant, *Risk anal.*, 2007, 27(4), Pages 991-998
- ⁷⁶ An Approach for Plant-Specific, Risk-Informed Decisionmaking: Inservice Testing, Regulatory Guide 1.175, US NRC, Washington, 1998
- ⁷⁷ An Approach for Plant-Specific, Risk-Informed Decisionmaking: Graded Quality Assurance, Regulatory Guide 1.176, US NRC, Washington, 1998
- ⁷⁸ An Approach for Plant-Specific, Risk-Informed Decisionmaking: Technical Specifications, Regulatory Guide 1.177, US NRC, Washington, 1998
- ⁷⁹ Early Site Permits; Standard Design Certifications; and Combined Licenses for Nuclear Power Plants, 10 CFR Part 52, US NRC, Washington, 2007
- ⁸⁰ Standard Review Plan for the Review of Safety Analysis Reports for Nuclear Power Plants (LWR Edition), NUREG-0800, US NRC, Washington, 1996
- ⁸¹ Hamzehee H., Hilsmeier T.; Use of Risk Insights in Support of USNRC Reviews of New Reactor Applications, PSAM 9, 18-23 May 2008, Hong Kong, China
- ⁸² Allan R. N., Billinton R.; Probabilistic methods applied to electric power systems - are they worth it?, *Power Engineering Journal*, Volume 6, Issue 3, May 1992, Pages 121 – 129B
- ⁸³ IEEE Guide for Electric Power Distribution Reliability Indices, IEEE Std 1366™-2003

- ⁸⁴ Data development, Volume 6, NUREG/CR 4350/6, US NRC, Washington, 1985
- ⁸⁵ RiskSpectrum® PSA Professional, 1998-2003 RELCON AB
- ⁸⁶ Grainger J. J., Stevenson W. D.; Power System Analysis, McGraw-Hill, 1994
- ⁸⁷ I. Papic; Mathematical analysis of FACTS devices based on a voltage source converter: Part 1: mathematical models, Electric Power Systems Research, 2000, 56(2), Pages 139-148
- ⁸⁸ Ačkovski R.; Contribution on methods for planning and development of power systems using Monte Carlo simulation -, PhD Thesis, Faculty of Electrical Engineering – Skopje, 1989
- ⁸⁹ Todorovski M.; Approximate calculation of power flows through high voltage network, Graduation work, Faculty of Electrical Engineering – Skopje, 1995
- ⁹⁰ Aswani D., Badreddine B., Malone M., Gauthier G., Proietty J.; Criteria for evaluating protection from single points of failure for partially expanded fault trees, Reliability Engineering & System Safety, 2008, 93(2), Pages 206-216
- ⁹¹ Strategija razvoja elektroenergetskega sistema Republike Slovenije, Načrt razvoja prenosnega omrežja v Sloveniji od leta 2007 do 2016, ELES, Ljubljana, 2007
- ⁹² Evaluation of Loss of Offsite Power Events at Nuclear Power Plants: 1980-1996, NUREG-5496, US NRC, Washington, 1997
- ⁹³ Rates of Initiating Events at U.S. Nuclear Power Plants: 1987–1995, NUREG-5750, US NRC, Washington, 1996
- ⁹⁴ Losses of Off-Site Power at U.S. Nuclear Power Plants Through 1991, NSAC-182, Electric Power Research Institute, 1992
- ⁹⁵ Analysis of Core Damage Frequency: Surry, Unit 1 Internal Events, NUREG/CR-4550, SAND86-2084, Vol.3, Rev.1, Part 1, US NRC, Washington, 1990
- ⁹⁶ Analysis of Core Damage Frequency: Surry, Unit 1 Internal Events Appendices, NUREG/CR-4550, SAND86-2084, Vol.3, Rev.1, Part 2, US NRC, Washington, 1990
- ⁹⁷ NRC Proposed License Renewal Interim Staff Guidance LR–ISG–2008–01: Staff Guidance Regarding the Station Blackout Rule (10 CFR 50.63); Associated With License Renewal, ADAMS Accession No. ML080520620, US NRC, Washington, 2008
- ⁹⁸ Jordan R., Mavko B., Žunko.; Raziskava razpoložljivosti sistema električnega napajanja z uporabo verjetnostnih varnostnih metod, Elektrotehniški vestnik, 58(1), 1991, Ljubljana
- ⁹⁹ Surry Power Station, NRC supplemental inspection report 05000280/2004011 and 05000281/2004011, US NRC, Washington, 2005
- ¹⁰⁰ Čepin M., Prosen R.; Update of the Human Reliability Analysis for a Nuclear Power Plant, Proceedings, International Conference Nuclear Energy for New Europe, Portorož, Slovenia, 2006
- ¹⁰¹ Krajnc B., Mavko B.; Safety importance determination of design changes in nuclear installations, Proceedings, Regional meeting Nuclear Energy in Central Europe, Bled, Slovenia, 1997

APPENDIX A. PRINCIPLES OF ENGINEERING SAFETY

The 24 safety principles and their categorization are given in Table A-1. The categories in the third column of Table A-1 are the following: (1) inherently safe design, (2) safety reserves, (3) fail safe and (4) procedural safeguards.

Table A-1 Principles of engineering safety

Principle/method	Brief description	Category
Inherently safe design	Potential hazards are avoided rather than controlled.	1
Safety factor	The system is constructed to resist loads and stresses exceeding what is necessary for the intended usage by multiplying the intended load by a factor (>1).	2
Safety margin	An (additive) margin is used for acceptable system performance as a precautionary measure.	2
Stress margins	The system is designed so that statistical variations in stresses do not lead to failure.	2
Screening	Control measure to eliminate components that may pass operating tests for specific parameters but show signs of possible future failure (or reduced sustainability).	3, 4
Safety barriers	Physical barriers providing multiple layers of protection; if one layer fails, the next will protect from system failure.	3
Reliability	A measure of system failure rate. High reliability against certain types of failures is necessary for system safety.	3
Redundancy	Method of achieving reliability for important system functions. Redundant parts protect the system in case of failure of one part.	3
Diversity	Redundant system parts are given different design characteristics to avoid failures from a common cause-to-cause failure in all redundant parts.	3
Segregation (Independence, Isolation)	Redundant parts should not be dependent on each other. Malfunction in part should not have any consequences for a redundant part. One way to avoid this is to keep the parts physically apart.	3
Fail-safe design	Even if a failure of one part occurs, the system remains safe, often by system shut down or by entering a “safe mode” where several events are not permitted.	3
Proven design	Relying on design that has been proven by the “test of time”, i.e. using solutions or materials that have been used on many occasions and over time without failure.	3
Single failure criterion (Independent malfunction)	Design criteria stating that a failure of a single system part should not lead to system failure. System failure should only be possible in case of independent malfunction.	3
Pilotability (safe information load)	The system operator should have access to the control means necessary to prevent failure, and the work should not be too difficult to perform	3
Quality	Reliance on materials, constructions etc of proven quality for system design.	3, 4

Principle/method	Brief description	Category
Operational interface control	Focusing on controlling the interface between humans and (the rest of) the system and equipment. For example, using interlocks to prevent human action to have harmful consequences.	3
Environmental control	The environment should be controlled so that it cannot cause failures. Especially, neither extremes of normal environmental fluctuations nor energetic events such as fire should be able to cause failures.	4
Operating and maintenance procedures	Automatic as well as manual procedures are used as a defense against failures. Training in order to follow procedures is a part of such safety procedures.	4
Job study observations	Identifying potential causes through collecting data from observations and audits, e.g., interviewing staff about potential or existent hazardous practices.	4
Controlling behavior	Controlling certain types of behavior (e.g., alcohol and drug abuse, lack of sleep), e.g., by tests and audits.	4
Standards	Standardized solutions of system design, material usage, maintenance procedures etc. Standards may be applied to all areas of safety engineering.	1–4
Timed replacement	Replacing components before their performance has decreased as a precautionary procedure. This can be done regularly without any signs of decreased performance, or by using indicators of potential failure such as component degradation or drift.	4
Procedural safeguards	Procedures such as instructions to operators to take or avoid specific actions in general or in special circumstances.	4
Warnings	Warning devices and information are provided when control measures are insufficient (or in addition to them).	

APPENDIX B. SUBSTATIONS CONFIGURATIONS

The substations have different complexity, which depend on their configuration (single bus, sectionalized single bus, breaker-and-a-half, double bus double breaker, and ring bus), number of generators, number of lines and number of loads connected into it.

The configurations of the substations used in the analysis are given in the following sections.

I.1 IEEE Test System

The IEEE test system includes 24 substations, 7 substations have identical configurations to others, and therefore there are 17 unique substation configurations. The fault trees are developed for all substations. The Figure B-1 shows the configuration of the substation 1 from IEEE RTS. The components (e.g. bus, disconnect switches and circuit breakers), which are active in the normal regime (i.e. closed), and components, which are not active (i.e. open), are identified on Figure B-1 using different coloring schemes. Components in blue are normally open.

The connected elements (lines, load and generators) are transferred from primary to secondary bus with disconnection of the active elements and transfer of the energy thought secondary bus in the case of identified error (e.g. short circuit to ground or between phases) from the protection. The following naming procedure is used for the substation components and their corresponding fault trees: the first letters identify the component type (e.g. bus, disconnect switch, circuit breaker), the following two letters identify the substation number and the last three numbers represent the identification of the component. For example, DS01011 identifies disconnect switch (DS) 011 situated in substation 01.

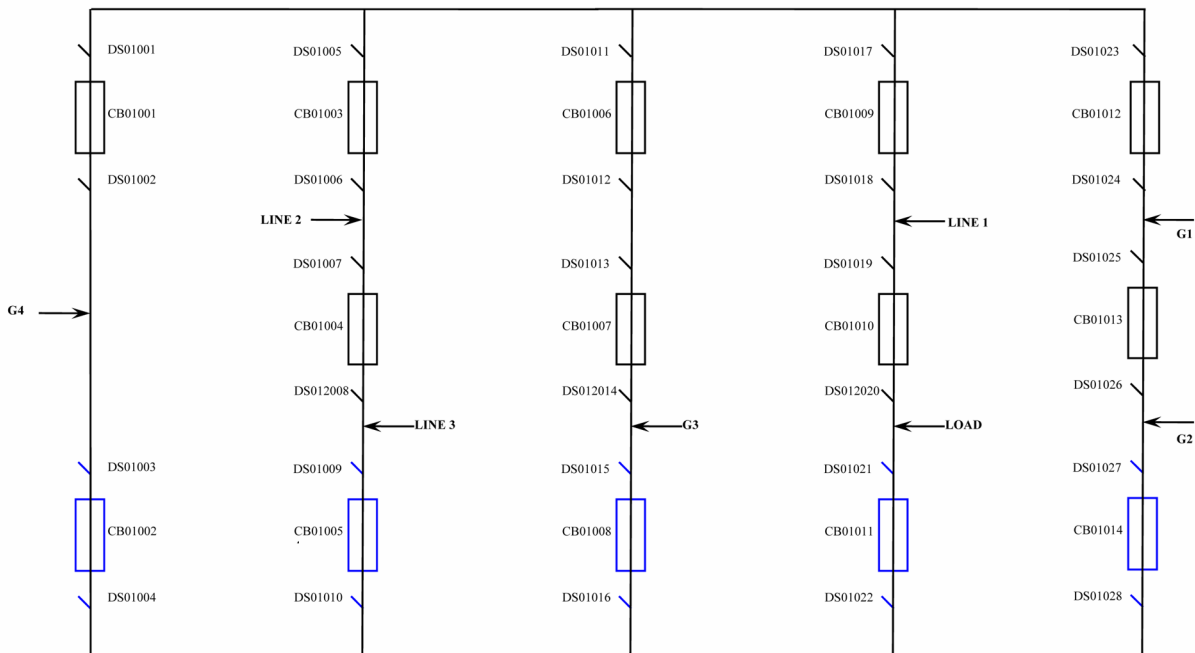


Figure B-1 Configuration of substation 1 from IEEE RTS

Substation 2 has the same scheme as substation 1, therefore the same FT is used.

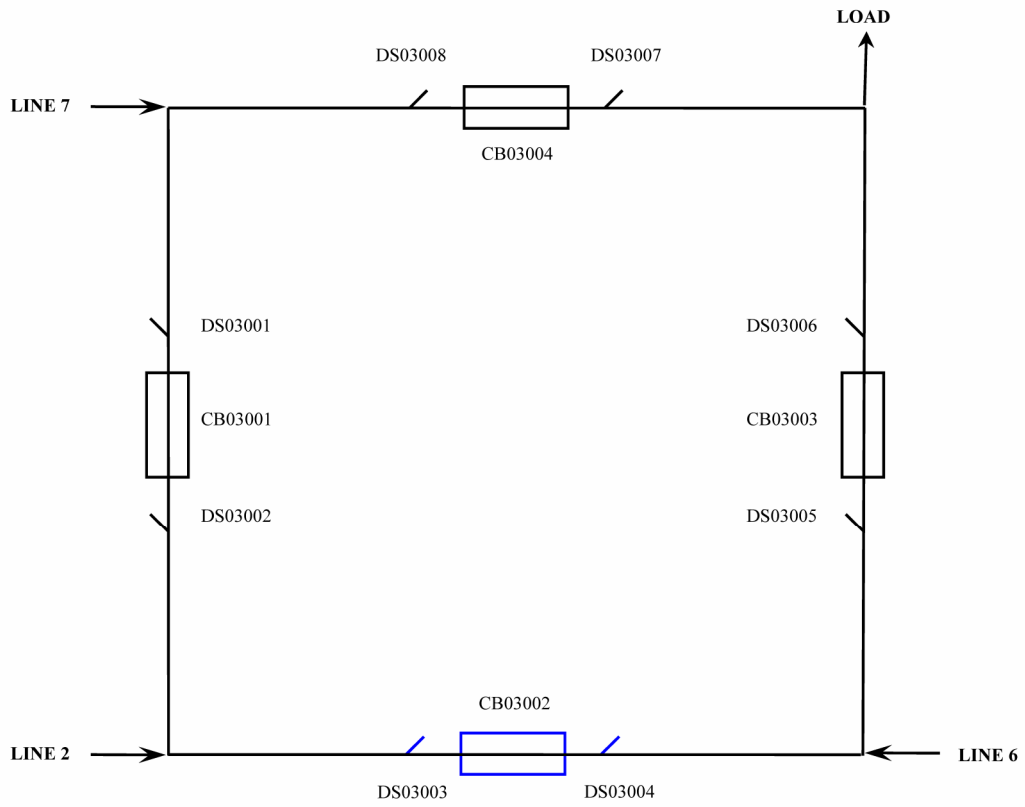


Figure B-2 Configuration of substation 3 from IEEE RTS

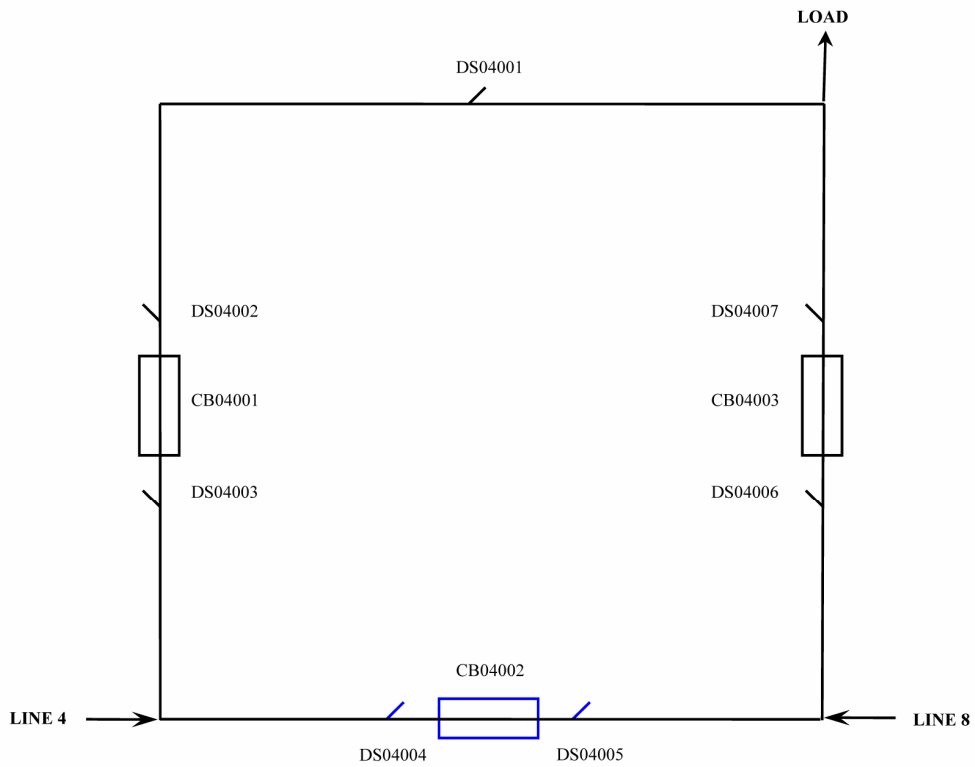


Figure B-3 Configuration of substation 4 from IEEE RTS

Substations 5 and 6 have the same configurations as substation 4.

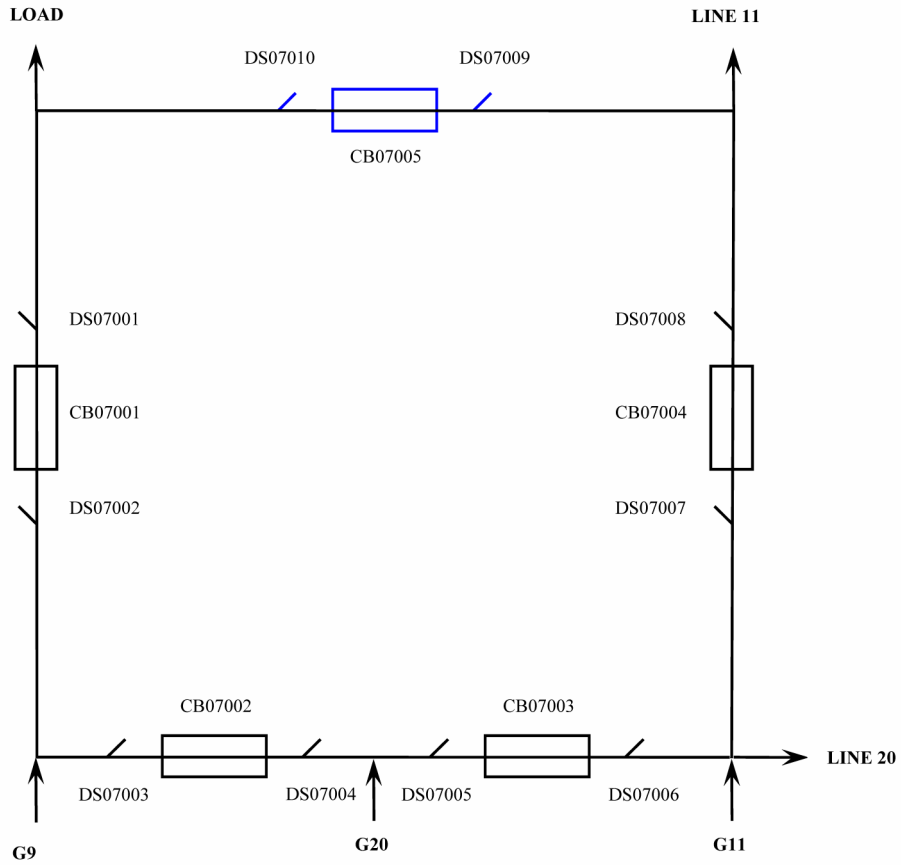


Figure B-4 Configuration of substation 7 from IEEE RTS

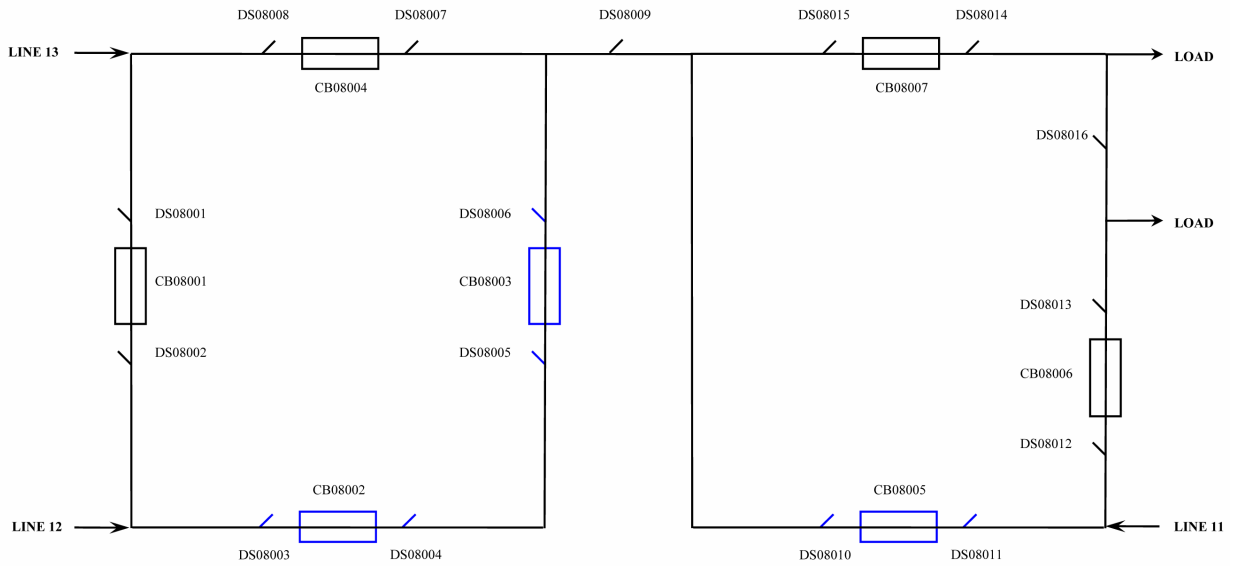


Figure B-5 Configuration of substation 8 from IEEE RTS

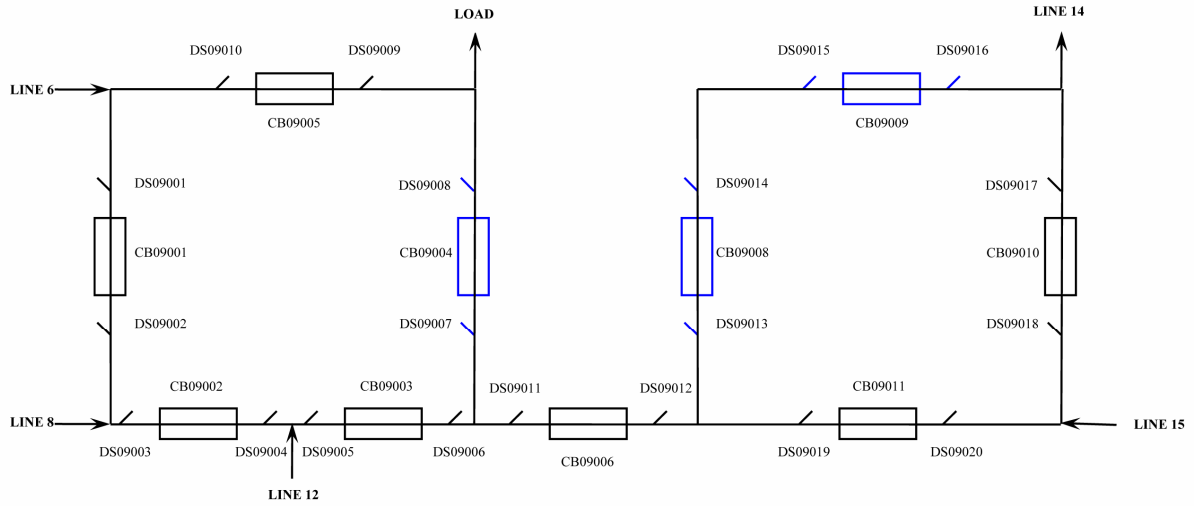


Figure B-6 Configuration of substation 9 from IEEE RTS

Substation 10 has the same scheme as substation 9, therefore the same FT is used.

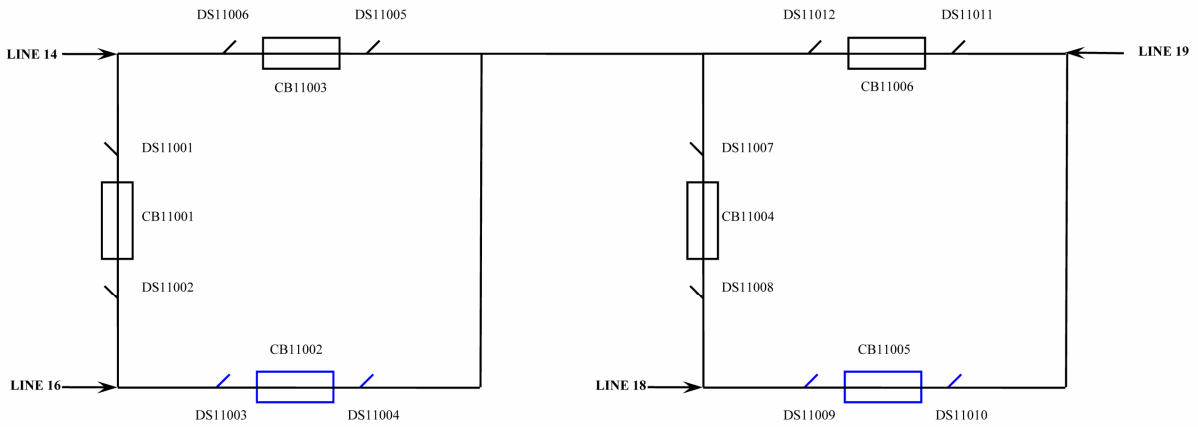


Figure B-7 Configuration of substation 11 from IEEE RTS

Substation 12 has the same scheme as substation 11, therefore the same FT is used.

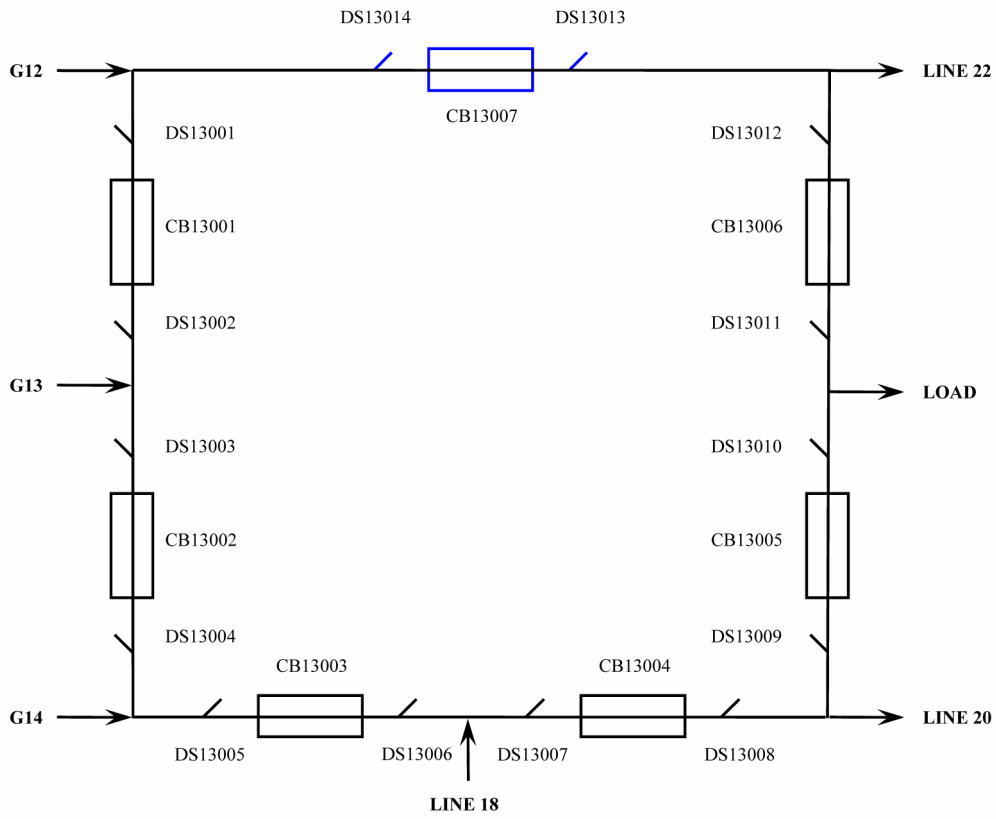


Figure B-8 Configuration of substation 13 from IEEE RTS

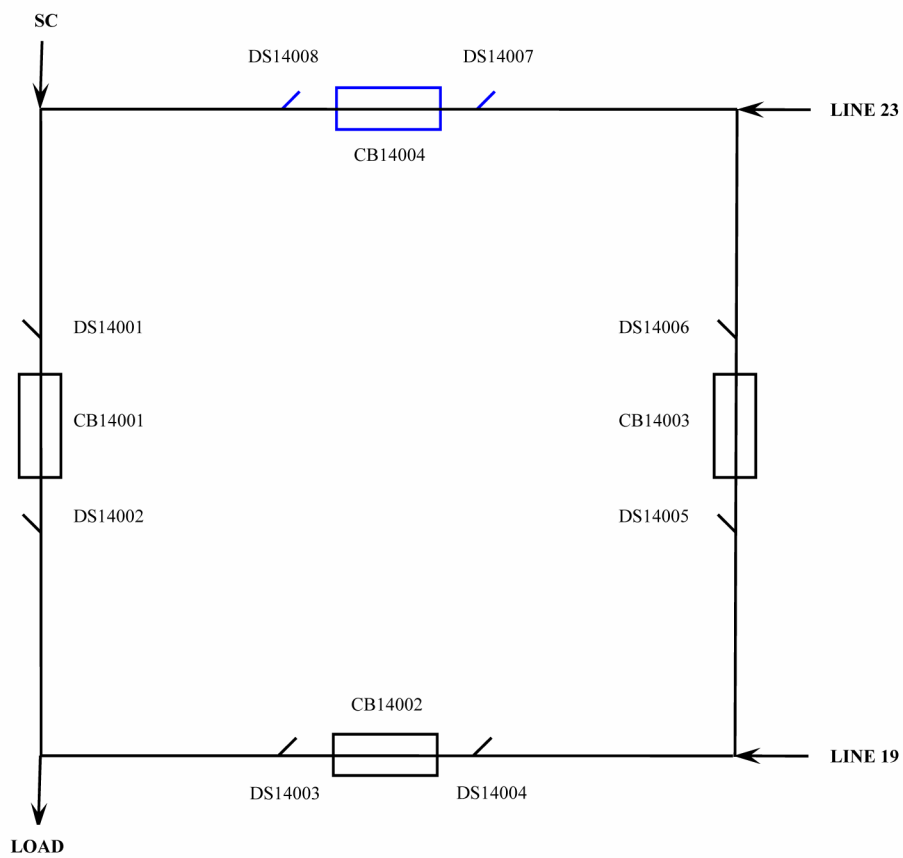


Figure B-9 Configuration of substation 14 from IEEE RTS

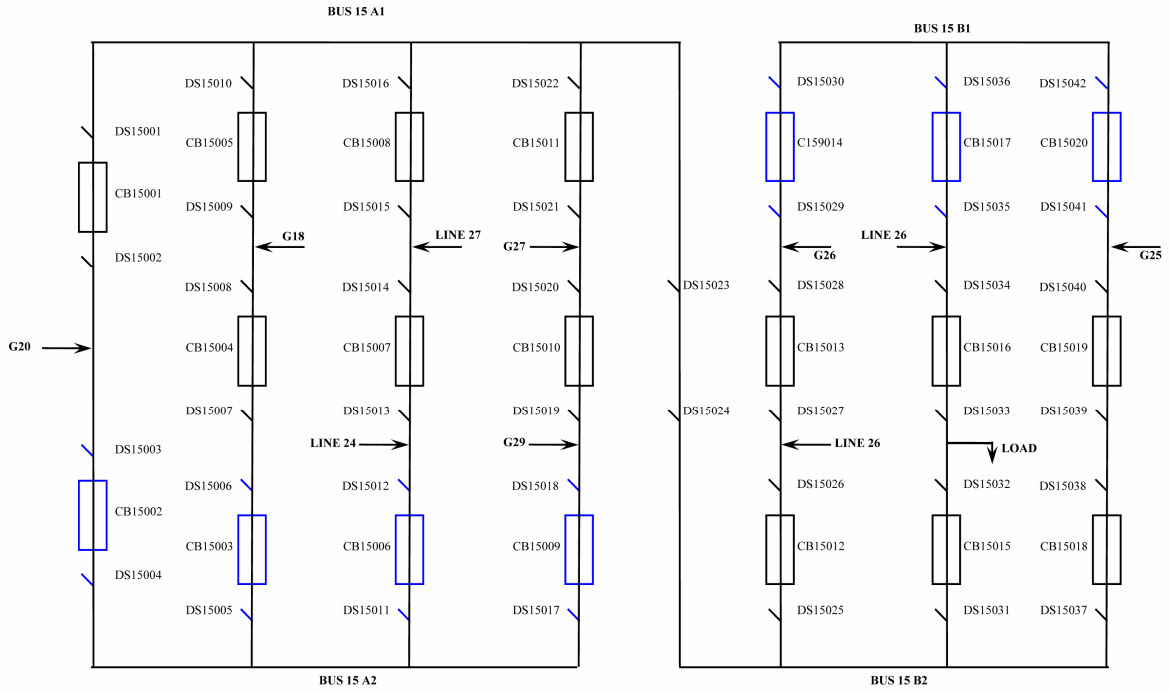


Figure B-10 Configuration of substation 15 from IEEE RTS

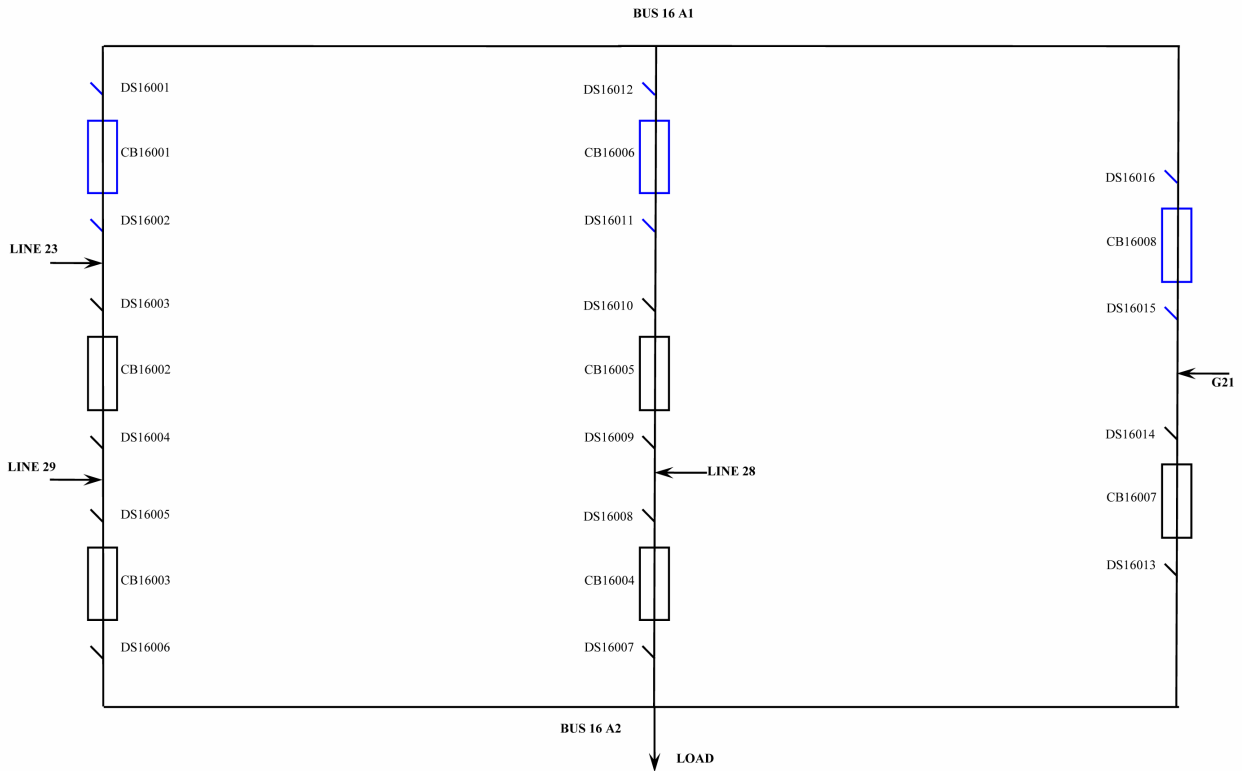


Figure B-11 Configuration of substation 16 from IEEE RTS

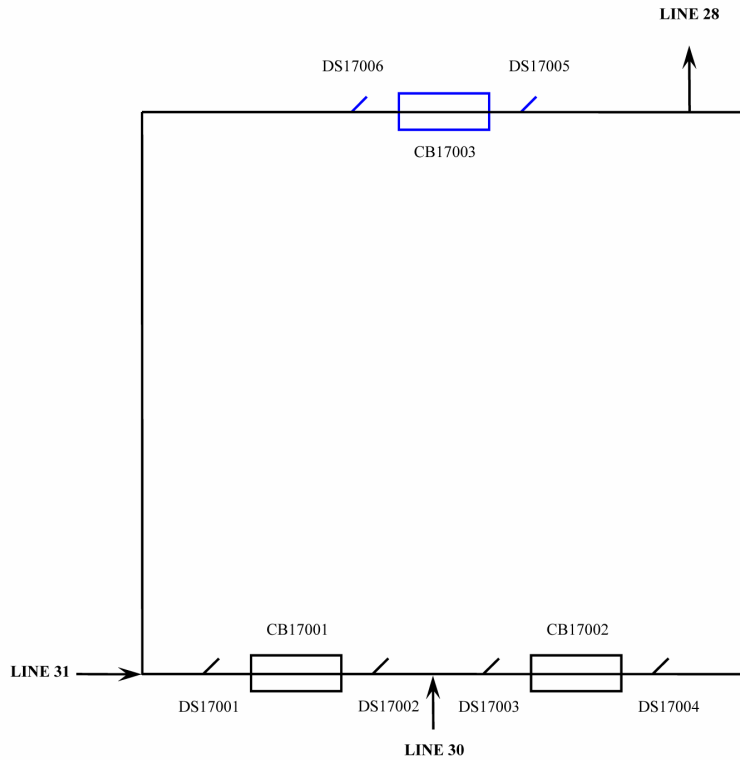


Figure B-12 Configuration of substation 17 from IEEE RTS

Substation 18 has the same scheme as substation 16, therefore the same FT is used.
 Substation 19 has the same scheme as substation 8, therefore the same FT is used.

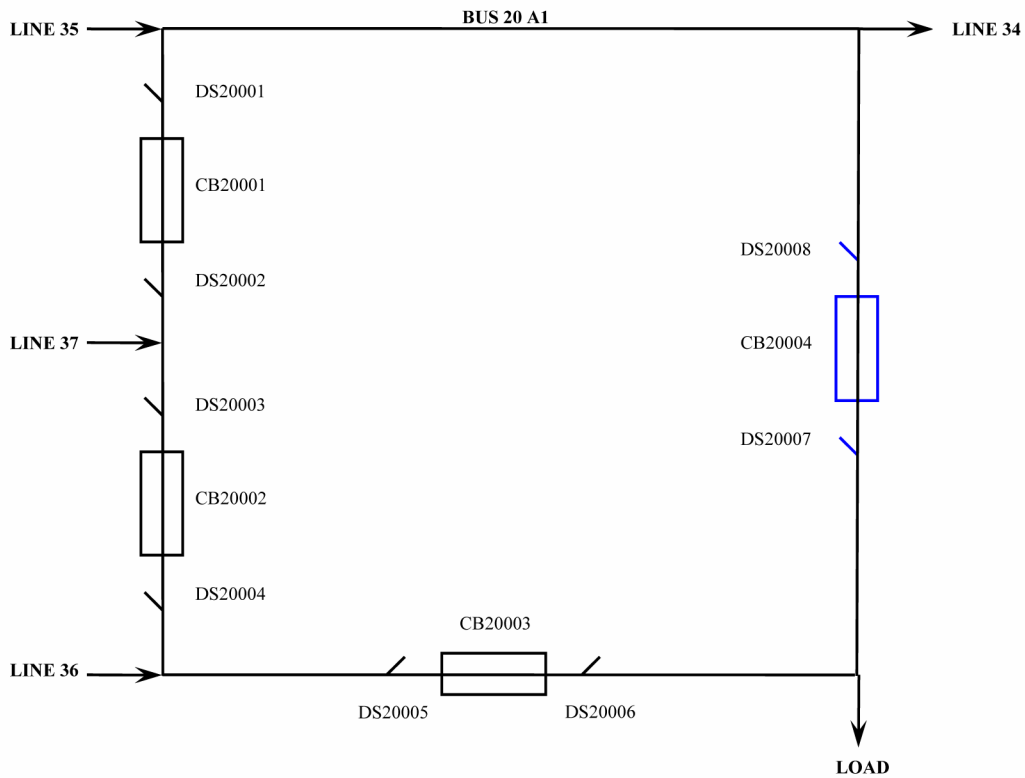


Figure B-13 Configuration of substation 20 from IEEE RTS

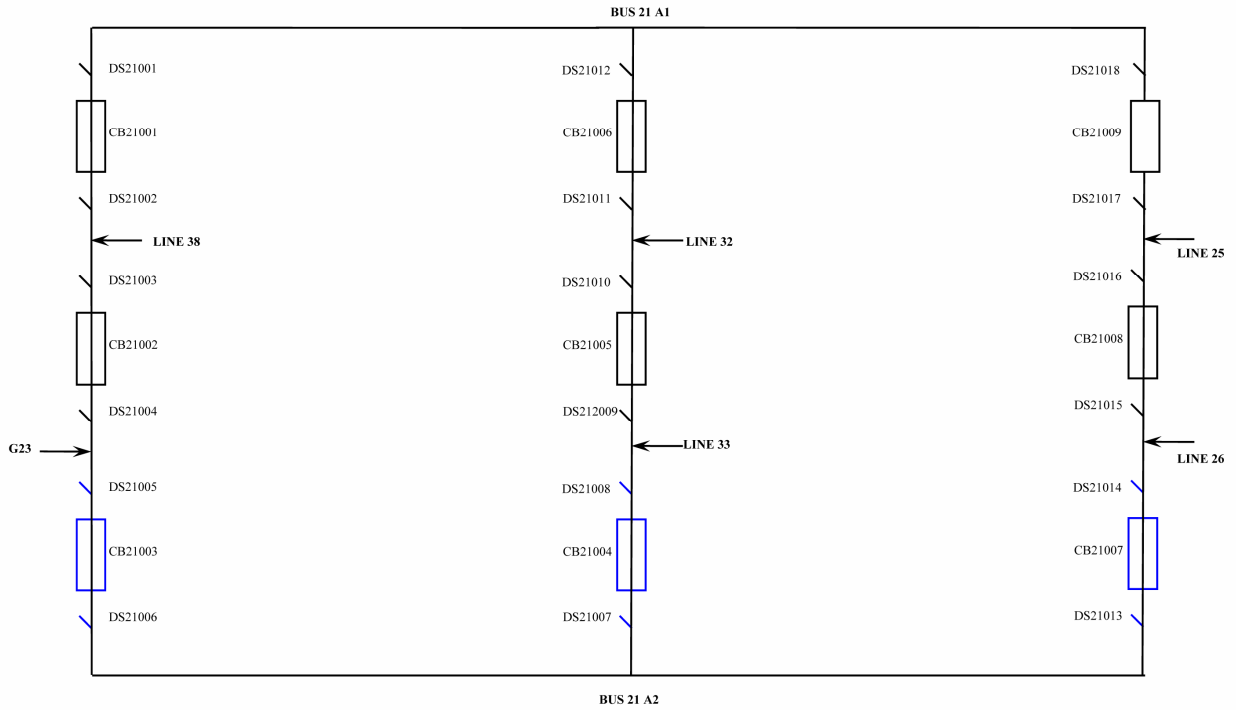


Figure B-14 Configuration of substation 21 from IEEE RTS

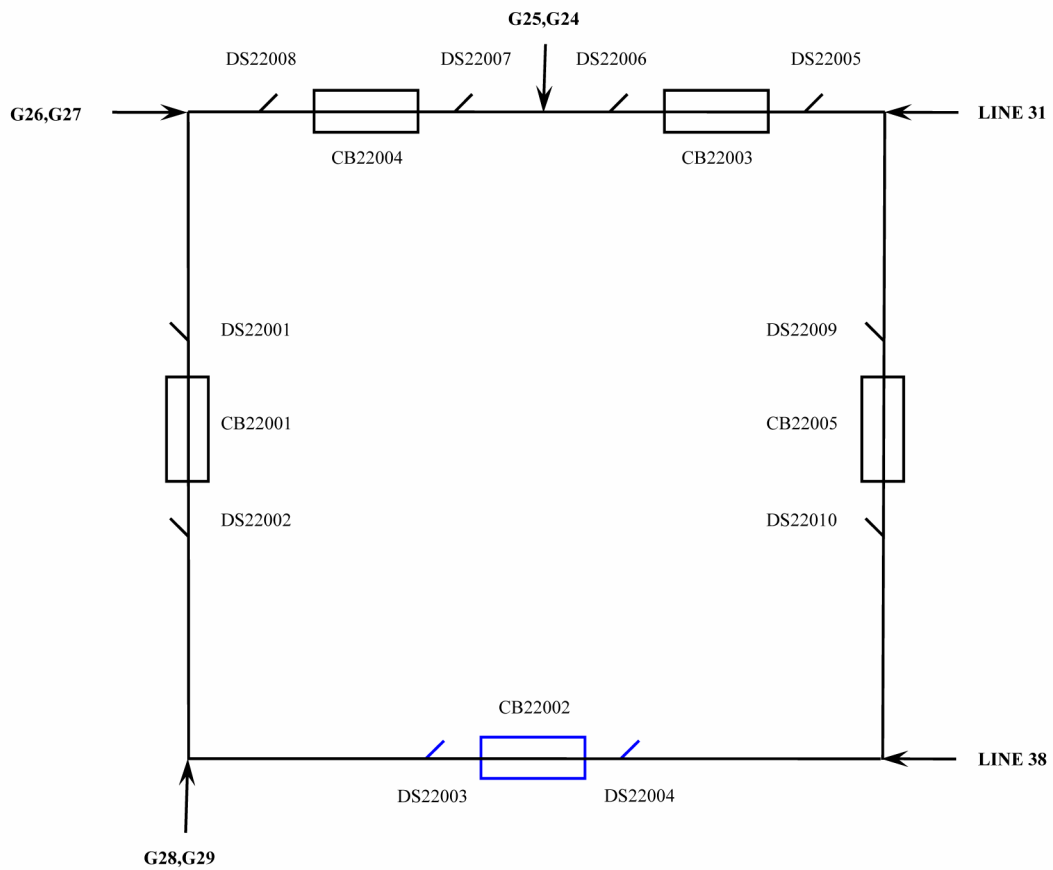


Figure B-15 Configuration of substation 22 from IEEE RTS

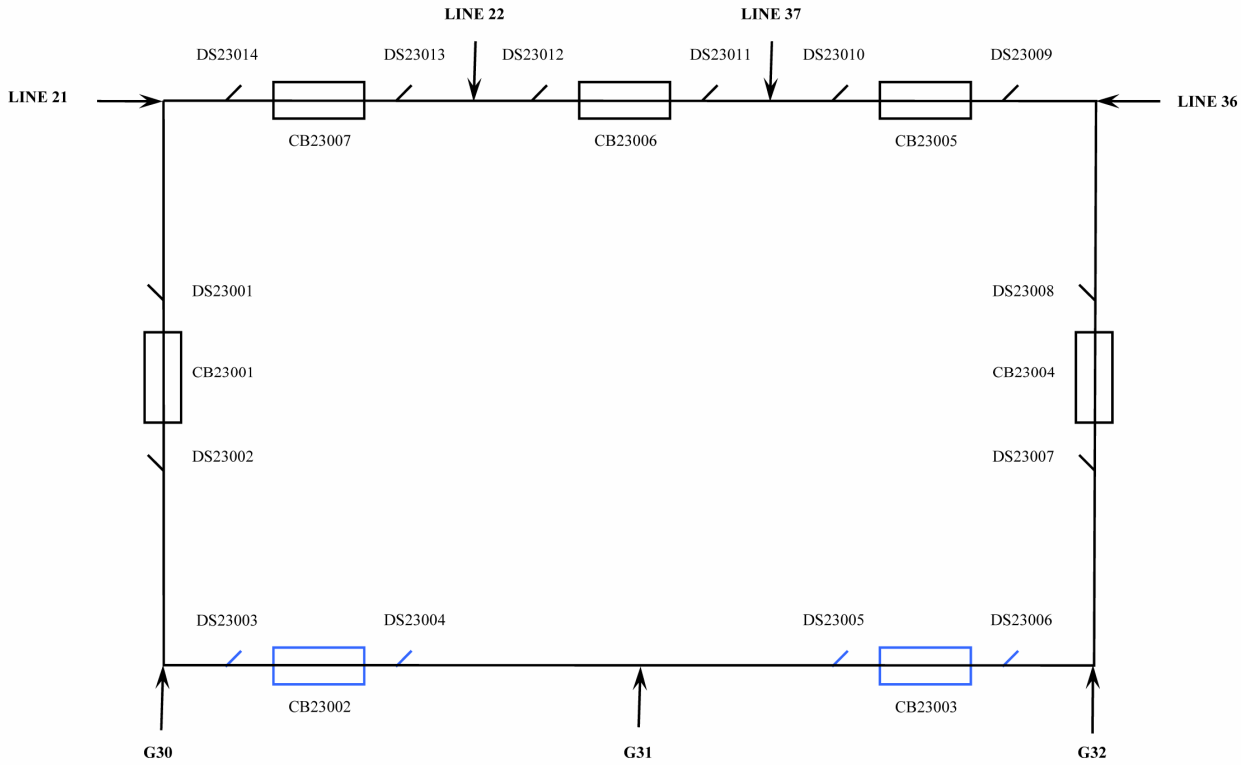


Figure B-16 Configuration of substation 23 from IEEE RTS

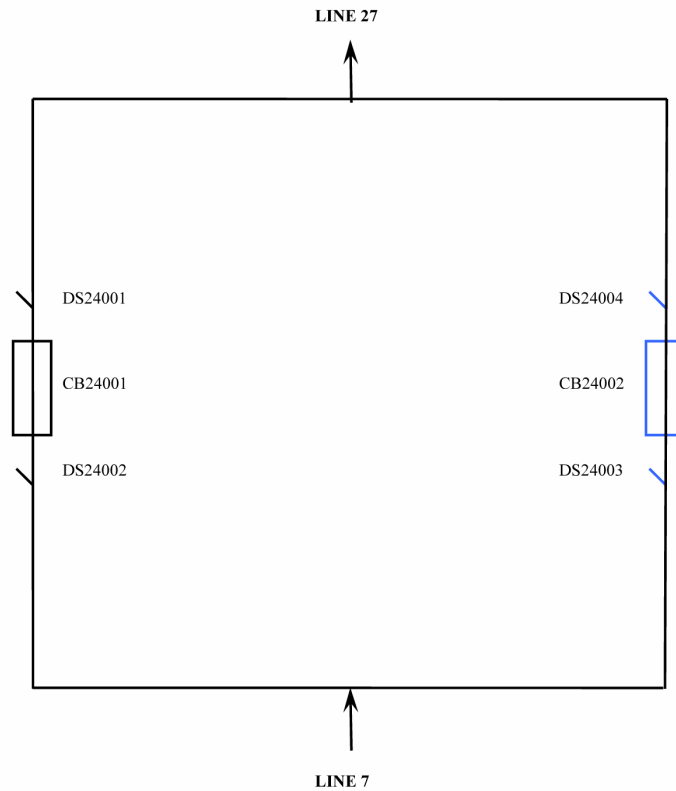


Figure B-17 Configuration of substation 24 from IEEE RTS

I.2 Slovenian power system

Configurations of the substations in the Slovenian power system are given in the following figures.

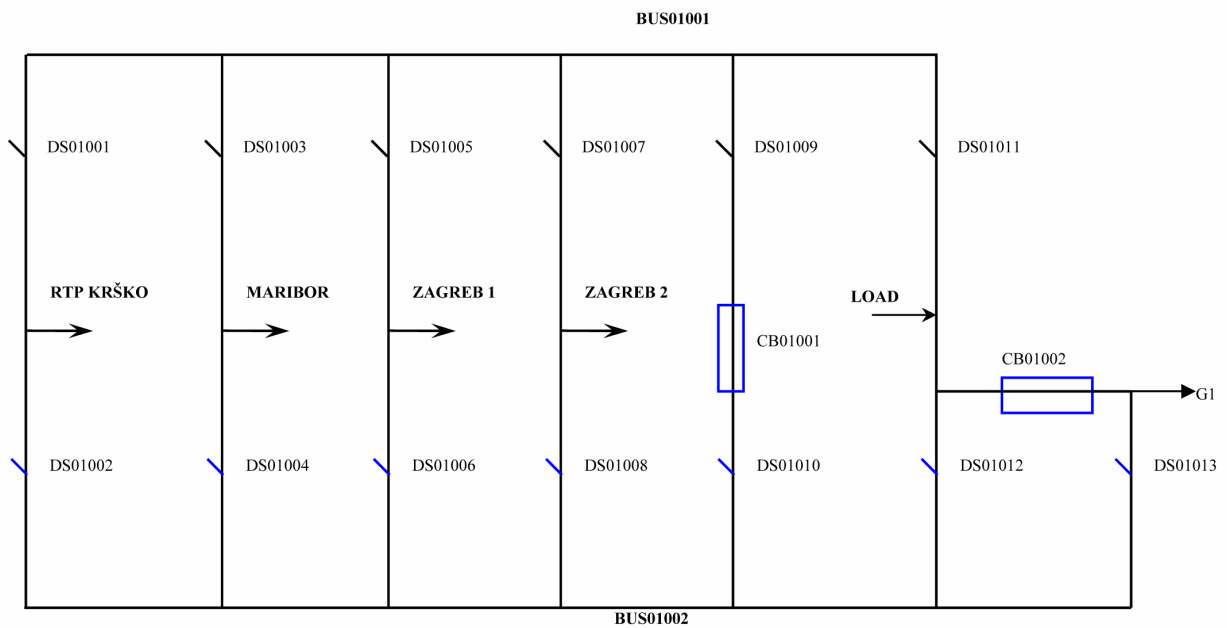


Figure B-18 Configuration of the substation NPP Krško

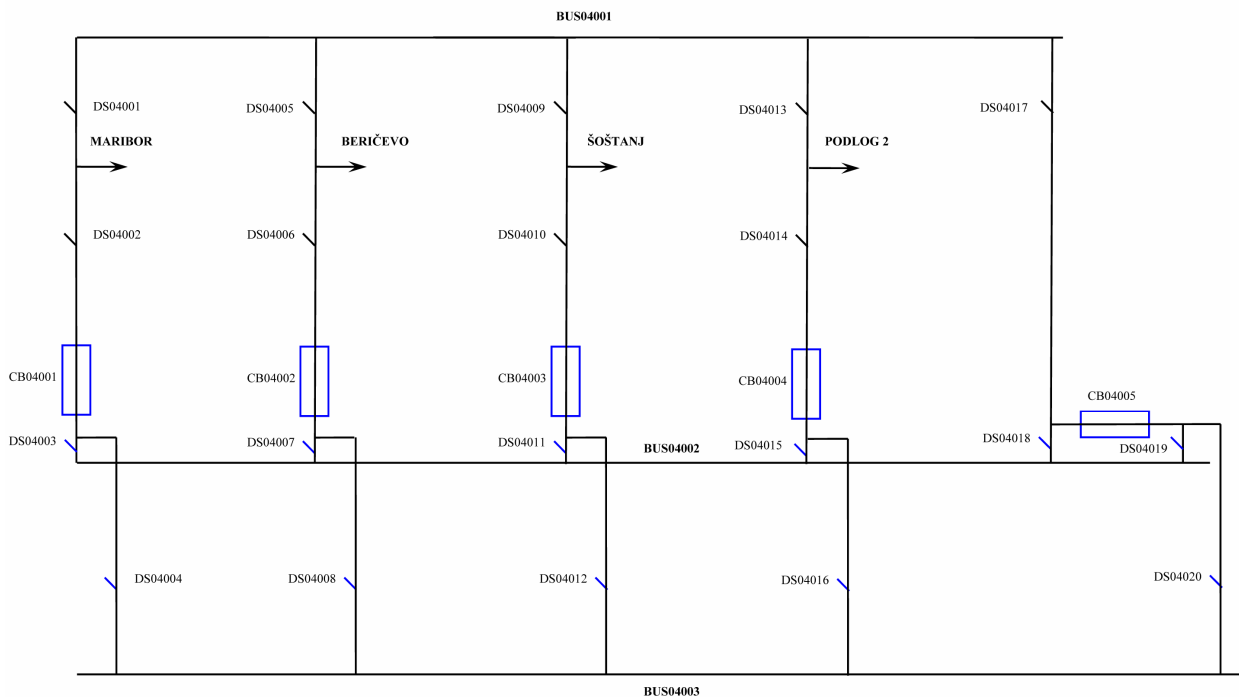


Figure B-19 Configuration of the substation Podlog

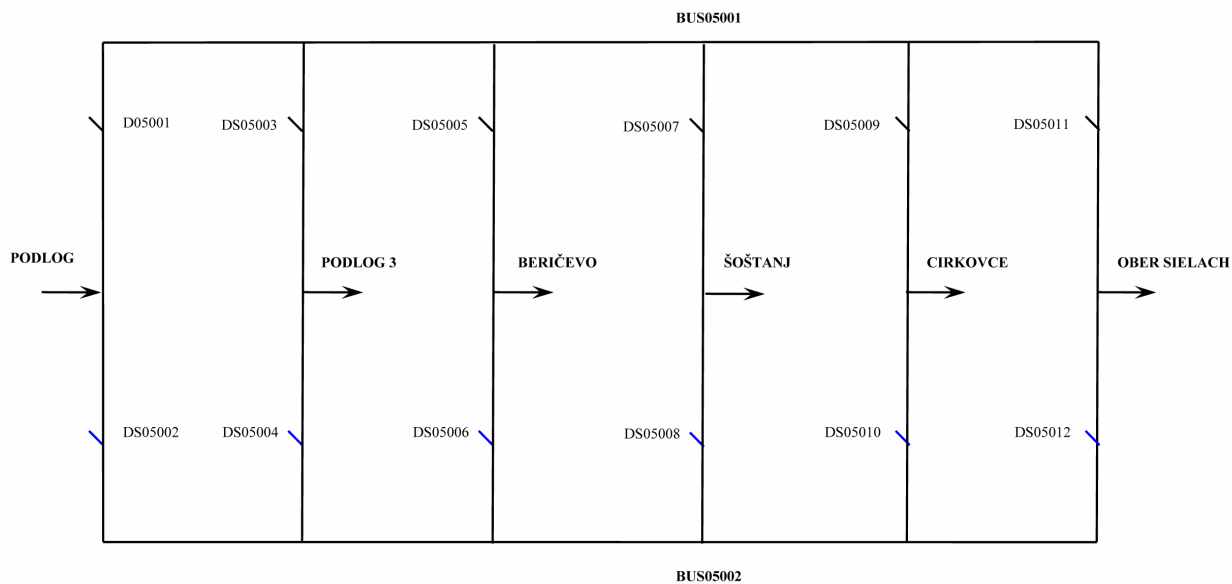


Figure B-20 Configuration of the substation Podlog 2

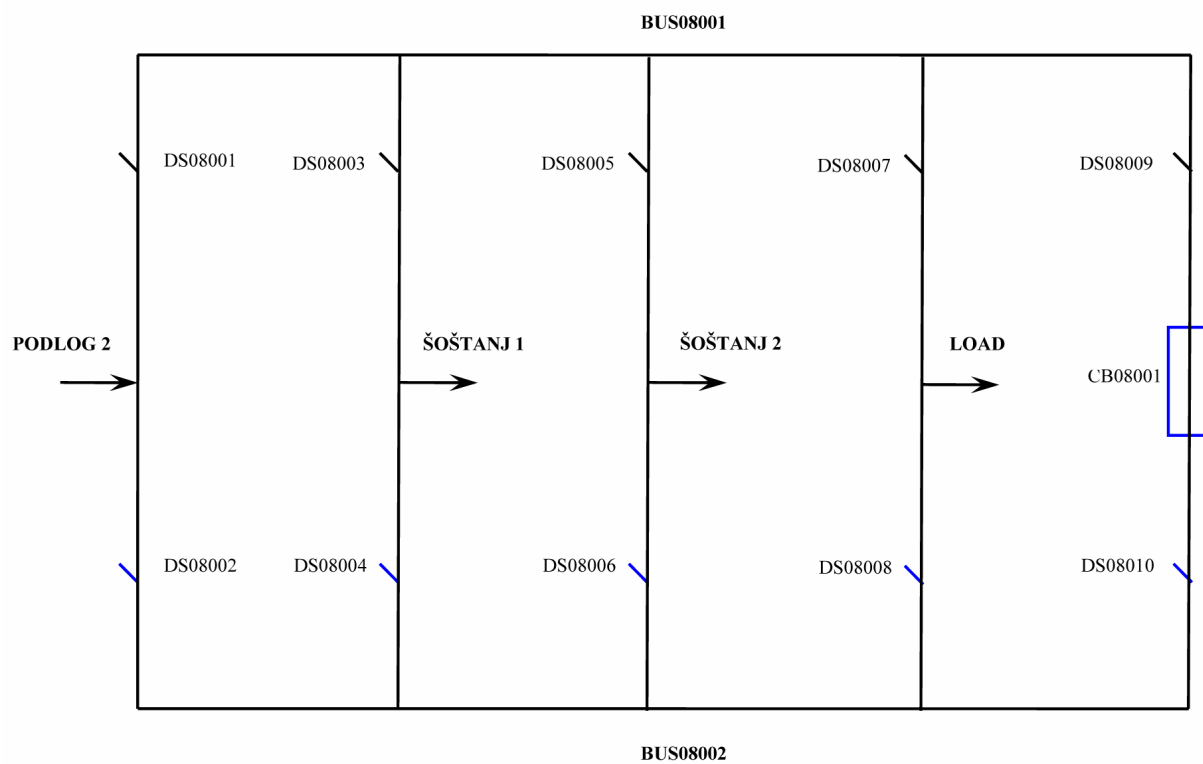


Figure B-21 Configuration of the substation Podlog 3

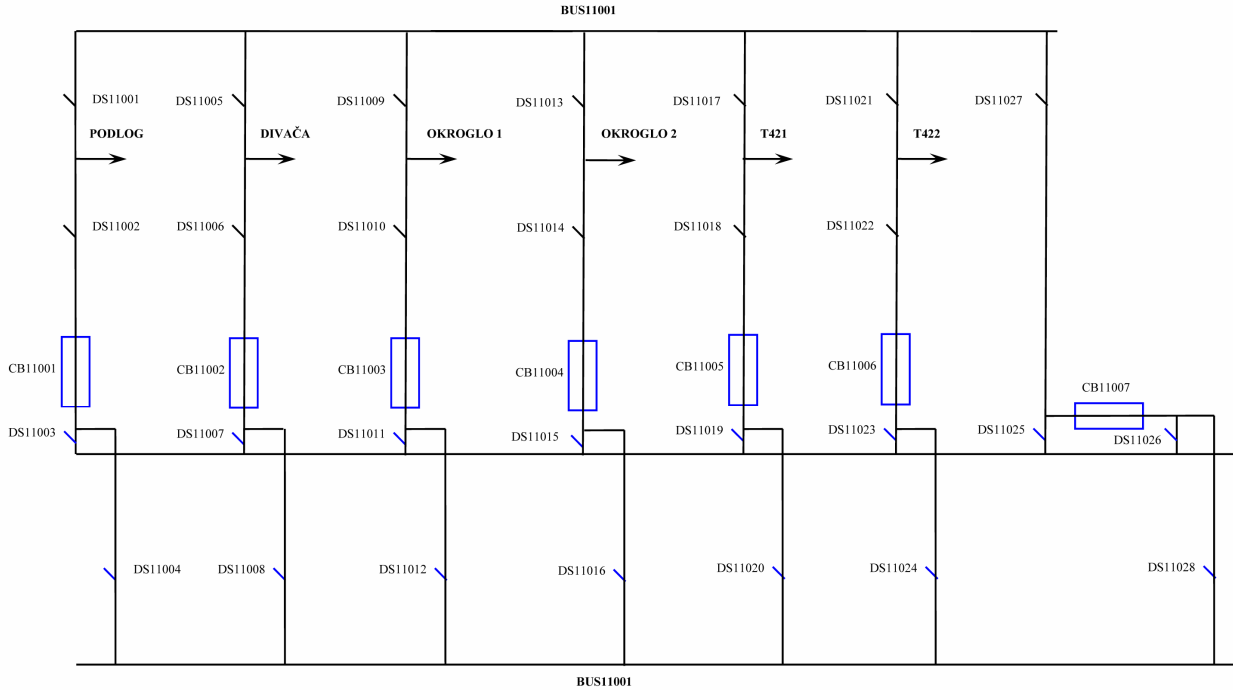


Figure B-22 Configuration of the substation Beričevo

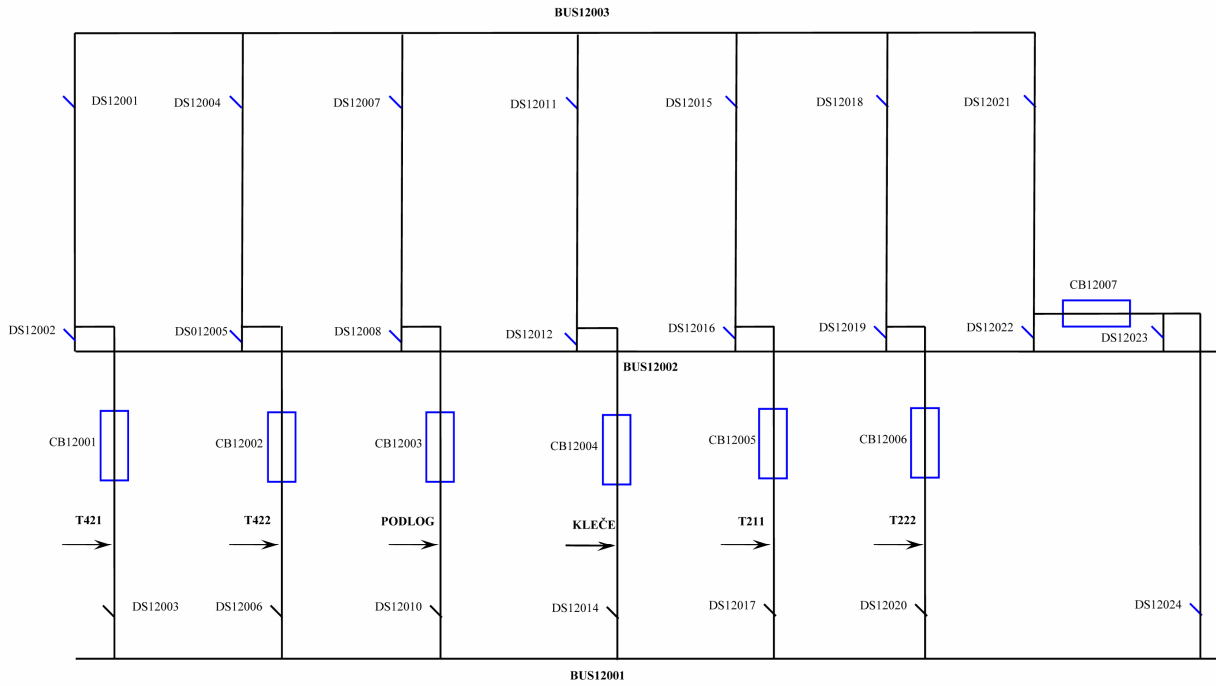


Figure B-23 Configuration of the substation Beričevo 2

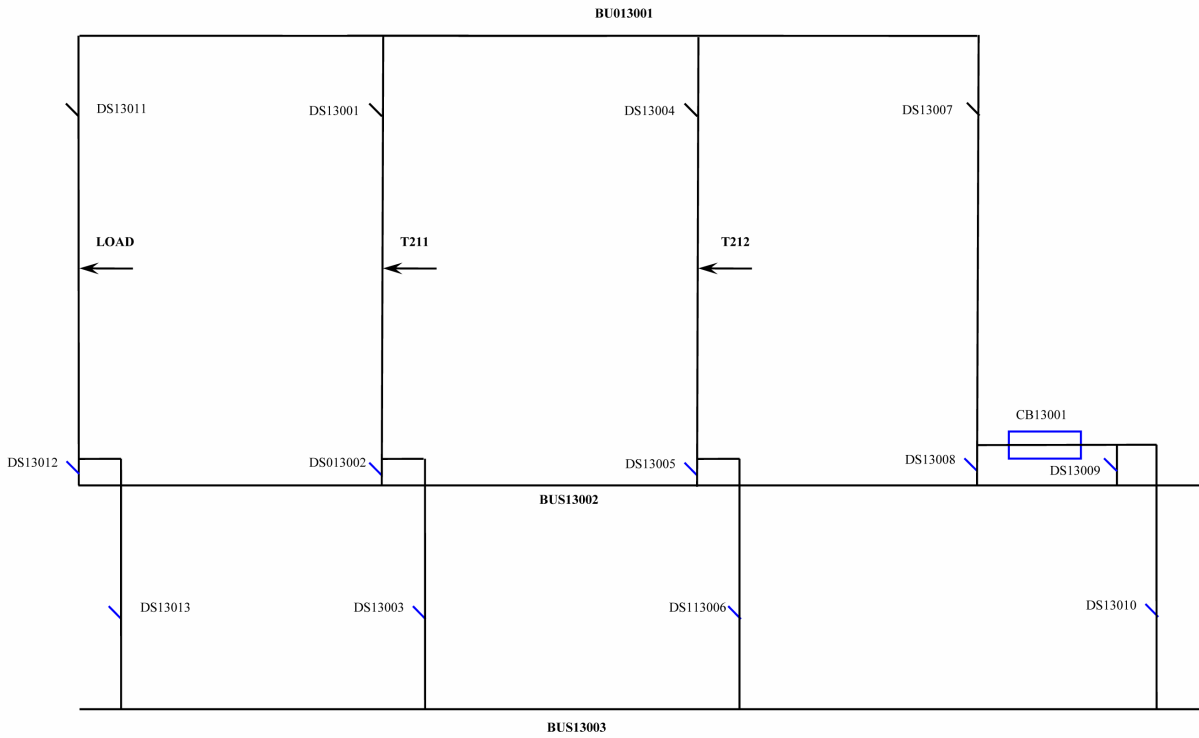


Figure B-24 Configuration of the substation Beričevo 3

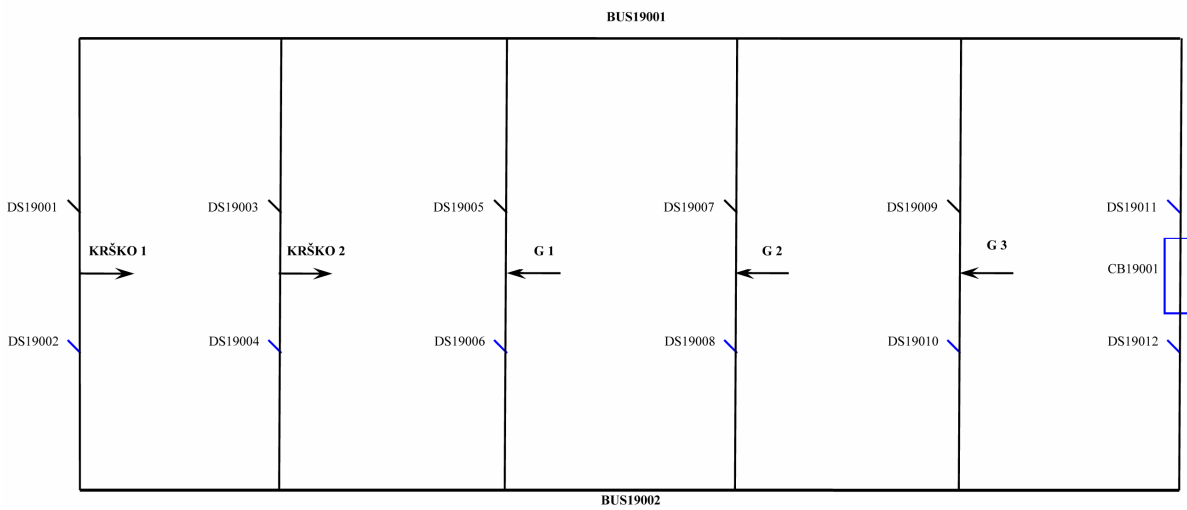


Figure B-25 Configuration of the substation Brestanica

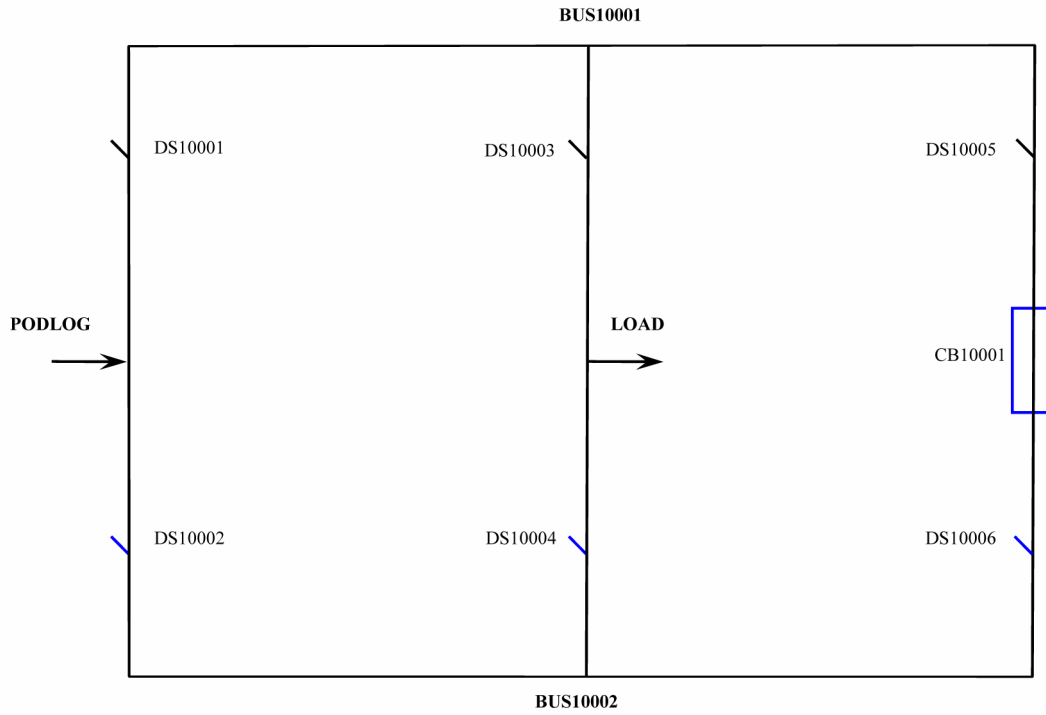


Figure B-26 Configuration of the substation Cirkovce

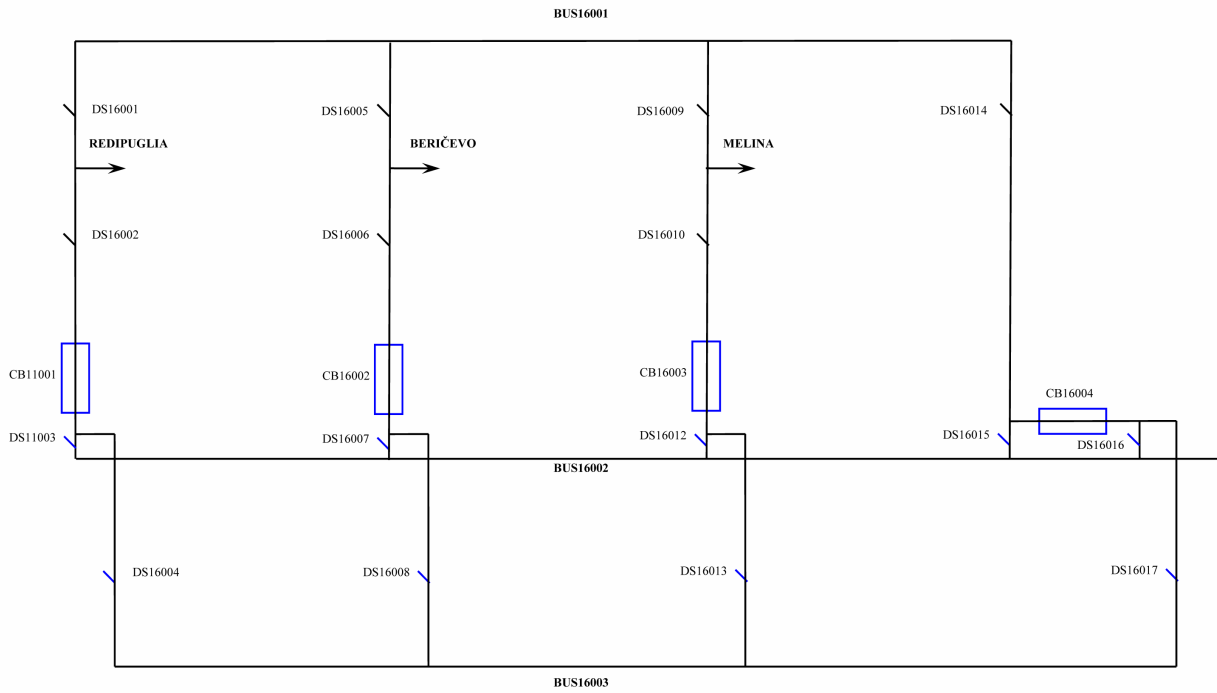


Figure B-27 Configuration of the substation Divača

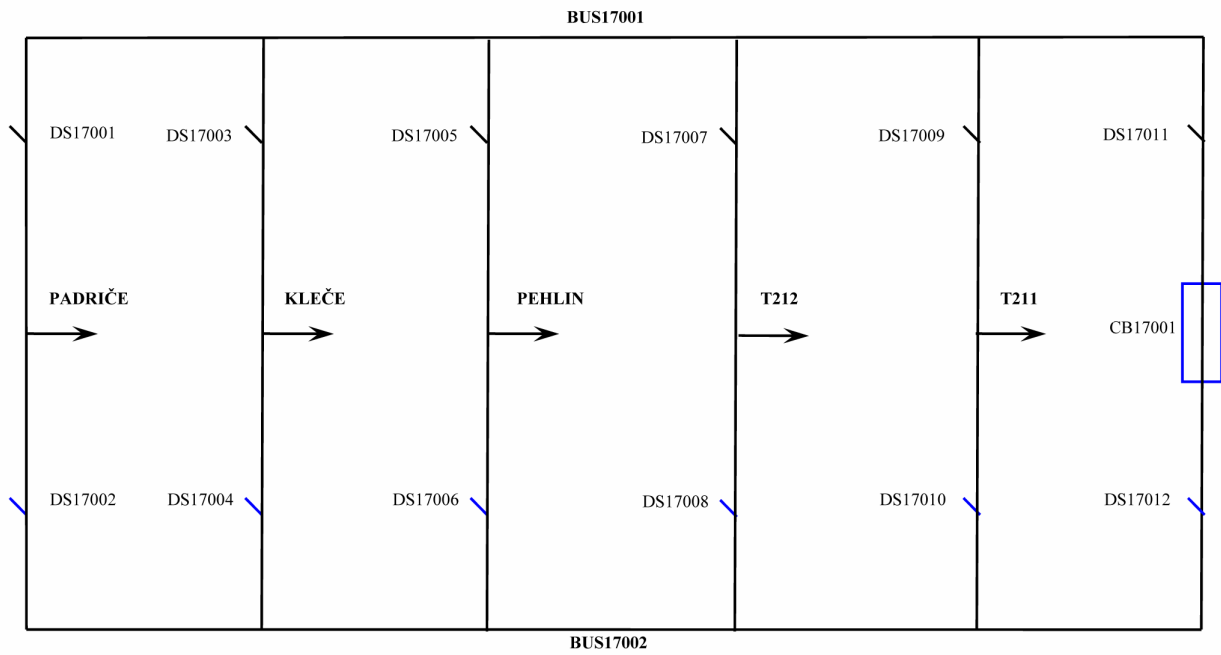


Figure B-28 Configuration of the substation Divača 2

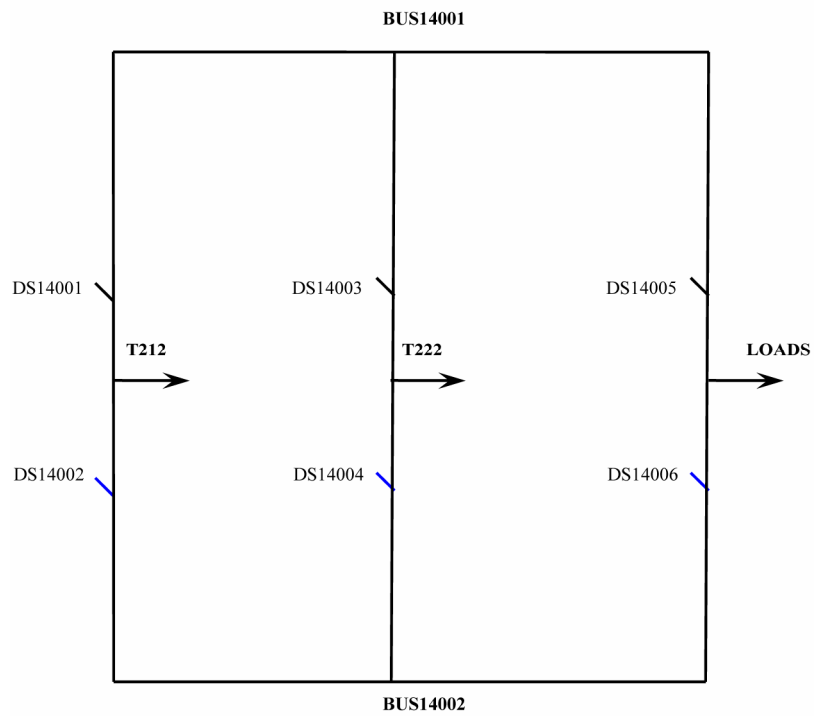


Figure B-29 Configuration of the substation Kleče

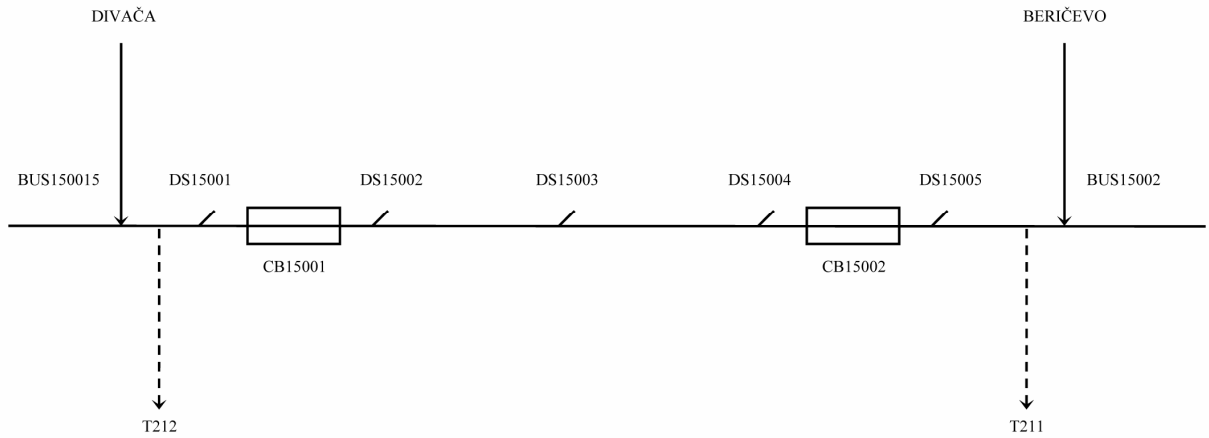


Figure B-30 Configuration of the substation Kleče 2

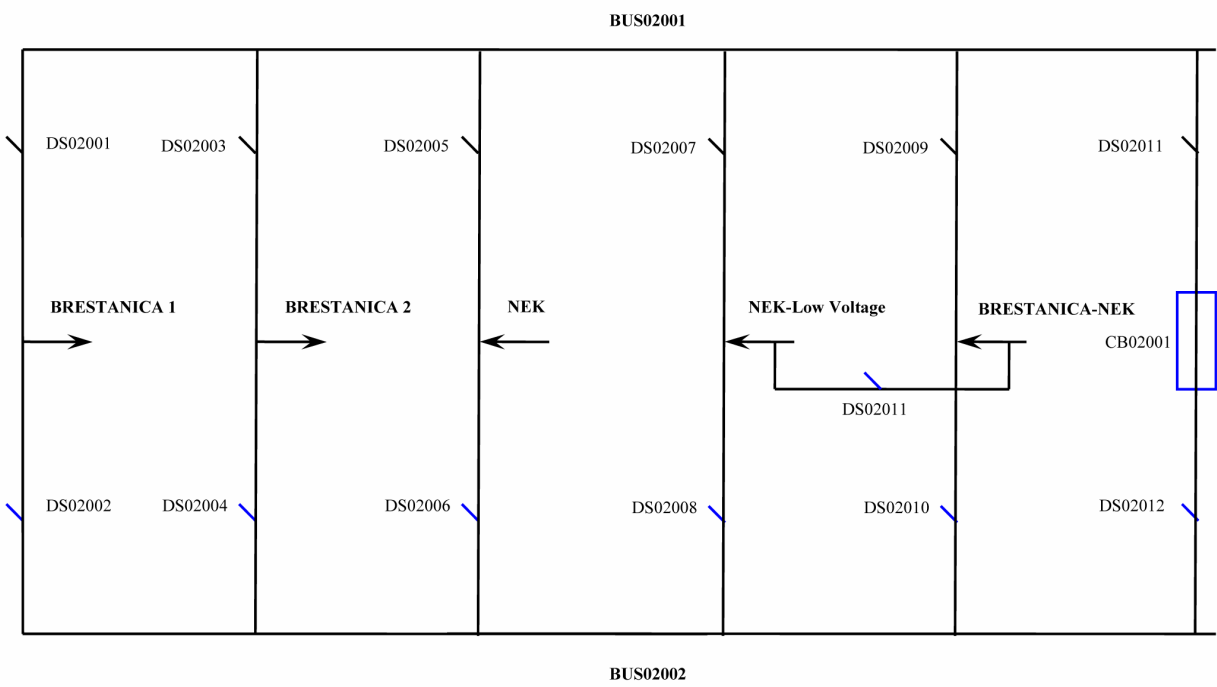


Figure B-31 Configuration of the substation RTP Krško

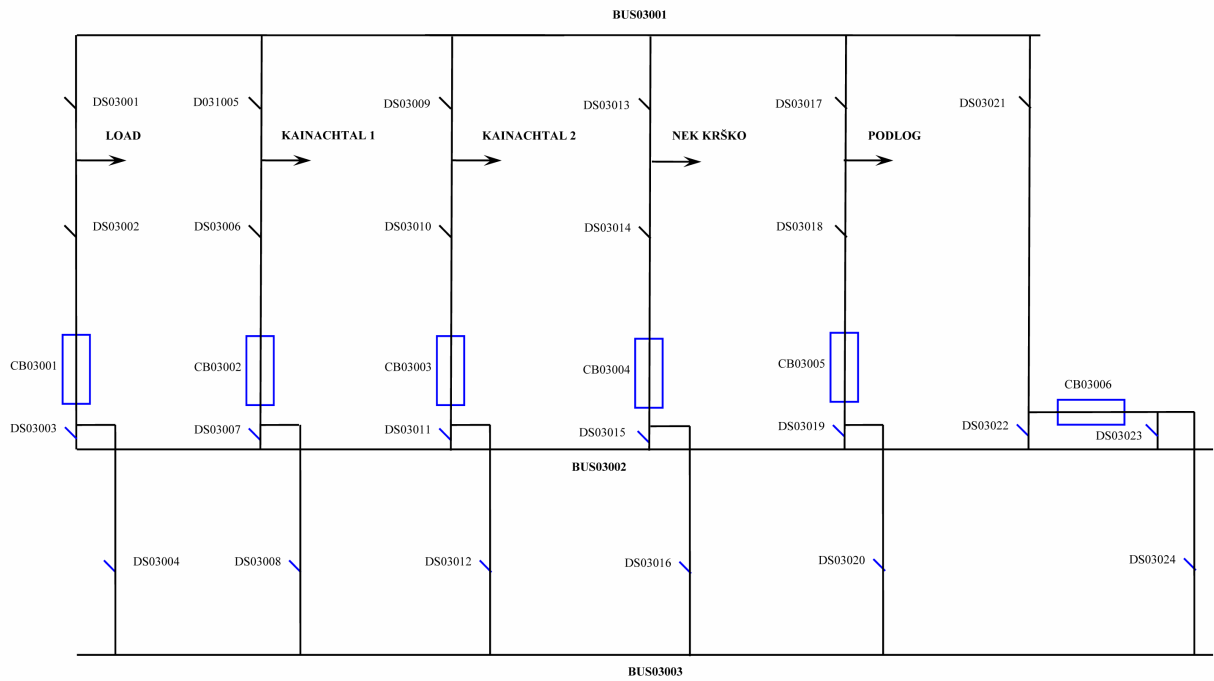


Figure B-32 Configuration of the substation Maribor

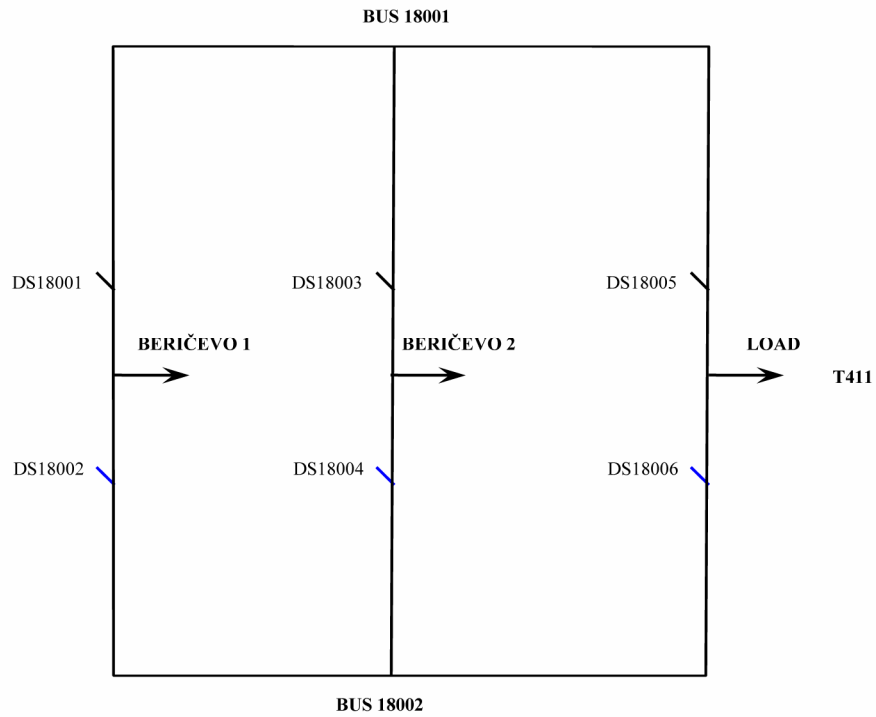


Figure B-33 Configuration of the substation Okroglo

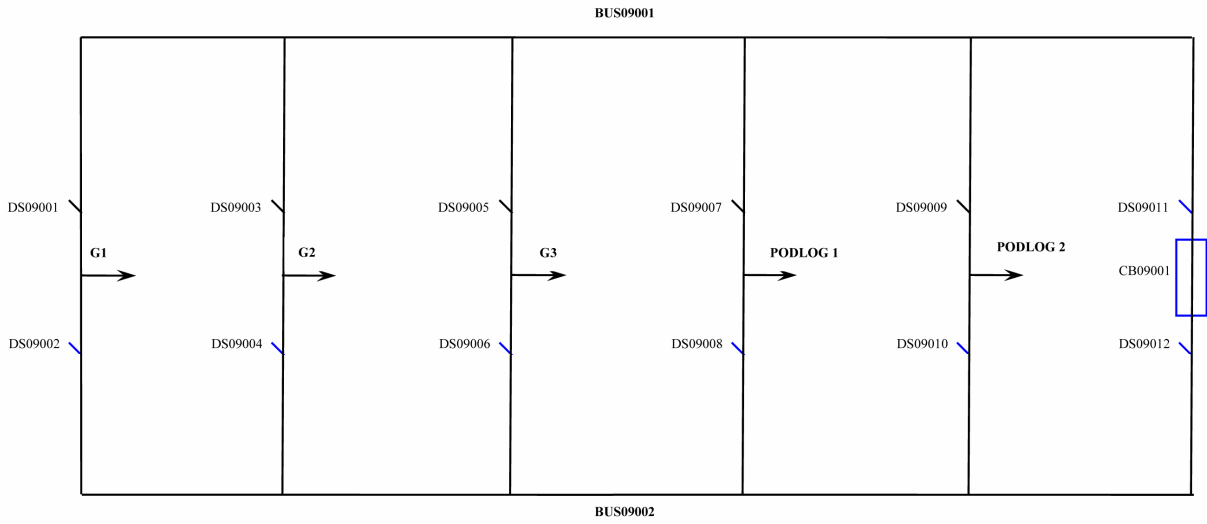


Figure B-34 Configuration of the substation TE Šoštanj

APPENDIX C. VERIFICATION OF THE METHOD AND COMPUTER CODE

The verification of the method and the corresponding computer code FTASYS is done by comparing the obtained results with those obtained from the commercial software for the small example systems. The verification is done in two steps:

- Verification of the fault tree (FT) construction and the identification of the minimal cut sets (MCS).
- Verification of the results obtained for load flow calculations.

The verification of the FT construction and MCS identification is done by comparing the results obtained from FTASYS and those calculated from commercial software for several small example systems. The FT built by the FTASYS is converted to format compatible to commercial software. The inspection of the built FT is done. The next step is identification of the list of MCS with commercial software and comparison with the list of MCS obtained from FTASYS. The results showed that:

1. Program FTASYS builds FT in accordance with the method.
2. Program FTASYS identifies the same MCS as commercial software, verifying the software section responsible for qualitative FT analysis.

The test systems and a part of the obtained results are given in the following sections.

I.1 Verification of FT construction and MCS identification

The configuration of the simplest 3NET.v1 test system, consisting of three substations, each with generator and load, interconnected with three power lines is given on Figure C-35. All energy flow paths are accounted during the construction of the FT for the loads. The FT built for the power delivery to the load in the substation 1 is given on Figure C-36.

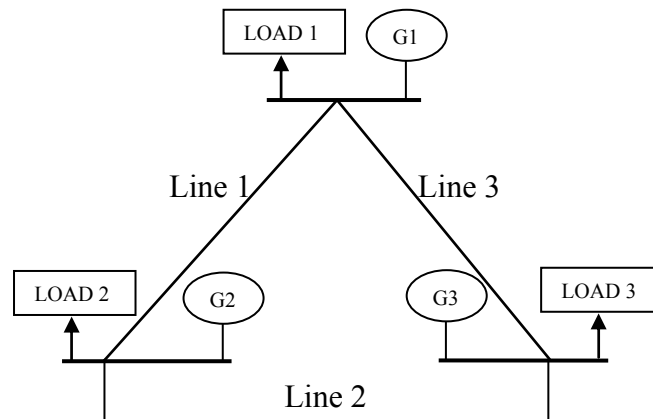


Figure C-35 Test system 3NET.v1

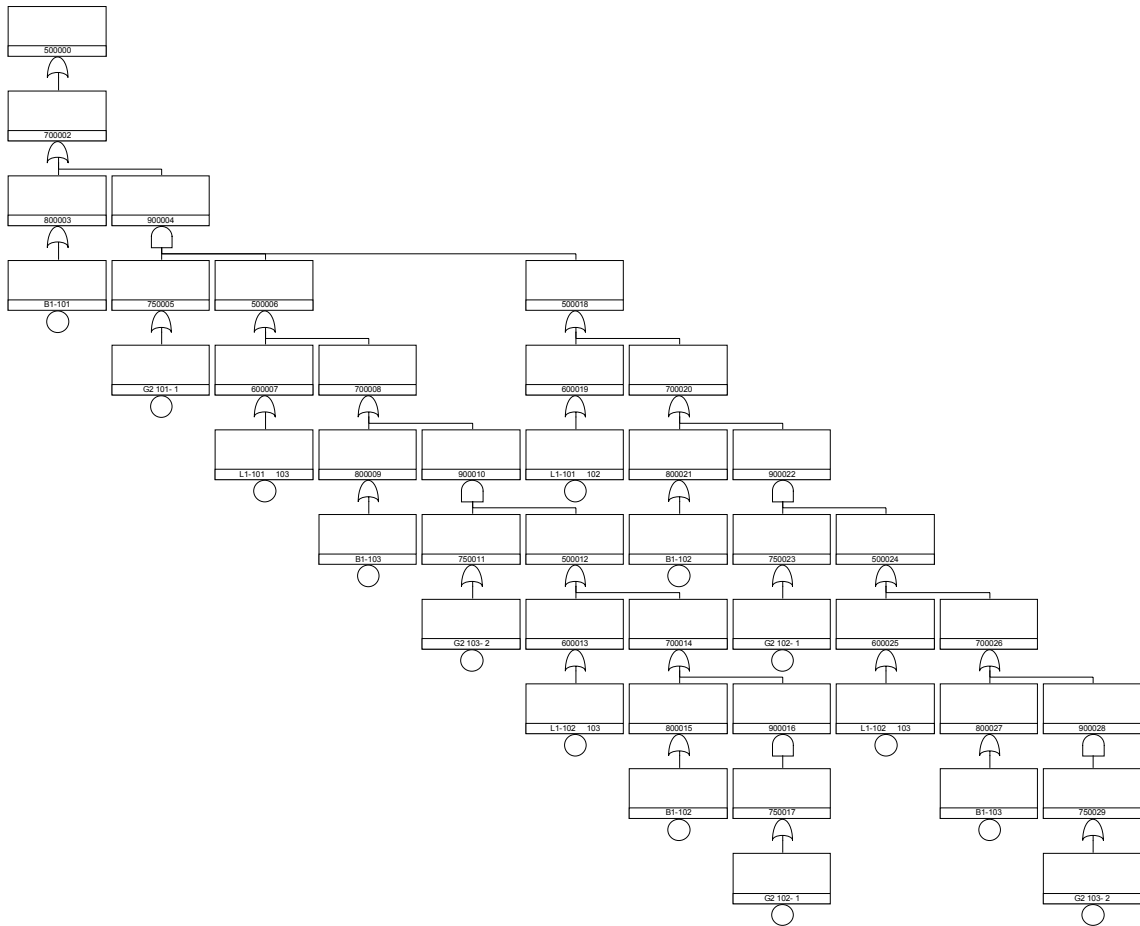


Figure C-36 Fault tree for test system 3NET.v1

The list of the identified MCS for the FT given on the Figure C-36 for the test system 3NET.v1 given on Figure C-35 is shown in Table C-2. The same MCS are identified with FTASYS computer code.

Table C-2 Identified MCS for test system 3NET.v1

MCS No.	Event 1	Event 2	Event 3	Event 4
1	B1-101			
2	G2 101- 1	L1-101 102	L1-101 103	
3	G2 101- 1	G2 102- 1	G2 103- 2	
4	B1-102	G2 101- 1	L1-101 103	
5	B1-103	G2 101- 1	G2 102- 1	
6	B1-103	G2 101- 1	L1-101 102	
7	B1-102	G2 101- 1	G2 103- 2	
8	B1-102	B1-103	G2 101- 1	
9	G2 101- 1	G2 102- 1	L1-101 103	L1-102 103
10	G2 101- 1	G2 103- 2	L1-101 102	L1-102 103

The test system 4NET.v1, which has one additional bus compared to 3NET.v1, is shown on Figure C-37. The FT built for load 1 in the test system 4NET.v1 is shown on Figure C-38. Comparison of the FT for power delivery to the load 1 in test systems 3NET.v1 and 4NET.v1 indicates the increase of the size and the complexity of the built FT resulting from addition of one interconnection and one substation.

MCS No.	Event 1	Event 2	Event 3	Event 4	Event 5
7	B1-103	G2 101- 1	G2 102- 1	L1-101 104	
8	B1-104	G2 101- 1	L1-101 102	L1-101 103	
9	B1-103	G2 101- 1	L1-101 102	L1-101 104	
10	B1-102	G2 101- 1	G2 104- 2	L1-101 103	
11	B1-102	G2 101- 1	G2 103- 2	L1-101 104	
12	B1-103	G2 101- 1	G2 102- 1	G2 104- 2	
13	B1-104	G2 101- 1	G2 102- 1	G2 103- 2	
14	B1-103	G2 101- 1	G2 104- 2	L1-101 102	
15	B1-102	G2 101- 1	G2 103- 2	G2 104- 2	
16	B1-102	B1-103	G2 101- 1	L1-101 104	
17	B1-102	B1-104	G2 101- 1	L1-101 103	
18	B1-103	B1-104	G2 101- 1	G2 102- 1	
19	B1-103	B1-104	G2 101- 1	L1-101 102	
20	B1-102	B1-103	G2 101- 1	G2 104- 2	
21	B1-102	B1-104	G2 101- 1	G2 103- 2	
22	G2 101- 1	G2 102- 1	L1-101 103	L1-101 104	L1-102 103
23	B1-102	B1-103	B1-104	G2 101- 1	
24	G2 101- 1	G2 102- 1	G2 104- 2	L1-101 103	L1-102 103
25	G2 101- 1	G2 103- 2	L1-101 102	L1-101 104	L1-102 103
26	G2 101- 1	G2 103- 2	G2 104- 2	L1-101 102	L1-102 103
27	B1-104	G2 101- 1	G2 102- 1	L1-101 103	L1-102 103
28	B1-104	G2 101- 1	G2 103- 2	L1-101 102	L1-102 103

The test system 4NET.v2, which has similar configuration as 4NET.v1, with changed interconnections to the substation four is shown on Figure C-39. The FT constructed for the load 1 in the 4NET.v2 test system is shown on Figure C-40. The increase of the size of the FT with the increase of the number of the interconnections is demonstrated on Figure C-40.

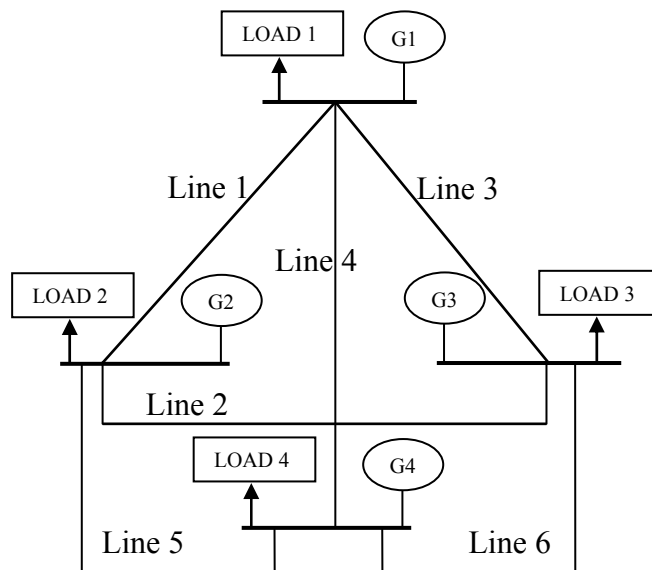


Figure C-39 Test system 4NET.v2

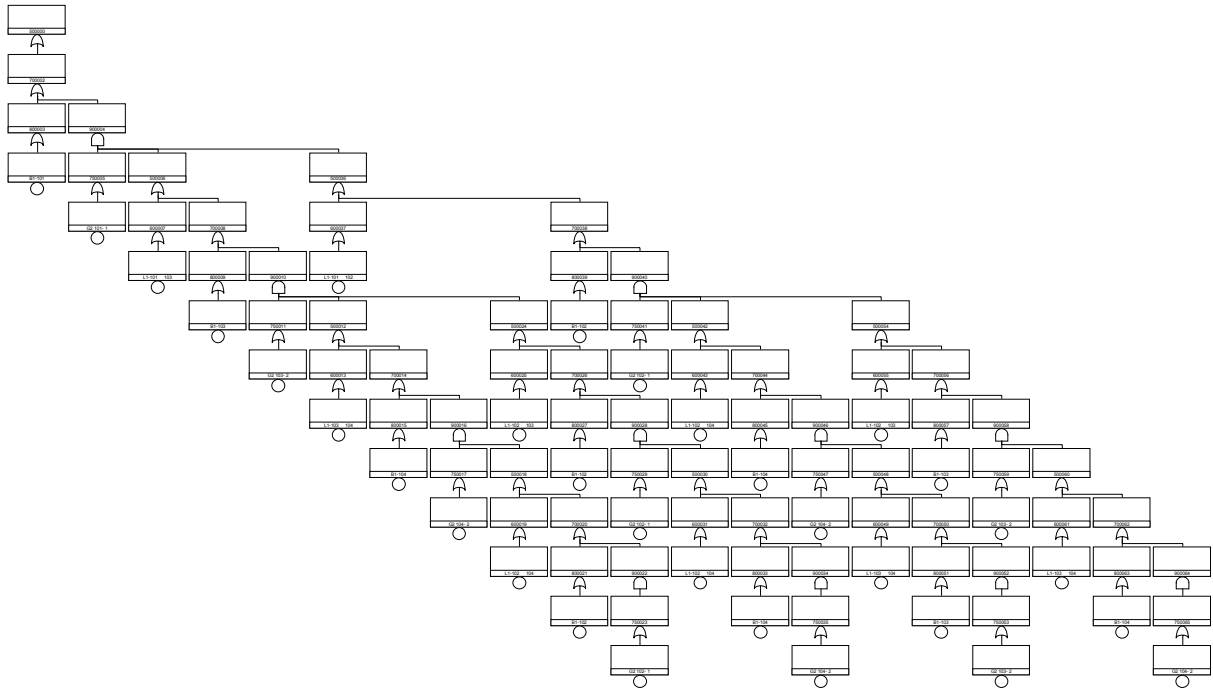


Figure C-40 Fault tree for test system 4NET.v2

The list of MCS for test system 4NET.v2 given on Figure C-39 and FT shown on Figure C-40 is given in Table C-4. The same MCS are identified with FTASYS.

Table C-4 Identified MCS for test system 4NET.v2

MCS No.	Event 1	Event 2	Event 3	Event 4	Event 5	Event 6
1	B1-101					
2	G2 101- 1	L1-101 102	L1-101 103			
3	B1-102	G2 101- 1	L1-101 103			
4	B1-103	G2 101- 1	L1-101 102			
5	B1-102	B1-103	G2 101- 1			
6	G2 101- 1	G2 102- 1	G2 103- 2	G2 104- 2		
7	B1-103	G2 101- 1	G2 102- 1	L1-102 104		
8	B1-102	G2 101- 1	G2 103- 2	L1-103 104		
9	B1-103	G2 101- 1	G2 102- 1	G2 104- 2		
10	B1-104	G2 101- 1	G2 102- 1	G2 103- 2		
11	B1-102	G2 101- 1	G2 103- 2	G2 104- 2		
12	B1-103	B1-104	G2 101- 1	G2 102- 1		
13	B1-102	B1-104	G2 101- 1	G2 103- 2		
14	G2 101- 1	G2 102- 1	L1-101 103	L1-102 103	L1-102 104	
15	G2 101- 1	G2 103- 2	L1-101 102	L1-102 103	L1-103 104	
16	G2 101- 1	G2 102- 1	G2 103- 2	L1-102 104	L1-103 104	
17	B1-104	G2 101- 1	G2 102- 1	L1-101 103	L1-102 103	
18	B1-104	G2 101- 1	G2 103- 2	L1-101 102	L1-102 103	
19	G2 101- 1	G2 102- 1	G2 104- 2	L1-101 103	L1-102 103	L1-103 104
20	G2 101- 1	G2 103- 2	G2 104- 2	L1-101 102	L1-102 103	L1-102 104

The test system 4NET.v3 in which all substations are interconnected is shown on Figure C-41. The constructed FT is omitted from the results for 4NET.v3 due to the reasons of space.

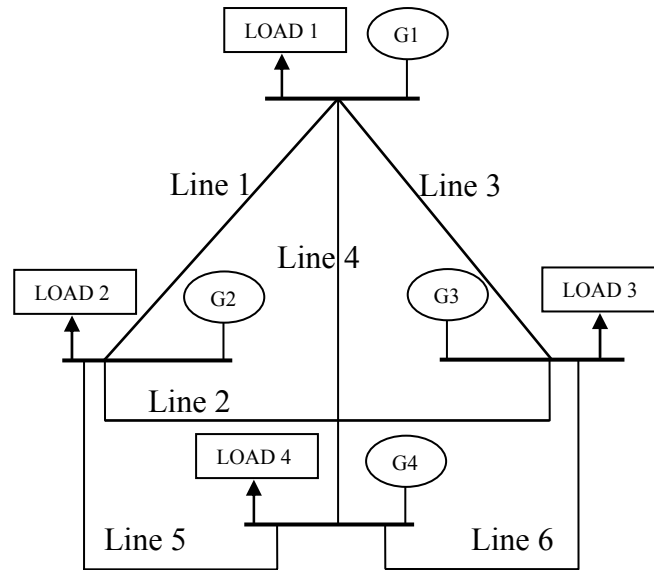


Figure C-41 Test system 4NET.v3

The list of the identified MCS for test system 4NET.v3 is given in Table C-5. The same MCS are identified with FTASYS as those in Table C-5.

Table C-5 Identified MCS for test system 4NET.v3

MCS No.	Event 1	Event 2	Event 3	Event 4	Event 5	Event 6
1	B1-101					
2	G2 101- 1	L1-101 102	L1-101 103	L1-101 104		
3	G2 101- 1	G2 102- 1	G2 103- 2	G2 104- 2		
4	B1-102	G2 101- 1	L1-101 103	L1-101 104		
5	B1-104	G2 101- 1	L1-101 102	L1-101 103		
6	B1-103	G2 101- 1	L1-101 102	L1-101 104		
7	B1-104	G2 101- 1	G2 102- 1	G2 103- 2		
8	B1-103	G2 101- 1	G2 102- 1	G2 104- 2		
9	B1-102	G2 101- 1	G2 103- 2	G2 104- 2		
10	B1-102	B1-103	G2 101- 1	L1-101 104		
11	B1-102	B1-104	G2 101- 1	L1-101 103		
12	B1-103	B1-104	G2 101- 1	G2 102- 1		
13	B1-103	B1-104	G2 101- 1	L1-101 102		
14	B1-102	B1-104	G2 101- 1	G2 103- 2		
15	B1-102	B1-103	G2 101- 1	G2 104- 2		
16	B1-102	B1-103	B1-104	G2 101- 1		
17	B1-104	G2 101- 1	G2 102- 1	L1-101 103	L1-102 103	
18	B1-103	G2 101- 1	G2 102- 1	L1-101 104	L1-102 104	
19	B1-104	G2 101- 1	G2 103- 2	L1-101 102	L1-102 103	
20	B1-102	G2 101- 1	G2 104- 2	L1-101 103	L1-103 104	
21	B1-102	G2 101- 1	G2 103- 2	L1-101 104	L1-103 104	
22	B1-103	G2 101- 1	G2 104- 2	L1-101 102	L1-102 104	
23	G2 101- 1	G2 102- 1	L1-101 103	L1-101 104	L1-102 103	L1-102 104
24	G2 101- 1	G2 102- 1	G2 104- 2	L1-101 103	L1-102 103	L1-103 104
25	G2 101- 1	G2 103- 2	L1-101 102	L1-101 104	L1-102 103	L1-103 104
26	G2 101- 1	G2 102- 1	G2 103- 2	L1-101 104	L1-102 104	L1-103 104

MCS No.	Event 1	Event 2	Event 3	Event 4	Event 5	Event 6
27	G2 101- 1	G2 103- 2	G2 104- 2	L1-101 102	L1-102 103	L1-102 104
28	G2 101- 1	G2 104- 2	L1-101 102	L1-101 103	L1-102 104	L1-103 104

The test system 5NET.v1, which has one additional substation connected through one line compared to the test system 4NET.v3, is given on Figure C-42.

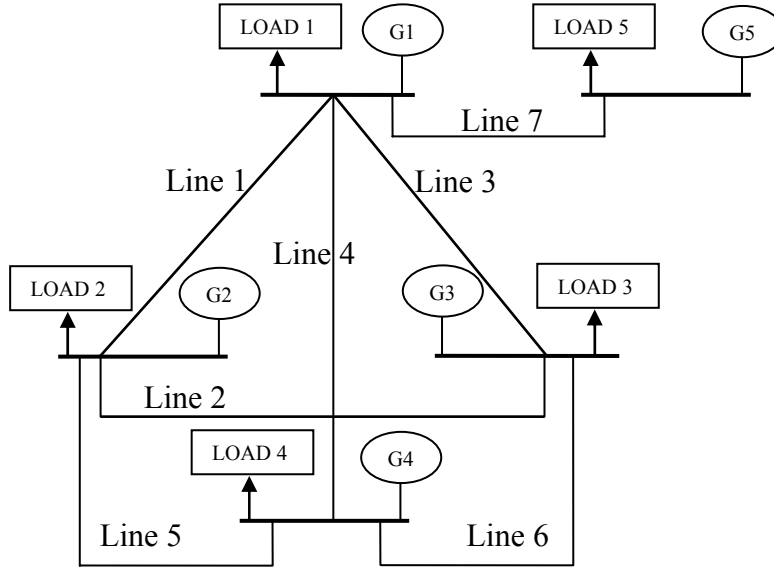


Figure C-42 Test system 5NET.v1

The first 20 identified MCS from total 82 for test system 5NET.v1 are given in Table C-6. The same MCS are identified with FTASYS.

Table C-6 First 20 identified MCS from total 82 for test system 5NET.v1

MCS No.	Event 1	Event 2	Event 3	Event 4	Event 5
1	B1-101				
2	G2 101- 1	L1-101 102	L1-101 103	L1-101 104	L1-101 105
3	G2 101- 1	G2 105- 2	L1-101 102	L1-101 103	L1-101 104
4	G2 101- 1	G2 102- 1	G2 103- 2	G2 104- 2	L1-101 105
5	G2 101- 1	G2 102- 1	G2 103- 2	G2 104- 2	G2 105- 2
6	B1-102	G2 101- 1	L1-101 103	L1-101 104	L1-101 105
7	B1-105	G2 101- 1	L1-101 102	L1-101 103	L1-101 104
8	B1-104	G2 101- 1	L1-101 102	L1-101 103	L1-101 105
9	B1-103	G2 101- 1	L1-101 102	L1-101 104	L1-101 105
10	B1-102	G2 101- 1	G2 105- 2	L1-101 103	L1-101 104
11	B1-103	G2 101- 1	G2 102- 1	G2 104- 2	L1-101 105
12	B1-104	G2 101- 1	G2 102- 1	G2 103- 2	L1-101 105
13	B1-103	G2 101- 1	G2 105- 2	L1-101 102	L1-101 104
14	B1-104	G2 101- 1	G2 105- 2	L1-101 102	L1-101 103
15	B1-102	G2 101- 1	G2 103- 2	G2 104- 2	L1-101 105
16	B1-104	G2 101- 1	G2 102- 1	G2 103- 2	G2 105- 2
17	B1-105	G2 101- 1	G2 102- 1	G2 103- 2	G2 104- 2
18	B1-103	G2 101- 1	G2 102- 1	G2 104- 2	G2 105- 2
19	B1-102	G2 101- 1	G2 103- 2	G2 104- 2	G2 105- 2
20	B1-102	B1-104	G2 101- 1	L1-101 103	L1-101 105

The two additional versions of the 5NET test system used during the verification are given on Figure C-43 and Figure C-44. The difference between the 5NET.v1 and 5NET.v2 and 5NET.v3 are the additional interconnections to newly added substation. The eight bus system which is the last test system for which inspection of the built FT is done, is shown on Figure C-45. Program FTASYS passed all tests for FT construction verifying the obtained results.

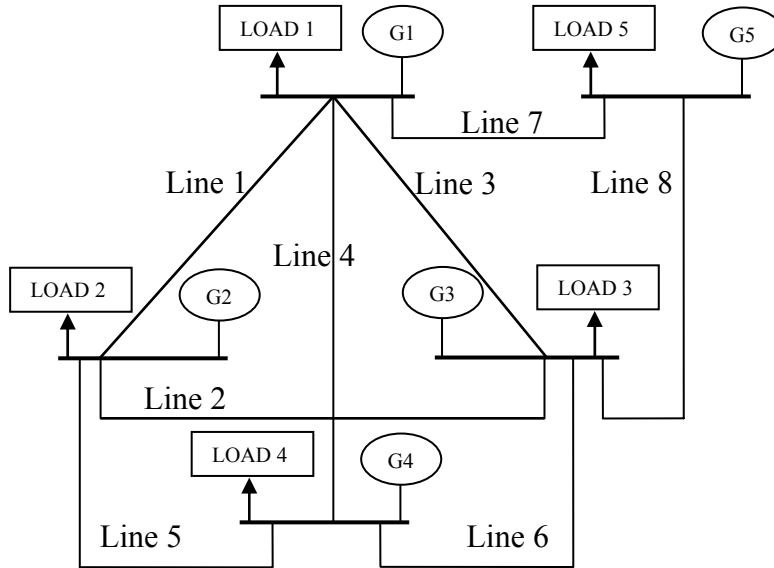


Figure C-43 Test system 5NET.v2

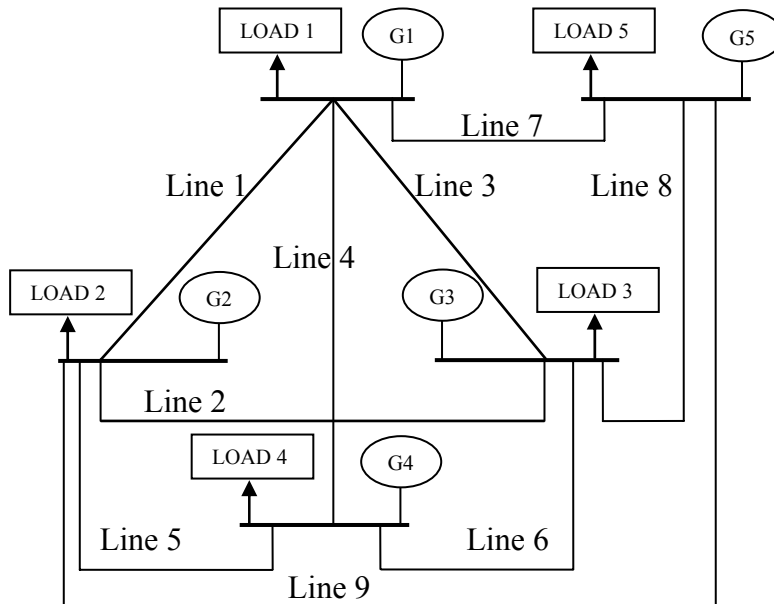


Figure C-44 Test system 5NET.v3

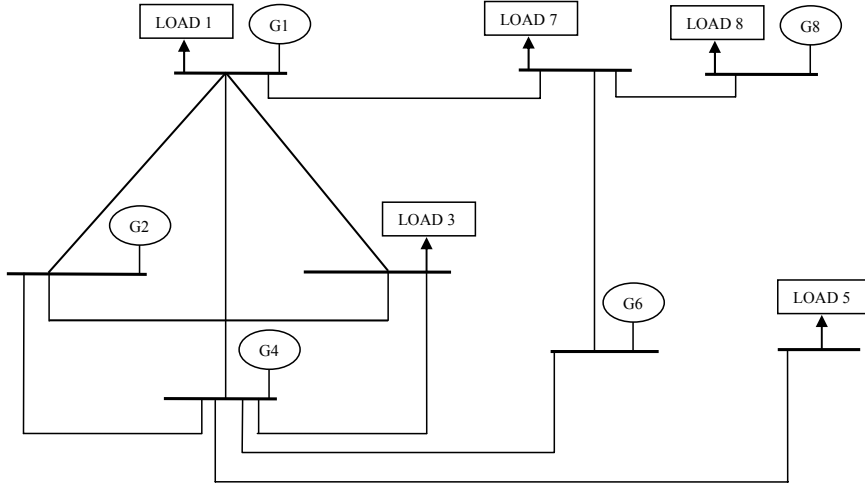


Figure C-45 Test system 8NET.v1

The IEEE RTS is used for the final examination of the FTASYS and the module for MCS identification. The commercial software calculated about 200000 MCS before demodularization for the house load of the NPP situated in the substation 18 of the IEEE RTS. In the final results only 121 MCS are identified. In the FTASYS the 4087 MCS are identified for the house load of the NPP in the substation 18. The truncation limits used during the analysis with the commercial software were maximum 5 BE in MCS and probability less than $Q_{MCS} < 10^{-12}$. The change of the truncation limits in the commercial software didn't result with the increase of the number of the identified MCS. In the developed computer code default truncation limits used in the analysis are maximum 7 BE in MCS and probability less than $Q_{MCS} < 10^{-14}$. These truncation limits were changed for the specified loads. The comparison of the MCS verified the MCS identification module in the developed computer code.

I.2 Verification of the DC Flow calculations

Verification of the results obtained for approximate DC load flow calculations is performed using MATPOWER, a MATLABTM Power Simulation Package. The MATPOWER Version 3.0.0 freely available together with MATLABTM Version 6.5.0 Release 13, commercial software from the MathWorks, Inc is used in the analysis.

The analysis of errors of the approximate DC model is done with load flows through line.

Error is defined as:

$$G_p \% = \frac{G_{p1}(\%) + G_{p2}(\%)}{2} \quad \text{C-(1)}$$

Where:

G_{p1} -Error of calculated power flows on start of the line.

G_{p2} -Error of calculated power flows on the end of the line.

$$G_{p1}(\%) = \frac{Pl_{DC1} - Pl_{AC1}}{Pl_{AC1}} 100 \quad \text{C-(2)}$$

$$G_{p2}(\%) = \frac{Pl_{DC2} - Pl_{AC2}}{Pl_{AC2}} 100 \quad \text{C-(3)}$$

The errors of the reactive power flows are calculated with the same approach.

The errors of the calculated voltages are calculated using the relation:

$$G_u(\%) = \frac{U_{DC} - U_{AC}}{U_n} 100 = U_{DC}(\%) - U_{AC}(\%) \quad \text{C-(4)}$$

The power flows and voltages are calculated and compared for IEEE test system for normal regime (no failed lines) using two of five MATPOWER power flow solvers. The runpf is the default power flow solver based on a standard Newton's method using a full Jacobean. The second method is a DC power flow, which is obtained by executing rundcpf solver. The calculated difference G_u , using Equation C-(4), between voltages calculated in MATPOWER using runpf and voltages obtained from FTASYS is given in Table C-7. The obtained results verify the module used for voltage calculation in the FTASYS.

Table C-7 Difference between calculated voltages

Bus No.	Matpower Voltage(p.u)	FTASYS Voltage(p.u)	Diference G_u(%)
101	1.04	1.07	3.89
102	1.04	1.08	4.04
103	0.99	0.99	0.85
104	1.00	1.02	2.32
105	1.03	1.06	2.77
106	1.09	1.10	1.43
107	1.03	1.05	2.86
108	1.00	1.02	2.13
109	1.01	1.01	0.95
110	1.05	1.07	1.63
111	1.00	1.03	3.13
112	1.01	1.04	3.01
113	1.02	1.05	2.91
114	0.98	1.01	2.96
115	1.01	1.01	-0.01
116	1.02	1.02	0.65
117	1.04	1.04	0.33
118	1.05	1.05	0.22
119	1.02	1.03	1.13
120	1.04	1.05	1.63
121	1.05	1.05	0.13
122	1.05	1.05	0.09
123	1.05	1.07	1.87
124	0.98	0.99	0.74

The calculated power flows from MATPOWER are given in Table C-8. The DC power flow solver included in the MATPOWER provides only active power flows in the system, and it doesn't account transformers off-nominal ratio. The power flows at line start (calculated by runpf), power flows at the line end (calculated by runpf) and flows calculated using rundcpf are given in Table C-8. The power flows obtained from the FTASYS are given in Table C-9. Evaluation of the results for the calculated power flows is done using Eqs. C-(1), C-(2), C-(3) and the obtained results are given in Table C-10. The $G_pRDC(\%)$ is relative error of results obtained from rundcpf and runpf (exact AC model), both from MatPower. The $G_pPDC(\%)$ and $G_qPDC(\%)$ are relative errors of active and reactive power flows calculated from FTASYS and runpf. The G_qPDCS and G_qPDCE are the absolute errors of reactive power flows, given in MVar, at the start(G_qPDCS) and at the end of the line(G_qPDCE) calculated from FTASYS and runpf. The results show that for the active power flows, results from FTASYS have small difference compared to results from the exact AC model. The value of relative error is decreasing with the increase of the line power flow. The results obtained from

FTASYS are equal or better from those obtained from rundcpf. There is an error for reactive power flows $G_{qPDC}(\%)$, especially for lines which have smaller flows of reactive power, marked with “*” in Table C-10. This result is expected accounting the approximations in the methodology. The absolute errors are small (important for overload lines identification), and calculated voltages (important for the identification of the violated bus voltages) are comparable to those obtained from the exact AC model, shown in Table C-7.

Table C-8 Calculated power flows using runpf and rundcpf

Bus no.	Start	End	P(MW)	Q(MVAr)	P(MW)	Q(MVAr)	P(MW) rundcpf
1	101	102	14.1	-27.7	-14.1	-21.7	14.5
2	101	103	-10.4	24.5	10.9	-28.6	-15.3
3	101	105	60.3	-10.6	-59.5	11.1	64.8
4	102	104	40.0	17.2	-39.4	-18.4	37.9
5	102	106	49.2	-39.4	-47.4	40.3	51.6
6	103	109	30.6	-25.2	-30.2	23.8	37.7
7	103	124	-221.5	16.7	222.6	27.3	-233.0
8	104	109	-34.7	3.4	35.0	-4.9	-36.1
9	105	110	-11.5	-25.1	11.6	23.1	-6.2
10	106	110	-88.6	-67.1	90.2	-207.0	-84.4
11	107	108	115.0	16.2	-112.9	-10.1	115.0
12	108	109	-35.8	4.7	36.3	-7.0	-39.2
13	108	110	-22.3	-29.6	22.8	26.9	-16.8
14	109	111	-94.4	-18.3	94.6	26.5	-93.9
15	109	112	-121.7	-29.6	122.1	43.4	-118.7
16	110	111	-145.1	63.9	145.6	-44.4	-138.7
17	110	112	-174.6	53.1	175.2	-27.1	-163.8
18	111	113	-105.2	-37.8	105.9	33.5	-83.2
19	111	114	-135.0	55.7	136.1	-55.0	-149.4
20	112	113	-56.7	-20.3	56.9	11.7	-38.5
21	112	123	-240.5	4.0	247.4	29.8	-243.9
22	113	123	-239.9	9.8	246.0	19.2	-250.7
23	114	116	-330.1	-4.9	335.8	63.6	-343.4
24	115	116	103.7	-31.0	-103.5	29.2	105.8
25	115	121	-216.0	-43.0	218.8	55.0	-220.4
26	115	121	-216.0	-43.0	218.8	55.0	-220.4
27	115	124	226.2	43.6	-222.6	-27.3	233.0
28	116	117	-320.9	-36.2	323.9	56.5	-326.3
29	116	119	143.6	-45.2	-143.0	45.1	143.6
30	117	118	-185.3	-61.0	186.0	62.6	-184.6
31	117	122	-138.7	4.5	141.2	-9.6	-141.7
32	118	121	-59.5	4.3	59.6	-9.5	-58.8
33	118	121	-59.5	4.3	59.6	-9.5	-58.8
34	119	120	-19.0	-41.1	19.1	32.9	-18.7
35	119	120	-19.0	-41.1	19.1	32.9	-18.7
36	120	123	-83.1	-45.9	83.3	42.7	-82.7
37	120	123	-83.1	-45.9	83.3	42.7	-82.7

Table C-9 Calculated power flows in FTASYS

Bus no.	Start	End	P (MW)	Q(MVAr)	P (MW)	Q(MVAr)
1	101	102	14.5	-40.0	-14.5	-13.2
2	101	103	-15.3	40.8	15.3	-43.4
3	101	105	64.8	1.2	-64.8	0.3
4	102	104	37.9	31.3	-37.9	-31.0
5	102	106	51.6	-28.4	-51.6	28.4
6	103	109	37.7	-27.3	-37.7	26.1
7	103	124	-236.5	35.4	236.5	10.6
8	104	109	-36.1	16.9	36.1	-18.4
9	105	110	-6.2	-13.4	6.2	10.9
10	106	110	-84.4	-73.0	84.4	-210.1
11	107	108	115.0	26.5	-115.0	-18.2
12	108	109	-39.2	12.9	39.2	-15.0
13	108	110	-16.8	-27.2	16.8	24.3
14	109	111	-96.7	-10.4	96.7	18.8
15	109	112	-122.2	-20.1	122.2	34.0
16	110	111	-140.7	66.3	140.7	-45.9
17	110	112	-166.2	57.2	166.2	-30.3
18	111	113	-83.2	-36.4	83.2	30.0
19	111	114	-149.4	63.9	149.4	-62.5
20	112	113	-38.5	-21.4	38.5	11.5
21	112	123	-243.9	21.9	243.9	19.8
22	113	123	-250.7	31.6	250.7	9.0
23	114	116	-343.4	38.0	343.4	25.3
24	115	116	105.7	-69.3	-105.7	68.0
25	115	121	-220.4	-40.6	220.4	57.6
26	115	121	-220.4	-40.6	220.4	57.6
27	115	124	233.0	28.6	-233.0	-10.2
28	116	117	-326.3	-18.2	326.3	42.8
29	116	119	143.6	-68.0	-143.6	68.4
30	117	118	-184.6	-51.2	184.6	53.9
31	117	122	-141.7	10.2	141.7	-11.4
32	118	121	-58.8	8.9	58.8	-14.0
33	118	121	-58.8	8.9	58.8	-14.0
34	119	120	-18.7	-53.0	18.7	45.1
35	119	120	-18.7	-53.0	18.7	45.1
36	120	123	-82.7	-58.3	82.7	55.7
37	120	123	-82.7	-58.3	82.7	55.7

The values of reactive power flows calculated in the FTASYS are larger than actual verifying that obtained results are conservative. The obtained results verified the used algorithm and computer code.

Table C-10 Calculated errors of power flows (%)

Bus No.	Start	End	G_pRDC(%)	G_pPDC(%)	G_qPDC(%)	G_qPDCS MVar	G_qPDCE MVar
1	101	102	2.5	2.5	2.7	12.29	-8.45
2	101	103	46.3	43.5	59.4	-16.34	14.83
3	101	105	7.4	8.2	-104.3*	-11.82	10.82
4	102	104	-5.1	-4.4	75.4	-14.12	12.62
5	102	106	4.9	6.8	-28.7	-10.97	11.86
6	103	109	23.0	24.0	9.1	2.15	-2.29
7	103	124	5.2	6.5	25.3	-18.68	16.69
8	104	109	4.2	3.7	337.0*	-13.52	13.48
9	105	110	-45.8	-46.3	-49.7	-11.72	12.19
10	106	110	-4.7	-5.6	5.2	5.92	3.13
11	107	108	0.0	0.9	72.3	-10.32	8.13
12	108	109	9.6	8.8	145.9*	-8.24	8.02
13	108	110	-24.7	-25.6	-8.9	-2.38	2.60
14	109	111	-0.5	2.3	-36.1	-7.93	7.69
15	109	112	-2.5	0.3	-26.9	-9.48	9.43
16	110	111	-4.4	-3.2	3.6	-2.37	1.55
17	110	112	-6.2	-5.0	9.7	-4.14	3.17
18	111	113	-20.9	-21.2	-7.1	-1.41	3.50
19	111	114	10.7	10.2	14.2	-8.24	7.47
20	112	113	-32.1	-32.3	1.9	1.07	0.16
21	112	123	1.4	0.0	205.0*	-17.87	9.95
22	113	123	4.5	3.2	85.4	-21.84	10.15
23	114	116	4.0	3.1	-471.1*	-42.86	38.34
24	115	116	1.9	2.0	128.2*	38.30	-38.79
25	115	121	2.0	1.4	-0.5	-2.44	-2.62
26	115	121	2.0	1.4	-0.5	-2.44	-2.62
27	115	124	3.0	3.8	-48.5	14.96	-17.09
28	116	117	1.7	1.2	-37.0	-17.96	13.72
29	116	119	0.0	0.2	51.0	22.78	-23.29
30	117	118	-0.4	-0.5	-15.0	-9.79	8.73
31	117	122	2.2	1.3	73.7	-5.73	1.84
32	118	121	-1.2	-1.2	78.3	-4.64	4.52
33	118	121	-1.2	-1.2	78.3	-4.64	4.52
34	119	120	-1.7	-1.9	33.1	11.94	-12.21
35	119	120	-1.7	-1.9	33.1	11.94	-12.21
36	120	123	-0.5	-0.6	28.8	12.41	-13.03
37	120	123	-0.5	-0.6	28.8	12.41	-13.03

APPENDIX D. RELIABILITY PARAMETERS

The basic event is an event which is not further developed in the fault tree. Each basic event is linked to its probabilistic model in order to quantify the probability of the event. The probability of the basic event corresponding to the failure probability of the modelled component or system is calculated using one of the parametric reliability models. The selection of a specified model is based on the available data and characteristics of the modelled components.

The unavailability of the components is calculated as mean^a (long-term) unavailability:

$$Q_{mean} = \frac{\lambda}{\lambda + \mu} \quad D-(5)$$

The following relations can be written for failure and repair rate:

$$\lambda = \frac{1}{MTTF} \quad D-(6)$$

$$\mu = \frac{1}{MTTR} \quad D-(7)$$

λ - Failure rate of the component.

μ - Repair rate of the component.

MTTF- Mean time to failure. The mean time expected until the first failure.

MTTR- Mean time to recovery. The average time that a device will take to recover from a non-terminal failure.

Table D-11 Reliability parameters of the components used in the analysis

Component type	MTTF (Yr)	MTTR (Yr)	$\lambda(1/yr)$	$\mu(yr)$	Q_{mean}
Generator P=12MW	3.36E-01	6.85E-03	2.98E+00	1.46E+02	2.00E-02
Generator P=20MW	5.14E-02	5.71E-03	1.95E+01	1.75E+02	1.00E-01
Generator P=50MW	2.26E-01	2.28E-03	4.42E+00	4.38E+02	1.00E-02
Generator P=76MW	2.24E-01	4.57E-03	4.47E+00	2.19E+02	2.00E-02
Generator P=100MW	1.37E-01	5.71E-03	7.30E+00	1.75E+02	4.00E-02
Generator P=155MW	1.10E-01	4.57E-03	9.13E+00	2.19E+02	4.00E-02
Generator P=197MW	1.08E-01	5.71E-03	9.22E+00	1.75E+02	5.00E-02
Generator P=350MW	1.31E-01	1.14E-02	7.62E+00	8.76E+01	8.00E-02
Generator P=400MW	1.26E-01	1.71E-02	7.96E+00	5.84E+01	1.20E-01
Transformer V>550kV					2.48E-02
Transformer 243-346kV					1.70E-02
Transformer 146-242kV					1.61E-02
Transformer 73-145kV					1.24E-02
Bus 138kV			1.13E-02	2.09E+02	5.44E-05
Bus 230kV			9.03E-03	2.04E+02	4.43E-05
Circuit breaker Active			6.60E-03	8.11E+01	8.14E-05
Circuit breaker Passive			5.00E-04	8.11E+01	6.16E-06
Disconnect switch Active					8.14E-05
Disconnect switch Passive					6.16E-06

^a Risk Spectrum Theory Manual, Relcon AB, 1998

The mean (long-term) reliability model of monitored repairable component is selected for elements of the power system because only MTTF and MTTR were available as input data and because this model quickly approach asymptotic value given by Eq. D-(5).

The input data and obtained unavailability used in the analysis is given in Table D-11.

The input data and calculated unavailability of the lines and transformers of the IEEE RTS is given in Table D-12. The unavailability Q_{CCF} resulting from the CCF of the interconnections is calculated as product of the Q_{mean} of the other interconnection multiplied by the length (percentage of whole line length) of the interconnection exposed to the CCF.

Table D-12 Line data for IEEE RTS

Line No.	From bus	To bus	$\lambda(1/yr)$	$\mu(yr)$	Q_{mean}	Q_{CCF}
1	1	2	0.24	547.5	4.38E-04	
2	1	3	0.51	876	5.82E-04	
3	1	5	0.33	876	3.77E-04	
4	2	4	0.39	876	4.45E-04	
5	2	6	0.48	876	5.48E-04	
6	3	9	0.38	876	4.34E-04	
7	3	24	0.02	11.40625	1.75E-03	
8	4	9	0.36	876	4.11E-04	
9	5	10	0.34	876	3.88E-04	
10	6	10	0.33	250.2857	1.32E-03	
11	7	8	0.3	876	3.42E-04	
12	8	9	0.44	876	5.02E-04	5.02E-04
13	8	10	0.44	876	5.02E-04	5.02E-04
14	9	11	0.02	11.40625	1.75E-03	
15	9	12	0.02	11.40625	1.75E-03	
16	10	11	0.02	11.40625	1.75E-03	
17	10	12	0.02	11.40625	1.75E-03	
18	11	13	0.4	796.3636	5.02E-04	5.02E-04
19	11	14	0.39	796.3636	4.89E-04	
20	12	13	0.4	796.3636	5.02E-04	5.02E-04
21	12	23	0.52	796.3636	6.53E-04	
22	13	23	0.49	796.3636	6.15E-04	
23	14	16	0.38	796.3636	4.77E-04	
24	15	16	0.33	796.3636	4.14E-04	
25	15	21	0.41	796.3636	5.15E-04	5.15E-04
26	15	21	0.41	796.3636	5.15E-04	5.15E-04
27	15	24	0.41	796.3636	5.15E-04	
28	16	17	0.35	796.3636	4.39E-04	
29	16	19	0.34	796.3636	4.27E-04	
30	17	18	0.32	796.3636	4.02E-04	
31	17	22	0.54	796.3636	6.78E-04	3.48E-04
32	18	21	0.35	796.3636	4.39E-04	4.39E-04
33	18	21	0.35	796.3636	4.39E-04	4.39E-04
34	19	20	0.38	796.3636	4.77E-04	4.77E-04
35	19	20	0.38	796.3636	4.77E-04	4.77E-04
36	20	23	0.34	796.3636	4.27E-04	4.27E-04
37	20	23	0.34	796.3636	4.27E-04	4.27E-04
38	21	22	0.45	796.3636	5.65E-04	6.49E-04

The reliability parameters of the elements of the power system are taken from multiple sources^{b,c,d}. The used input data for calculation of the unavailability of the interconnections of the Slovenian power system is given in Table D-13. The data is the same as the data used for the Macedonian power system^e.

Table D-13 Slovenian power system lines reliability parameters

Line No.	From bus	To bus	λ (/yr)	μ (yr)	Q_{mean}
1	Krško	Krško 2			2.897E-03
2	Krško	Maribor	7.5	705.7	1.052E-02
3	Maribor	Podlog	3.75	705.7	5.286E-03
4	Podlog	Šoštanj G5	3	705.7	4.233E-03
5	Podlog	Beričevo	3	705.7	4.233E-03
6	Okroglo	Beričevo	6	705.7	8.431E-03
7	Okroglo	Beričevo	6	705.7	8.431E-03
8	Beričevo	Divača	5.25	705.7	7.385E-03
9	Divača2	Kleče	2.16	839.5	2.566E-03
10	Beričevo	Kleče	1.8	839.5	2.140E-03
11	Beričevo	Podlog 2	1.44	839.5	1.712E-03
12	Podlog 2	ŠoštanjG4	1.44	839.5	1.712E-03
13	Podlog 2	Cirkovce	1.62	839.5	1.926E-03
14	Beričevo1	Beričevo2			2.897E-03
15	Beričevo1	Beričevo2			2.897E-03
16	Podlog	Podlog2			2.897E-03
17	Podlog3	Šoštanj	2.24	938.6	2.381E-03
18	Krško2	Brestanica	2.24	938.6	2.381E-03
19	Krško2	Brestanica	2.24	938.6	2.381E-03
20	Beričevo2	Beričevo3			1.069E-03
21	Beričevo2	Beričevo3			1.069E-03
22	Podlog2	Podlog3			1.069E-03
23	Podlog2	Podlog3			1.069E-03
24	Kleče2	Kleče			1.069E-03
25	Kleče2	Kleče			1.069E-03

The size and location of the loads and generators in the Slovenian power system model is given in ta.

Table D-14. The substations marked with “*” at the end of the name have representative and not actual generators in the power system.

The generators in the substations Maribor, Divača and Divača 2 represent power flows with the neighboring power systems. The generator in substation Maribor additionally represent adjacent hydro power plants connected to 110 kV power system network. The generators in Podlog 2 and Okroglo represent adjacent hydro power plants that are not directly connected to the specified substations. The size and reposition of the loads and generators in Table D-14

^b Billinton R., Allan R. N; Reliability assessment of large electric power systems, Kluwer Academic Publishers,1988

^c IEEE Std 500-1984, IEEE Guide to the Collection and Presentation of Electrical, Electronic, Sensing Component, and Mechanical Equipment Reliability Data for Nuclear-Power Generating Stations, 1983

^d IAEA-TECDOC-478, Component reliability data for use in probabilistic safety assessment, 1988

^e Todorovski M.; Approximate calculation of the power flows in the high voltage networks, Graduation work, Faculty of Electrical engineering - Skopje, Macedonia, 1995

doesn't represent the actual Slovenian power system but the nearest approximation developed on the basis of the available data.

Table D-14 The size of the loads and generators of the Slovenian power system

Substation number	Substation name	Load MW	Load MVar	Generator MW	Generator MVar
1	NPP Krško	30	0	600	130
2	RTP Krško	254	54	0	42
3	Maribor*	139	17	77	0
4	Podlog	0	0	0	0
5	Podlog 2*	0	0	10	0
6	Šoštanj 4	0	0	232	65
7	Šoštanj 5	0	0	246	29
8	Podlog 3	100	50	0	0
9	Šoštanj 1	0	0	35	50
10	Cirkovce	94	105	0	0
11	Beričevo	115	0	0	0
12	Beričevo2	74	60	0	0
13	Beričevo3	80	15	0	0
14	Kleče 2	113	68	0	0
15	Kleče	0	0	0	0
16	Divača*	77	32	0	106
17	Divača 2*	48	47	0	81
18	Okroglo*	159	58	53	0
19	Brestanica	70	0	100	197